DIVERSE PAGP::LIPID INTERACTIONS IN GRAM-NEGATIVE BACTERIA

MOLECULAR BASIS OF DIVERSE PAGP::LIPID INTERACTIONS IN GRAM-NEGATIVE BACTERIA

By SANCHIA MILLER, B.Sc, M.Sc.

A Thesis Submitted to the School of Graduate Studies in Partial Fulfilment of the Requirements for the Degree Doctor of Philosophy

DOCTOR OF PHILOSOPHY (2018) McMaster University

(Biochemistry and Biomedical Sciences) Hamilton, Ontario

TITLE: Molecular Basis Of Diverse PagP::Lipid Interactions In Gram-Negative Bacteria

AUTHOR: Sanchia Miller, B.Sc., M.Sc.

SUPERVISOR: Dr. Russell Bishop

NUMBER OF PAGES: xxii, 265

Abstract

PagP is an integral outer membrane enzyme that transfers a palmitoyl group from a phospholipid to lipid A and the polar headgroup of phosphatidylglycerol (PG). Palmitoyl-lipid A and palmitoyl-PG (PPG) have been implicated in resistance to host immune defenses. PagP proteins are diverse, the *E. coli* PagP belongs to the major clade of PagP homologs and palmitoylates lipid A regiospecifically at the 2-position, whereas *P. aeruginosa* PagP belongs to the minor clade of PagP homologs and instead palmitoylates lipid A regiospecifically at the 3'-position. Our objective was to understand how PagP has been adapted in nature to interact with multiple lipid substrates and products. We investigated the structure-function relationships of key major clade homologs, to show that *Bordetella* PagP palmitoylates lipid A at the 3'-position and employs surface residue T29 in its palmitoyltransferase reaction. *Legionella* PagP palmitoylates lipid A at the 2-position and was confirmed to select a palmitate chain from a pool including *iso*-methyl branched phospholipids characteristic of this species. PagP is usually encoded as a single copy on the chromosome in most bacteria, but two copies of *pagP* are found in endophytic bacteria. These duplicated PagP homologs from the major clade branch into two subclades, namely chromosomal and plasmid-based PagP homologs. The chromosomal PagP homologs exhibit interacting periplasmic D61 and H67 residues, which are naturally mutated in plasmid-based PagP homologs, and are associated with a conformational change in the β-barrel that determines its ability to palmitoylate PG. Chromosomal PagPs can convert PPG to

bis(monoacylglycero)phosphate (BMP) and lysophosphatidylglycerol (LPG) through a periplasmic active site controlled by the invariant Y87 residue of *E. coli* PagP. Plasmid-based PagP homologs appear to have been adapted instead as monofunctional lipid A palmitoyltransferases. These results points to a common ancestor for PagP proteins. Knowledge gained from these studies can be applied to protein engineering.

Acknowledgement

I thank my supervisor, Dr. Russell Bishop, for the opportunity to pursue graduate research in his lab. I appreciate the independence you gave me and your unwavering confidence in me over the years.

I thank my committee members Dr. Brian Coombes and Dr. Radhey Gupta for their constructive criticism and wise counsel during our committee meetings. I also thank Drs. Juliet Daniel and Lesley Macneil for their invaluable advice on how to prepare and expedite the thesis!

I thank Charneal and Liset for our discussions, and for their support and encouragement during this journey. I thank other present and past members of the Bishop, Borrows, Epand and the Gupta laboratories who assisted me greatly during this process.

To my family and friends, too many to name, words cannot express how grateful I am for you. I especially thank my son, Aziel, for being such an awesome sport and allowing me to complete this degree. Last but not least, I thank the Almighty God for guidance and strength to endure the difficult times during this process.

Table of Contents

List of Figures

Chapter 1

Chapter 2

Chapter 3

Chapter 4

List of Tables

Chapter 2

Chapter 3

Chapter 4

List of Abbreviations

Abbreviations	**Name**
ABC	ATP binding cassette
ACP	Acyl carrier protein
Amp	Ampicillin
ATCC	American Type Culture Collection
ATP	Adenosine triphosphate
BMP	*bis*(monoacylglycerol)phosphate
CAMP	Cationic Antimicrobial Peptide
CD	Circular Dichroism
CL	Cardiolipin
ClsA	Cardiolipin synthase A
ClsB	Cardiolipin synthase B
ClsC	Cardiolipin synthase C
CLSI	Clinical Laboratory Standards Institute
CSI	Conserved Signature Indel
DDM	*n*-dodecyl-β-D-maltoside
DNA	Deoxyribonucleic acid
dNTP	Deoxynucleotide triphosphate
DPPC	*sn*-1,2-dipalmitoyl-phosphatidylcholine

DPPG	*sn*-1,2-dipalmitoyl phosphatidylglycerol
EDTA	Ethylenediaminetetraacetic acid
ESBL	Extended-spectrum β-lactamases
ESI	Electrospray Ionisation
FLP	Flippase recombinase
FNR	Fumarate nitrate reduction regulator
FRT	Flippase recognition target
GalNAc	*N*-acetyl galactosamine
GlcNAc	*N*-acetyl glucosamine
HGT	Horizontal gene transfer
HPLC	High performance liquid chromatography
IM	Inner membrane
IPTG	Isopropyl β-D-thiogalactoside
Kdo	3-deoxy-D-*manno*-oct-2-ulosonic acid
L-Ara4-N	L-4-aminoarabinose
LB	Lysogeny broth
LC	Liquid chromatography
LDAO	Lauroyldimethylamine-*N*-oxide
LPG	Lyso-phosphatidylglycerol
LPS	Lipopolysaccharide
MAMP	Microbe-associated molecular patterns
MCE	Mammalian cell entry

MD-2	Myeloid differentiation factor 2
MGE	Mobile genetic elements
MHII	Mueller Hinton II
MIC	Minimal inhibitory concentration
MPD	*2*-methyl-*2, 4*-pentanediol
MS	Mass spectrometry
MS/MS	Tandem Mass Spectrometry
MurNAc	*N*-acetylmuramic acid
NCBI	National Center for Biotechnology Information
NMR	Nuclear Magnetic Resonance
OD	Optical Density
OM	Outer membrane
PAGE	Polyacrylamide gel electrophoresis
PDB	Protein Data Bank
PBS	Phosphate buffered saline
PC	Phosphatidylcholine
PCR	Polymerase chain reaction
PE	Phosphatidylethanolamine
PG	Phosphatidylglycerol
PGP	PG-phosphate
PLA_2	Phospholipase A_2
PL	Phospholipid

POPC	*1*-palmitoyl-*2*-oleoyl-*sn*-glycero-*3*-phosphatidylcholine
POPG	*1*-palmitoyl-*2*-oleoyl-*sn*-glycero-*3*-phosphotidylglycerol
P-POPG	Palmitoyl-POPG
POPE	*1*-palmitoyl-*2*-oleoyl-*sn*-glycero-*3*-phosphatidylethanolomine
PPG	Palmitoyl phosphatidylglycerol
PRR	Pattern recognition receptor
PTI	Pattern triggered immunity
TLC	Thin layer chromatography
TLR4	Toll like receptor-4
SDS	Sodium dodecyl sulfate
SOC	Super optimal broth with catabolite media
UDP-GlcNAc	UDP-*N*-acetylglucosamine
UV	Ultra violet

Chapter 1.0

General Introduction

1.1 The Gram-negative bacterial cell envelope

Gram-negative bacteria are endowed with a multilayered cell envelope, which functions to protect them from an environment of high internal osmotic pressure. Three principal layers make up the cell envelope: the inner membrane (IM), the peptidoglycan or murein layer, and the outer membrane (OM) (Figure 1.1). The IM and OM are separated by an aqueous cellular compartment called the periplasmic space, which houses the rigid murein sacculus that surrounds the cell and determines cell shape (Glauert & Thornley 1969; Silhavy et al. 2010). The OM is tethered to the peptidoglycan layer by the murein lipoprotein. The OM is studded with β-barrel membrane proteins known as porins that can facilitate exchange of nutrients and waste products.

1.1.1 Inner membrane

The IM is a semipermeable membrane that facilitates transfer of materials necessary for bacterial growth and cell division (Figure 1.1). The IM is crucial for energy production, protein secretion, cell signaling, and lipid biosynthesis and transport. This membrane is a phospholipid bilayer that contains integral α-helical membrane proteins, lipoproteins anchored to the membrane by an attached lipid, and peripheral membrane proteins (Costerton et al. 1974; Strahl & Errington 2017). Early models of the IM depicted a homogeneous matrix of a fluid phospholipid bilayer with mobile integral membrane proteins (Singer & Nicolson 1972). However, recent research demonstrates the important roles of specialized lipid domains and protein complexes in the membrane architecture (Strahl & Errington 2017; Nicolson 2014). Major glycerophospholipids of

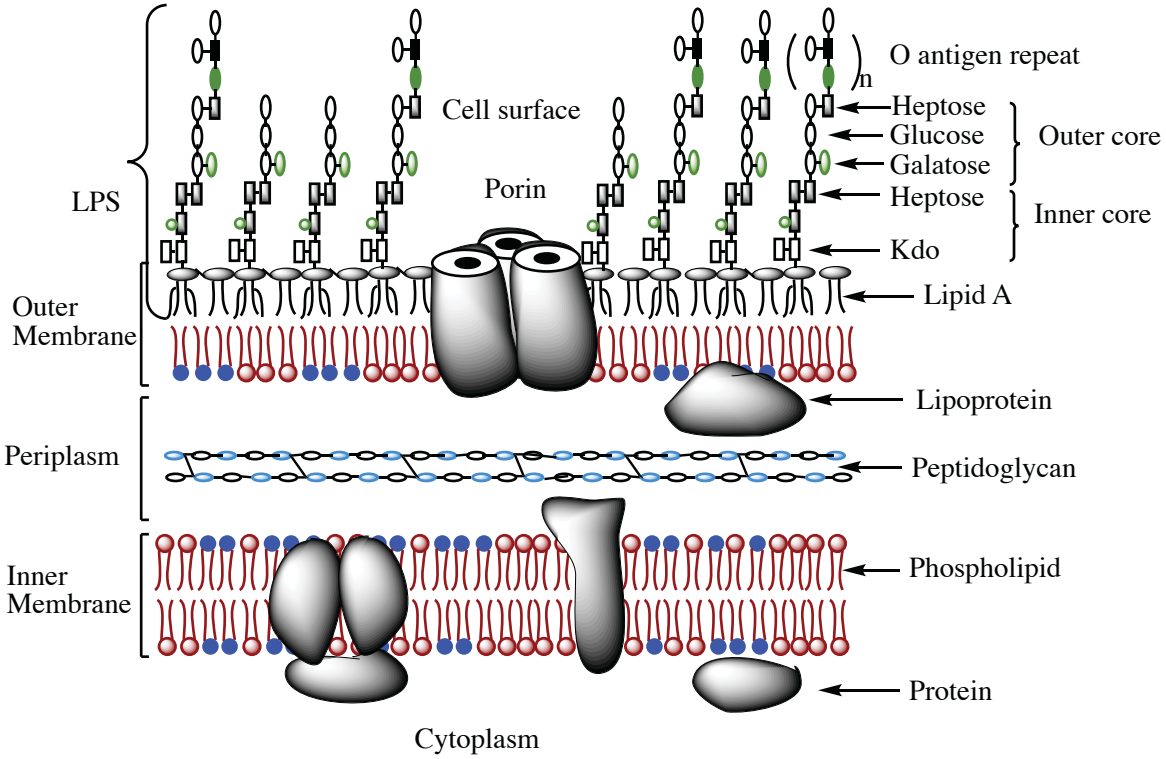

Figure 1.1. The Gram - negative bacterial cell envelope. The inner and outer membrane is separated by a peptidoglycan layer. Both inner and outer membranes house integral membrane proteins and lipoproteins. The lipid fraction of the outer membrane consists of phospholipids in the inner leaflet and lipopolysaccharides (LPS) in the exterior leaflet. LPS consists of a lipid A anchor decorated with inner and outer core sugars and the O-antigen (repeating polysaccharides).

the *Escherichia coli* IM include 70-75% zwitterionic phosphatidylethanolamine (PE), 20-25% anionic phosphatidylglycerol (PG), and ~5% anionic cardiolipin (López-Lara & Geiger 2017; Cronan 2003). Of these, only PG has the requisite cylindrical shape to function on its own as a bilayer-forming lipid, whereas PE, and cardiolipin in the presence of divalent cations, are conical in shape and instead form inverse hexagonal phases. Therefore, the composition of these major phospholipids in the *E. coli* membrane is balanced by their individual polymorphic phase behavior to achieve a lamellar bilayer membrane architecture with its embedded proteins (Bishop 2016; de Kruijff 1987; Rietveld et al. 1993).

1.1.2 Periplasm and peptidoglycan

The periplasmic compartment is packed with proteins that facilitate protein folding and assembly, oxidation/reduction processes, lipid transport, and signal transduction. Recently, it has become evident that the size of the periplasmic space is non-uniform, with some sections being bridged by proteins that connect the IM and OM together. The periplasmic space is necessary for intermembrane communication and its size is regulated by lipoproteins that anchor the peptidoglycan to the OM (Miller & Salama 2018; Asmar et al. 2017). The peptidoglycan layer found in Gram-negative bacteria (Figure 1.1) is between 2 and 8 nm thick compared to the multilayered structure found in Gram-positive bacteria, which exhibits a thickness of 30-60 nm. The peptidoglycan is made up of alternating units of *N*-acetylglucosamine (GlcNAc) and *N*-acetylmuramic acid (MurNAc) linked by β-(1,4) glycosidic bonds and cross-linked

together by short peptides attached to the MurNAc residues (Silhavy et al. 2010; Vollmer et al. 2008).

1.1.3 Outer membrane

The OM is approximately 4 nm thick and it provides the cell with a permeability barrier to hydrophobic antibiotics and detergents (Nikaido 2003; Ursell et al. 2012). The OM must protect Gram-negative bacteria from harmful compounds in the environment, but at the same time, it must also allow for the passage of nutrients the bacteria need to survive. The Gram-negative OM is distinguished from the IM because it is an asymmetric lipid bilayer consisting of phospholipids in the inner leaflet and lipopolysaccharides (LPS) in the outer leaflet (Figure 1.1) (Nikaido et al. 1985; Silhavy et al. 2010). The negatively charged LPS molecules are bridged together by divalent cations, which form ionic bonds to repel hydrophobic compounds that would normally permeate through a phospholipid bilayer (Clifton et al. 2014). Perturbations to OM lipid asymmetry that allow phospholipids to accumulate in the external leaflet will create patches of symmetric phospholipid bilayers that provide sites for hydrophobic compounds to enter the Gram-negative cell envelope (Doerrler 2006; Nikaido 2003). Bile salts in the mammalian gastrointestinal tract are detergents that normally disrupt bacterial phospholipid bilayers, but only the enteric Gram-negative bacteria survive in this environment due to their asymmetric OM lipid bilayers (Begley et al. 2005; Nikaido 2003).

1.1.3.1 Outer membrane proteins

Similar to the IM, roughly half of the mass of the OM is protein. Although numerically fewer OM proteins are present, the porins and murein lipoprotein are present in very high abundance (Nikaido et al. 1985). A few OM proteins function as enzymes and these are present in very low abundance. The integral OM β-barrel proteins serve important functions for the cell including nutrient uptake, cell adhesion, cell signaling, and OM lipid asymmetry maintenance. Most OM proteins are unique in that they have an even number of β-strands aligned in an antiparallel β-barrel with hydrogen bonds between adjacent β-strands (Galdiero et al. 2007; Koebnik et al. 2000). They range in size from 8-26 strands, with short turns on the periplasmic side and long extended loops on the extracellular side (Rollauer et al. 2015). Another general feature of OM β-barrel protein is the presence of an aromatic belt made up of the aromatic amino acid residues Trp, Tyr and Phe that demarcate the interfacial boundaries between the hydrophobic membrane and the aqueous environment on either side. OM proteins have a hydrophobic surface that contacts with the lipid component of the membrane, whereas the interior region can be either polar or nonpolar (Bishop 2008; Schulz 2002). The hydrophobic surface of β-barrel membrane proteins helps to keep them folded in detergents. In fact, detergents can facilitate the refolding of many OM proteins that have been purified in their unfolded state using guanidine or urea (Bannwarth & Schulz 2003; Bishop 2008). The architecture of OM proteins contributes to their high thermal stability and resistance to unfolding by anionic detergents such as sodium dodecyl sulfate (SDS). As the first line of defense between bacteria and their environment, OM β-barrel proteins help Gram-negative

bacteria to withstand various conditions including extremes of temperature, pH, and pressure (Beveridge 1999; Bishop 2008; Rollauer et al. 2015).

OM proteins, like all other proteins, are synthesized by ribosomes in the cytoplasm and need to traverse the IM and the aqueous periplasmic space before they can be inserted in the OM. They are able to do this because of a tripartite *N*-terminal signal sequence consisting of a positively charged *N*-terminal domain, a hydrophobic core consisting of ~10-15 residues, and a *C*-terminal domain with polar residues including the site for cleavage by signal peptidases (Hegde & Bernstein 2006; Sjostrom et al. 1987). OM proteins are transported in their unfolded states to the SecYEG translocon in the IM either post-translationally by SecAB chaperones or co-translationally during synthesis (Baars et al. 2008). On the periplasmic side of the IM, the signal peptide is cleaved by the enzyme signal peptidase, releasing the mature protein (Hegde & Bernstein 2006). It is believed that unfolded OM proteins are protected and delivered by periplasmic chaperones to the β-barrel assembly machinery known as the Bam complex in the OM (Rollauer et al. 2015). The Bam complex acts to insert β-barrel proteins into the OM, but it is unclear whether Bam inserts unfolded, partially or pre-folded β-barrel proteins (Noinaj et al. 2013; Sikdar et al. 2017; Wu et al. 2005). Recently it was shown that some β-barrel proteins begin folding in the periplasm prior to their interaction with Bam (Sikdar et al. 2017). IM α-helical proteins also depend on the Sec translocon for insertion, but their very hydrophobic nature prevents them from being exported to the OM (Baars et al. 2008). Since the murein sacculus surrounds the Gram-negative cell envelope, α-helical

membrane proteins in the IM cannot be transported to the OM by vesicle budding and fusion as occurs in the Golgi apparatus of eukaryotic cells (Palade 1975; Bonifacino & Glick 2004). Consequently, all integral OM proteins assume β-barrel structures. Most integral IM proteins are α-helical in design because β-barrels would presumably create pores in the IM that would depolarize the transmembrane electrochemical potential or proton-motive force (Nikaido & Vaara 1985).

1.1.3.2 Phospholipids

Bacterial OMs consist of phospholipids with a glycerol backbone, a hydrophilic phosphate head-group and hydrophobic acyl chains. Bacteria synthesize a diverse array of phospholipids, with differences including the number, distribution and length of acyl chains, the number, position and geometry of unsaturated bonds, and the nature of the headgroup (Lin & Weibel 2016). In enterobacteria, the phospholipid composition is usually similar for both the IM and OM under normal growth conditions (Raetz & Dowhan 1990).

Phospholipids are synthesized on the inner leaflet of the IM through two pathways starting from the central metabolite cytidine diphosphate-diacylglycerol (CDP-DAG), which is generated by a series of reactions using the precursor *sn*-glycerol-3-phosphate (Raetz & Dowhan 1990) (Figure 1.2). PE is formed in two steps from CDP-DAG: first, phosphatidylserine (PS) is formed by the enzyme phosphatidylserine synthase (Pss) and then it is converted to PE by phosphatidylserine decarboxylase (Psd) (Figure 1.2). Cells

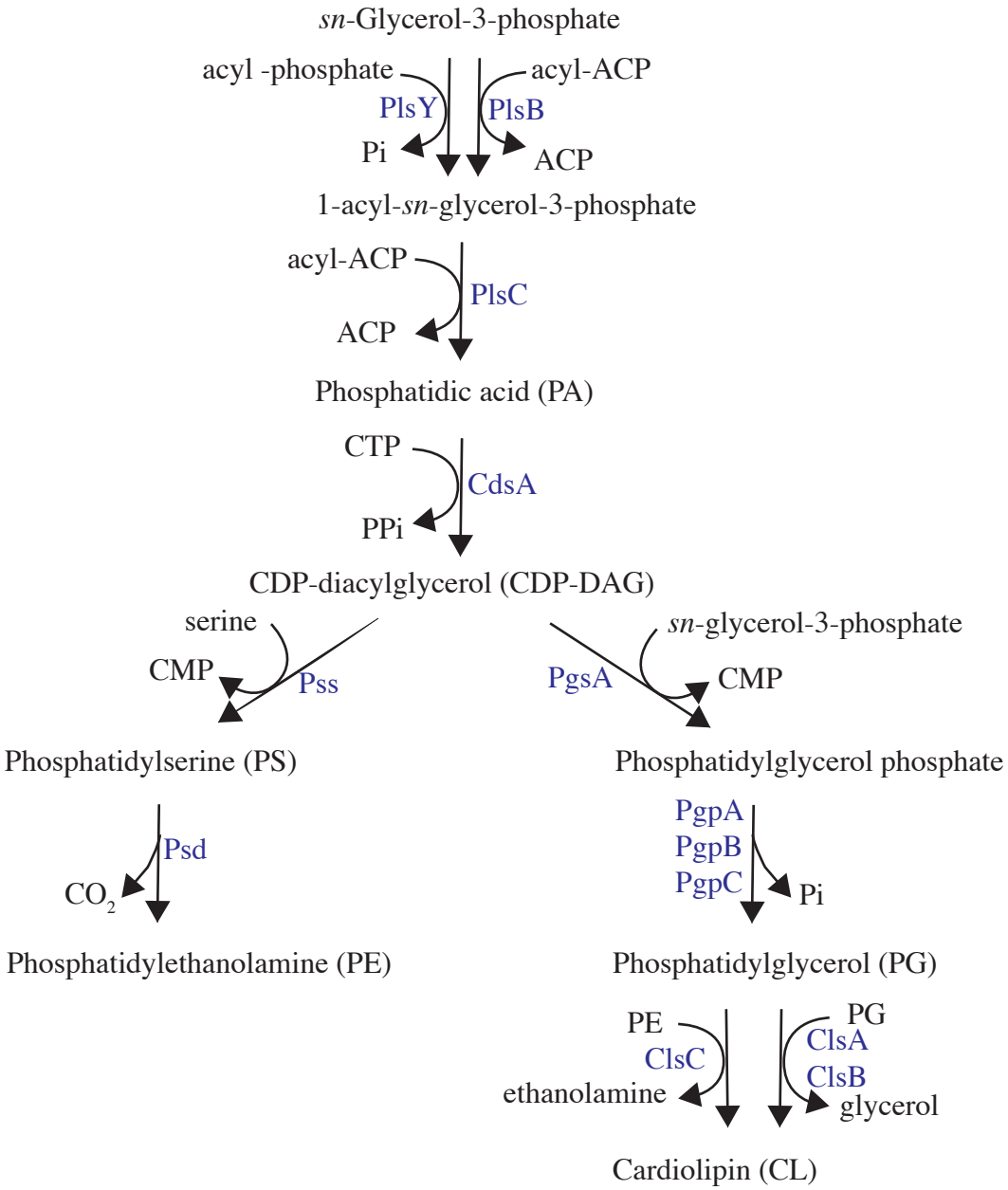

Figure 1.2. Phospholipid biosynthesis in *E. coli*. Biosynthesis of the zwitterionic PE, and the anionic PG and CL phospholipids are synthesized from the central metabolite CDP-DAG, which is made from a series of reactions from *sn*-glycerol-3-phosphate. These enzymes are found on the inner leaflet of the inner membrane. Enzymes are indicated in blue.

devoid of PE are viable only if the medium is supplemented with Ca^{2+} or Mg^{2+} (Rietveld et al. 1993; Rietveld et al. 1994). In these mutant cell lines, PE is largely replaced by phosphatidic acid (PA), which can only assume the required conical shape to replace PE when its anionic headgroup is reduced in size upon charge neutralization due to the binding of divalent cations (DeChavigny et al. 1991; Parsons & Rock 2013; Rilfors et al. 1984). The anionic PG and CL are synthesized first through the condensation of *sn*-glycerol-3-phosphate (G3P) with CDP-DAG, which is catalyzed by PG-phosphate (PGP) synthase PgsA to form PGP (Figure 1.2). PGP is then dephosphorylated to form PG, a reaction catalyzed by any of the three phosphatases PgpA, PgpB, or PgpC (Figure 1.2). PG is essential for bacterial growth since double mutants in PG forming phosphatases are viable, but a triple mutant is lethal (Lu et al. 2010; Raetz & Dowhan 1990). While the backbone of PG is *sn*-glycerol-3-phosphate, the polar headgroup is *sn*-glycerol-1-phosphate. CL is usually formed from two PG molecules; this reaction is catalyzed by either ClsA or ClsB (Guo & Tropp 2000). A third CL synthase, ClsC, catalyzes the formation of CL from PG and PE (Figure 1.2) (Tan et al. 2012; López-Lara & Geiger, 2017). CL is a non-bilayer forming lipid that is dispensable to bacterial cells, but it also performs a variety of functions such as protein stabilization, membrane curvature and long-term viability in stationary phase (Tan et al. 2012). Despite the narrow phospholipid profile of bacterial membranes, the lipid distribution is dynamic (Furse & Scott. 2016). Bacteria have the ability to alter their lipid composition for survival and adaptation in response to environmental stress (Lin & Weibel 2016; Rowlett et al. 2017).

Although the details of phospholipid biosynthesis have been described, how phospholipids are transported back and forth between the IM and OM is only recently being clarified (Cronan 2003; Shrivastava et al. 2017). Phospholipid movement is bidirectional between the IM and OM (Jones & Osborn 1977; Langley et al. 1982). A number of mechanisms for the retrograde movement of phospholipids from the outer leaflet of the OM to the IM are being investigated (Abellón-Ruiz et al. 2017; Shrivastava et al. 2017; Malinverni & Silhavy 2009). The Mla system has at least one component in each compartment of the cell envelope, which includes the MlaBDEF ATP-binding cassette (ABC) transporter in the IM, MlaC in the periplasmic space, and MlaA in the OM (Thong et al. 2016; Malinverni & Silhavy 2009). Cells lacking any of these proteins exhibit phospholipid accumulation in the OM outer leaflet. The structure of MlaA bound to the OmpC/F porins as a scaffold was solved to reveal an amphipathic α-helical protein that is embedded in the inner leaflet of the OM (Abellón-Ruiz et al. 2017; Chong et al. 2015). MlaA acts as a pore for the uptake of phospholipids in the outer leaflet of the OM, but is not accessible to the OM inner leaflet phospholipids. MlaA transports phospholipids via MlaC and MlaBDEF to the IM, where the phospholipids might be recycled in the IM pool or transported back to the OM, but the precise pathway remains elusive (Abellón-Ruiz et al. 2017). MlaD is a member of the mammalian cell entry (MCE) protein family, which form hexameric assemblies with a central channel capable of mediating lipid transport. Two additional MCE proteins in *E. coli* YebT and PqiB create channels of sufficient length to span the periplasmic space and have been shown to bind phospholipids and modulate membrane homeostasis, but their role in anterograde

phospholipid transport is still being evaluated (Ekiert et al. 2017; Isom et al. 2017). PbgA uses a distinctly different mechanism to transport cardiolipin to the OM (Dalebroux et al. 2015; Dong et al. 2016). Phospholipid retrograde transport and OM stability has also been described via a Tol-Pal complex. The Tol-Pal complex is also highly conserved in Gram-negative bacteria and transverses the IM and OMs. Mutants of Tol-Pal complex components have OM defects and with accumulation of phospholipids in the outer leaflet of the OM (Shrivastava et al. 2017).

1.1.3.3 Lipopolysaccharide

LPS is a phospholipid, but unlike glycerophospholipids that have two to four acyl chains attached to a glycerol backbone, LPS can have four to seven acyl chains connected to a glucosamine disaccharide backbone depending on the bacteria and growth conditions from which it is being isolated (Nikaido 2003). LPS is anchored to the OM by lipid A, which is decorated with inner and outer core oligosaccharides and can be coupled to an O-antigen polysaccharide (Figure 1.1). The hydrophilic O-antigen is highly variable and approximately 180 different O-antigens have been identified in *E. coli* alone. The variability in sugar content contributes to the different antigenic types between species and within Gram-negative bacterial strains (Lerouge & Vanderleyden 2001). The outer core is less variable than the O-antigen and is more conserved among bacterial strains. It consists of more common hexoses and hexosamines, such as glucose, galactose, *N*-acetyl galactosamine (GalNAc) and GlcNAc (Caroff & Karibian 2003; Erridge et al. 2002). The inner core is connected to lipid A and consists of the unusual 8-carbon sugar 3-deoxy-D-

manno-octulosonic acid (Kdo) and the 7-carbon sugar L-*glycero*-D-manno-heptose (Hep). The ketosidic bond between the first Kdo residue and lipid A is very labile and can be hydrolyzed upon boiling in detergent solutions with a pH of 4.5 to release the core from lipid A (Rosner et al. 1979; Caroff 1988); this mild acid hydrolysis method is useful when isolating lipid A from cells (Zhou 1999). Lipid A represents the conserved microbial structure required to elicit an immune response in host cells. The primary structure of lipid A in *E. coli* and related bacteria is phosphorylated at the 1 and 4'-positions, acylated with four *R*-3-hydroxymyristate, one laurate and one myristate chains, attached to a *β*-1',6-linked disaccharide of glucosamine (Figure 1.1 and 1.3). The sugars and phosphates provide LPS with a net negative charge, which would cause electrostatic repulsion between the LPS molecules. However, the negatively charged LPS molecules are held together in the outer monolayer of the OM by electrostatic bridges with divalent cations in the surroundings, and hydrophobic interactions between the acyl chains (Clifton et al. 2014; Nikaido 2003).

1.1.3.3.1 Lipid A biosynthesis

Lipid A is synthesized in the cytoplasm through a nine-step enzymatic Raetz pathway, which is conserved in most Gram-negative bacteria and was elucidated primarily in *E. coli* (Raetz et al. 2007) (Figure 1.3). The genes for these enzymes are usually present in single copy in the genome. In the first step of this pathway, LpxA catalyzes the fatty acylation of UDP-GlcNAc. LpxA is a soluble protein that requires the fatty acyl chain to be activated as a thioester donor substrate on acyl carrier protein

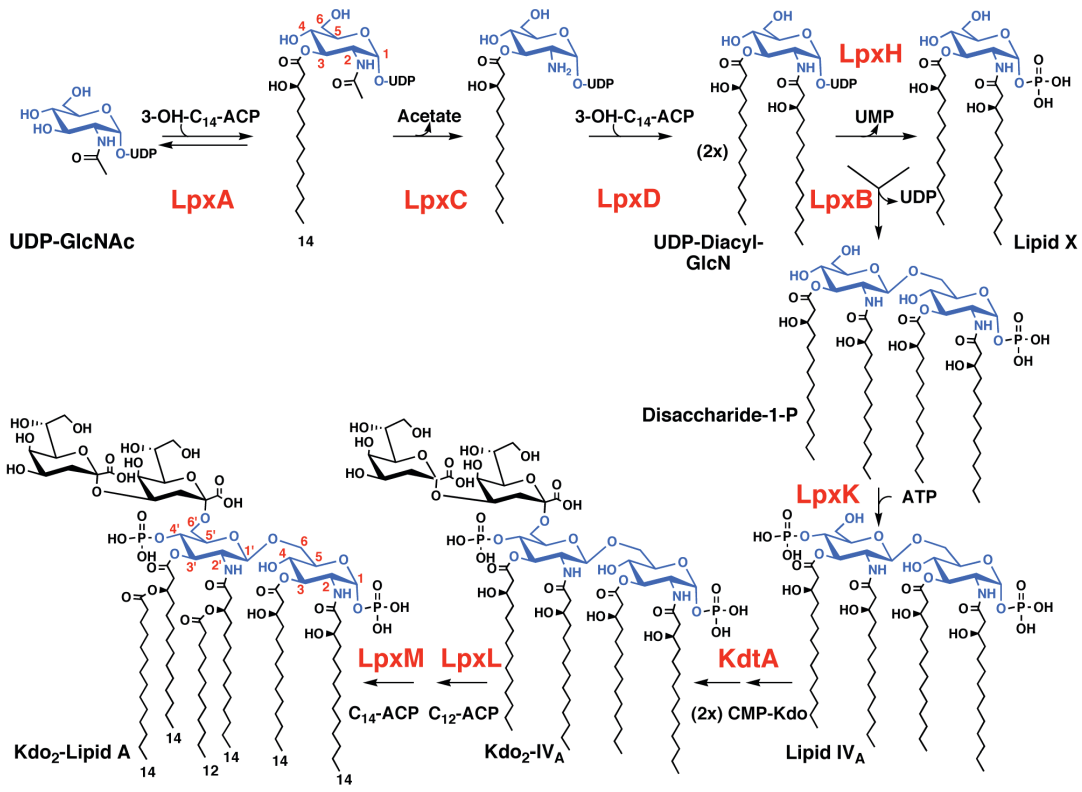

Figure 1.3. Raetz Pathway for Kdo_2 lipid A biosynthesis. Lipid A from *E. coli* is synthesized by a series of nine enzymes in the cytoplasm and inner membrane, known as the Raetz Pathway. The initial enzymes LpxA, LpxC and LpxD are soluble proteins found in the cytoplasm, whereas LpxB and LpxH are peripheral membrane proteins. The final steps are executed by intergral membrane proteins LpxK, KdtA, LpxL and LpxM with active sites facing the cytoplasm. Figure adopted from Raetz et al., 2007.

(ACP). *E. coli* LpxA is highly selective for *R*-3-hydroxymyristoyl-ACP, whereas *Neisseria* LpxA selects *R*-3-hydroxylauroyl-ACP, and *Pseudomonas* LpxA selects *R*-3-hydroxydecanoyl-ACP for esterification of the UDP-GlcNAc 3-OH group; as such, the active site of LpxA measures the selected acyl chain using a precise hydrocarbon ruler (Smith et al. 2015; Raetz et al. 2007). The first committed step is the irreversible deacetylation of the UDP-3-*O*-(acyl)-GlcNAc by hydrolysis of its 2-acetamido group catalyzed by the conserved zinc-dependent LpxC, which is a target for antibiotic development (Figure 1.3). Next, a second *R*-3-hydroxymyristate chain is added, this time in amide linkage, by LpxD to make UDP-2, 3-diacyl-GlcN. Hydrolytic cleavage of the diphosphate bond by the peripheral IM enzyme LxpH forms 2,3-diacyl-GlcN-1-phosphate (lipid X), releasing uridine monophosphate in the process. LpxB, another peripheral IM protein, then condenses UDP-2,3-diacyl-GlcN and lipid X to form the β, 1'-6 glycosidic linked disaccharide characteristic of most lipid A molecules. The disaccharide-1-phosphate is then phosphorylated using ATP by the 4'-kinase LpxK to produce lipid IV_A (Figure 1.3). The integral IM protein KdtA (WaaA) then incorporates two Kdo residues to the 6' position of the distal glucosamine unit. LpxL (HtrB) and LpxM (MsbB) execute the final steps of the Raetz pathway, transferring a lauroyl and a myristoyl chain in acyloxyacyl linkage to the distal glucosamine unit at the 2' and 3' positions, respectively (Figure 1.3). LpxL and LpxM require the presence of the Kdo residues on the disaccharide for activity (Raetz et al. 2009).

The vast majority of lipid A diversity observed in nature arises as a consequence of additional enzymes that serve to modify the basic lipid A scaffold initially assembled by Raetz pathway enzymes. In a few notable cases, modification of the Raetz pathway enzymes can occur. For example, lipid A with two amide-linked hydroxyacyl chains is observed when UDP-GlcNAc is replaced with UDP-2-acetamido-3-amino-2,3-dideoxy-α-D-glucopyranose (Sweet et al. 2004). Additionally, under cold growth conditions (12 ^{o}C), LpxL can be replaced with LpxP, which substitutes laurate with an unsaturated palmitoleate chain (Raetz et al. 2007). Another regulated covalent lipid A modification involves the hydroxylation of the acyloxyacyl-linked myristate chain by LpxO to produce *S*-2-hydroxymyristate (Gibbons et al. 2008). However, the majority of regulated covalent lipid A modifications (see below) are performed in the extracytoplasmic compartments, at the periplasmic leaflet of the IM and in the OM, and their discovery provided molecular markers to follow LPS on its journey from its site of synthesis in the inner leaflet of the IM to the outer leaflet of the OM. As such, remarkable progress in the structural biology of LPS transport has been made in the past decade.

1.1.3.3.2 LPS transport

Raetz pathway enzymes all require cytoplasmic substrates and have their active sites exposed to the cytoplasm. The subsequent glycosylation reactions similarly depend on nucleotide activated sugars to assemble the core oligosaccharide on lipid A in the inner leaflet of the IM. The O-antigen polysaccharide is synthesized in the same location, except it is attached to the isoprenoid lipid carrier undecaprenyl diphosphate. Both core-

lipid A and undecaprenyl-O-antigen are separately translocated to the periplasmic face of the IM by MsbA and Wzx, respectively. The structure of the ABC transporter MsbA has been solved by x-ray crystallography (Ward et al. 2007) and its mechanism for transporting the macroamphiphile core-lipid A substrate across the IM (Mi et al. 2017), and its targeting for antibiotic development (Ho et al. 2018), have been described recently. The O-antigen is polymerized in the periplasmic space and then ligated *en bloc* to core lipid A by WaaL to produce so-called "smooth" LPS. In the absence of O-antigen, the resulting core lipid A is referred to as "rough" LPS, as in the case of *E. coli* K12, or as lipooligosaccharide (LOS), as in the case of *Neisseria* (Raetz et al. 2007). Seven LPS transport proteins, LptA-LptG, form a transenvelope complex to transport LPS from the IM to the OM (Okuda et al. 2016; Sherman et al. 2018). All seven LPS transport proteins are required since a deletion of any Lpt component results in accumulation of LPS in the IM (Okuda et al. 2016). An ABC transporter complex comprised of $LptB_2FG$ (Luo et al. 2017; Dong et al. 2017) extracts the LPS from the periplasmic leaflet of the IM and delivers it to LptC. The energy from ATP hydrolysis drives the process by an alternating lateral access mechanism as LPS is ushered from LptC to LptA. LPS is delivered to its destination by an OM translocon containing two membrane proteins LptD and LptE (Qiao et al. 2014; Dong et al. 2014). LptE is a lipoprotein that is inserted into LptD like a plug. LptD is a 26-strand β-barrel protein (the largest β-barrel protein described so far) and it delivers LPS directly into the external leaflet of the OM (Okuda et al. 2016; Dong et al. 2014).

1.2 Host-LPS interaction

1.2.1 LPS and cationic antimicrobial peptides (CAMPs)

CAMPs are polycationic compounds of the innate immune system. Initially, CAMPs are unstructured in solution, but they competitively displace the divalent cations that neutralize the negative charges of LPS. As CAMPs approach the OM their peptide bonds are stripped of water molecules, which drives their folding into α or β secondary structures, thus revealing their amphipathic structure with polar and non-polar faces. By this "self-promoted" uptake pathway (Hancock & Bell 1988) CAMPs migrate across the OM and continue their journey toward the IM. CAMPs can disrupt the asymmetric organization of the OM and cause phospholipids to migrate into the outer leaflet (Bonnington & Kuehn 2016; Rosenfeld & Shai 2006). Reaching the IM, CAMPs are faced with the semipermeable IM layer. The symmetric bilayer nature of the IM makes it prone to becoming damaged by CAMPs. Several mechanisms have been proposed to explain how CAMPs interact and damage the IM, including pore formation and membrane depolarization, which can lead to cell lysis (Epand & Epand 2011; Zasloff 2002). CAMPs can trigger the IM sensor kinase PhoQ (Bader et al. 2005), which activates transcription of genes that fortify OM barrier function. One such strategy is to modify lipid A structure, which will be discussed below.

1.2.2 LPS and the inflammatory response

Dissociated LPS is recognized by the Toll-like receptor 4 (TLR4) in association with myeloid differentiation factor – 2 (MD-2) found primarily on dendritic cells and

macrophages of the innate immune system (Park et al. 2009; Rietschel et al. 1994). The characteristic structural features of *E. coli* lipid A (Figure 1.3), in particular the length and arrangement of the acyl chains, two on the proximal and four on the distal sugar moieties, in addition to the two phosphate groups, makes this lipid A the optimal ligand to cause a dimerization of the TLR4/MD-2 complex (Figure 1.4) (Park et al. 2009). Five of the six acyl chains labeled R3, R2', R3', R2", and R3" of this lipid A are buried within the MD-2 pocket, but the acyl chain at position 2 (R2) is partially exposed to the surface of this protein and interacts with a second TLR4 (Figure 1.4). Modification of the acyl chain at position 2 in lipid A with an acyloxyacyl-linked palmitate chain by the OM enzyme PagP from *E. coli* is believed to attenuate the inflammatory response by interfering with TLR4 dimerization. Modification of lipid A with a palmitate chain at 3'-position by PagP in *Pseudomonas aeruginosa* serves instead to improve lipid A binding within MD-2 and thus stimulates the inflammatory response (Thaipisuttikul et al. 2014). Additionally, the phosphate groups of lipid A interact with positively charged groups in TLR4. Altogether this causes the dimerization of the TLR4/MD-2 complexes resulting in a signaling cascade stimulating phagocytic activity and production of pro-inflammatory cytokines and mediators (Figure 1.4). Initially this is beneficial in helping to clear the infection, however, if the infection persists, this unresolved inflammation can lead to septic shock (Park et al. 2009; Rietschel et al. 1994).

With an ever increasing resistance of bacteria to antibiotics, there is need for not only new antibiotics but alternative anti-infective therapeutics for the effective treatment

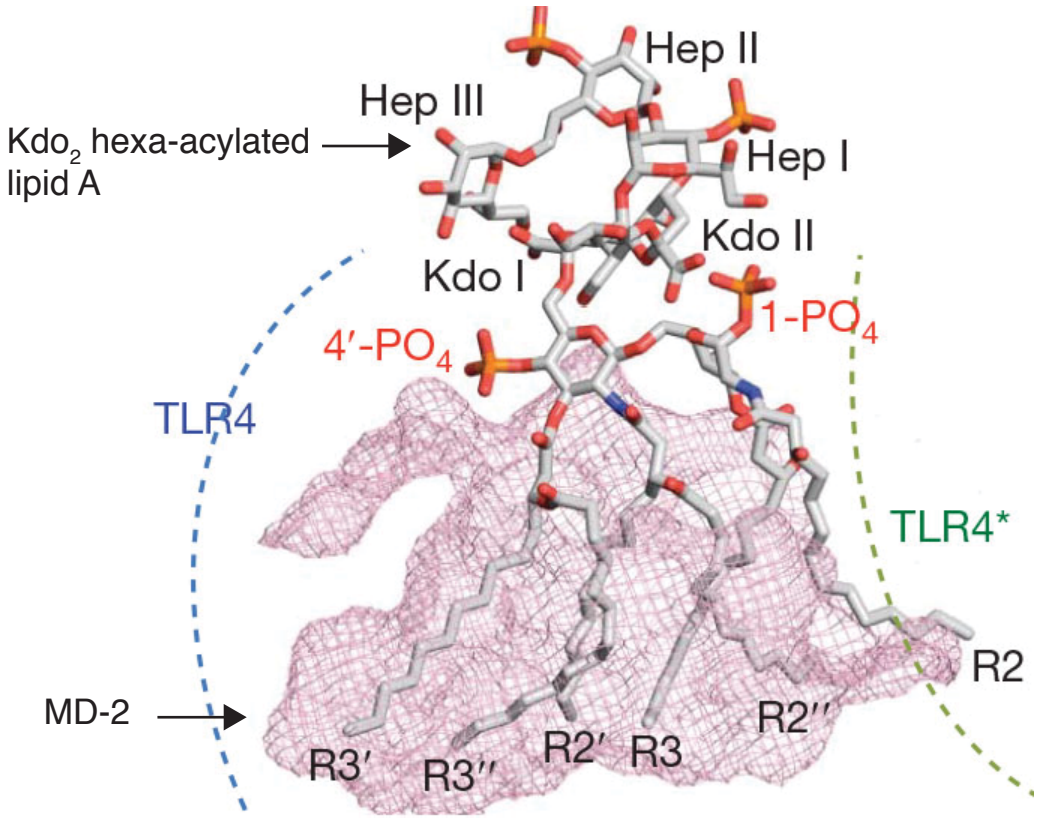

Figure 1.4. Lipid A -TLR4-MD-2 complex dimerization. Kdo_2 hexa-acylated lipid A binds to TLR4/MD-2. Five of the six acyl chains of lipid A are buried in the MD-2 pocket (mesh), but the acyl chain at position 2 (R2) extends outside the pocket to interact with the second TLR4* molecule and initiates dimerization of the complexes. TLR4 in blue dashed lines is from the first complex and TLR4* in green dashed lines is from the second complex. Acyl chains are labelled R2, R3 on the proximal glucosamine and R2', R3' on the distal glucoseamine. R2'' and R3'' are secondary acyl chains on the distal sugar. Figure adopted from Park et al. 2009.

of infectious diseases that continue to be major causes of morbidity and mortality worldwide (Gregg et al. 2017). Potential strategies are the development of endotoxin antagonist and adjuvants from lipid A substructures. Endotoxin adjuvants are used in vaccine formulations to mediate partial activation of the innate immune system, causing altered production of cytokines that are beneficial in triggering the immune response without eliciting sepsis (Raetz et al. 2007). Endotoxin antagonists are designed to treat sepsis by blocking the inflammatory response altogether (Park et al. 2009; Kim et al. 2007). Studies of lipid A antagonists are also important to elucidate mechanisms of endotoxin and host cell interactions and may lead to new pharmacological strategies to control early stage bacterial infections (Rietschel et al. 1994). Currently, monophosphoryl lipid A (MPL adjuvant™) is being used in vaccine formulations marketed by GlaxoSmithKline (Didierlaurent et al. 2017; Garçon et al. 2007). Monophosphoryl lipid A is a substructure of lipid A with five or six acyl chains and a phosphate removed from the 1-position, which renders the molecule ~0.1% as toxic as LPS in rabbits (Casella & Mitchell 2013; Evans et al. 2003). PagP is an enzyme that palmitoylates lipid A and was instrumental to develop MPL in the vaccine Cervarix™ used to target the human papilloma virus for the prevention of cervical cancer, but it is potentially a tool for the synthesis of lipid A-based vaccine adjuvants and endotoxin antagonists for treatment for infectious diseases (Bishop 2005).

1.2.3 Plant host – bacterial LPS interaction

Plants are hosts to pathogenic and non-pathogenic microorganisms. They possess an innate immune system that has many similarities with that of mammals, including the ability to recognize LPS. In plants, sensing of microbe-associated molecular patterns (MAMP) such as LPS by pattern recognition receptors (PRRs) induces a defense mechanism known as pattern triggered immunity (PTI), resulting in local (affecting only infected areas) and systematic resistance (affecting the entire plant system) (Ranf 2016). Initial resistance includes the release of secondary metabolites (such as polyphenols) and pathogen-related proteins (such as CAMPs). Different domains of LPS (O-antigen, core region, and lipid A) can be sensed by these PRRs, but studies have suggested that the lipid A acylation pattern and phosphorylation status plays a key role in recognition by plants (Ranf et al. 2015; Silipo et al. 2008). Intriguingly, many of the LPS biosynthesis genes have been identified in plants and they produce precursors similar to the enterobacterial LPS, but their function in plants has not been elucidated (Li et al. 2011). It seems likely that plant LPS receptors may not sense the enterobacterial LPS as this might trigger auto-immunity against its own LPS structures or substructures (Ranf 2016). Nevertheless, lipid A modification may play a role in the ability of bacteria not only to escape the immune system, but also to fortify the OM permeability barrier against the unpredictable environment in and around plants.

1.3 Regulated lipid A modifications

Bacteria have developed several mechanisms to modify LPS to increase survival in unpredictable and often hostile environments. Modifications of Kdo_2-lipid A that occur

in the extracytoplasmic compartments of many enterobacteria are shown in Figure 1.5 (Raetz et al 2007). Covalent lipid A modification enzymes can be regulated by two-component sensory transduction systems and small regulatory sRNAs (Needham & Trent 2013). Bacteria modify their lipid A by two main mechanisms: (1) modification of lipid A phosphate groups and (2) modification of lipid A acyl chains (Needham & Trent 2013; Raetz et al. 2007).

1.3.1 Regulated modification of lipid A phosphate groups

The modification of lipid A phosphate groups by either dephosphorylating lipid A or incorporating 4-amino-4-deoxy-L-arabinose (L-Ara4N) into the phosphate groups serves to neutralize the negative charge of the bacterial surface. Incorporating the zwitterionic phosphoethanolamine (pEtN) into the lipid A phosphate groups does not neutralize charge, but it does alter the covalent structure of the lipid A phosphate groups. The antibiotic polymyxin directly binds to the lipid A 1 and 4'-phosphate groups and the modification of these groups by pEtN and L-Ara4N moieties effectively controls polymyxin resistance. The enzymes EptA and ArnT modify the 1 and 4' phosphates of lipid A with pEtN and L-Ara4N, respectively, using active sites exposed to the periplasmic side of the IM (Anandan et al. 2017; Petrou et al. 2016) (Figure 1.5). Under low Mg^{2+} and low pH growth conditions, or in the absence of ArnT, EptA may also modify the 4' phosphate of lipid A (Gibbons et al. 2005). EptA uses PE as a donor to add a pEtN group to lipid A, and a homolog EptB adds pEtN to the outer Kdo residue (Reynolds et al. 2005). ArnT transfers L-Ara4N from an undecaprenyl phosphate-

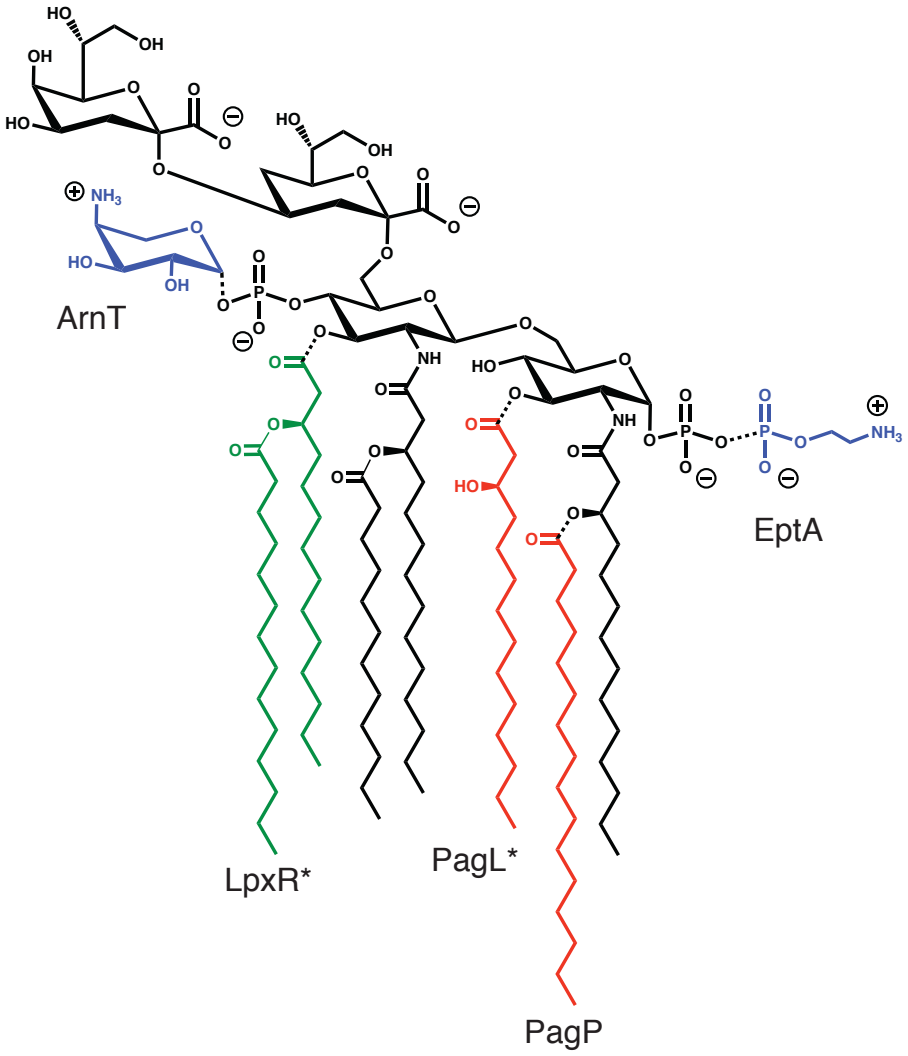

Figure 1.5. Regulated Kdo$_2$ lipid A modifications. Acyl chains in red are added (PagP) or removed (PagL) by OM enzymes of PhoPQ activated genes. Modifications in blue (by EptA and ArnT) are regulated by PmrA/B; these enzymes are located on periplasmic side of the IM. Modification in green by LpxR is controlled by Ca^{2+}; these enzymes are also located on the periplasmic side of the inner IM. An asterisk means that the modification does not occur in *E. coli*. Adapted from Trent et al., 2006.

linked precursor that depends on a metabolic pathway controlled by ArnABCDEF (Yan et al. 2007).

In *Salmonella*, these modifications occur when the PmrAB two-component regulatory system is directly activated upon sensing Fe^{3+} or Al^{3+}, or secondarily via PmrD when the PhoPQ two-component system is activated under Mg^{2+} limitation or by CAMPs (Needham & Trent 2013; Gunn 2008; Raetz et al. 2007; Bader et al. 2005). PmrD is inactive in *E. coli* where PhoPQ and PmrAB function independently of each other. These lipid A modifications fortify the OM permeability barrier in the presence of antimicrobial peptides and limited cations (Needham & Trent 2013).

Some Gram-negative bacteria reduce the net negative charge of LPS by expressing enzymes that remove one or both phosphate groups from lipid A. *Francisella tularensis, Helicobacter pylori* and *Porphyromonas gingivalis* encode phosphatases that cleave lipid A 1 or 4' phosphates, called LpxE and LpxF, respectively (Needham & Trent 2013; Trent 2006). Removal of one or both phosphates can be beneficial to bacteria during infections by reducing the endotoxic activities of lipid A because both phosphates play an essential role in the optimal binding of lipid A to the TLR4/MD-2 complex (Park et al. 2009; Trent et al. 2006). Enteric bacteria do not express lipid A phosphatases (Trent et al. 2006).

1.3.2 Regulated modification of lipid A acyl chains

Several factors govern the immunological property of LPS, but the total number of lipid A acyl chains is the most important (Park et al. 2009). PagP is one of three OM enzymes that modifies the number of lipid A acyl chains. PagP transfers a palmitate chain from the *sn*-1 position of a glycerophospholipid to the 2-position of lipid A (Figure 1.5; 1.6). Lipid A palmitoylation at position 2 provides resistance to some CAMPs and attenuates inflammation signaled through TLR4. PagL is a lipase in the OM of some Gram-negative bacteria such as *Salmonella* and *Pseudomonas*, but it is not present in *E. coli*. PagL removes the 3-O-linked acyl chain from lipid A, which attenuates TLR4 signaling without affecting bacterial resistance to CAMPs (Kawasaki et al. 2004) (Figure 1.5). PagP and PagL are both activated during exposure of the bacterium to CAMPs or limiting Mg^{2+} concentrations (Guo et al. 1998). The third enzyme, LpxR, removes the 3'-acyloxyacyl moiety of lipid A in the presence of Ca^{2+} ions (Figure 1.5). The regulation of this enzyme is yet to be elucidated (Rutten et al. 2006).

1.4 PagP

PagP is a lipid modification enzyme that resides in the OM of some Gram-negative bacteria. The *pagP* gene was first identified in *S. typhimurium* as a PhoPQ-activated gene important for CAMP resistance and increased palmitoylation of lipid A (Guo et al. 1998). The biochemical reaction was later established for the *E. coli* homolog, which enzymatically transfers of a palmitate chain from the *sn*-1 position of a phospholipid to the *R*-3- hydroxymyristate chain at the 2-position of lipid A (Bishop et al. 2000). Subsequently, PagP was shown in *Salmonella* OMs to palmitoylate the *sn-3'*

position in the headgroup of PG (Dalebroux et al. 2014) (Figure 1.6 and 1.7). PagP is known to confer resistance to host CAMPs and attenuates the inflammatory response of the host immune system. When PagP palmitoylates lipid A, converting it to a hepta-acylated species, it is implicated that the seventh chain at the 2-position interferes with TLR4-MD-2 dimerization, thus attenuating inflammation by 10-100 fold (Figure 1.4) (Park et al. 2009; Feist et al. 1989). Additionally, a seventh acyl chain increases the overall hydrophobic interactions between the acyl chains and so fortifies the OM permeability barrier. As such, PagP and other lipid A modification enzymes that affect bacterial-host interactions are seen as targets for the development of therapeutics to combat certain infectious diseases (Bishop 2005). Interestingly, palmitoylated lipid A and palmitoylated PG (PPG) were observed in a 1:1 ratio in *Salmonella* bacterial OM (Dalebroux et al. 2014). The function of PPG is yet to be elucidated, but it has been suggested that it increases the hydrophobicity of the OM (Dalebroux et al. 2014).

In most bacteria, PagP expression is regulated by the PhoPQ two-component system that senses Mg^{2+}-limited growth conditions and CAMPs as previously mentioned (Wang et al. 2018; Thaipisuttikul et al. 2014; Bishop 2005; Guo et al. 1998). However, in biofilms formed by a number of Gram-negative bacteria, PagP is regulated by the histone-like protein repressor H-NS and SlyA regulator. Also, *E. coli* biofilms show an increased level of palmitoylated lipid A compared to isolated cells, and increased biofilm bacterial survival in animal models. Increased lipid A palmitoylation demonstrated in biofilms is possibly a new phenotype to monitor biofilms (Chalabaev et al. 2014).

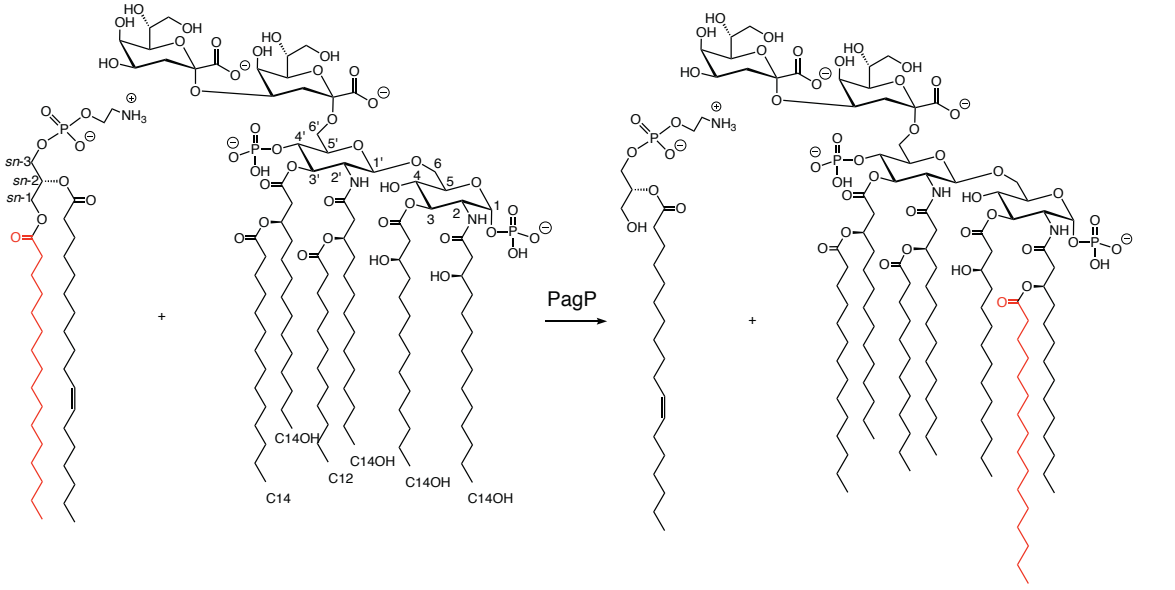

PE Kdo$_2$ lipid A Lyso-PE Hepta acylated - Kdo$_2$ lipid A

Figure 1.6. Enzymatic palmitoylation of lipid A catalyzed by PagP. PagP biochemical reaction using Kdo$_2$ lipid A as an acceptor substrate. PagP takes a palmitate (in red) from the *sn*-1 position of a phospholipid (PE) and transfers it to the 2-position of the *R*-3 hydroxymyristate on Kdo$_2$ lipid A creating a hepta-acylated lipid A and lyso-PE as a byproduct.

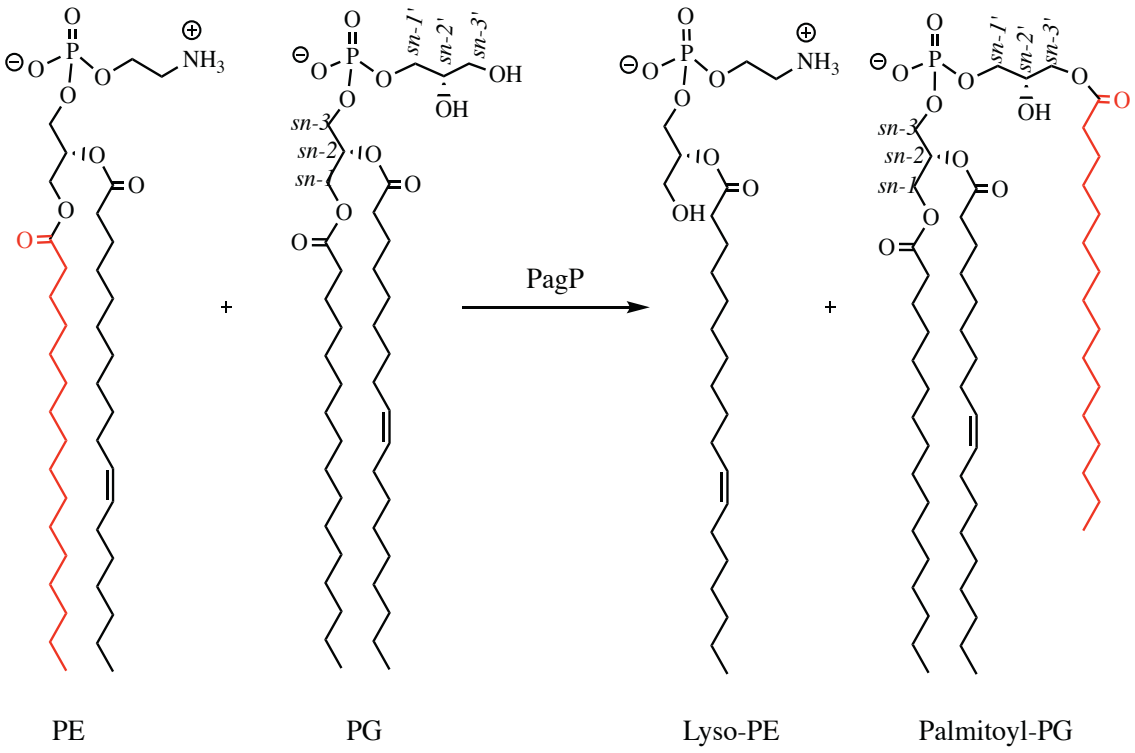

Figure 1.7 . Enzymatic palmitoylation of PG catalyzed by PagP. PagP transfers a palmitate from the *sn*-1 position of a phospholipid (PE in this reaction) to the *sn*-3 position of PG's headgroup generating palmitoyl-PG. .

1.4.1 PagP Structure and dynamics

The structure of *E. coli* PagP was solved by x-ray crystallography and NMR spectroscopy to reveal an eight-strand antiparallel β-barrel (Figure 1.8) (Cuesta-Seijo et al. 2010; Ahn et al. 2004; Hwang et al. 2002; Hwang et al. 2004). The β-barrel is preceded by a short amphipathic *N*-terminal α-helix that functions to stabilize the barrel as a post-assembly clamp (Iyer & Mahalakshmi 2016; Huysmans et al. 2007; Jia et al. 2004). Like other β-barrel membrane proteins, PagP displays a rigid membrane domain with flexible external loops and smaller periplasmic turns in addition to the aromatic belts, which demarcate the membrane interfaces. PagP is a small protein of 161 amino acids and spans the membrane with a tilt of roughly 25^{o}. The three catalytic residues His33, Ser77 and Arg114 are located on the external side of the membrane (Ahn et al. 2004; Bishop Unpublished). PagP possesses a palmitoyl-chain binding pocket known as the hydrocarbon ruler, which is delineated by a bound detergent molecule in the crystal structure (Figure 1.8). NMR studies revealed a dynamic protein with an inhibited R and activated T states, which likely depicts the two conformations exhibited in the bacterial OM (Hwang et al. 2004; Hwang et al. 2002).

1.4.2 Crenel and embrasure

Phospholipids and lipid A gain access to the hydrocarbon ruler from the OM exterior by lateral diffusion through two gateways in the β-barrel wall known as the crenel and embrasure, respectively (Khan & Bishop 2009) (Figure 1.8). The crenel is where phospholipid regioselectivity is enforced. It is gated by a hydrogen bond between

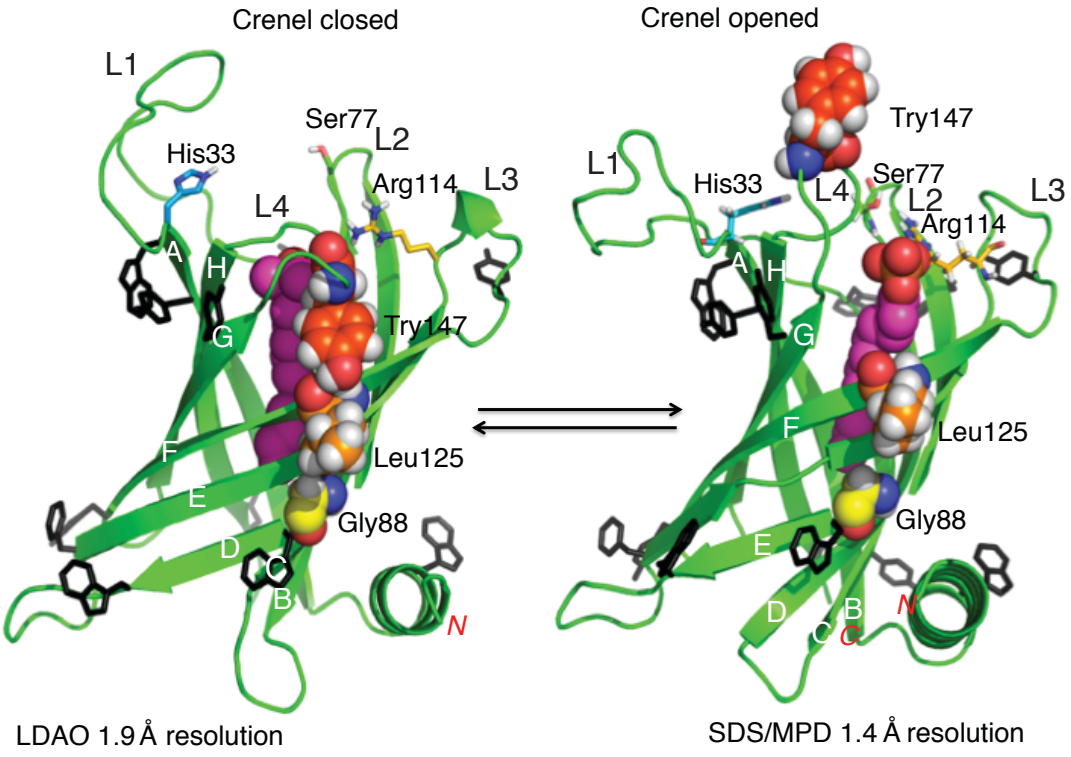

Figure 1.8. PagP crenel lateral gating mechanism. PagP is an 8-stranded β-barrel protein with an amphipathic *N*-terminal α-helix (green). A bound detergent molecule delineates the hydrocarbon ruler lined by Gly88 at its base. The *N*-terminus (*N*) and *C*- terminus (*C*) are shown in red and the β-strands are marked with white letters (A-H). The crenel is gated by Try147 in the L4 loop and Leu125 in β-strand E. The aromatic belt residues (black wireframe) demarcate the membrane interfaces between the extracellular and the periplasmic spaces.

the phenolic hydroxyl group of Tyr147 in the L4 loop and the backbone amide of Leu125 (Figure 1.8). The Tyr147Phe mutant unlatches the crenel resulting in an enzyme with two to three-fold higher specific activity, but with relinquished phospholipid regioselectivity (Cuesta-Seijo et al. 2010; Bishop Unpublished). Opposite the crenel between Pro28 and Pro50 is the embrasure, where lipid A or PG gain access to the hydrocarbon ruler. The *E. coli* PagP has no Cys residues, but a Pro28Cys/Pro50Cys double mutant is fully active unless the two cysteine residues are oxidized to form a disulfide bond. In this case, Pro28Cys/Pro50Cys PagP retains its slow phospholipase activity, but it can no longer palmitoylate lipid A or PG. Reducing the disulfide bond fully restores all palmitoyltransferase activity (Khan & Bishop 2009; Bishop Unpublished). PagP requires both substrates in a ternary complex for the acyltransferase reaction to occur through a sequential mechanism as indicated by enzyme kinetics and spectroscopic properties observed in a detergent-micellar assay system (Bishop Unpublished). Details of the mechanism by which lipid A binds to the enzyme in a regiospecific manner remain to be elucidated, but judging from the diversity of palmitoylated lipid A structures found in bacterial OMs the embrasure is quite flexible in recognizing acceptor substrates. In addition to lipid A and PG, palmitoylation of non-specific lipid alcohols can be observed *in vitro* (Dalebroux et al. 2014; Khan & Bishop 2009).

1.4.3 Molecular mechanism for selecting a palmitate

PagP selects a palmitate chain with exquisite precision through collaboration between the hydrocarbon ruler and crenel. In *E. coli*, the phospholipid pool is mainly

esterified by C14, C16 and C18 acyl chains. The C14 and C16 acyl chains are primarily found at the *sn*-1 position, while C16 and C18 chains are found at the *sn*-2 position (Oursel et al. 2007). The crenel gating mechanism effectively blockades *sn*-2 C18 phospholipids from entering the hydrocarbon ruler. The phospholipid acyl chain enters through the crenel to access the hydrocarbon ruler while its headgroup is stabilized by an electrostatic interaction with the catalytic residue Arg114 in the L3 loop (Figure 1.8) (Bishop Unpublished). The hydrocarbon ruler tightly binds the distal six carbons on the acyl chain, therefore excluding *sn*-1 C14 myristate chains, which are too short to register with the catalytic residues when fully extended. Consequently, only *sn*-1 C16 acyl chains are selected (Khan et al. Unpublished). C14 acyl chains can be selected both *in vitro* and *in vivo* if the dimensions of the hydrocarbon ruler are shortened by Gly88Ser/Thr/Val substitutions (Khan et al. 2007; Khan et al. 2010; Khan et al. 2010). Tyr147Phe mutants reveal a significant amount of C18 stearate chains in lipid A *in vivo*, indicating that the hydrocarbon ruler cannot exclude stearate. Interestingly, unsaturated fatty acyl chains of any length have never been observed to be incorporated into lipid A by PagP *in vivo*. Considering the abundance of unsaturated fatty acyl chains in the *E. coli* phospholipid pool, a mechanism must exist to exclude these acyl chains from the PagP active site, but the molecular mechanism for that exclusion remains to be determined.

His33 and Ser77 residues are essential for the transesterification reaction to occur (Hwang et al. 2002). The reaction mechanism remains to be elucidated with certainty, but all existing data is consistent with a mechanism like that described for the carnitine

acyltransferases, which similarly operate through a sequential ternary complex mechanism governed primarily by a catalytic dyad of conserved His and Ser residues (Jogl & Tong 2003; Jogl et al. 2004). We similarly propose that His33 in PagP functions as a general base to deprotonate the acceptor substrate hydroxyl group for nucleophilic attack on the carbonyl carbon of the *sn*-1 palmitoyl ester bond in the phospholipid donor. Ser77 is proposed to function not as a nucleophile, but to simply stabilize the oxyanion that forms in the tetrahedral transition state of the ternary complex. Finally, protonated His33 is proposed to function as a general acid by donating its proton to the *sn*-1 hydroxyl group of the lyso-phospholipid leaving group.

1.4.4 OM lipid asymmetry

OM lipid asymmetry is maintained by systems that prevent the appearance or removal of phospholipids in the exterior leaflet of the OM. These systems include the MlaABCDEF six component system, the OM phospholipase PldA, which hydrolyzes both *sn*-1 and *sn*-2 phospholipid acyl chains, and PagP (Chong et al. 2015; Malinverni & Silhavy 2009). The asymmetric lipid organization of the OM, with LPS in the external leaflet and phospholipids in the internal leaflet, means PagP with its active site residues in the external loops is topologically separated from its substrates. Consequently, for PagP to access its substrates there needs to be a perturbation in the OM causing ectopic cell-surface exposure of the phospholipids. This likely occurs upon attack by host antimicrobial agents recruited to disrupt the OM permeability barrier (Nikaido 2003; Silhavy et al. 2010). Defects in the Mla system contribute to phospholipid accumulation

in the outer leaflet and provide PagP with access to its substrates (Malinverni & Silhavy 2009). Similarly, the *lptD4213* mutation in *E. coli* provides insufficient LPS transport to the OM and allows phospholipids to accumulate in the external leaflet, thus providing PagP with its necessary substrate to palmitoylate lipid A (Wu et al. 2006; Bishop 2014). The divalent cation chelator ethylenediaminetetraacetic acid (EDTA) similarly activates PagP (Jia et al. 2004). Brief exposure of *E. coli* cell cultures to millimolar concentrations of EDTA effectively strips a fraction of LPS from the OM without affecting nucleic acid function within the cell (Leive 1968). Lipid A palmitoylation induced by EDTA is rapid and independent of the *de novo* synthesis of PagP, but cells cannot grow continuously in the presence of EDTA since Mg^{2+} is an essential nutrient. Brief EDTA treatment before harvesting bacteria has proven to be an effective method to activate PagP in the OM for monitoring lipid A palmitoylation or ectopic cell-surface phospholipid exposure (Chong et al. 2015; Jia et al. 2004).

1.5 PagP diversity in Gram-negative bacteria

PagP is found in a number of Gram-negative bacteria, most having a pathogenic or intracellular lifestyle (Bishop 2005). Diversity in PagP is observed with respect to the enzyme's preference to palmitoylate the 2 and/or 3' position of lipid A. PagP homologs are known to have a lipid A 2-position regiospecificity in most bacteria including *E. coli* (Figure 1.6; 1.9) (Bishop et al. 2000; Bishop 2005). Previous studies indicate that a lipid A 3'-position regiospecificity also exists in the β-Proteobacteria represented by *Bordetella* PagP homologs (Preston et al. 2003). Another PagP homolog

was identified in *Bordetella parapertussis* that palmitoylates the 2 and 3' positions of its lipid A (Figure 1.9) (Hittle et al. 2015). Interestingly, the discovery of PagP in *Pseudomonas aeruginosa,* which shares no primary sequence similarity with *E. coli* PagP, revealed that it palmitoylates lipid A at the 3'-position of the distal glucosamine unit (Figure 1.9) (Thaipisuttikul et al. 2014). Although *P. aeruginosa* PagP shows close structural and functional relationships with *E. coli* PagP, the *P. aeruginosa* PagP has diverged into a distinct clade (Thaipisuttikul et al. 2014). The PagP family of proteins is therefore separated into two clades: the major clade homologs, including those from *E. coli*, *Salmonella*, *Legionella* and *Bordetella*, and the minor clade homologs, including PagP from *Pseudomonas*; a complete phylogenetic analysis of either the major or the minor PagP clades have not yet been reported. A few members of PagP from each clade will be discussed here to illustrate its importance to particular bacterial lifestyles.

1.5.1 *Bordetella* PagP

Bordetella bronchiseptica infects many mammals, but rarely humans, and is one of three closely related β-Proteobacteria that infect the respiratory tracts of mammals; the other two bacteria are *B. parapertussis*, which infects humans and sheep, and *B. pertussis*, the causative agent of whooping cough in humans. PagP palmitoylates the 3'-position of lipid A in *B. bronchiseptica* (Figure 1.9) and is regulated by the BvgAS two-component regulatory system that responds to environmental stimuli. In *B. bronchiseptica,* PagP is required for resistance to antibody-mediated complement lysis during infection and the persistent colonization of the mouse respiratory tract, but not for initial colonization

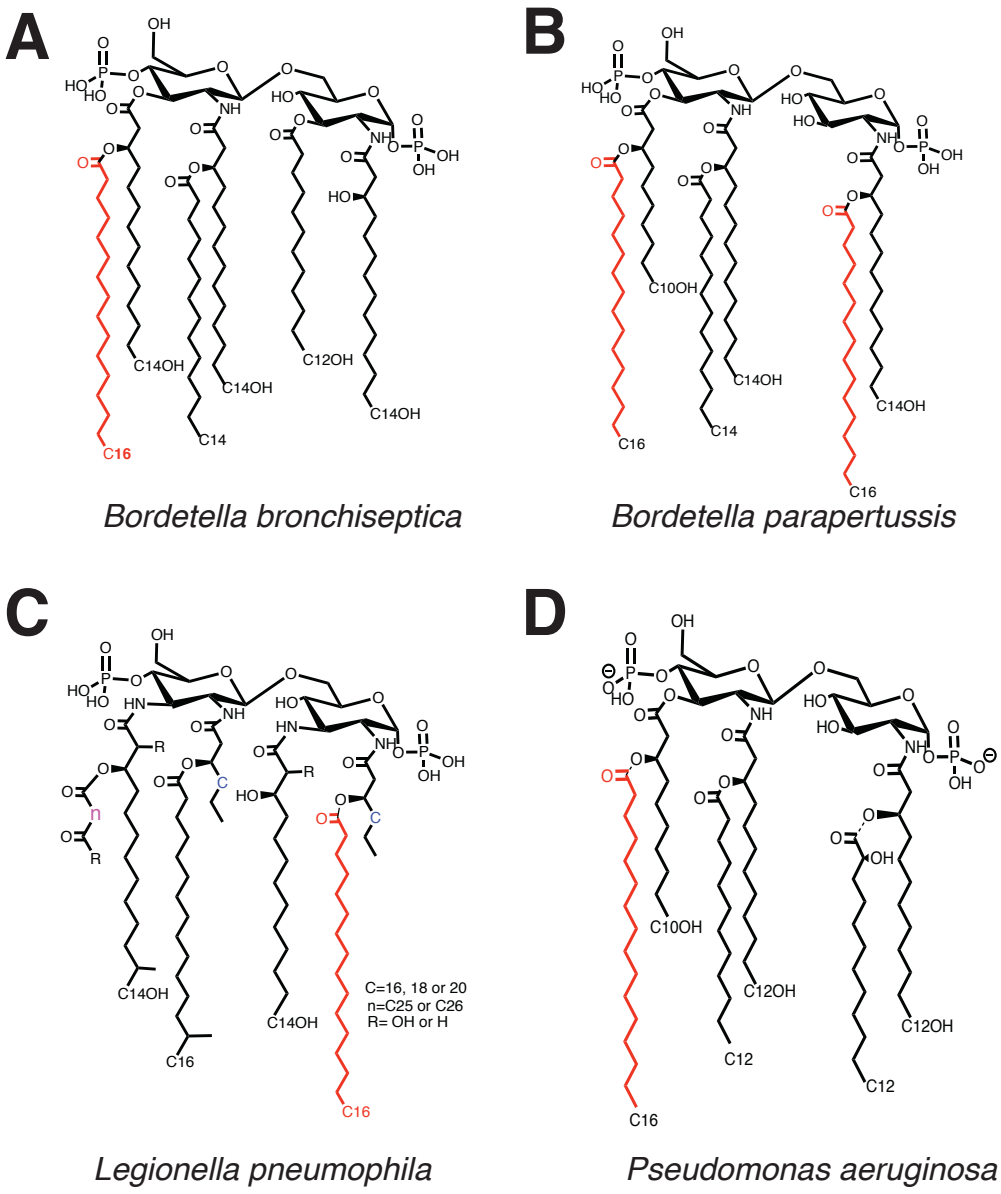

Figure 1.9. Palmitoylated lipid A diversity. A-C. Lipid A palmitoylated by PagP homologs from the major clade. A. Palmitoylated lipid A displayed in *Bordetella bronchiseptica.* B. Predominant palmitoylated lipid A displayed in *Bordetella parapertussis*. C. The proposed palmitoylated lipid A displayed in *Legionella pneumophila.* D. Palmitoylated lipid A displayed in *Pseudomonas aeruginosa,* which has a lipid A 3'-position regiospecific PagP.

(Pilione et al. 2004; Preston et al. 2003). Interestingly, *B. bronchiseptica* and *B. parapertussis* each encode PagP homologs with 99% amino acid sequence identity, yet *B. parapertussis* PagP palmitoylates its lipid A at the 2 and 3' positions of lipid A, whereas *B. bronchiseptica* PagP palmitoylates lipid A exclusively at the 3'-position (Figure 1.9). The *Bordetella* genus is known to show remarkable heterogeneity in their lipid A structures, which is a reflection of their adaptation to various niches or hosts (Zarrouk et al. 1997). *B. parapertussis* PagP confers resistance to antimicrobial peptides and decreases the endotoxicity of the lipid A (Hittle et al. 2015). *B. pertussis* has a *pagP* sequence, but its expression is inactivated due to the insertion of a transposable element in the promoter region (Hittle et al. 2015; Parkhill et al. 2003).

1.5.2 *Legionella* PagP

Legionella pneumophila is an intracellular bacterium that causes Legionnaires' disease. A *pagP* gene was identified in *Legionella pneumophila* that conferred resistance to CAMPs and promoted intracellular infection. *Legionella* lipid A is known to be acylated with long and *iso*-methyl-branched chains attached to a 2,3-diamino-2,3-dideoxy-D-glucopyranose backbone, which contributes to its low endotoxicity and, therefore, successful intracellular lifestyle (Zähringer et al. 1995). The palmitoylated lipid A structure was never identified in *L. pneumophila*, but it is suspected to have a similar hepta-acylated lipid A pattern like that of *E. coli* and *Salmonella* with the palmitate added to the 2-position of lipid A (Figure 1.9). However, *Legionella*, unlike the bacteria from the Enterobacterales, have 40-90% branched acyl chains bearing *iso*- or *anteiso*-methyl

groups in their phospholipid pool; therefore, it is possible for an *iso*-methyl-branched acyl chain to be selected by PagP instead of a palmitate (Geiger 2010; López-Lara & Geiger 2017). Additionally, in the multiple sequence alignment the conserved G88, which lines the base of the hydrocarbon ruler in *E. coli* PagP, is replaced by an alanine in *Legionella* PagP, raising the possibility that this enzyme might select an acyl chain other than palmitate (Ahn et al. 2004).

1.5.3 *Pseudomonas* PagP

Pseudomonas aeruginosa is an opportunistic pathogen of humans that chronically infects the lungs of cystic fibrosis patients. The lipid A extracted from *P. aeruginosa* cells that have been isolated from cystic fibrosis patients is constitutively palmitoylated (Ernst et al. 2003). However, for several years no *pagP* gene was found in the genome of *P. aeruginosa.* A combined genetic and biochemical approach was used to identify the *P. aeruginosa pagP* gene, which displayed little or no identity in deduced amino acid sequence with *E. coli* PagP. Nevertheless, this PagP is functionally and even structurally similar to the *E. coli* PagP. The *Pseudomonas* PagP palmitoylates lipid A at the 3' position, which contributes to the stimulation of the innate immune system instead of an attenuation as observed in *E. coli* and *Salmonella* (Thaipisuttikul et al. 2014; Guo et al. 1998). The lipid A exhibited by *Pseudomonas spp*. is typically acylated with five acyl chains; therefore, a sixth chain incorporated by PagP equips the lipid A with the optimum number of acyl chains to elicit a pro-inflammatory response of the innate immune system. However, the response in not as strong as that of a hexa-acylated lipid A from *E. coli*,

because the length of the *Pseudomonas* lipid A acyl chains are of 10 and 12 carbons instead of 12 and 14 as in the *E. coli* lipid A (Figure 1.9) (Park et al. 2009; Ernst et al. 2003). The addition of a sixth chain also reinforces the permeability barrier of the OM and increases resistance to CAMPs (Thaipisuttikul et al. 2014).

Bordetella, Legionella and *Pseudomonas* are highly pathogenic bacteria that show diversity of PagP lipid A regioselectivity (Thaipisuttikul et al. 2014; Preston et al. 2003; Robey et al. 2001). PagP is found in many other bacteria that are pathogenic and even in some that are non-pathogenic, but it is apparent that PagP lipid A regioselectivity is dependent on the bacterial lifestyle and the lipid A being presented (Bishop 2005). Although other factors need to be considered, elucidating the molecular basis of PagP selectivity for the 2 and/or 3'position is important because it seems regulated lipid A acylation is necessary for bacterial pathogenesis (Trent 2004).

1.7 Thesis objectives

The ultimate goal envisioned is that PagP will be used to develop anti-infective agents, endotoxin antagonists and adjuvants. However, before any effective therapeutic value can come to realization, certain areas of PagP structure-function relationships need to be addressed, including the molecular diversity of lipid A palmitoylation and characterizing new functions of this enzyme. In particular, the overarching objectives of this dissertation was to understand the molecular mechanisms by which diverse PagP homologs interact with their lipid substrates. To this end, Chapter 2 details the

distribution of PagP among Gram-negative bacteria and demonstrates structure-function relationships among major clade PagP homologs. In Chapter 3 we characterized duplicate PagP homologs from *Klebsiella oxytoca* that represented chromosomal and plasmid-based subclades of PagP. In Chapter 4 we attempted to elucidate a role for the two PagP homologs from *K. oxytoca*. Chapter 5 summarizes the contents of this thesis and highlights areas for future studies.

Chapter 2.0

Structure-function relationships among a major clade of PagP homologs.

2.1 Preface

The work in this chapter describes structure-function relationships among a major clade of PagP homologs. Dr. Radhey Gupta and his PhD student Bijendra Khadka conducted the original phylogenetic analysis that led to the discovery of a major clade of PagP homologs and the identification of conserved signature indels in the L3 loop and T2 turn of the protein. Results from structure-functional studies of the minor clade of PagP homologs were provided by Charneal Dixon and Emily DeHaas. Dr. Bishop and I designed experiments and wrote the manuscript together. We received *iso*-methyl branched phospholipids from Dr. Ronald McElhaney and Dr. Ruthven Lewis of the University of Alberta to carry out acyl chain specificity reactions using *Legionella* PagP. Mass spectrometry experiments were carried out by Dr. Theresa Garrett of Vassar College.

2.2 Summary

The outer membrane (OM) enzyme PagP from *Escherichia coli* EcPagP modifies the lipid A component of lipopolysaccharide and the polar headgroup of phosphatidylglycerol (PG) with a palmitoyl group; these modifications have been implicated in providing resistance to host immune defenses. EcPagP belongs to a major clade of PagP homologs, but a minor clade represented by PagP from *Pseudomonas aeruginosa* PaPagP has evolved to fulfill distinctly different functions. We have conducted a phylogenetic analysis of the major and minor clades of PagP homologs and investigated structure-function relationships within the major clade. The known lipid A

regiospecificity at the 2-position for EcPagP versus the 3'-position for PaPagP was extended to show that particular major clade PagP homologs can palmitoylate lipid A specifically at the 3'-position or at both the 2 and 3'-positions. PagP lipid A regioselectivities observed *in vitro* are not always reflective of the lipid A structures exhibited *in vivo* in wild type bacteria. We demonstrate that Thr28 in the embrasure of PagP from *Bordetella bronchiseptica* BbPagP of the β-Proteobacteria is necessary for lipid A palmitoylation at the 3'-position. We also demonstrate that PagP from *Legionella pneumophila* LpPagP of the γ-Proteobacteria selects palmitate from a pool of phospholipids that include *iso*-methyl branched acyl-chains in order to palmitoylate lipid A at the 2-position. Among the *Enterobacterales* order of the γ-Proteobacteria we identified a conserved signature indel or CSI in the L3 loop of duplicated PagP homologs from *Klebsiella oxytoca* Ko1PagP and Ko2PagP, and demonstrate that the CSI controls the enzymatic palmitoylation of PG *in vitro*. The duplicated Ko2PagP homolog belongs to a subclade that appears to be disseminated by plasmids among bacteria known to live as endophytes within plant host. The specific structure-function relationships observed among both the minor and major clades point to a common ancestor for all PagP homologs.

2.3 Introduction

PagP from *Escherichia coli* EcPagP is an OM enzyme that catalyzes the transfer of a palmitate chain from the *sn*-1 position of a phospholipid to the 2-position of lipid A. Lipid A palmitoylation confers bacterial resistance to host cationic antimicrobial peptides

(CAMPs) and attenuates inflammation signaled through the host TLR4/MD2 receptor (Bishop 2005; Kawasaki et al. 2004). EcPagP also catalyzes the transfer of a palmitate chain from the *sn*-1 position of a phospholipid to the headgroup of phosphatidylglycerol (PG), which is implicated in increasing the hydrophobicity of the OM (Dalebroux et al. 2014). EcPagP is a small 161 amino acid eight-stranded β-barrel protein with an *N*-terminal amphipathic α-helix (Figure 2.1) (Cuesta-Seijo et al. 2010; Ahn et al. 2004; Hwang et al. 2004; Hwang et al. 2002). The β-barrel is tilted by ~25^{o} with respect to the membrane normal and displays its catalytic residues His33, Ser77 and Arg114 in loops on the extracellular surface. At the center of the β-barrel is a palmitoyl group binding pocket known as the hydrocarbon ruler (Figure 2.1) (Ahn et al. 2004; Cuesta-Seijo et al. 2010; Hwang et al. 2002; Hwang et al. 2004).

PagP precisely selects a 16-carbon palmitate chain from the *sn*-1 position of its phospholipid donor by using the hydrocarbon ruler combined with lateral gating through an opening in the β-barrel wall known as the crenel (Figure 2.1) (Cuesta-Seijo et al. 2010). The crenel enforces regioselectivity at the *sn*-1 position of the phospholipid donor and thereby blockades 18-carbon acyl chains esterified to the *sn*-2 position (Khan et al. Unpublished). Crenel mutants devoid of phospholipid regiospecificity are found to incorporate some C18 stearate chains into lipid A. The hydrocarbon ruler excludes 14-carbon acyl chains present at the *sn*-1 position (Khan et al. Unpublished). The floor of the hydrocarbon ruler is lined by Gly88 (Figure 2.1A), and Gly88 mutations can raise this

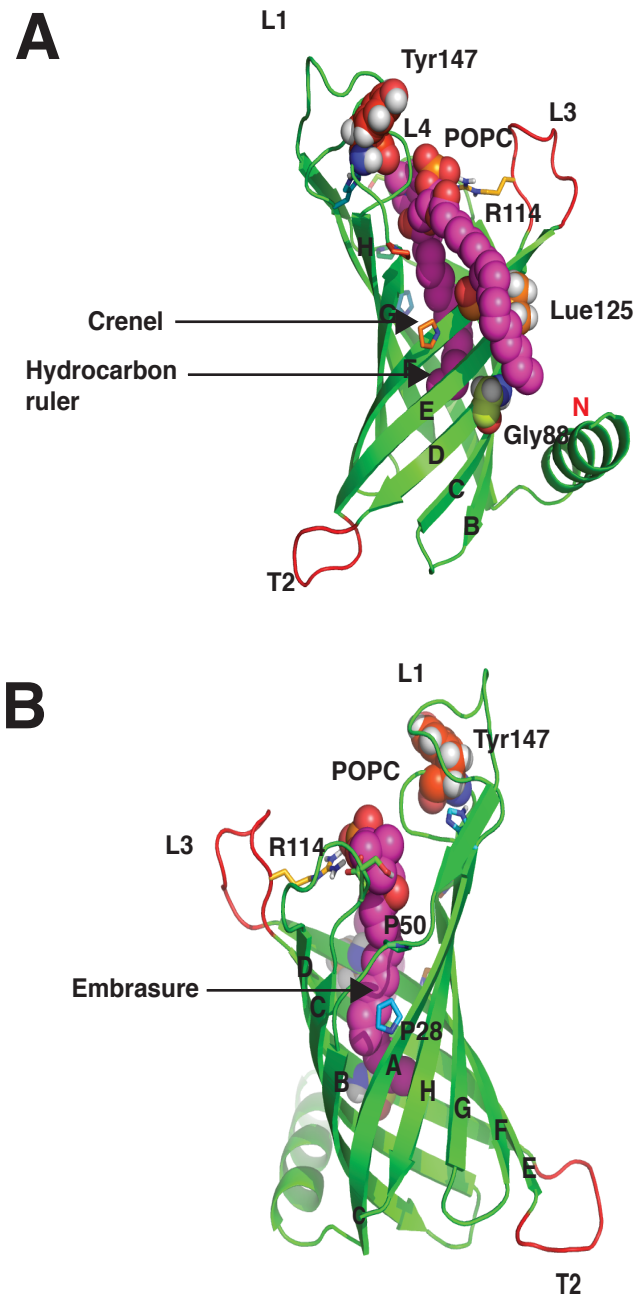

Figure 2.1. The crenel and the embrasure. A. Cartoon of PagP from a molecular dynamics simulation (Bishop Unpublished) showing elements of the gating mechanism of the crenel between Tyr147 and Lue125. The palmitate group from 1-palmitoyl-2-oleoyl-*sn*-phosphatidylcholine (POPC) enters the hydrocarbon ruler, which is lined at the base by Gly88, through the unlatched crenel. B. Cartoon in (A) rotated by 180° to show the embrasure located between Pro28 and Pro50.

floor to enable selection of C14 myristate chains (Khan et al. 2007; Khan et al. 2010a; Khan et al. 2010b). Unsaturated fatty acyl chains have never been observed to be incorporated into lipid A by PagP in bacterial OMs.

Lipid A gains lateral access to the hydrocarbon ruler through another opening in the β-barrel wall known as the embrasure, which is flanked by Pro28 and Pro50 (Figure 2.1B). The function of the embrasure was established by mutating the flanking prolines to cysteines in order to reversibly form a disulfide bridge. The oxidized Pro28Cys/Pro50Cys double mutant loses its rapid lipid A palmitoyltransferase activity while retaining its slow phospholipase activity until lipid A palmitoyltransferase activity is restored upon reduction of the disulfide bond (Khan & Bishop 2009). Kinetic and spectroscopic observations demonstrate that PagP catalysis proceeds through a sequential or ternary complex mechanism (Bishop Unpublished). Diversity in lipid A palmitoylation at the 2- versus 3'-positions is likely attributed to the nature of specific PagP::lipid A interactions occurring at the embrasure, which is located underneath the structurally dynamic and disordered L1 loop (Figure 2.1B).

PagP homologs have been reported in a number of Gram-negative bacteria that colonize eukaryotic hosts (Bishop 2005). Particular PagP homologs can differ in their regiospecificity for the lipid A acceptor substrate by distinguishing between the 2 and/or 3'-positions for incorporating the palmitate chain (Trent et al. 2006; Raetz et al. 2007; Bishop 2005). EcPagP and its close relatives from the γ-Proteobacteria display lipid A 2-

position regiospecificity (Bishop et al. 2000; Bishop 2005). Lipid A 3'-position regiospecificity has been reported in PagP from *Bordetella bronchiseptica* BbPagP and in PagP from *Pseudomonas aeruginosa* PaPagP, which belong to the β- and γ-Proteobacteria, respectively (Preston et al. 2003; Thaipisuttikul et al. 2014). Interestingly, the BbPagP displays primary sequence similarity with EcPagP and belongs to the major clade PagP proteins, whereas the PaPagP lacks obvious primary sequence similarity with EcPagP and belongs instead to the minor clade PagP proteins. Lipid A 3'-regiospecificity is thus shared between the minor clade and certain members of the major clade, whereas lipid A 2-position regiospecificity appears to be a derived characteristic arising within the major clade (Thaipisuttikul et al. 2014).

PagP from *Legionella pneumophila* LpPagP confers resistance to CAMPs and promotes intracellular infection, but the lipid A regiospecificity remains to be established (Robey et al. 2001). *L. pneumophila* is an intracellular bacterium that causes Legionnaires' disease in humans (Winn 1988). Although *L. pneumophila* belongs to the γ-Proteobacteria, it is distinguished from *E. coli* by the unusual lipids in it membranes. The major phospholipid in *L. pneumophila* is phosphatidylcholine (PC), most of which is esterified with *iso*-C16:0, *anteiso*-C15:0, *anteiso*-C17:0, *iso*-C14:0 or *iso*-C16:1 branched acyl chains (Shevchuk et al. 2011; Lambert & Moss 1989). *L. pneumophila* lipid A contains a 2, 3-dideoxyglucose (GlcN3N) backbone and lacks glucosamine that is found in the backbone of *E. coli* and related bacterial lipid A (Zähringer et al. 1995). *L. pneumophila* lipid A is decorated with unusually long branched (27 and 28 carbons) acyl

chains, but the distribution is the same as that of a hexa-acylated lipid A from *E. coli*; consequently, it is expected that PagP would palmitoylate lipid A at the 2-position (Geiger 2010; Zähringer et al. 1995). LpPagP is known to be important for pathogenesis in animal models, but because of the peculiarities of *L. pneumophila* lipids it would be interesting to determine the nature of the acyl chain selected and the lipid A regiospecificity.

Due to our limited understanding of the distribution and phylogenetic relationships among PagP from Gram-negative bacteria we decided to perform a phylogenetic study of the proteins. We selected key PagP homologs for structure-function investigations. The question of how PagP palmitoylates lipid A in a regiospecific manner was also investigated. Knowing the structure-function relationships and lipid A regiospecificities for diverse PagP homologs will expand our knowledge of PagP::lipid interactions for the development of novel lipid A adjuvants and endotoxin antagonists.

2.4 Methods

2.4.1 Sequence alignment and phylogenetic analysis

BlastP searches were performed using the *E. coli* K12 PagP sequence against the NCBI non-redundant database and sequences of 25-30% amino acid similarity from 64 bacteria were retrieved (Altschul 1997). The *P.* aeruginosa PAO1 PagP sequence was used to conduct BlastP searches for the minor clade PagP sequences using the same criteria as for the major clade. For the minor clade, sequences from 35 bacteria were

retrieved (Thaipisuttikul et al. 2014). Multiple sequence alignments of PagP proteins were created using Clustal Omega (Sievers et al. 2011). Separate multiple sequence alignments for generating phylogenetic trees were conducted using Clustal X (which is compatible to MEGA 6.0 software). The sequences were examined for the presence of CSIs, that were flanked on both sides by at least 5-6 residues in the neighboring regions of 30-40 aa residues (Gupta 2014; Gupta 1998; Gupta & Epand 2017). The identification of CSIs was done as previously described (Gupta 2014). A maximum-likelihood phylogenetic tree was generated by MEGA 6.0 (Tamura et al. 2013). Sequence alignment excluded all indels for the generation of maximum-likelihood phylogenetic trees (Figures not shown). The Neighbor-Joining method was applied to a matrix of pairwise distances and trees were bootstrapped 100 times. The numbers shown on the branches identifies clades in which associated taxa clustered together >60% of the time in bootstrap replicates (Pattengale et al. 2009).

2.4.2 Bacterial strains, plasmids and growth conditions

The bacterial strains and plasmids used are described in Table 2.1. Cells were generally grown at 37 ºC on semi-solid or liquid LB media consisting of 10 g Tryptone, 5 g yeast extract, 10 g NaCl and 15 g agar (for semi-solid media). Antibiotics were added as necessary at final concentrations of 100 μg/mL for ampicillin, 15 μg/mL for gentamicin, 25 μg/mL for kanamycin and 30 μg/mL for chloramphenicol. The term “overnight culture” refers to a liquid culture in LB broth inoculated with a single bacterial colony from semi-solid media and allowed to incubate for 16 to 18 hours.

Table 2.1. Bacterial strains and plasmids used

Strains /Plasmids	Description	Source
***E. coli* strains**		
MC1061	F^-, λ^-, *araD139, Δ(ara-leu)7697, Δ (lac)X74, galU, galK, hsdR2* (r_K-m_K+), *mcrB1, rpsL*	(Casadaban & Cohen 1980)
WJ0124	MC1061 *pagP::amp*^{r}	(Jia et al. 2004)
SK1061	MC1061 *msbB::*Tn5 (kan^r), *pagP::amp*^{r}	(Smith et al. 2008)
C41(DE3)	F^- *ompT hsdS*B (rB- mB-) *gal dcm* (DE3)	Lucigen
BKTO9	BW25113Δ*pagP*, Δ*lpxP*, Δ*lpxL*, Δ*lpxM::*Kan	(Tan et al. 2012)
Plasmids		
pET21a(+)	*T7 lac promoter and terminator MCS, C-terminal His-tag Amp*^{R}	Novagen
BbPagP	pET21a(+) with *BbpagP* gene	This study
BbPagPT28A	Derivative of BbPagP	This study
BbPagPR44A	Derivative of BbPagP	This study
BbPagPS30A	Derivative of BbPagP	This study
BbPagPS33A	Derivative of BbPagP	This study
LpPagP	pET21a(+) with *LppagP* gene	This study
Ko1PagP	pET21a(+) with *Ko1pagP* gene	This study
Ko1PagPN117_Y118insN	Derivative of Ko1PagP	This study
Ko2PagP	pET21a(+) with *Ko2pagP* gene	This study
Ko2PagPN118del	Derivative of Ko2PagP	This study
Ko2PagPN118A	Derivative of Ko2PagP	This study
Ko2PagPN118R	Derivative of Ko2PagP	This study
pBADGr	*ori araC-*P_{BAD} *dhfr*::Gm^r mob$^+$	(Asikyan et al. 2008)
pBADcm-18	*ori araC-*P_{BAD} Amp^r	(Guzman et al. 1995)
pBBPagP	pBADcm-18 with *BbpagP* gene	This study
pLPPagP	pBADcm-18 with *LppagP* gene	This study
pKo1PagP	pBADGr with *Klebsiella Ko1pagP* gene	This study
pKo2PagP	pBADGr with *Klebsiella Ko2pagP* gene	This study

2.4.3 DNA manipulations

Plasmid constructs were isolated using a QIAprep Spin Miniprep Kit from Qiagen or Invitrogen. Isolations were done according to manufacturer's instructions for high copy number plasmids (e.g. pET21a+). For low copy plasmids (e.g. pBADcm-18) 5 or 10 mL of the sample was harvested initially and the remainder of the protocol followed according to manufacturer's instruction. Site directed mutagenesis on various protein sequences were done using the QuikChange site directed mutagenesis kit by Agilent according to the manufacturer's specification, and using primers listed in Table 2.2.

Briefly, the reaction included 20 ng DNA template, 125 ng each of the forward and reverse primers, 5 µL 10X reaction buffer, 1µL dNTPs, 3 µL QuikSolution, sterile distilled water was added for a total volume of 50 µL and 1µL *Pfu* DNA polymerase. The PCR conditions for site directed mutagenesis include an initial 1 min denaturation at 95 ^{o}C, 18 cycles of 50 secs at 95 ^{o}C, 50 secs at 60 ^{o}C, 1 min/kb of plasmid length at 68 ^{o}C, with a final extension for 7 mins at 68 ^{o}C and the reaction was then held at 4 ^{o}C. 1 µL of *Dpn*1 restriction enzyme was added to the reaction mixture and then it was incubated at 37 ^{o}C for 1 hr. The mutated DNA was transformed into XL1 Gold competent cells and the cells of interested selected on LB agar supplemented with ampicillin. Mutations were confirmed by DNA sequencing.

Table 2.2 Primers and electrospray mass spectrometry values for BbPagP, Ko1PagP, and Ko2PagP wild type and CSI mutants

PagP protein	Primer (3'-5')	ESI Mw
BbPagP		19002
T28A	F: CACGAGTAGCCGGCCAGGTAGAGGTCG	18973
	R: CGACCTCTACCTGGCCGGCTACTCGTG	
R44A	F: CAGCTCGTTGAAGCTGGCGATCTTGTCGCTGCTG	18918
	R: CAGCAGCGACAAGATCGCCAGCTTCAACGAGCTG	
S31A	F: CGGTTGTGCCACGCGTAGCCGGTCAGG	18987
	R: CCTGACCGGCTACGCGTGGCACAACCG	
S39A	F: CTGCGGATCTTGTCGGCGCTGTACATGGCCCG	18987
	R: CGGGCCATGTACAGCGCCGACAAGATCCGCAG	
Ko1PagP		20367
N117_Y118insN	F: CAACCGGAATCGGGATATAATTATTCCAATTATCACGTGCG	20481
	R: CGCACGTGATAATTGGAATAATTATATCCCGATTCCGGTTG	
Ko2PagP		21403
N118del	F: ATCGGCAGCGGAACATATGCAAAATCATCACGTG	21291
	R: CACGTGATGATTTTGCATATGTTCCGCTGCCGAT	
N118A	F: AATCGGCAGCGGAACATAAGCTGCAAAATCATCACGTGCG	21362
	R: CGCACGTGATGATTTTGCAGCTTATGTTCCGCTGCCGATT	
N118R	F: TAATCGGCAGCGGAACATACCTTGCAAAATCATCACGTGCG	21447
	R: CGCACGTGATGATTTTGCAAGGTATGTTCCGCTGCCGATTA	

2.4.4 Chemical transformation

To prepare chemically competent cells for protein analysis in the outer membrane, the calcium chloride method was used. 50 mls of LB was inoculated with a 1% overnight culture of the appropriate bacteria and allowed to grow at 37 ^{o}C at 200 rpm to OD 0.4-0.6. The cells were placed on ice for 10 mins. All remaining steps were carried out at 4 ^{o}C. The cells were harvested at 6000 rpm for 3 mins. The supernatant was discarded, and the pellet resuspended in 10 ml cold 0.1M $CaCl_2$, very gently. The resuspended cells were incubated on ice for 20 mins then centrifuged as above. The supernatant was discarded and gently resuspended in 5 ml solution of cold 0.1M $CaCl_2$ and 15% glycerol. This was then dispensed into microtubes and placed at 80 ^{o}C.

To transform these cells, 1 µl of the plasmid DNA was added to 100 µl of thawed competent cells in a microtube. The microtube was then placed on ice for 30 mins. The cells were then heat shocked at 42 ^{o}C for 45 secs and then chilled on ice for 2 mins. 500 µl of SOC media was added to the cells and they were outgrown at 37 ^{o}C for 1 hr. The cells were centrifuged at 8000 rpm for a min, 400 µl of the supernatant was discarded. The remaining 100 µl of supernatant was used to resuspend the cells for plating on LB with appropriate antibiotic.

2.4.5 Protein expression and purification

The DNA sequences for all proteins without the signal peptide used in this study

were synthesized and purchased from Invitrogen GeneArt™. The PagP sequences from *Bordetella bronchiseptica* strain RB50, *Legionella pneumophila* pneumophilia strain FFI329 and *Klebsiella oxytoca* ATCC 8724 were cloned into the pET21a+ plasmid using restriction enzymes *Nde*I, which adds a Met residue to the mature *N*-terminal end of the protein and *Xho*I. Two residues Leu and Glu at the carboxylic end of the protein precedes the X6 His-tag that were also added by the plasmid. The protein expression procedure depends on isopropyl β-D-thiogalactoside (IPTG) induction in *E. coli* C41(DE3) (Table 2.1) (Khan et al. 2007).

1L cultures of *E. coli* C41(DE3) overexpression cells with the pET21a-*pagP* construct were grown at 37 °C and 200 rpm, after a 1% overnight inoculum, until the culture reached an OD_{600} of 0.5 (~2.5 hrs). The cells were then inoculated with IPTG for a final concentration of 1 mM, and grown for 4 hrs. The cells are harvested by centrifugation, the supernatant was discarded, and the pellet stored at -80 °C or protein isolation continued. The harvested cells were resuspended in isolation buffer (50 mM Tris-HCl at pH 8.0, 5mM EDTA) and lysed mechanically with a French Press 40K cell at 800 psi. The lysate was pelleted at 27000 rpm using an optima ultracentrifuge MLA-80 rotor at 4 °C for 20 mins. The pellet was resuspended in 50 mM Tris-HCl pH 8.0, 2% Triton X-100 and centrifuged as above. The pellet was again resuspended in 50 mM Tris-HCl at pH 8.0 and centrifuged using a Sorval RC-58 at 8000 rpm in a Sorval SS-34 rotor for 20 mins. This pellet was resuspended in 50 mM Tris-HCl at pH 8.0, 6 M guanidine-

HCl, centrifuge as previous and the resulting supernatant is crude denatured protein. All supernatants were collected for further analysis.

Crude protein was purified using Ni^{2+} charged ion-exchange chromatography. The His-bind column was charged with 5 column volumes of 50 mM $NiSO_4$ and equilibrated with 3 column volumes of 100 mM Tris-HCl (pH 8.0), 250 mM NaCl, 6 M guanidine and 5 mM imidazole. The crude protein was added to the column slowly and washed with 10 column volumes of the previous buffer and then with 20 column volumes with the same buffer adjusted with 20 mM imidazole. The protein was then eluted step-wise with 5 mL of the same buffers, but with increasing concentration of imidazole 35, 50, 75, 100 and 125 mM. The 100 and 125 mM fractions were pooled and dialyzed against water. The precipitated protein is collected by centrifugation using the Sorval SS-34 rotor at 8000 rpm for 20 mins.

2.4.6 Protein Electrospray Mass Spectrometry

Approximately 1ng/μL of the wet pellet from the water dialyzed protein was sent to the McMaster Regional Centre for Mass Spectrometry (MRCMS). Protein samples were diluted 50-fold into a solution of 1:1 (v/v) 1% formic acid and acetonitrile just prior to injection into an Agilent G1696 TOF mass spectrometer using methanol as the mobile phase. Data was obtained using the Agilent MassHunter Workstation and analyzed using the Agilent MassHunter Workstation Software Qualitative Analysis. The multiple

charged ion region was selected and the mass to charge ratio of the protein was deconvoluted using max entropy in BioConfirm Software.

2.4.7 Protein refolding and analysis on SDS PAGE

Precipitated protein samples after dialysis against water were dissolved in 10 mM Tris-HCl (pH 8.0) and 6 M Gdn-HCl. These samples were diluted dropwise into a 10-fold excess of 100 mM Tris-HCl (pH 8.0) and 0.5% LDAO at room temperature with vigorous stirring and left to stir overnight at 4 ^{o}C. The samples were then loaded on a 4 mL bed of His-bind resin charged with 50 mM $NiSO_4$ and equilibrated with 10 mM Tris-HCl (pH 8.0), 0.1% LDAO, and 5 mM imidazole. The protein samples were washed with 10 column volumes with the equilibrium buffer and then with 10 column volumes with 10 mM Tris-HCl (pH 8.0), 0.1% LDAO, and 20 mM imidazole. The refolded proteins were eluted with 10 mM Tris-HCl (pH 8.0), 0.1% LDAO, and 250 mM imidazole. The protein is then dialyzed against 100 mM Tris-HCl (pH 8.0), 0.1% LDAO overnight.

Refolded protein (KoPagP) concentrations were determined using the bicinchoninic acid assay (BCA) (Smith et al. 1985). 40 μg of protein extracts were solubilized in an equal volume of 2X SDS buffer (100 mM Tris-HCl pH 6.8, 4% (w/v) SDS, 0.2% (w/v) bromophenol blue, 200 mM DTT) with or without boiling for 10 min where indicated. For BbPagP and LpPagP, lysate, supernatants, crude and refolded protein were analyzed. SDS-PAGE on 1.5 mm thick 13 or 15% acrylamide gels were performed with Bio-Rad Protean II XI apparatus and operated at 150 V. Gels were

stained with Coomassie Blue dye and destained (methanol, acetic acid and water 40/10/50 v/v) overnight.

2.4.8 Far-UV circular dichroism spectroscopy

The samples were analysed by CD according to Khan et al (2007). Briefly, samples were maintained at 0.3 mg/mL in 0.1% LDAO and 100 mM Tris-HCl (pH 8.0) in a 1 mm path length cuvette specific for CD analysis. The samples were analyzed with an Aviv 250 CD spectrometer which was linked to a Peltier device Merlin Series M25 for temperature control. The temperature was maintained at 25 ^{o}C for wavelength scans and data sets were obtained between 200 to 260 nm for most samples. The samples were maintained at the same concentration for thermal unfolding profiles. The samples were heated from 25 to 100 ^{o}C at a rate of 2 ^{o}C/min, with a response time of 16 secs.

2.4.9 Phospholipase assay

Phospholipase activity assays are performed without an acceptor substrate. Phospholipase activity reactions were set up with a final concentration of 20 μM of ^{14}C-labeled *sn-1,2*-dipalmitoyl phosphatidylcholine (^{14}C-DPPC) at 4000 cpm/ul to monitor the phospholipase reaction on a thin layer chromatography (TLC) plate. To the radio-labeled lipid final concentrations of 1 mM cold DPPC and 10 ng/μL of the enzyme were added in a 25 μL reaction that was buffered by100 mM Tris HCl (pH 8.0), 0.25% *n*-dodecyl-β-D-maltoside (DDM) and 10 mM EDTA. Specifically, phospholipids dissolved in chloroform were first dried down (one and then the other) under a stream of nitrogen

prior to the addition of 22.5 µL of reaction buffer, and the reaction was initiated with the addition of 2.5 µL of a 10 ng/µL aliquot of the enzyme. The enzyme was serially diluted from the inhibitory lauroyldimethylamine-*N*-oxide (LDAO) detergent, into a DDM dilution buffer that supports activity (100 mM Tris HCl pH 8 and 0.25% DDM). A no enzyme negative control (DDM dilution buffer), and a phospholipase A_2 (PLA_2) positive control were also used in these reactions. PLA_2 uses its own aqueous reaction buffer (100 mM Tris HCl pH 8.0, 0.25% DDM and 10 mM $CaCl_2$). Reactions were carried out at 30 ^oC overnight (16-18 hrs) and were terminated by adding 2.5 µL (10000 cpm ^{14}C-DPPC) of the reaction directly to the origin of G25 silica TLC plates. The plates were resolved in sealed glass tanks that were previously equilibrated for ~ 3 hrs with solvent system chloroform/methanol/water (65:25:4 v/v), dried and exposed to a Molecular Dynamics Phosphorimager screen overnight. The products were visualized using a Molecular Dynamic Typhoon 9200 Phosphorimager.

2.4.10 Lipid A palmitoyltransferase assay

Palmitoyltransferase assays were done either with ^{14}C-DPPC or with ^{32}P orthophosphate lipid IV_A to monitor the reactions. For ^{14}C-DPPC reactions, final concentrations of 20 µM of the ^{14}C-DPPC, 1 mM of cold DPPC, 100 µM of synthetic lipid IV_A (resuspended in the reaction buffer 100 mM Tris HCl pH 8.0, 0.25% DDM and 10 mM EDTA) with 10 ng/µL of the enzyme were used in a 25 µL reaction volume. For ^{32}P orthophosphate lipid IV_A assays reactions were set up with final concentrations of 1 mM of cold DPPC, 100 µM ^{32}P orthophosphate lipid IV_A (extracted from *E. coli* cells see

below) along with 10 ng/μL of the enzyme. The phospholipids dissolved in chloroform were dried separately under a stream of N_2 prior to the addition of 22.5 μL of lipid IV_A dissolved in the aqueous reaction buffer. The lipids were resuspended by alternately sonicating and vortexing. A no enzyme control and a PLA_2 positive control (PLA_2 control only for ^{14}C-DPPC reactions) were also used for these reactions. The reactions are initiated with the addition of 2.5 μL of a 10 ng/μL of the enzyme. The reactions progressed for various time periods from 10 mins to 16 hrs and were terminated by adding 2.5 μL (~10000 cpm for ^{14}C-DPPC or ~1000 cpm for ^{32}P orthophosphate lipid IV_A) of the reaction directly to the origin of a G25 (^{14}C-DPPC reactions) or Silica 60 (^{32}P orthophosphate lipid IV_A) TLC plate. For ^{14}C-DPPC reactions the plates were resolved in sealed glass tanks that were equilibrated with the solvent system chloroform/methanol/water 65/25/4 (v/v). For ^{32}P orthophosphate lipid IV_A reactions the plates were resolved in sealed glass tanks that were previously equilibrated for ~ 3 hrs with solvent system chloroform/pyridine/88% formic acid/water 50/50/16/5 (v/v). The plates were dried and exposed to a Molecular Dynamics Phosphorimager screen overnight. The products were visualized using a Molecular Dynamics Typhoon 9200 Phosphorimager and quantified by ImageQuant software.

2.4.10.1 Headgroup specificity assay

For headgroup specificity assays different phospholipids, *1*-palmitoyl-*2*-oleoyl-*sn*-glycero-*3*-phosphatidylcholine (POPC), *1*-palmitoyl-*2*-oleoyl-*sn*-glycero-*3*-phosphatidylethanolomine (POPE), and *1*-palmitoyl-*2*-oleoyl-*sn*-glycero-*3*-

phosphatidylglycerol (POPG) were used as donors along with ^{32}P orthophosphate lipid IV_A (see below) as the acceptor substrate. Reactions were set up with final concentrations of 1 mM of POPC, POPE or POPG, 50 μM of ^{32}P orthophosphate lipid IV_A and 10 ng/ul of the enzyme in a 25 μl volume reaction. The remainder of the procedure follows the acyltransferase assays as above.

2.4.10.2 Acyl chain specificity assay

These reactions were conducted as acyltransferase assays with a suite of phospholipid donors and a ^{32}P orthophosphate lipid IV_A acceptor for monitoring on a TLC plate. Reactions were set up with final concentrations of 1 mM of cold C14-C16 symmetrical *iso*-methyl branched and straight-chained phosphatidylcholines (PCs), 100 μM ^{32}P orthophosphate labeled lipid IV_A (extracted from *E. coli* cells see below) along with 10 ng/μL of the enzyme. The phospholipids in chloroform were dried separately under a stream of N_2 prior to the addition of 22.5 μL of ^{32}P orthophosphate lipid IV_A dissolved in the aqueous reaction buffer. The lipids are resuspended by alternately sonicating and vortexing. The remainder of the procedure is as described for acyltransferase assays above.

2.4.11 Mass spectrometry of palmitoylated lipids

To confirm the location of palmitoylation in lipid IV_A, the products were generated from acyltransferase reactions with nonradiolabeled substrates. The palmitoyltransferase reaction was carried out with 1 mM DPPC and 100 μM of lipid IV_A

with 10 ng/μL of the enzyme in a reaction volume of 25 μL. The lipids were dried down under a stream of N_2 and dissolved into 22.5 μL of the reaction buffer (100 mM Tris-HCl pH 8.0, 10 mM EDTA, 0.25% DDM). The reaction was initiated with the addition of 2.5 μL of 10 ng/μL of the enzyme, conducted at 30 °C overnight. The reaction was terminated by adding 55 μL of chloroform: methanol (1:1 v/v) to form a two-phase Bligh/Dyer mixture, the lower organic phase was extracted and dried down under a stream of N_2. The non-radioactive dried lipid films were dissolved in chloroform: methanol (2:1 v/v) and analyzed by normal phase liquid chromatography electrospray ionization quadrupole time-of-flight tandem mass spectrometry (LC-ESI-QTOF MS/MS) as described previously (Garrett et al. 2011).

2.4.12 ^{32}P orthophosphate lipid IV_A extraction

^{32}P orthophosphate lipid IV_A extractions were performed using a mild acid hydrolysis reaction that disrupts the labile ketosidic bond and cleaves the Kdo sugar residues from lipid A without affecting the distribution of acyl chains (Smith et al. 2008; Zhou et al. 1999). *E. coli* BKTO9 strain (Table 2.1) was used for these extractions. A 1% inoculum of overnight culture was subcultured into 20 mL of fresh LB media with 12.5 μg/μL kanamycin and 5 μC_i/mL of ^{32}P orthophosphate for labeling. The cells were grown for 2 hrs 55 mins after which 25 mM of EDTA was added and the cells allowed to grow for an additional 5 mins prior to harvesting in a clinical centrifuge at high speed for 10 mins. The cells were then washed with 10 mL 1 X PBS before being resuspended in 0.8 mL PBS followed by addition of 1 mL chloroform and 2 mL methanol, then left at room

temperature for 1 hr. The cells were pelleted and washed with 5 mL of single phase Bligh/Dyer (chloroform/methanol/PBS - 1:2:0.8) and pelleted at high speed in a clinical centrifuge for 5 mins. The pellet was then dispersed in 1.8 mL of 12.5 mM sodium acetate pH 4.5 and 1% SDS by sonic irradiation. This suspension was incubated at 100 ^{o}C for 30 mins (or until suspension goes clear) and then cooled. The mixture was then converted to a two-phase Bligh/Dyer by adding 2 mL chloroform and 2 mL methanol, vortexed and centrifuged at high speed for 10 mins. The lower phase was collected and washed with 4 mL of upper phase from a fresh two-phase Bligh/Dyer mixture (chloroform/methanol/PBS – 2:2:1.8) centrifuged for 8 mins, collected lower phase and dried under a stream of N_2. The dried lipid was resuspended in 100 μL of chloroform/methanol (4:1 v/v) by sonication while being periodically cooled on ice. The resuspended lipid was applied to a TLC plate and resolved in a sealed tank that was previously equilibrated for ~3 hrs with solvent system chloroform/ pyridine/ 88% formic acid/ water (50:50:16:5 v/v).

The resolved plate was air-dried or blow dried on cool setting. The TLC plate was exposed to a Phosphorimager screen for at least 1 hr. The relevant spot for lipid IV_A was located and scratched from the plate. The lipid was extracted from the scrapings with 5 mL single phase Bligh/Dyer after incubation for 1 hour. The mixture was centrifuged at high speed for 5 mins and passed through a glass Pasteur pipette fitted with about a 2 cm plug of glass wool. The filtered liquid was converted to two-phases by adding 1.3 mL chloroform and 1.3 mL 1x PBS vortexed and centrifuged for 5 mins. The lower phase

was collected and dried under a stream of N_2. The dried pure lipid IV_A was resuspended in 100 µL of chloroform/methanol (4:1 v/v). 2 µL was used for scintillation counting and the remaining lipid dried again. The lipid was then resuspended in a sufficient volume of reaction buffer (100 mM Tris HCl pH 8.0, 0.25% DDM and 10 mM EDTA) to give each reaction spot a count of 1000 cpm on the TLC plate (i.e. spotting 5µL x 200 cpm/µL in the assay). The pure ^{32}P orthophosphate labeled lipid IV_A is then fed into enzymatic assays as described above.

2.4.13 Protein expression in bacterial OM

The DNA sequences for all proteins with an *N*-terminal signal peptide used in this study were synthesized and purchased from Invitrogen GeneArt™. The *pagP* sequences with their *N*-terminal signal peptides were cloned into *Eco*RI and *Hin*dIII restriction sites of pBADcm-18 and pBADGr with an arabinose-inducible promoter. The plasmid-*pagP* constructs were then transformed chemically into *E. coli* strains WJ0124 and SK1061 (Table 2.1). Lipid A was isolated from these strains and their parental strains as controls to analyze protein expression in bacterial OMs. Lipid A species were isolated by the mild acid hydrolysis method. A 1% inoculum of overnight culture was subcultured into 5 mL fresh LB media with 30 mg/mL chloramphenicol for cultures with pBADcm-18, 15 mg/mL gentamicin and 5 μC_i/mL of ^{32}P orthophosphate for labeling. The cells were grown for 2 hrs 55 mins after which 25 mM of EDTA was added and the cells allowed to grow for an additional 5 mins prior to harvesting in a clinical centrifuge at high speed for 10 mins. The mild acid hydrolysis method was followed as mentioned above for ^{32}P

orthophosphate lipid IV_A extraction. After the suspension was incubated at 100 ^oC for 30 mins and then cooled. The mixture was then converted to two-phase Bligh/Dyer by adding 2 mL chloroform and 2 mL methanol vortexed and centrifuged at high speed for 10 mins. The lower phase was collected and washed with 4 mL of fresh upper phase from a two-phase Bligh/Dyer (chloroform/methanol/PBS – 2:2:1.8) mixture and centrifuged for 8 mins before collecting the lower phase to be dried under a stream of nitrogen. 2 μL was added to 2 mL of scintillation fluid for counting. 1000 cpm of the lipid A samples were spotted on the silica 60 TLC plate. The plate was resolved in a sealed tank that was previously equilibrated for ~ 3 hrs with solvent system chloroform/ pyridine/ 88% formic acid/ water (50:50:16:5 v/v). Plates were visualized, and spots quantified as above.

2.4.14 Identification of potential lipid A binding residues

PagP sequences from *E. coli*-K12, *B. bronchiseptica*, *L. pneumophila* and *K. oxytoca* were aligned using Clustal O (Sievers et al. 2011). Variant positive or polar uncharged residues were identified within the area of the embrasure. The sequence of BbPagP was uploaded to the I-TASSER database which predicts secondary structure and models three dimensional structures of the protein (Roy et al. 2010). Visualization of the BbPagP model and verification of possible surface exposed embrasure lipid A binding residues were conducted in PyMOL (PyMOL, Schrodinger, LLC).

2.5 Results

2.5.1 Minor clade PagP phylogenetic analysis and structure-function

relationships

2.5.1.1 Minor clade PagP distribution in Gram-negative bacteria

PaPagP lacks obvious amino acid sequence similarity with EcPagP (Thaipisuttikul et al. 2014), which divides the PagP protein family into two distinct clades: the minor and the major clade, respectively. Thirty five sequences with >25% amino acid similarity to PaPagP were retrieved from BlastP searches. We aligned the sequences using Clustal Omega (Figure 2.2) (Sievers et al. 2011). A phylogenetic tree was generated with these 35 sequences to reveal PagP homologs distributed among bacteria from the β-Proteobacteria, γ-Proteobacteria, δ-Proteobacteria, and Firmicutes (Figure 2.3). However, the random distribution of the protein among bacteria and low bootstrap scores (<60) deemed any inference of evolutionary relationships unreliable (Gupta & Epand 2017). Therefore, another approach was necessary to gain a better understanding.

A conserved signature indel (CSI) molecular marker-based study was conducted (Gupta 1998). To be useful for evolutionary studies, a CSI within a protein family is required to have a fixed length, and be flanked by conserved sequences on both sides for reliability. CSIs found in the same protein from various species provides an indication of a common ancestry (Gupta 1998; Gupta 2014; Naushad et al. 2014). A four-amino acid CSI was identified in the T2 turn region of the protein, suggesting that these minor clade PagP homologs originated from a common ancestor (Figure 2.2 and 2.3).

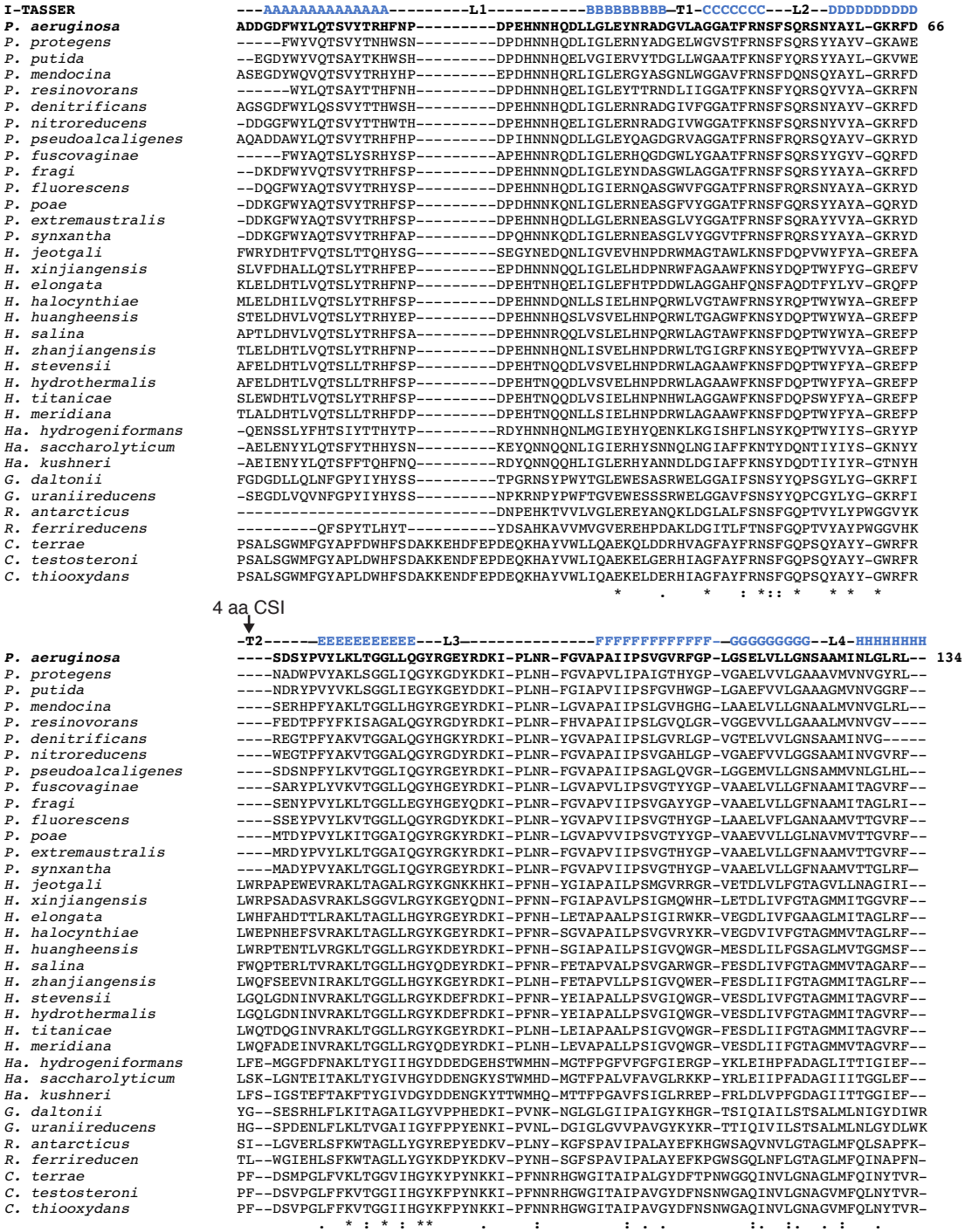

Figure 2.2. Minor clade PagP multiple sequence alignment. Multiple sequence alignment of 35 minor clade PagP sequences. The predicted secondary structural elements (I-TASSER) are placed above the *P. aeruginosa* PagP sequence (Thaipisuttikul et al., 2014). The β-barrel strands are highlighted in blue letters. Surface exposed loops (L) and periplasmic exposed turns (T) are represented by dashed lines. The location of a four amino acid conserved indel (CSI) is displayed in the sequences. *P-Pseudomonas, H-Halomonas, Ha-Halanaerobium, G-Geobacter, R-Rhodoferax , C-Comamonas.*

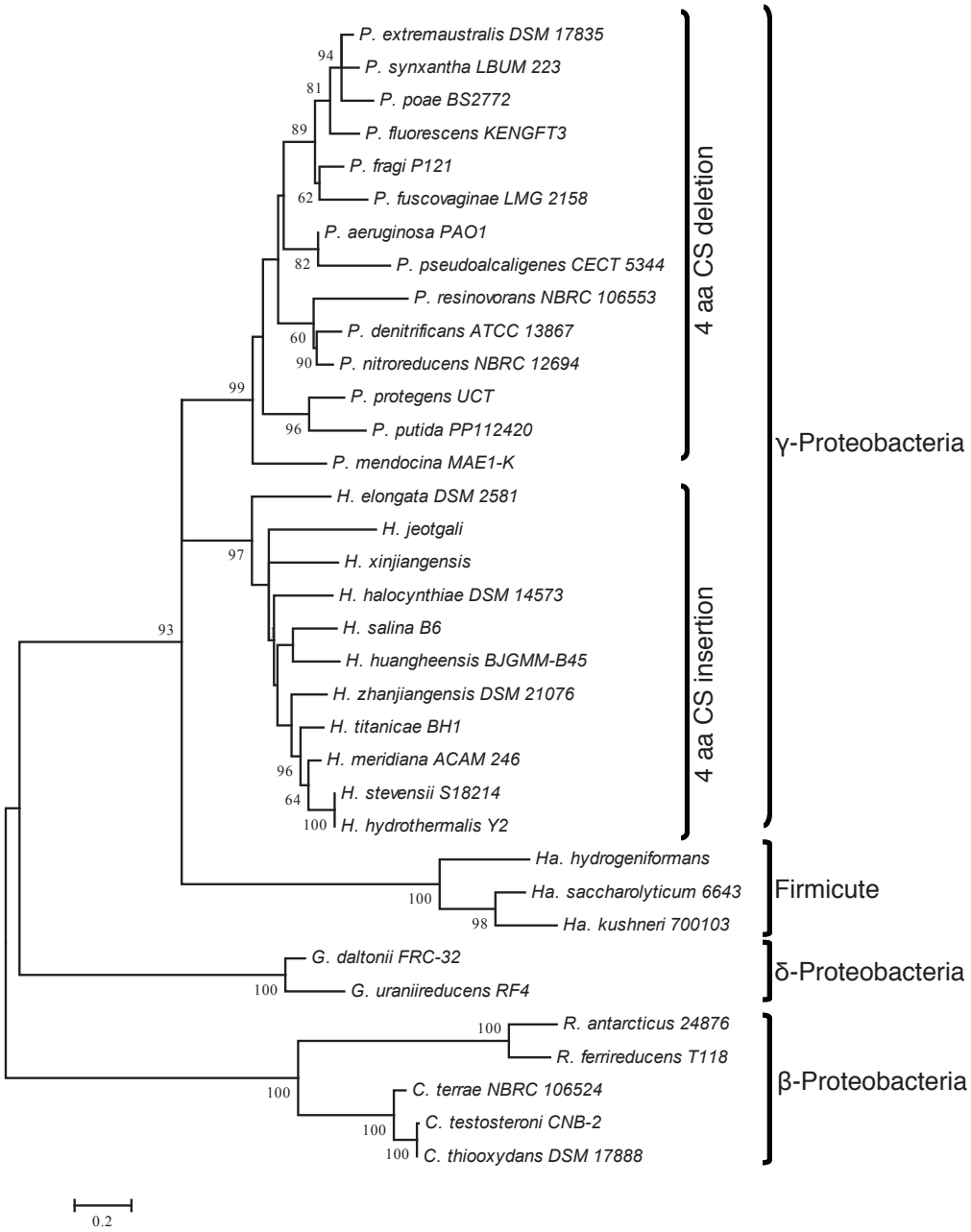

Figure 2.3. Minor clade PagP phylogenetic tree. Maximum - likelihood tree showing the distribution of PagP from the minor clade. PagP from the minor clade are distributed among the β-Proteobacteria, γ-Proteobacteria and δ-Proteobacteria, as well as *Halanaerobium* of the Firmicutes. The tree was generated by MEGA 6.0 (Tamura et al., 2013), amino acids were aligned with Clustal X. The nodes and branches supported by >60% bootstrap scores are marked. All species containing four amino acid (4 aa) conserved signature (CS) insertions and deletions are marked. *P-Pseudomonas, H-Halomonas, Ha-Halanaerobium, G-Geobacter, R-Rhodoferax , C-Comamonas*

2.5.1.2 Minor clade structure-function relationships

At the primary structure level PaPagP and EcPagP appear to be unrelated, but the β-barrel tertiary structure with an interior hydrocarbon ruler appears to be conserved (Thaipisuttikul et al. 2014). In the absence of a solved structure for a minor clade PagP homolog, we exploited secondary structure predictions of PaPagP and of PagP from *Halomonas elongata* HePagP (Figures 2.2) by aligning their structures with each other and with the structure of EcPagP (PDB 3GP6), which reveals their structural similarities and differences (Figure 2.4). The catalytic surface residues H17 and S51 of PaPagP align with corresponding residues in HePagP and with the catalytic EcPagP residues H33 and S77 (Hwang et al. 2002; Ahn et al. 2004; Cuesta-Seijo et al. 2010; Dixon Unpublished). EcPagP additionally requires major clade invariant R114 to stabilize the polar headgroup of the phospholipid donor as it docks inside the hydrocarbon ruler, but the minor clade PagP homologs do not have any invariant arginine residues (Figure 2.1, 2.2 and 2.3). Instead, the minor clade homologs have an invariant tyrosine corresponding to Y84 in PaPagP, which lies at a nearly identical position as R114, except Y84 is displaced by one residue and becomes exposed on the β-barrel exterior. Therefore, the function of Y84 in PaPagP cannot be analogous to that of R114, suggesting a potential role in gating the phospholipid donor through a crenel aperture instead of stabilizing the phospholipid inside the hydrocarbon ruler. Additionally, both PaPagP and HePagP exhibit lipid A 3'-position regiospecificity and they lack any ability to palmitoylate PG (Thaipisuttikul et al. 2014; Dixon Unpublished). The four amino acid CSI in the T2 turn is required for function in HePagP, and a stabilizing *N*-terminal extension in HePagP corresponds to the

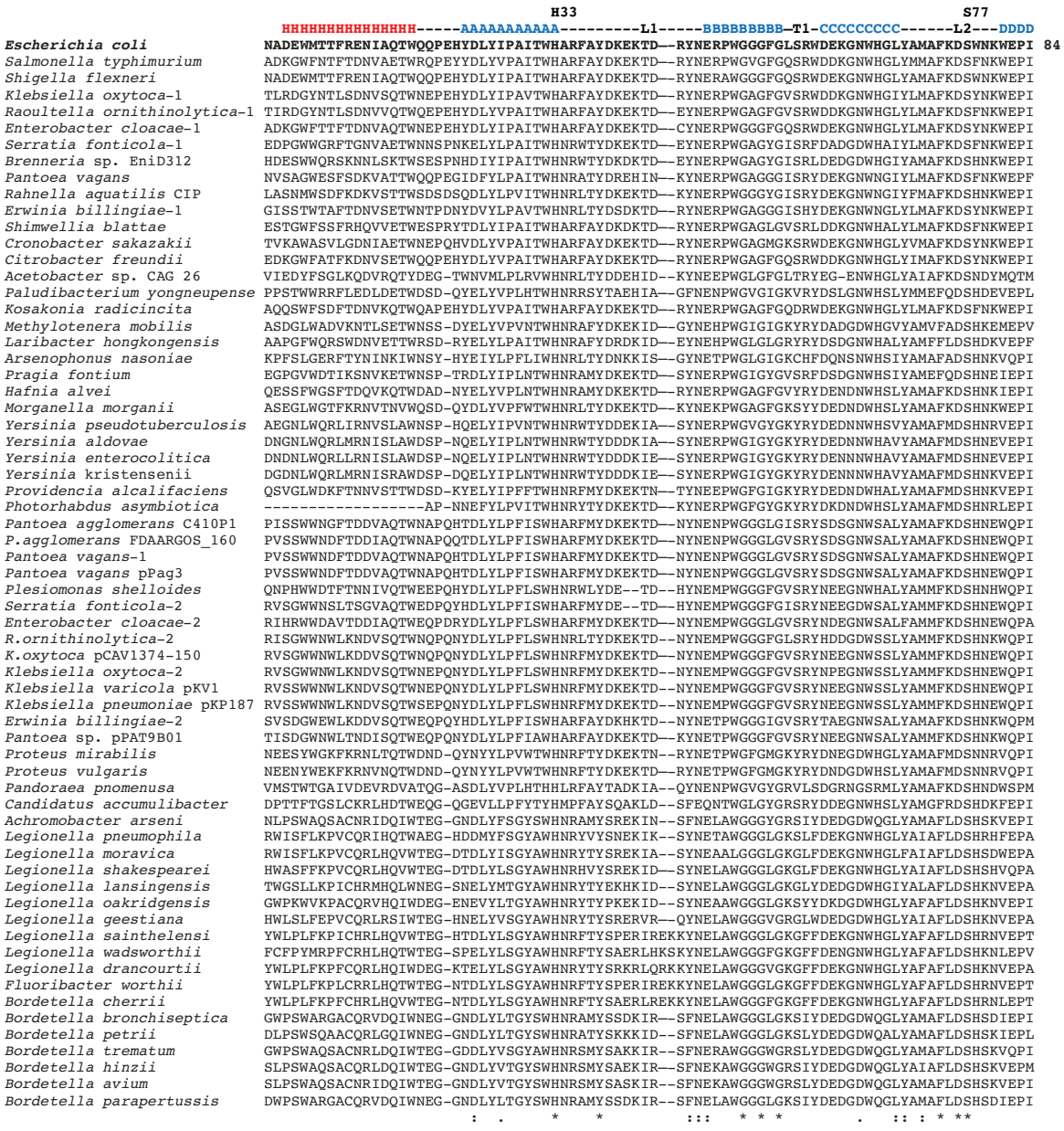

Figure 2.5. PagP major clade multiple sequence alignment. Multple sequence alignment of 64 PagP sequences from various bacteria from the β- and γ-Proteobacteria. The secondary structural elements are placed above the PagP sequence for *Escherichia coli*. The amphipathic α-helix is highlighted in red block letters and β-barrel strands are highlighted in blue block letters. Cell surface loops (L) and periplasmic turns (T) are represented by dash lines. The conserved catalytic residues H33, S77 and R114 are shown. The location of a one amino acid conserved signature indel (CSI) is also displayed in the sequences.
Figure 2.5 continues unto following page...

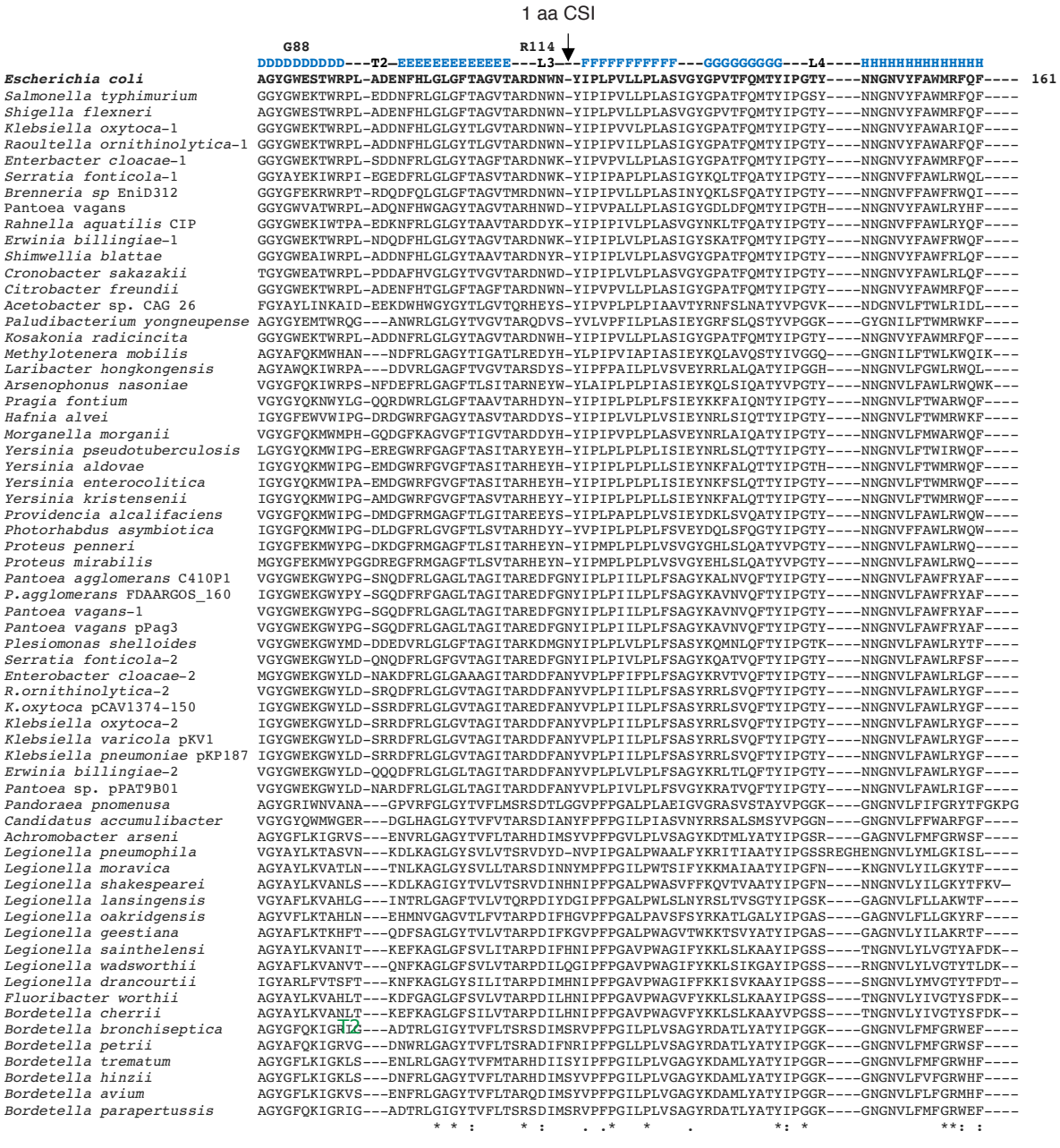

Figure 2.5 continued...

PagP major clade multiple sequence alignment. Multple sequence alignment of 64 PagP sequences from various bacteria from the β- and γ-Proteobacteria. The secondary structural elements are placed above the PagP sequence for *Escherichia coli*. The amphipathic α-helix is highlighted in red block letters and β-barrel strands are highlighted in blue block letters. Cell surface loops (L) and periplasmic turns (T) are represented by dash lines. The conserved catalytic residues H33, S77 and R114 are shown. The location of a one amino acid conserved signature indel (CSI) is also displayed in the sequences.

stabilizing amphipathic α-helix of EcPagP that is missing from PaPagP (Figure 2.4) (Dixon Unpublished).

2.5.2 Major clade PagP phylogenetic analysis

2.5.2.1 Major clade PagP distribution in Gram-negative bacteria

Sequences with over 30% amino acid similarity to EcPagP were retrieved from BlastP searches. Sixty four sequences from various bacteria were aligned to the EcPagP structure (PDB 3GP6) (Figure 2.5) (Cuesta-Seijo et al. 2010). These major clade PagP sequences were aligned and subjected to a phylogenetic analysis. A maximum-likelihood tree based on 100 bootstrapped sequences was constructed (Figure 2.6). Clear distinction between PagP homologs from the β- and the γ-Proteobacteria class was observed. The node connecting the β- and the γ-Proteobacteria major clade PagP homologs (and many other nodes within the γ-Proteobacteria section of the tree) had low bootstrap scores suggesting that the evolutionary relationship was not reliably determined as observed for the minor clade (Figure 2.6; 2.3). The CSI molecular marker approach was also applied to the major clade PagP homologs. Two CSIs were identified in the PagP sequences from the major clade; CSIs of one amino acid and two amino acids were located in the L3 loop and T2 turn, respectively (Figure 2.4 and 2.6). The one amino acid CSI seems to be relevant because of its location in the L3 loop where the catalytic residue R114 is situated. Structure-function studies of this L3 loop CSI will be discussed in section 2.5.5. No specific biochemical relevance has been associated to the T2 turn on the

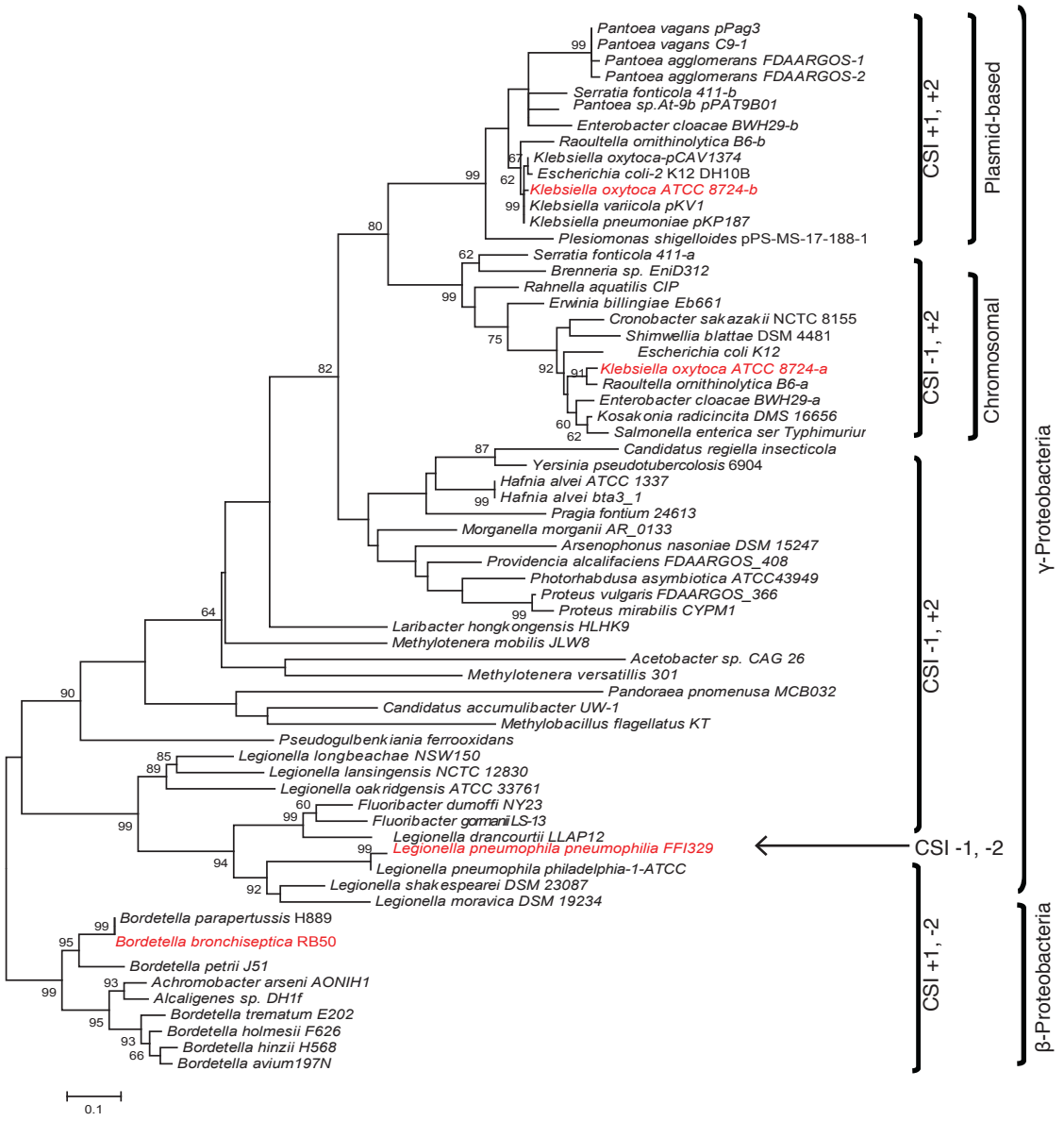

Figure 2.6. PagP major clade phylogenetic tree. Maximum-likelihood tree showing PagP homologs from the major clade that are distributed mainly in the β- and γ-Proteobacteria. Homologs highlighted in red were biochemically investigated. Within the γ-Proteobacteria, a group of bacteria has two genes encoding for PagP; these have a (a) or (b) at the end of the bacterial species name. The tree was generated by MEGA 6.0 (Tamura et al., 2013). The Neighbor-Joining method was applied to a matrix of pairwise distances and trees were bootstrapped 100 times. The nodes and branches supported by >60% bootstrap scores are marked. Conserved signature indels (CSI) of one (+/-1) amino acid and two (+/-2) amino acid are displayed e.g. CSI +1, -2 means a 1 aa insertion in the L3 loop and a 2aa deletion in the T2 turn for proteins in the labeled clade.

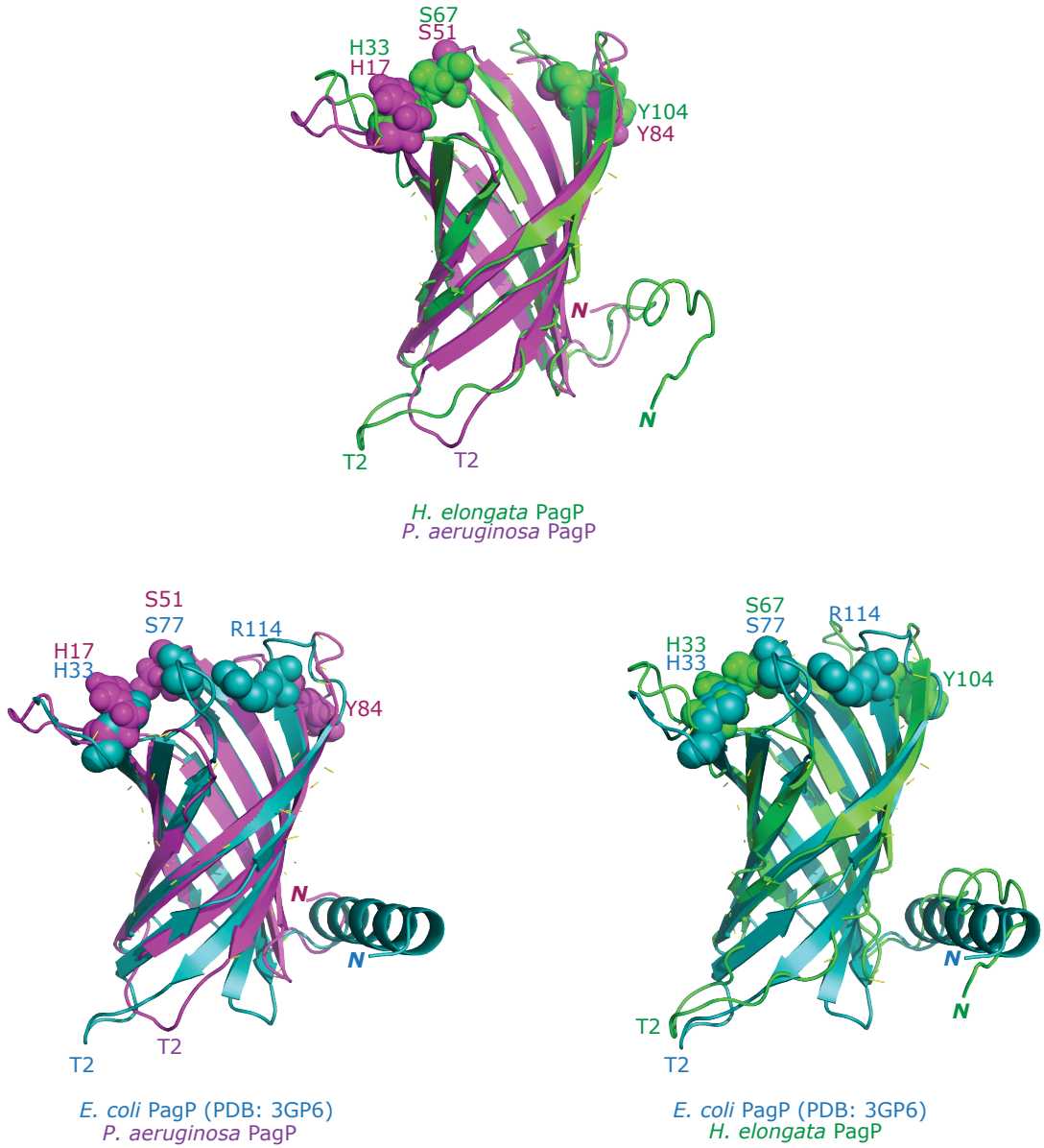

Figure 2.4. Structural alignment of PagP proteins from minor and major clade. Predicted structures from I-TASSER (Roy et al. 2011) for *P. aeruginosa* (magenta) and *H. elongata* PagP (green) were aligned to the SDS/MPD (1.4 Å) solved crystal structure of the *E. coli* PagP (cyan) using PyMOL (Schrodinger, NY). Residues critical for catalysis are shown as spheres. The *N*-terminus (*N*) and second periplasmic turn (T2) for each enzyme are labeled (Dixon Unpublished).

periplasmic surface of major clade PagP. Therefore, the two-amino acid CSI in T2 turn was not investigated further.

Examining the distribution of the major clade homologs, the protein appears to have been introduced in the β-Proteobacteria represented by the *Bordetella spp.*, was then passed on to the γ-Proteobacteria through the *Legionella spp*., and then disseminated among members of the *Enterobacterales* order within the γ-Proteobacteria (Figure 2.6). The issue with this vertical inheritance of the protein is that PagP is not found in all β or γ-Proteobacteria. It would be difficult to account for the loss of this protein from the other members of these groups (Gupta 1998). Alternatively, PagP could have been distributed through horizontal gene transfer (HGT; the lateral transfer of genes between different species), as observed for many proteins in bacterial genomes (Nakamura et al. 2004; Wiedenbeck & Cohan 2011). The seemingly random distribution of the protein of the minor clade, especially those from the distantly related bacteria, suggests HGT was involved (Figure 2.3) (Koonin et al. 2001). HGT in the prokaryotic world is facilitated by mobile genetic elements (MGE) such as plasmids. Plasmids may transfer from one bacterium to another by conjugation, transduction or natural transformation. In addition, genes from the plasmid can be incorporated in the bacterial genome through various types of recombination, and plasmid reconstitution (Brigulla & Wackernagel 2010).

2.5.2.2 Discovery of two *pagP* genes in bacterial genomes

Interestingly, within the γ-Proteobacteria, a group of bacteria from the *Enterobacterales* order (Alnajar & Gupta 2017) has two copies of *pagP* genes on the chromosome, or one on the chromosome and another on a plasmid (Figure 2.6). The two *pagP* genes separate into different subclades: the *pagP* gene that shows up first in the genome, which are highly similar in primary sequence (>70%) to the *E. coli* PagP is called "chromosomal" *pagP*; the other subclade of *pagP* genes from this branch are either randomly placed on the chromosome or found on plasmids, and these are called "plasmid-based" *pagP* or their protein products (Figure 2.6). Interestingly, the conserved signature deletion of one amino acid in the L3 loop identified in chromosomal PagP homologs that aligns to a conserved signature insertion in plasmid-based homologs (Figure 2.5 and 2.6). Plasmid-based PagP homologs (even those found on the chromosome) share over 90% sequence identity with PagP homologs from the plasmids. This gives grounds to the HGT theory for at least the plasmid-based PagP distribution (Treangen & Rocha 2011).

Multiple copies of a protein such as PagP in some bacteria usually indicate importance towards environmental adaptation, virulence or other survival strategies. An extra copy of the protein could mean establishment of a new function, or both could have the same function (complementing each other), or they could be expressed under different conditions (Bratlie et al, 2010; Zhang 2003). Bacteria with two *pagP* genes on the chromosome include *Klebsiella oxytoca, Enterobacter cloacae, Pantoea* strains, *Serratia* strains and *Raoultella ornithinolytica* (Figure 2.6). Common factors among bacteria with two PagP homologs include their association with plants and possibly their ability to fix

atmospheric N_2 (Cakmakci et al. 1981; Raju et al. 1972; Lin et al. 2012; Sandhiya et al. 2001; Thijs et al. 2014; Anisha et al. 2013). It is possible that these bacteria require an additional copy of PagP to protect themselves when invading plant tissues. Unlike animals, plants lack an adaptive immune system, and therefore rely entirely on the onslaught of the innate immune response of each cell to protect themselves from invaders (Chisholm et al. 2006; Jones & Dang 2006). Additionally, similar to mammals, plants use transmembrane protein recognition receptors that respond to microbial pathogen associated molecular patterns such as flagellin and LPS (Ranf et al. 2015; Ranf 2016). Therefore, lipid A modification by two copies of PagP might be necessary in this regard.

Our analysis also displayed a second *pagP* gene in *E. coli* (Figure 2.6). Examination of this *E. coli* strain DH10B genome revealed that the second *pagP* sequence was in close proximity (within 400bp) to the first *pagP* gene. This duplication possibly occurred as a result of an internal chromosomal duplication because flanking genes dicarboxylate transporter *dcuC* and a cold shock protein *cspE,* were also duplicated. This *E. coli* strain is a derivative of a laboratory K12 MC1061 strain (a strain with only one *pagP* gene), it has 226 mutations and more insertion sequence transposons compared to K12 MG1655 (wild type). These insertion elements appear to have remodeled the genome, providing homologous recombination sites resulting in tandem duplication and inversion (Durfee et al. 2008). This confirms that this second PagP in *E. coli* DH10B is a result of an internal duplication caused by unnatural mutations. As such this second PagP is not considered a true duplicate copy. No other complete E. coli genome had two copies

of PagP.

2.5.3 Major clade structure-function relationships: Determining PagP lipid A regioselection

To determine the diversity in major clade PagP lipid A regiospecificity we chose to investigate PagP homologs based on their distribution from *B. bronchiseptica* (BbPagP)*, L. pneumophila* (LpPagP) and the duplicate homologs from *K. oxytoca* (Ko1 and Ko2PagP). *Bordetella* and *Legionella* PagP homologs were chosen because their roles in bacterial pathogenesis have been established, and it appears that PagP lipid A regiospecificity might be important in this regard (Robey et al. 2001; Preston et al. 2006; Bishop 2005). The two PagP homologs from *K. oxytoca* were chosen because of the conserved signature indel and their close relatedness to PagP from the pathogenic *Klebsiella pneumoniae*, which serves to broaden our knowledge of PagP among the *Enterobacterales* order that is dominated by studies of EcPagP. These studies were performed in a detergent micellar enzymatic assay system and in a lamellar OM bilayer environment.

2.5.3.1 Detergent micellar enzymatic investigations: Evaluation of purification and refolding of BbPagP and LpPagP

BbPagP and LpPagP were expressed in a denatured state without their *N*-terminal signal peptide, solubilized in guanidine-HCl, purified using Ni^{2+}-ion affinity chromatography, and refolded by dilution into LDAO (Figure 2.7). Concentrations of

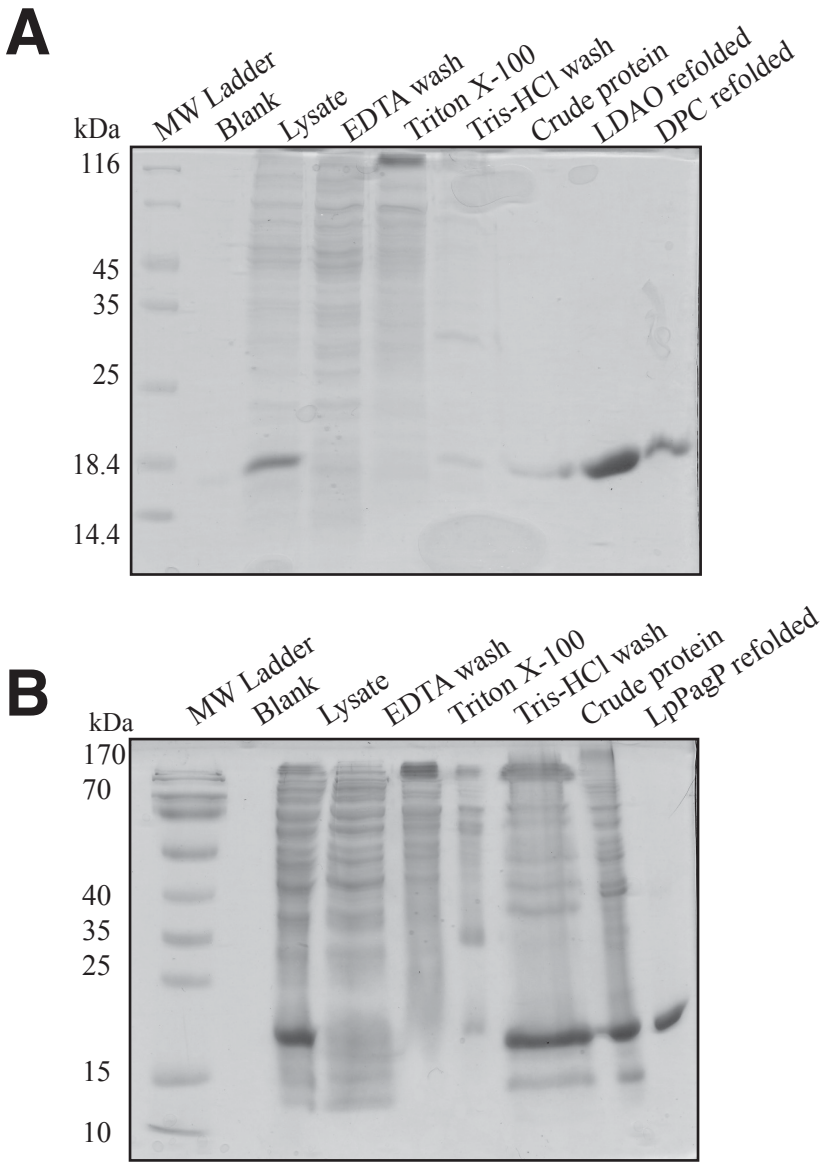

Figure 2.7. 13.5% SDS-PAGE assessment of BbPagP and LpPagP isolation and purification. Approximately 40 µg of samples of the lysate, supernatants, crude and refolded proteins were analyzed for BbPagP (A) and LpPagP (B). BbPagP was refolded in LDAO and DPC.

3 mg/mL were obtained of pure, refolded protein using this method, which gives similar yields as reported for EcPagP (Khan et al., 2007). The purified proteins refolded in LDAO migrated as pure single bands when analyzed by SDS-PAGE (Figure 2.7).

In previous studies of EcPagP, far-UV CD wavelength scans revealed a signature positive ellipticity maximum at 232 nm and a negative ellipticity maximum at 218 nm. The positive ellipticity at 232 nm arises from an exciton interaction involving buried aromatic residues Tyr26 and Trp66 when they are positioned in a specific geometric configuration (Khan et al. 2007). The negative ellipticity at 218 nm is characteristic of a β-barrel conformation (Khan et al. 2007; Miles & Wallace 2016). Although Tyr26 and Trp66 are conserved in BbPagP and LpPagP, the far-UV CD spectra showed only the negative ellipticity at 218 nm, likely because the aromatic residues interact in a unique configuration that fails to generate the exciton since these proteins share only 40% of their amino acid sequences with EcPagP (Figure 2.8A). BbPagP and LpPagP were also highly stable with thermal unfolding temperatures above 80 ^{o}C as observed for the EcPagP (Figure 2.8B) (Khan et al. 2007).

BbPagP palmitoylates lipid A at the 3'-position

To determine PagP lipid A regiospecificity we decided to use two different acceptor substrates in acyltransferase reactions: lipid IV_A, and Kdo_2 lipid A, which is the mature lipid A molecule with only the 2-position available for secondary acylation.

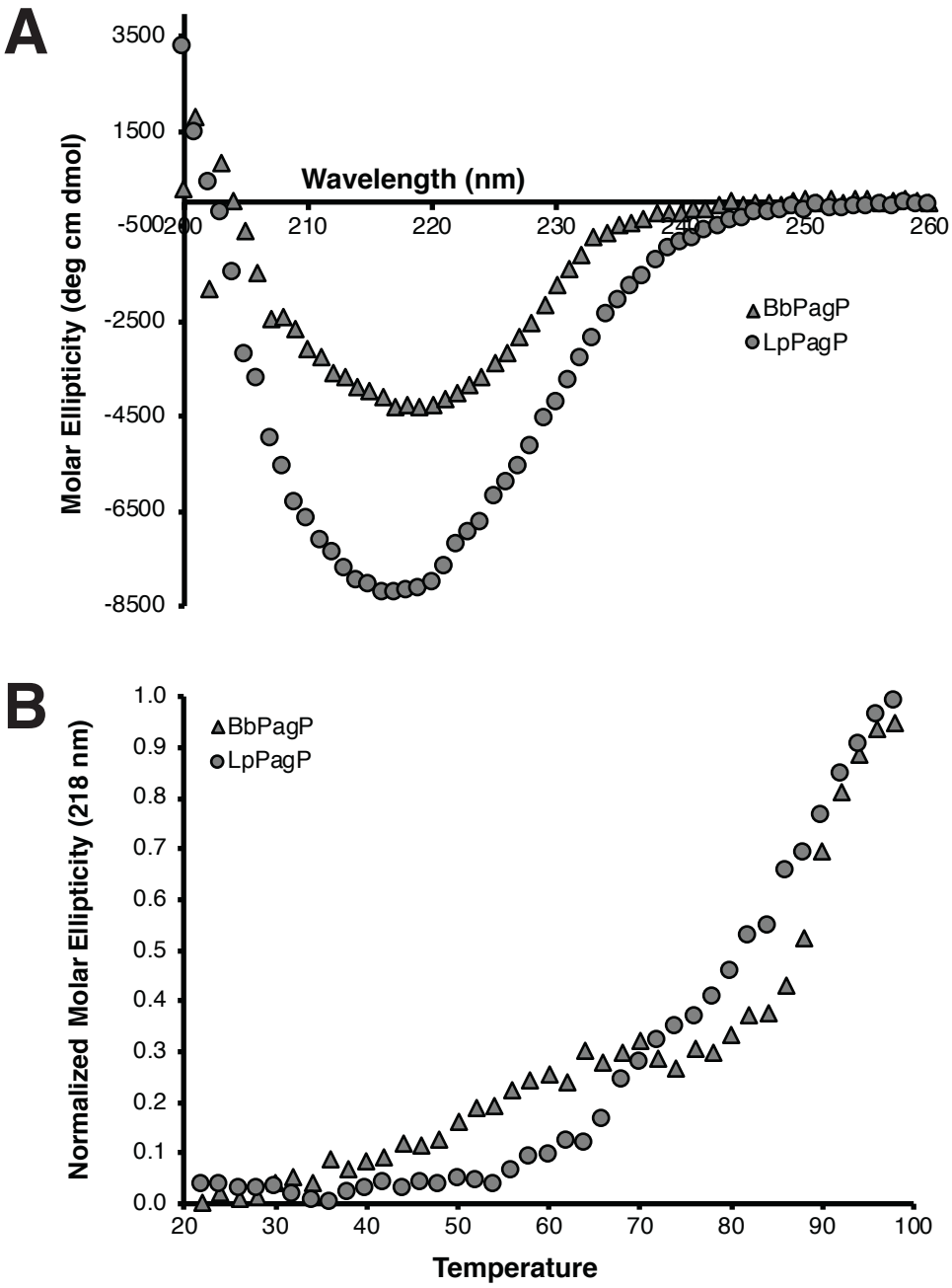

Figure 2.8. Far-UV CD spectroscopic analysis of BbPagP and LpPagP refolded in LDAO. A. Wavelength scans of each protein sample at 0.3 mg/mL was obtained between 200 and 260 nm at a constant temperature of 25 °C. Three scans were collected for each protein and the molar ellipticity calculated. B. Thermal unfolding profiles of BbPagP and LpPagP at 0.3 mg/mL of each protein sample which was heated from 20 to 100 °C at a rate of 2 °C/min. The molar ellipticity was calulated, normalized and plotted.

Lipid IV_A is a precursor of Kdo_2 lipid A that has all four positions available for secondary acylation (Figure 2.9) (Brozek & Raetz 1990). Therefore, using a lipid IV_A substrate the enzyme can be either specific or relaxed in choosing a position to palmitoylate (Figure 2.9). We incubated BbPagP with ^{14}C-DPPC as a donor with lipid IV_A and Kdo_2 lipid A as acceptor substrates in separate reactions. EcPagP was used as a positive control that palmitoylates both lipid IV_A and Kdo_2 lipid A at the 2-position (Bishop et al. 2000; Thaipisuttikul et al. 2014). The reactions were carried out overnight and were monitored by TLC (Figure 2.10A). BbPagP palmitoylated lipid IV_A, but not Kdo_2 lipid A. EcPagP palmitoylated both lipid IV_A and Kdo_2 lipid A substrates indicating a lipid A 2-position regiospecificity. These results suggest that BbPagP palmitoylates lipid IV_A at the distal 3'-position.

To confirm the lipid A position that was palmitoylated in the enzymatic assays, the products lipid IV_B (lipid IV_A palmitoylation at the 2-position) and lipid $IV_{B'}$ (lipid IV_A palmitoylation at the 3'-position) from the reaction without the use of radioactive-labeling were analyzed by collision-induced dissociation mass spectrometry (CID MS) (Figure 2.10B and 2.10C) (Thaipisuttikul et al. 2014). The products generated from EcPagP and BbPagP reactions were subjected to liquid chromatography ESI quadrupole TOF (LC-ESI-Q-TOF). The product detected in the positive mode $[M+H]^+$ with *m/z* value of 1644 and in the negative mode $[M-H]^-$ with *m/z* value of 1642 were consistent with those reported for lipid $IV_{B/B'}$ (Raetz et al. 1985). The positive mode $[M+H]^+$ ion was subjected to CID MS. The B^+_1 ion or oxonium product ion generated from the proximal glucosamine, after cleavage of the glycosidic bond in the lipid IV_B

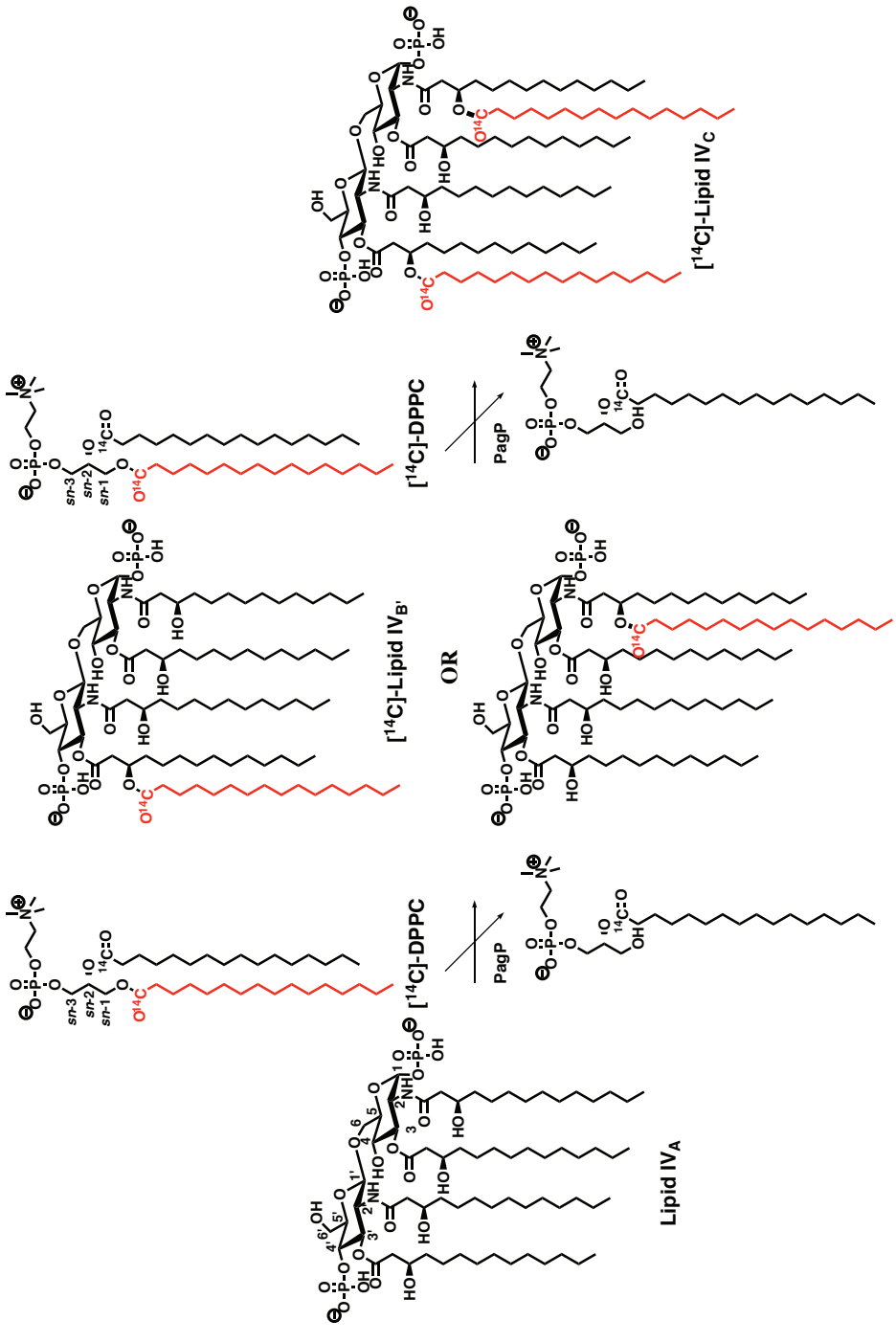

Figure 2.9. PagP acyltransferase reaction with ^{14}C-DPPC and lipid IV$_A$. PagP catalyzed acyltransferase reaction in a defined detergent micellar enzymatic assay system: synthetic ^{14}C labeled *sn*-1,2-dipalmitoyl phosphatidylcholine (DPPC) and lipid IV$_A$ react to form ^{14}C labeled lyso-PC and palmitoylated lipid IV$_A$. A radiolabeled ^{14}C palmitate chain can be incorporated into lipid IV$_A$ either at positions 2 or 3' (lipid IV$_B$ or lipid IV$_{B'}$), or at both positions (lipid IV$_C$). The reaction with Kdo$_2$ lipid A is similar except that only the 2-position would be available for secondary acylation.

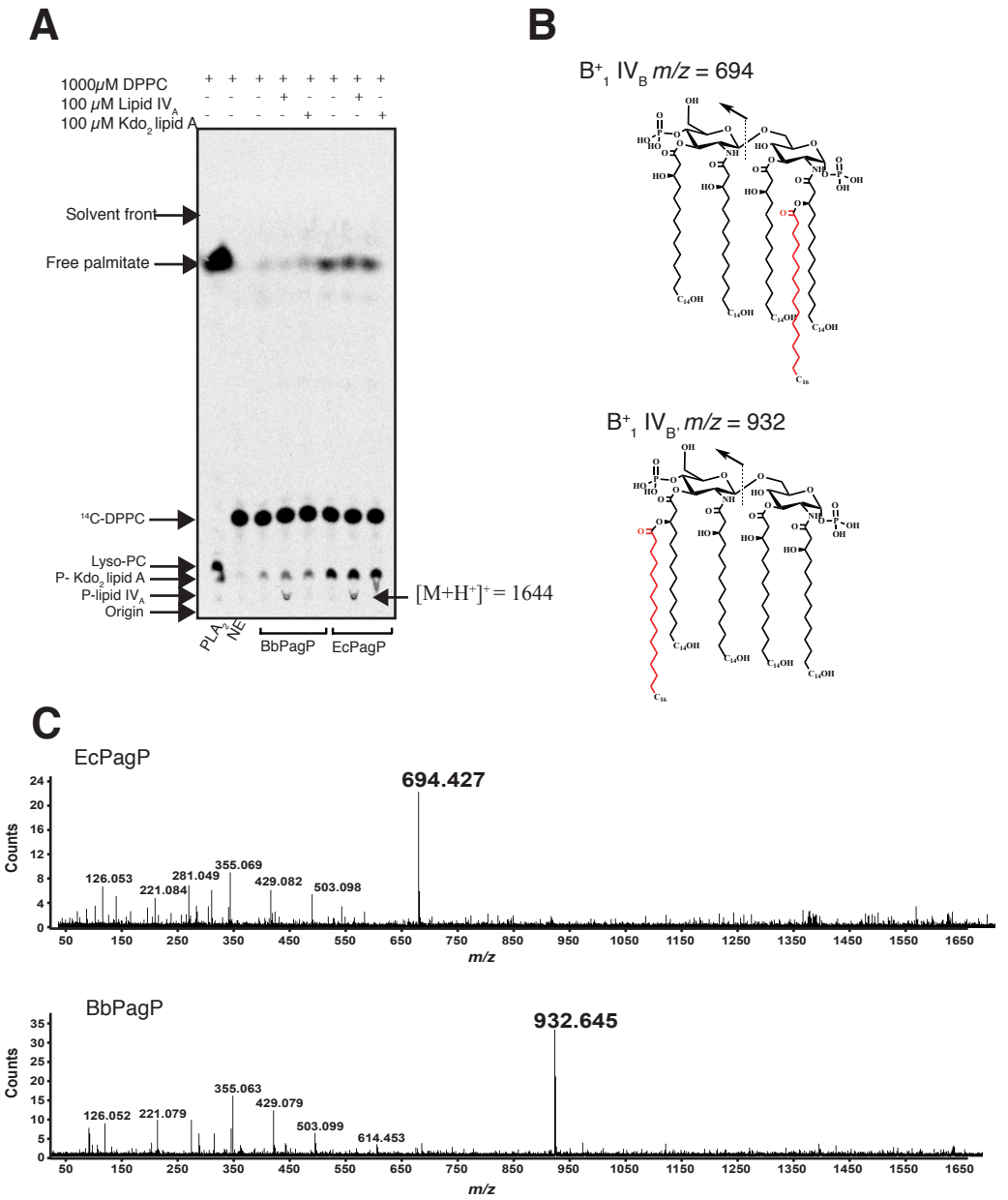

Figure 2.10. BbPagP palmitoylates lipid IV_A at the 3' position. A. BbPagP and EcPagP (control) were incubated with ^{14}C-DPPC as the donor, and lipid IV_A or Kdo_2 lipid A acceptor substrates in separate acyltransferase reactions to produce free palmitate and palmitoylated lipid IV_A (P-lipid IV_A could be lipid IV_B or lipid $IV_{B'}$ or both) or palmitoylated Kdo_2 lipid A (P-Kdo_2 lipid A). A no enzyme negative control and PLA_2 positive control showed unconverted ^{14}C-DPPC and hydrolyzed DPPC forming free palmitate, respectively. The TLC plate was developed in solvent system chloroform/methanol/water 65:25:4 (v/v). The TLC plates were exposed and visualized using Phosphorimaging. B. Structures of lipid IV_B and lipid $IV_{B'}$. C. Collision induced dissociation mass spectrometry was performed on the $[M+H^+]^+$ ion from liquid chromatography for the palmitoylated lipid IV_A species obtained from EcPagP and BbPagP catalyzed reactions.

product (EcPagP reaction), had an *m/z* value of 694, which is consistent with the palmitate attached to the 2-position of lipid IV_B (Figure 2.10B and 2.10C). The B^+_1 ion from BbPagP reactions had an *m/z* value of 932 as observed for a lipid $IV_{B'}$ product with the palmitate on the distal glucosamine unit (Garrett 2017). Altogether, these results validate that a purified BbPagP exhibits lipid A 3'-position regiospecificity.

LpPagP transfers a C16 palmitate to the 2-position of lipid A

To our knowledge there are no reports of the length or type of fatty acyl chain that PagP incorporates into lipid A in *L. pneumophila* OMs. The major acyl chains that decorate the *Legionella* phospholipids are mainly of methyl *iso*- or *anteiso*-branched forms, unlike those found in *E. coli,* which are primarily of the palmitic, steric, *cis*-vaccenic and cyclopropane forms (Geiger 2010; Oursel et al. 2007). Furthermore, the hydrocarbon ruler in LpPagP is lined at its base by an Ala instead of a Gly residue as found in EcPagP. This observation suggests that LpPagP might be adapted to select a 15-carbon long *iso*-methyl branched C16 acyl chain (Ahn et al. 2004; Bishop 2005; Khan et al. 2007). Prior to determining the lipid A regiospecificity of LpPagP, we decided to investigate the acyl chain specificity of this enzyme.

We used C14-C16 symmetrical *iso*-methyl branched and straight-chained phosphatidylcholines (PCs) as the donor substrates, and ^{32}P orthophosphate lipid IV_A as acceptor substrate in acyltransferase reactions (Figure 2.11A). Surprisingly, the enzyme preferred 16:0 straight chain PC of all the PCs investigated. LpPagP had no significant

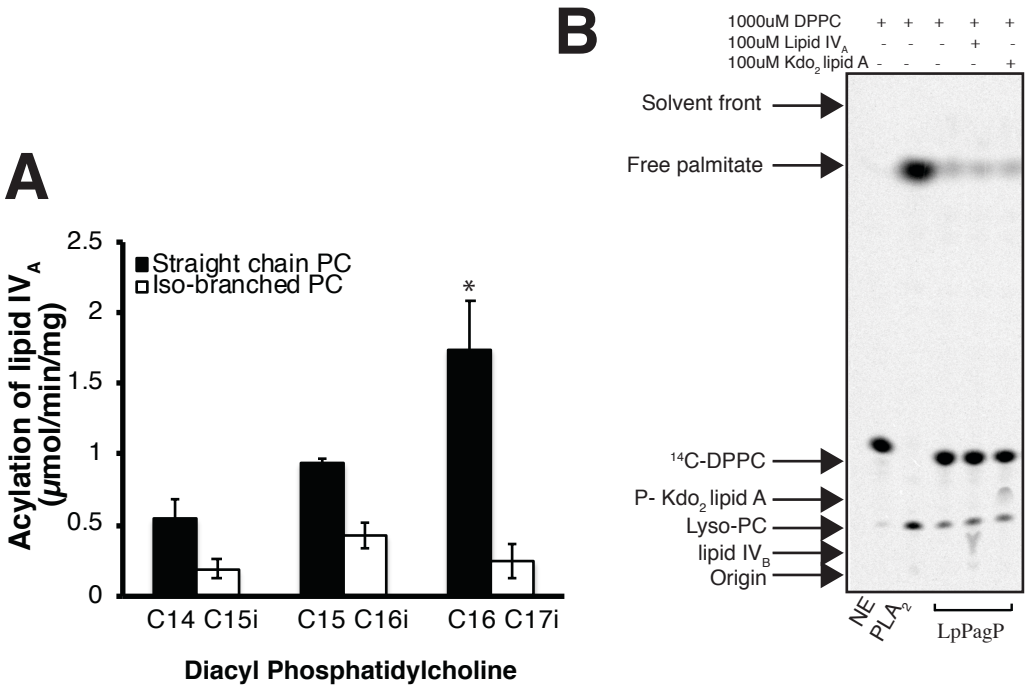

Figure 2.11. LpPagP transfers a C16 palmitate to the 2-position of lipid IV$_A$ *in vitro.* A. LpPagP was incubated with diacyl phosphatidylcholine of straight chain C14-C16 and iso-methyl branched chain C15i-C17i phospholipids. ^{32}P orthophosphate labeled lipid IV$_A$ was used as the acceptor substrate and for monitoring by TLC. The TLC plates were exposed to Phosphorimager screens and quantification was done by ImageQuant software. LpPagP significantly selects C16 straight acyl chain by unpaired Student t test, *P<0.05. B. LpPagP was incubated with ^{14}C-DPPC as the donor and nonradiolabeled lipid IV$_A$ or Kdo$_2$ lipid A acceptor substrates in separate acyltransferase reactions to produce free palmitate, palmitoylated lipid IV$_A$ (lipid IV$_B$) or palmitoylated Kdo$_2$ lipid A (P-Kdo$_2$ lipid A). A no enzyme negative control and PLA$_2$ positive control showed unconverted ^{14}C-DPPC and hydrolyzed DPPC, free palmitate and lyso-PC. The TLC plate was developed in solvent system chloroform/methanol/water 65:25:4 (v/v). The TLC plates were exposed and visualized by Phosphorimaging.

preference for any of the *iso*-methyl branched phospholipids employed. Overall, LpPagP had higher specific activities for straight chain PCs than for *iso*-methyl branched PCs (Figure 2.11A). This result suggests that 16:0 straight chain is the preferred acyl chain that is being transferred by LpPagP *in vitro*.

After determining the acyl chain specificity for LpPagP, we were able to determine the lipid A regiospecificity of the enzyme. We expected LpPagP to palmitoylate the 2-position of Kdo_2 lipid A and lipid IV_A, because *L. pnuemophila* lipid A has all sites on the distal glucosamine already blocked, leaving only the 2-position available for secondary acylation (Geiger 2010; Zähringer et al. 1995). Hence, we incubated the enzyme in separate acyltransferase reactions with lipid IV_A and Kdo_2 lipid A as acceptors along with ^{14}C-DPPC as a donor to monitor palmitoylation on a TLC plate (Figure 2.11B). LpPagP palmitoylated both lipid IV_A and Kdo_2 lipid A, as expected, confirming that it palmitoylates lipid A at the 2-position.

Ko1PagP and Ko2PagP transfer a palmitate to lipid A 2 and 3'-positions

To determine the lipid A regioselectivity of Ko1PagP and Ko2PagP we used the same system as for BbPagP and LpPagP (Figure 2.12). Both homologs palmitoylated lipid IV_A and Kdo_2 lipid A, indicating that the 2-position of Kdo_2 lipid A is being used. Interestingly, a doubly palmitoylated lipid IV_A (identified as lipid IV_C in Figure 2.9) was present (Figure 2.12). KoPagP homologs cannot palmitoylate position-3' in cells because this position is occupied by myristate in *K. oxytoca* (Süsskind et al. 1998), but their

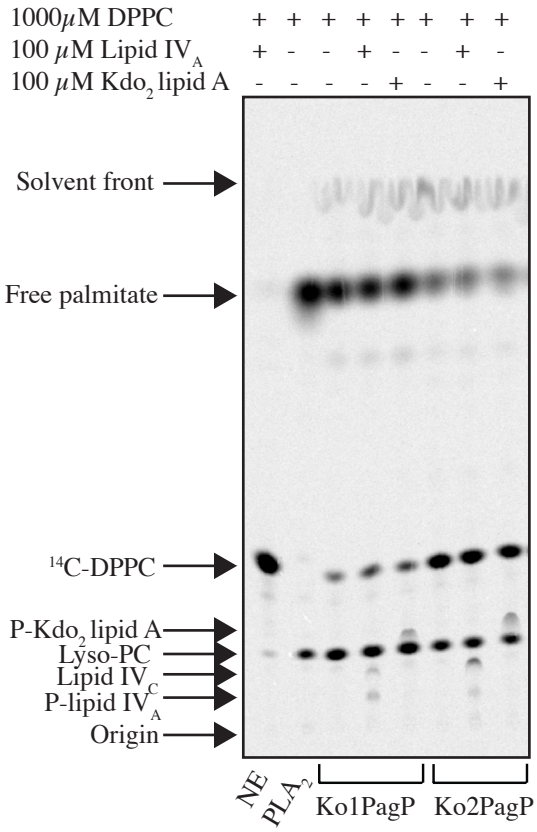

Figure 2.12. Ko1PagP and Ko2PagP palmitoylate Kdo_2 lipid A and doubly palmitoylate lipid IV_A. The enzymes were incubated in detergent micellar enzymatic assay system with ^{14}C-DPPC as the donor and nonradioactive lipid IV_A or Kdo_2 lipid A acceptor substrates. The separate reactions produce free palmitate, palmitoylated lipid IV_A (P-lipid IV_A could be lipid IV_B or lipid $IV_{B'}$ or both), dipalmitoylated lipid IV_A (lipid IV_C) and palmitoylated Kdo_2 lipid A (P-Kdo_2 lipid A). A no enzyme negative control and PLA_2 positive control showed unconverted ^{14}C-DPPC and hydrolyzed DPPC, free palmitate and lyso-PC. The TLC plate was developed in solvent system chloroform/methanol/water 65:25:4 (v/v). The TLC plates were exposed and visualized by Phosphorimaging.

capacity *in vitro* to display both lipid A position-2 and position-3' regioselectivity indicates that they are enzymatically distinctly different from EcPagP, which is regiospecific for the 2-position (Bishop et al. 2000).

2.5.3.2 Lamellar outer membrane bilayer investigations: BbPagP displays lipid A 3'-position regiospecificity

PagP purified in detergent micelles experience fewer restraints compared to the enzyme embedded in the lamellar OM bilayer. Therefore, to be certain of BbPagP lipid A 3'-position regiospecificity we expressed the enzyme in *E. coli* OMs. To carry out this investigation we expressed BbPagP with its native signal peptide for targeting the protein to the OM from an arabinose-inducible promoter. We also needed to employ *E. coli* mutants that expressed under-acylated lipid A so the 2 and/or 3' positions were available for acylation (Table 2.1). *E. coli* strains MC1061 (wild type), WJ0124 (Δ*pagP*) and SK1061 (Δ*pagP* and Δ*lxpM*) were used in these studies (Table 2.1). Lipid A exhibited in *E. coli* WJ0124 has the 2-position available for secondary acylation. The *E. coli* strain SK1061 has both *pagP* and *lpxM* knocked out, which leaves both the 2 and 3' position of lipid A available for acylation. *lpxM* gene encodes for the enzyme LpxM that incorporates a myristate at the 3'-position of lipid A (Raetz et al. 2007).

The *E. coli* strains with and without *pagP*-expressing plasmids were grown with ^{32}P orthophosphate for labeling the lipid A molecules and treated with and without EDTA to activate PagP in the OM. The lipids were extracted using mild acid hydrolysis and

analyzed by TLC (Figure 2.13). BbPagP acylated lipid A isolated from the OMs of the *E. coli* SK1061 strain, which had lipid A 2 and 3'-positions available, but the enzyme did not acylate lipid A from the WJ0124 strain that had lipid A with only the 2-position available. This confirmed lipid A 3'-position regiospecificity for BbPagP.

LpPagP does not function in heterologous *E. coli* OMs

We asked if the lipid A 2-position regiospecificity observed for LpPagP could be recapitulated in an *E. coli* OM background, despite the differences in the membrane lipid profiles for *Legionella* and *E. coli* (Geiger 2010; Oursel et al. 2007; Zähringer et al. 1995). We used the same system that was used for BbPagP to express LpPagP with its native signal peptide (optimized to be expressed in *E. coli*) from an arabinose-inducible promoter. The *E. coli* strains employed expressed lipid A structures with the 2-position available, and with the 2 and 3' positions available (Table 2.1). The percentage lipid A acylation of LpPagP was calculated for three biological replicates (Figure 2.14). LpPagP did not acylate lipid A in any of the *E. coli* strains. Only background measurements comparable to the *pagP* knockout strain were obtained. We conclude that LpPagP is either inactive in *E. coli* OMs or else it failed to be properly expressed and assembled.

KoPagP homologs acylate available 2 and/or 3'-positions of lipid A

K. oxytoca exhibits a hexa-acylated lipid A similar to that of *E. coli*, leaving only the 2-position available for palmitoylation (Süsskind et al. 1998). Therefore, it was

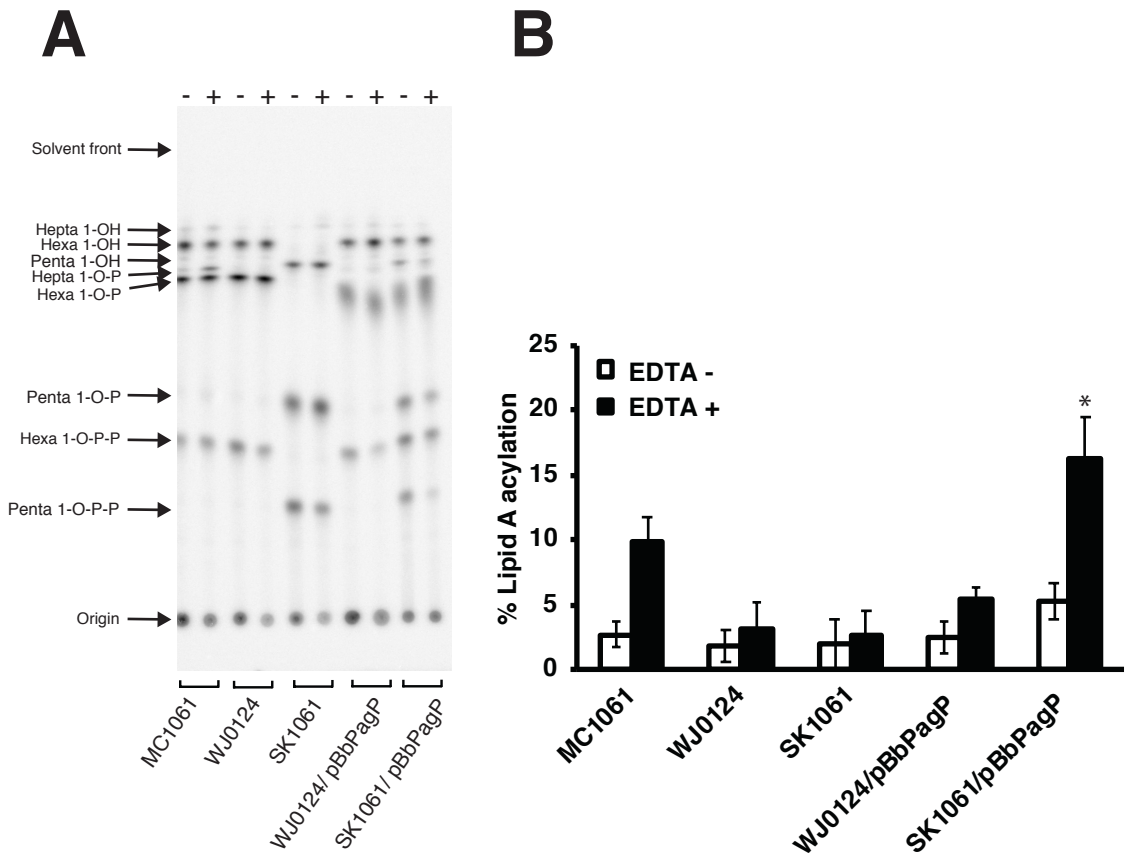

Figure 2.13. BbPagP acylates lipid A at the 3' position in *E. coli* OMs. Autoradiograph showing lipid A profile from *E. coli* MC1061 (wild type), WJ0124 (Δ*pagP*), SK1061 (Δ*pagP* and Δ*lpxM*) and pBbPagP (with its signal peptide) expressed in WJ0124 and SK1061. The bacterial cells were grown and treated with and without EDTA before harvesting to activate PagP in the presence of ^{32}P orthophosphate. Lipid A species were isolated, using a mild acid hydrolysis procedure, separated by TLC, and plates were visualized by Phosphorimaging. The main lipid A species are indicated on the left and include the hepta, hexa and penta-acylated lipid A with the 4'-monophosphate (1-OH), 1,4' *bis*-phosphate (1-O-P) or 1-diphosphate (1-O-P-P) derivatives of each species. Quantification of lipid A species was done by ImageQuant software. The average percent of lipid A acylation for the major 1,4'-bis-phosphorl-lipid A species was calculated and plotted for three biological replicates. Lipid A acylation by activated BbPagP expressed in SK1061 was significantly greater when compared to SK1061 with no PagP by unpaired Student t test, *P<0.05.

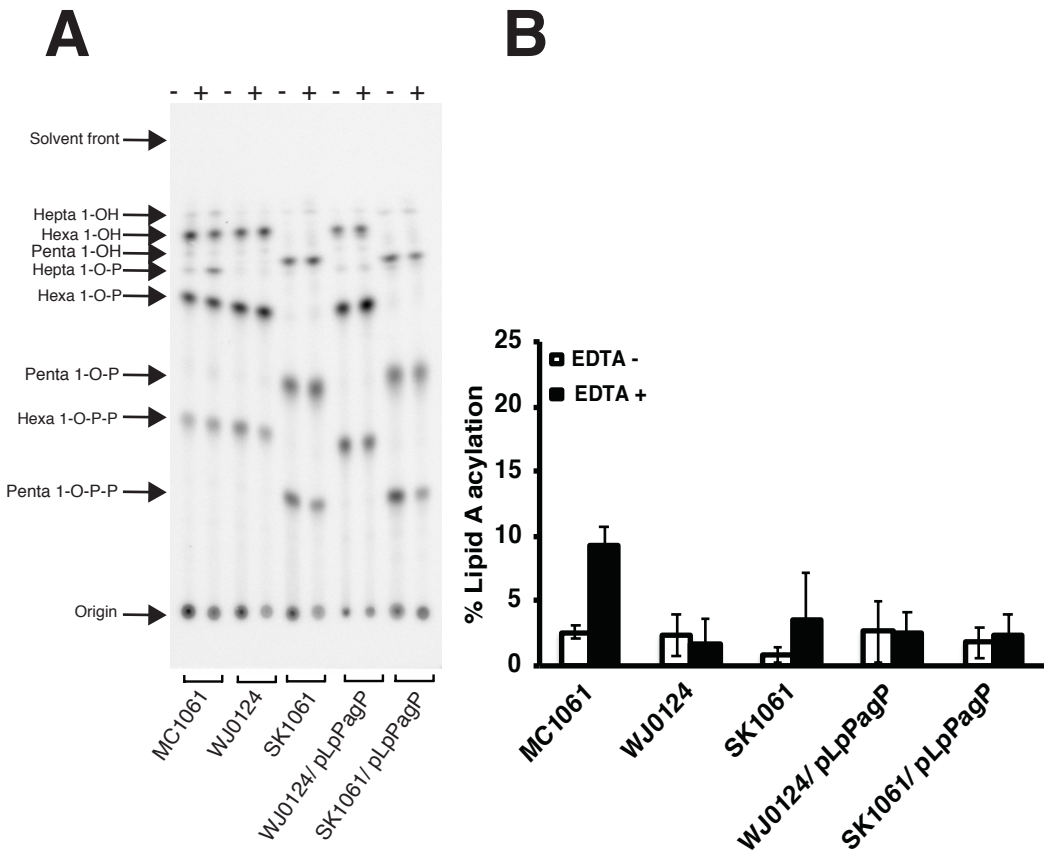

Figure 2.14. LpPagP does not acylate lipid A in *E. coli* OMs. A. Autoradiograph showing lipid A profile from *E. coli* MC1061 (wild type), WJ0124 (Δ*pagP*), SK1061 (Δ*pagP* and Δ*lpxM*) and pLpPagP (with its signal peptide) expressed in WJ0124 and SK1061. The bacterial cells were grown and treated with and without EDTA before harvesting to activate PagP in the presence of ^{32}P orthophosphate. Lipid A species were isolated, using a mild acid hydrolysis procedure, separated by TLC, and plates were visualized by Phosphorimaging. The main lipid A species are indicated on the left and include the hepta, hexa and penta-acylated lipid A with the 4'-monophosphate (1-OH), 1,4' *bis*-phosphate (1-O-P) or 1-diphosphate (1-O-P-P) derivatives of each species. B. Quantification of lipid A species was done by ImageQuant software. The average percent of lipid A acylation for the major 1,4'-bis-phosphorl-lipid A (1-O-P) species was calculated and plotted for three biological replicates. Lipid A acylation by activated LpPagP expressed in SK1061 or WJ0124 was no different when compared to SK1061 or WJ0124 with no PagP by unpaired Student t test.

surprising that KoPagP enzymes palmitoylated lipid IV_A twice *in vitro* (Figure 2.12). As such, we decided to also investigate the lipid A regioselectivity in bacterial OMs for the KoPagP homologs. The same procedure was used as for BbPagP and LpPagP (Figure 2.15). Both Ko1PagP and Ko2PagP acylated lipid A in WJ0124 and in SK1061 confirming that they both have lipid A 2-position and 3'-position regioselectivity. It was also noted that both PagP homologs exhibited ~20% palmitoylation of lipid A (Figure 2.15), which is comparable with EcPagP palmitoylation of lipid A in *E. coli* OMs (Jia et al. 2004).

2.5.4 BbPagP embrasure polar residue affects lipid A palmitoylation

Knowing the lipid A position regioselection of BbPagP, LpPagP and KoPagP homologs, our aim was to understand how the enzymes palmitoylate the different positions in lipid A. Lipid A accesses PagP through the embrasure, which is flanked by Pro28 and Pro50 (Khan & Bishop 2009). However, considering the size of the lipid A molecule (LPS is 32 Å x 28 Å x 12 Å in height, length and width, respectively) the enzyme may not be able to accommodate lipid A within the β-barrel interior (Qiao et al. 2014). It is more likely that lipid A binds on the exterior surface in the vicinity of the embrasure, probably by way of electrostatic neutralization between positively charged residues and the negatively charged phosphate groups (Graf et al. 1988; Batra et al. 2013). Additionally, polar uncharged residues may be involved in stabilizing the interaction by forming H-bonds (Holliday et al. 2009). The various modes of acylation observed by different PagP homologs suggests that lipid A binds to variant residues on

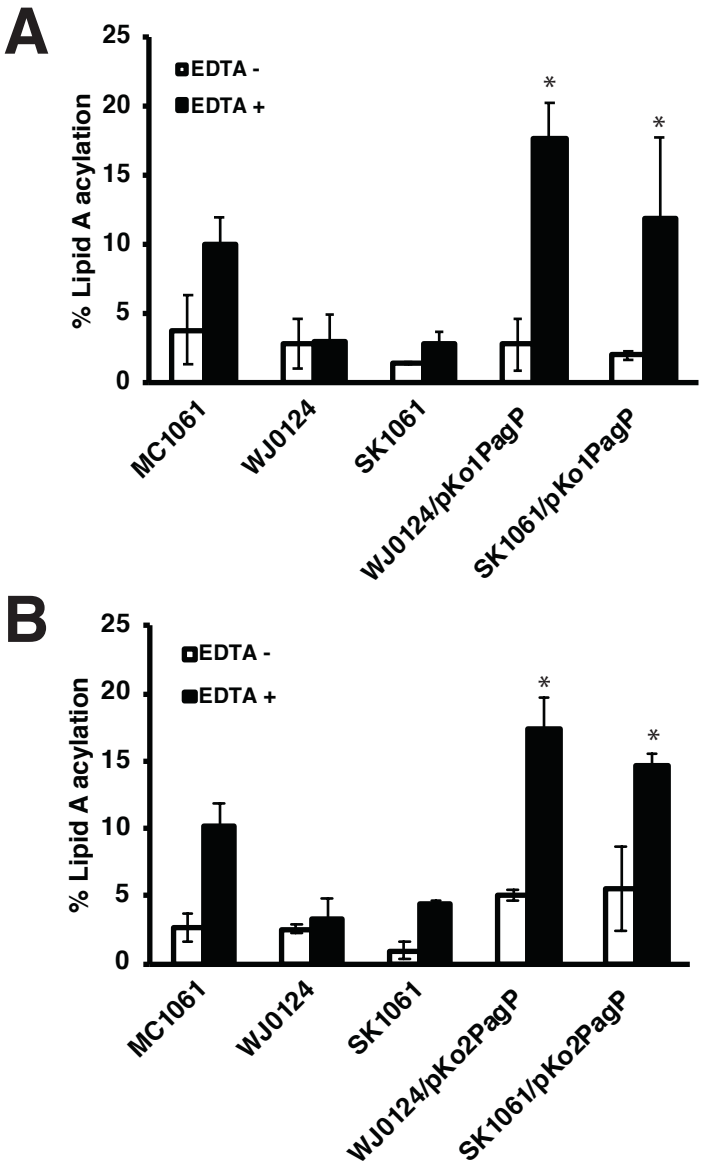

Figure 2.15. Ko1PagP and Ko2PagP acylate lipid A at the 2 and 3' positions in *E. coli* OMs. pKo1PagP (A) and pKo2PagP (B) were expressed with their signal peptide from an arabinose inducible promoter plasmid. The plasmids were transformed into *E. coli* strains WJ0124 (Δ*pagP*) and SK1061 (Δ*pagP and* Δ*lpxM*). The bacterial cells were grown and treated with and without EDTA to activate PagP in the presence of ^{32}P orthophosphate. Lipid A species were isolated, using a mild acid hydrolysis procedure, and separated by TLC. The TLC plates were exposed to Phosphorimaging screen and quantification was done by ImageQuant software. The average percent of lipid A acylation was calculated and plotted. Lipid A acylation by activated Ko1PagP and Ko2PagP expressed in SK1061 or WJ0124 were significantly greater when compared to SK1061 or WJ0124 with no PagP by unpaired Student t test, *P<0.05.

the surface of the enzymes. Therefore, we hypothesize that lipid A binds to variant extracellular residues in and around the embrasure.

Solving the structures of the various homologs, possibly with bound substrates, would have been ideal to understand how PagP interacts with lipid A. Attempts were made to obtain and solve crystal structures for BbPagP, LpPagP and KoPagP homologs, but these were unsuccessful. Alternatively, we decided to visualize the protein structures using structure modelling and sequence alignment to assist in our investigation (Figure 2.16). The amino acid sequence for BbPagP was uploaded to I-TASSER, an automated protein structure and function prediction tool that uses multiple threading alignment and related structural assembly simulations to predict the structure of the uploaded protein sequence (Roy et al. 2010). The top hit was the *E. coli* PagP structure solved at 1.4 Å in SDS/MPD. The model was structurally aligned to the solved *E. coli* PagP structure (PDB 3GP6) and the variant, positive and polar uncharged residues were identified around the area of the embrasure (Figure 2.16). Four possible non-conserved positively charged or polar uncharged residues were identified in BbPagP: T28, S39 and R44 (using PDB 3GP6 numbering) and mutated to Ala by site directed mutagenesis (Table 2.2). Residue S31 was chosen as a control as it is not a surface exposed residue, although it is located near the embrasure (Figure 2.16B).

The mutants BbPagPT28A, BbPagPR44A, BbPagPS31A were expressed and refolded into LDAO (Figure 2.17A). BbPagPS39A was expressed but we were unable to refold this protein, probably due to instability in the presence of detergent (Bowie 2005).

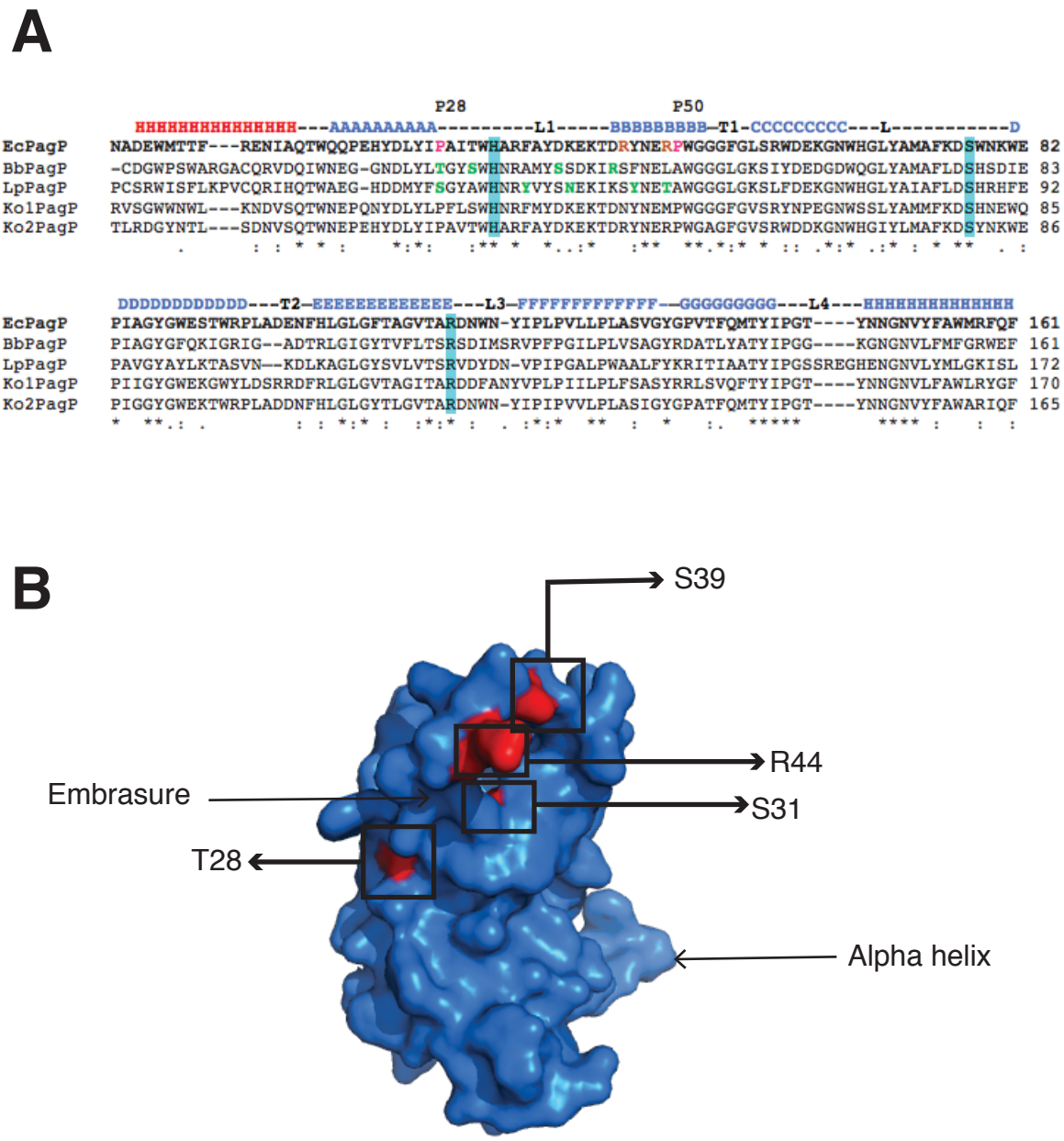

Figure 2.16. Identification of possible BbPagP residues involved in lipid A binding. A. Multiple sequence alignment of EcPagP, BbPagP, LpPagP, Ko1PagP and Ko2PagP. The EcPagP embrasure residues are highlighted in pink, and the potential lipid A binding residues are highlighted in green. The residues highlighted in orange were previously mutated, but had no effect on enzyme activities (Sapiano, 2014). B. Surface representation of BbPagP (model from I-TASSER) showing potential binding residues for lipid A in red.

Wild type and mutant proteins all had β-barrel conformation illustrated by a far-UV CD spectrum with a negative ellipticity maximum at 218 nm (Figure 2.17B). The BbPagPT28 mutant displayed an increase in its minimum ellipticity, suggesting a conformational change with increased β-sheet formation.

BbPagP and the embrasure mutants were used *in vitro* acyltransferase assays to investigate the effects on lipid IV_A palmitoylation (Figure 2.18). BbPagPT28A had a significantly reduced specific activity in lipid IV_A palmitoylation compared to the wild type. This suggests a possible role for threonine in the interaction between lipid IV_A and BbPagP. Interestingly, T28 in BbPagP aligns with P28 in EcPagP, one of the embrasure residues that was converted to cysteines for a cross linking studies described by Khan and Bishop (2009).

2.5.5 Major clade PagP structure-function relationships for KoPagP homologs: Determining the significance of a CSI in the L3 loop

Recently, studies on the significance of CSIs in soluble proteins have shown results that correlate CSIs with functions in protein-protein interaction and protein-lipid interaction (Gupta et al. 2017; Khadka & Gupta 2017). The one amino acid CSI in *K. oxytoca* PagP homologs is an insertion of an Asn at position 118 in Ko2PagP and a deletion at said position in Ko1PagP (Figure 2.5). These investigations of Ko1PagP and Ko2PagP in *K. oxytoca* were focused on establishing a significance, if any, for the presence of a CSI in the L3 loop in this non-essential outer membrane protein.

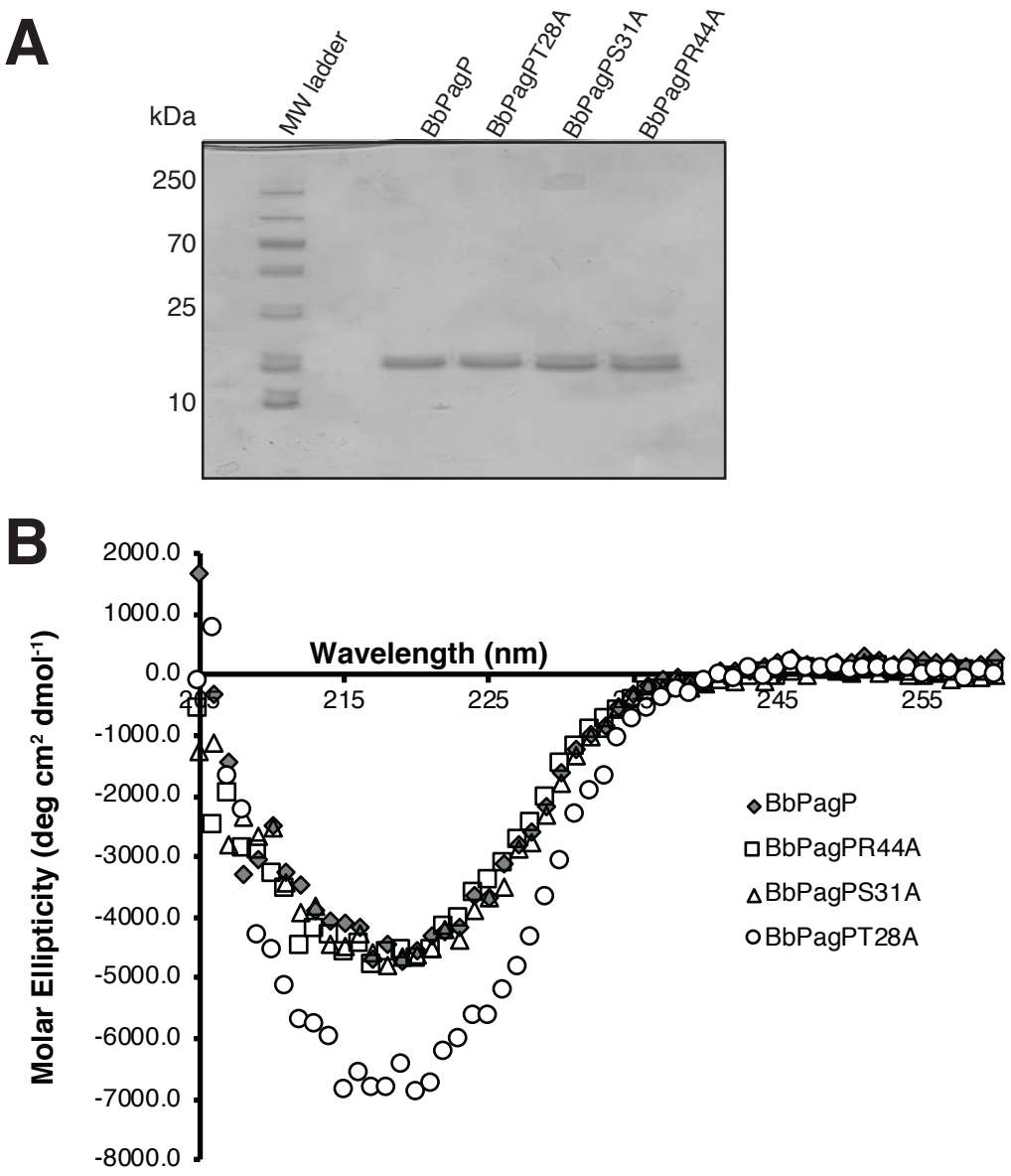

Figure 2.17. 13.5% SDS PAGE and far-UV CD spectroscopic analysis of BbPagP and the embrasure mutants. A. BbPagP, BbPagPT28A, BbPagPS31A and BbPag-PR44A were purified and refolded in LDAO. Aproximately 40 µg of each protein sample were solubilibized in 2XSDS loading buffer for analysis by electrophoresis. B. Far UV wavelength scan of BbPagP, BbPagPT28A, BbPagPS31A and BbPagPR44A showing minimum ellipticity at 218 nm. Samples were maintained 0.3 mg/mL in 10 mM Tris-HCl (pH 8.0) and 0.1% LDAO. Scans were made between 205 and 260 nm at a contstant temperature of 25 °C.

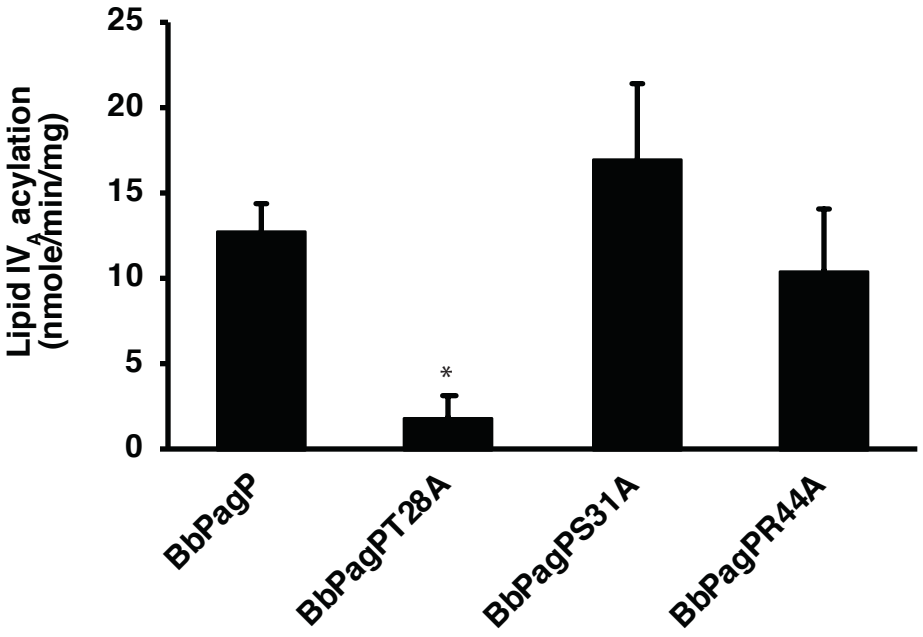

Figure 2.18. Lipid IV_A acylation for BbPagP and embrasure mutants. BbPagP and its mutants were incubated with ^{14}C-DPPC and lipid IV_A over a time course and aliquots were pippetted onto TLC plate at 30, 60, 120, 240 and 360 minutes. The plates were resolved, exposed and visualized by Phosphorimaging. Substrates and products were quantified by imageQuant. The average lipid A acylation was calculated for three replicates. Specific activity for BbPagPT28A was significantly less than wildtype BbPagP by an unpaired Student t test, *P=0.01.

2.5.5.1 Evaluation of refolded KoPagP homologs and the CSI mutants

The CSI of one amino acid seemed to be strategically located in the L3 loop in close proximity to R114 that stabilizes the phospholipid headgroup during the acyltransferase reaction (Figure 2.1) (Bishop Unpublished). In an unrestrained molecular dynamics simulation of EcPagP in a lamellar bilayer environment a POPC molecule was observed to dock itself inside the hydrocarbon ruler, and on its initial approach to the crenel this same POPC molecule grazed past the L3 loop. We asked if this one amino acid CSI might have an effect on the phospholipid headgroup preference for at least one of these enzymes from *K. oxytoca*. To investigate if the CSI in the L3 loop has an effect on the headgroup preference of the enzyme, we inserted an asparagine residue at position 118 in Ko1PagP and deleted the N118 from Ko2PagP using site directed mutagenesis, thus switching the CSI between Ko1PagP and Ko2PagP. We also made substitutions at position 118 in Ko2PagP to ensure that the effects observed could be attributed to the insertion/deletion and not to a simple substitution (Table 2.2). DNA sequencing and ESI MS confirmed the correct point mutations and enzyme masses, respectively (Table 2.2).

The purity, folding and conformation of the proteins were analyzed by heat modifiability SDS-PAGE, far-UV CD wavelength scan and thermal unfolding profiles (Figure 2.19, 2.20 and 2.21). All samples (heated and unheated) ran as single bands with a Mw of ~ 20 kDa demonstrating pure monomeric protein (Figure 2.19). The protein samples also showed a band shift for the heated and unheated samples, which is characteristic of denatured and folded β-barrel OM proteins (Khan et al. 2007).

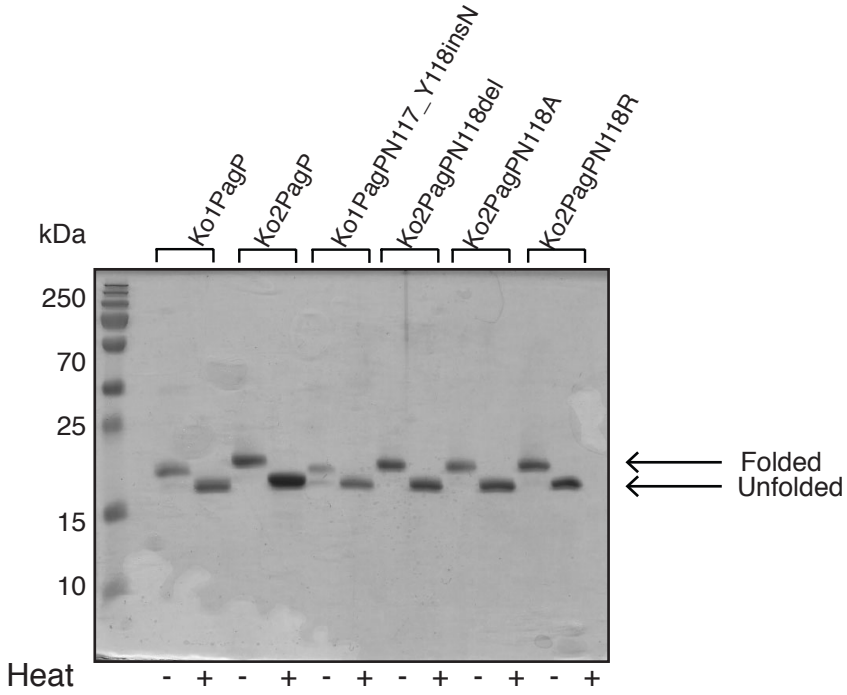

Figure 2.19. 15% SDS-PAGE analysis showing heat modifiability Ko1PagP and Ko2PagP and CSI mutants. Approximately 40 µg of protein samples were solubilized in equal volumes of SDS loading buffer at room temperature or heated (100 °C) prior to electrophoresis.

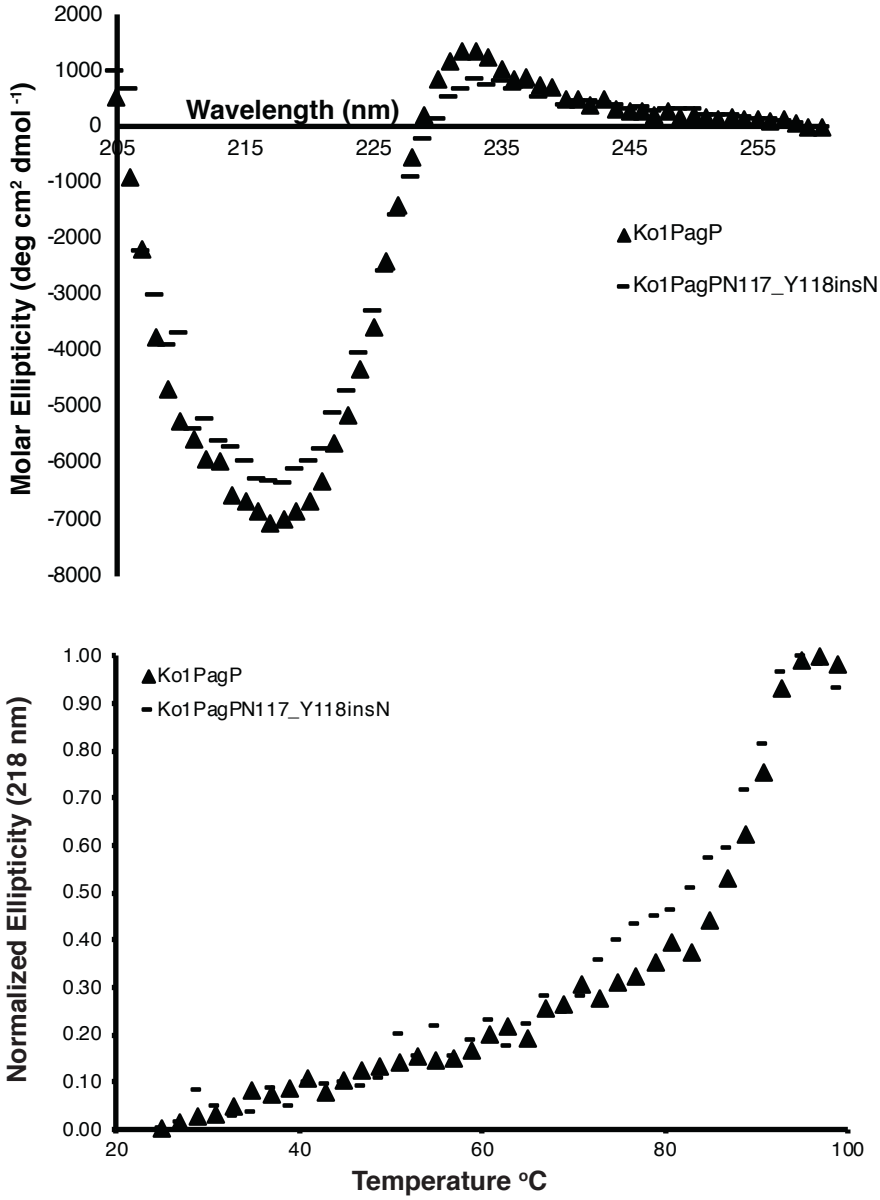

Figure 2.20. Far-UV CD spectroscopic analysis and thermal unfolding profiles for Ko1PagP and CSI mutant. A. Wavelength scan of LDAO refolded Ko1PagP and CSI mutants. Samples were maintained at 0.3 mg/mL in 10 mM Tris-HCl (pH 8.0) and 0.1% LDAO. Scans were made between 205 and 260 nm at a constant temperature of 25 °C. B. Thermal unfolding profiles for Ko1PagP and CSI mutants. Samples were the same as for wavelength scans, but were heated from 20 to 100 °C at a rate of 2 °C/min and response time of 16 sec.

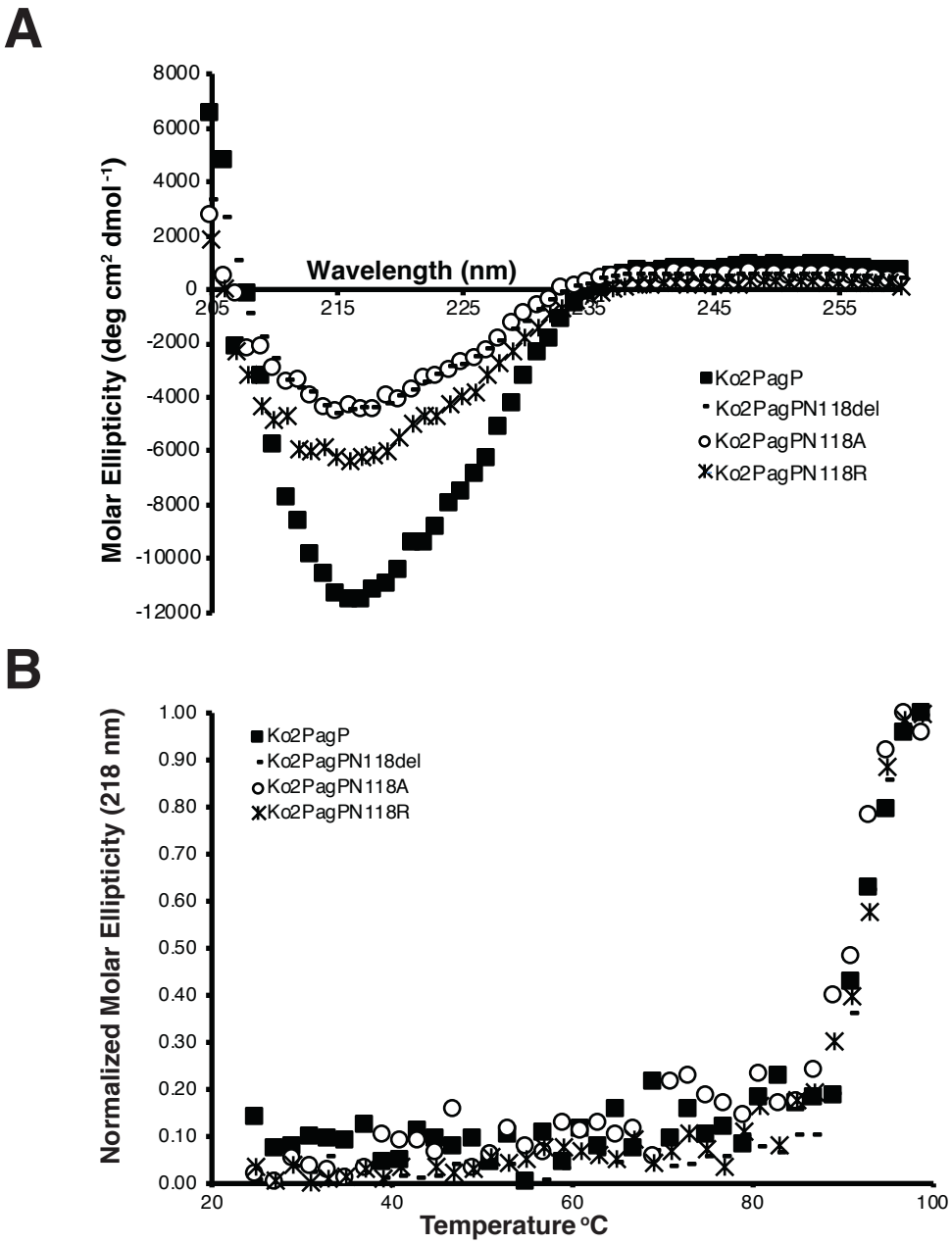

Figure 2.21. Far-UV CD spectroscopic analysis and thermal unfolding profiles for Ko2PagP and conserved indel mutants. A. Wavelength scan of LDAO refolded Ko2PagP and CSI mutants. Samples were maintained at 0.3 mg/mL in 10 mM Tris-HCl (pH 8.0) and 0.1% LDAO. Scans were made between 205 and 260 nm at a constant temperature of 25 °C. B. Thermal unfolding profiles for Ko2PagP and CSI mutants. Samples were the same as for wavelength scans, but were heated from 20 to 100 °C at a rate of 2 °C/min and response time of 16 sec.

Far-UV CD wavelength scans of these proteins displayed a negative ellipticity maximum at 218 nm indicating that the proteins exhibited β-barrel conformations (Figure 2.20A and 2.21A). The CD signal for Ko1PagPN117_Y118insN* had a decrease in molar ellipticity at 218 nm and 232 nm compared to the wild type (Figure 2.20A). Differences were also observed for the Ko2PagP mutants N118del*, N118A, N118R, which had significantly decreased molar ellipticity at 218 nm compared to the wild type (Figure 2.21A) (*Nomenclature for point mutations was adopted from den Dunnen & Antonarakis 2001). These changes in molar ellipticity at 218 nm suggests that the CSI mutations created a conformational change in the protein structures that could be detected by CD (Miles & Wallace 2016). No differences were observed in thermal unfolding temperatures for the CSI mutants compared to the wild type Ko1PagP or Ko2PagP proteins (Figure 2.20B and 2.21B). Overall, these outcomes suggest that the one amino acid switch in the L3 loop CSI resulted in structural perturbations without compromising the stability of the proteins.

2.5.5.2 L3 loop CSI does not affect KoPagPs' preference for a phospholipid polar headgroup

We asked if the CSI in the L3 loop would affect the enzymes' preference for the polar headgroup of a phospholipid. We used asymmetrically acylated phosphatidylethanolamine (PE) and phosphatidylglycerol (PG) phospholipids because they are the predominant phospholipid species found in *E. coli* and related bacterial OMs (Oursel et al. 2007). Phosphatidylcholine (PC) is not found in *E. coli*, but the availability

of synthetic symmetrical and asymmetrical PC combined with the relaxed specificity of PagP for this phospholipid headgroup (Bishop et al. 2000) suits their use as controls in these experiments. We incubated the enzyme with asymmetrical POPC, POPE and POPG as donor substrates and ^{32}P orthophosphate lipid IV_A extracted from *E. coli* BTKO9 as the acceptor molecule in acyltransferase reactions. This assay was repeated 4 -5 times and the specific activity was calculated for the acyltransferase reaction for each donor phospholipid (Figure 2.22). No significant preference was observed for Ko1PagP or Ko2PagP towards any relevant phospholipid (Figure 2.22). Therefore, Ko1PagP and Ko2PagP are unspecific for the phospholipid polar headgroups. This result concurs with previous findings that EcPagP displays relaxed specificity for the phospholipid polar headgroup despite its stringent selection of an *sn*-1 palmitoyl group (Bishop et al. 2000; Brozek et al. 1987).

2.5.5.3 The L3 loop CSI affects the specific activity of KoPagP enzymes when PG is used as an acceptor substrate.

Since there was no significant difference in lipid A palmitoylation despite differences in the phospholipid headgroup, we asked if the CSI would affect the enzymes' ability to palmitoylate PG. We decided to conduct the acyltransferase reaction by incubating the enzymes with ^{14}C-DPPC as the donor and POPG as the acceptor. This reaction was repeated 4-5 times to determine the specific activity of the enzyme for this reaction (Figure 2.23). The Ko2PagPN118del mutant had a significant increase in specific activity when POPG was used as an acceptor compared to the wild type suggesting that

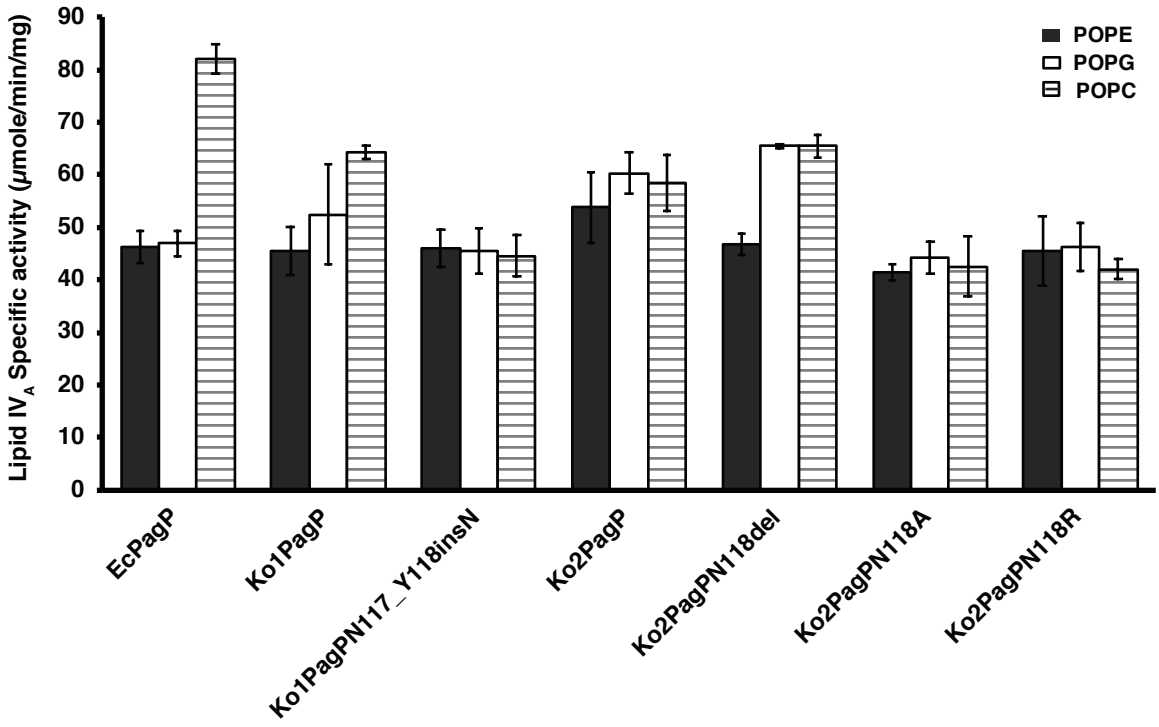

Figure 2.22. L3 conserved signature indel in Ko1PagP and Ko2PagP has no effect on phospholipid headgroup preference. Deleting the Asn at position 118 in Ko2PagP and inserting Asn at the same position in Ko1PagP created a switch in the CSI in the L3 loop of these proteins. Substitutions with Arg and Ala of the CSI in Ko2PagP were also created. The assays were carried out with 1mM POPE, POPG or POPC as a donor substrate, 50 µM ^{32}P orthophosphate labeled lipid IV_A as an acceptor substrate, for monitoring by TLC and using 10 ng/µl of each enzyme. The TLC plates were exposed to a Phosphorimager screen and quantification was done by ImageQuant software. The average specific activity of each enzyme and each phospholipid donor was calculated and plotted. No significant differences between mutants and wild types by unpaired Student t test.

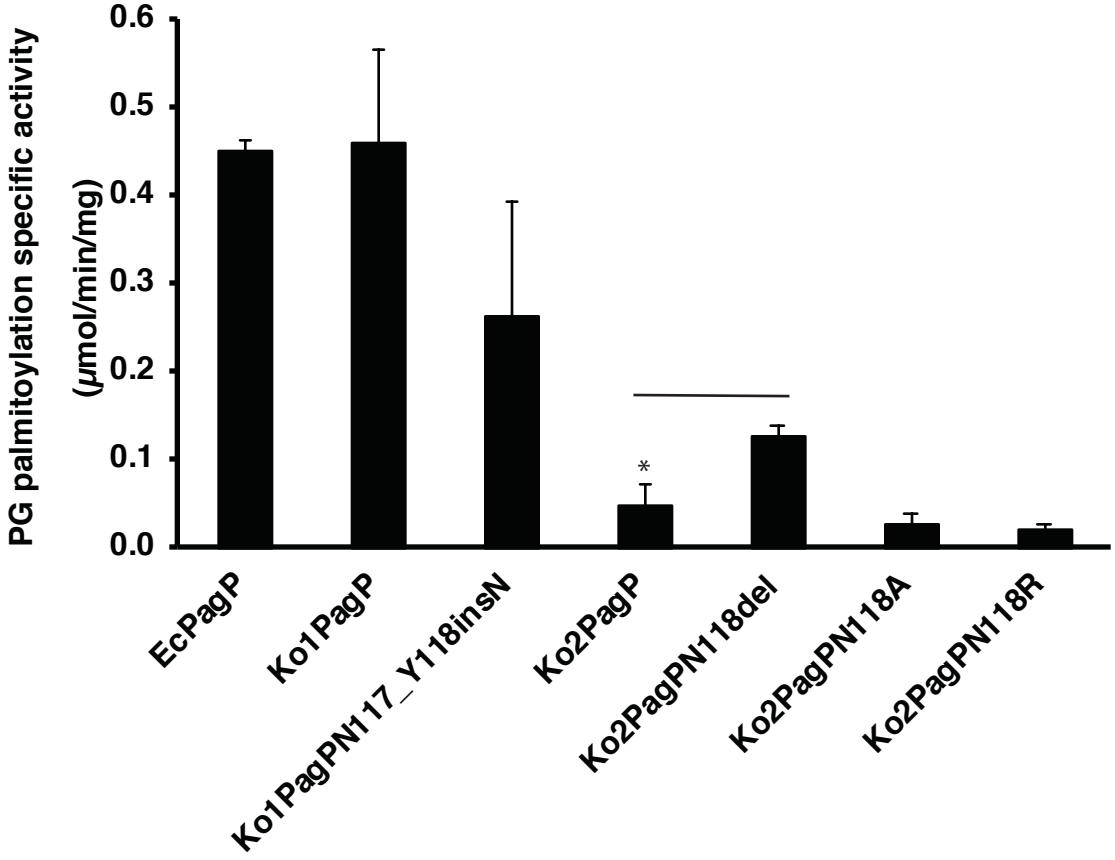

Figure 2.23. L3 loop conserved signature indel in Ko1PagP and Ko2PagP affects PG palmitoylation *in vitro*. Deleting the Asn at position 118 in Ko2PagP and inserting Asn at the same position in Ko1PagP created a switch in the CSI in the L3 loop of these proteins. Substitutions with Arg and Ala of the CSI in Ko2PagP were also created. The assays were carried out with 1 mM DPPC as a donor, 100 μM PG as an acceptor, 20 μM ^{14}C- DPPC, for monitoring by TLC and using 10 ng/μl of each enzyme. The TLC plates were exposed to a Phosphorimager screen and quantification was done by ImageQuant software. After 4-5 repeats of this assay, the average specific activity of each enzyme was calculated and plotted. Statistical analysis was done using unpaired Student t test, *P<0.05.

the specific activity was trending towards that of Ko1PagP (Figure 2.23). Ko1PagP was not significantly affected (Figure 2.23). The specific activity for Ko2PagPN118A and Ko2PagPN118R were unaffected, suggesting that substitutions did not have the same effects as the CSI (Figure 2.22). Therefore, the presence or absence of the CSI correlates to Ko2PagP's ability to palmitoylate PG. The effect was only partial, possibly because there are other features within the structure of the enzyme contributing to the difference between Ko1PagP and Ko2PagP in terms of their ability to palmitoylate PG. The difference in secondary structure content between Ko1PagP and Ko2PagP might be significant, considering that these enzymes are only 61% similar at the primary structure level (Figure 2.5).

2.6 Discussion

The work here demonstrates the distribution of PagP family proteins in Gram-negative bacteria, and elucidates structure-function relationships with regards to the lipid A position regioselection and conserved signature indels. We presented the distribution of PagP from the major and minor clades to select appropriate homologs for study. Using detergent micellar enzymatic assays and lamellar OM bilayer studies that employ a variety of lipid A acceptors we determined the lipid A regiospecificity for *B. bronchiseptica* PagP, *L. pneumophila* PagP and newly identified duplicate PagP homologs from *K. oxytoca* in the major clade. The PagP regiospecificity determined in this study indicates that major clade PagP homologs from the β-Proteobacteria exhibit lipid A 3'-position regiospecificity characteristic of the minor clade PagP enzymes.

Interestingly, *K. oxytoca* PagP homologs have the capacity to palmitoylate lipid A at both the 2- and 3'-position despite the fact that their lipid A is blocked at the 3'-position and their close relative from *E. coli* is decidedly regiospecific for the 2-position. Clearly, the ability of major clade PagP homologs to palmitoylate lipid A at the 3'-position is carried through the clade either in terms of function or as an evolutionary vestige. Variant residues around the embrasure of PagP might contribute to the lipid A positional regiospecificity as illustrated by our identification of a critical role of Thr28 in BbPagP. The one amino acid CSI in the L3 loop of major clade homologs clearly governs a switch between Ko1PagP and Ko2PagP that affects PG palmitoylation *in vitro*.

The sequence based phylogenetic analysis presented here aided our understanding of PagP distribution in Gram-negative bacteria, although the evolutionary relationships were not reliably resolved. Minor clade PagP homologs are found among diverse bacteria from β-Proteobacteria, γ-Proteobacteria, δ-Proteobacteria and Firmicutes (Figure 2.3). Previous structure-function studies of PaPagP from the minor clade reveals that the protein adopts a β-barrel structure with an interior hydrocarbon ruler. PaPagP specifically selects a palmitate and displays lipid A 3'-position regiospecificity (Thaipisuttikul et al. 2014). Current studies that highlight surface residues H17 and S51, which are responsible for catalytic function in PaPagP, are conserved in HePagP and superimpose onto EcPagP catalytic residues H33 and S77 (Figure 2.4). Additionally, the *N*- terminal extension and T2 turn characteristic of EcPagP are necessary for function of HePagP protein despite their absence from PaPagP. These results indicate that although PagP proteins of the

minor clade lacks the obvious primary sequence of the major clade homologs, the enzymes from these two clades are structural homologs and are consequently derived from a common ancestor (Thaipisuttikul et al. 2014; Aravind et al. 2002; Zhang et al. 1997).

Major clade PagP homologs that are similar in primary sequence to EcPagP are restricted to the β- and γ-Proteobacteria (Figure 2.6). Duplicate copies of PagP were discovered in the genomes of a number of bacteria from the γ-Proteobacteria that live as endophytes within plants. We were unable to fully resolve the evolutionary relationships among major clade homologs using the sequence-based phylogenetic analysis. As such, we chose major clade homologs for structure-function studies based on the distribution of the protein among these bacteria.

We confirmed that BbPagP palmitoylates lipid A at the 3'-position *in vitro* for the first time, and in bacterial OMs as described by Preston et al. (2003). Interestingly, this is not the case for all *Bordetella* PagP homologs because *B. parapertussis* PagP palmitoylates lipid A at the 2 and 3'- position (Hittle et al. 2015). At the primary sequence level, PagP from *B. bronchiseptica* and *B. parapertussis* are 99% identical with differences in only one amino acid substitution Gly4Asp in the α-helix near the *N*-terminus (using PDB 3GP6 numbering). The function of the alpha helix is to stabilize and anchor the protein into the membrane milieu (Iyer & Mahalakshmi 2016; Huysmans et al. 2007; Jia et al. 2004). Therefore, this change in amino acid within the alpha helix is not

expected to have such a profound effect on lipid A regiospecificity for these enzymes. Consequently, innate variations in the lipid A structures displayed in these different *Bordetella* species need to be considered as factors governing the outcome of PagP palmitoylation.

Bordetella sp. are known to display variability in lipid A structures, likely due to the range of host that these bacteria infect (El Hamidi et al. 2009a; Zarrouk et al. 1997). *B. bronchiseptica* infects a wide range of mammals, but it seldom infects humans, whereas *B. parapertussis* is known to infect humans and sheep. Interestingly, *B. parapertussis* isolates from humans are distinct from those taken from sheep; this difference is also reflected in LPS structures and, more specifically, lipid A modification by PagP (Hester et al. 2015; Parkhill et al. 2003; Basheer et al. 2011; Hamidi et al. 2009).

Our results suggest that LpPagP preferred to select a C16 palmitate to acylate the 2-position of lipid IV_A. *L. pneumophila* is a member of the γ-Proteobacteria, but it has unusual lipids in its membranes. With a 2,3-diamino-2,3-dideoxyglucose (GlcN3N) lipid A backbone decorated with unusually long branched (27 and 28 carbons) acyl chains, and with more than 50% *iso*- or *anteiso*-branched phospholipids in its membranes, investigating LpPagP in our detergent micellar and lamellar OM bilayer systems was challenging. Other than the phospholipid composition and branched acyl chains, there are no reports of unusual lengths of phospholipid acyl chains in the outer membranes of *L. pneumophila* (Geiger 2010; Lambert & Moss 1989). We expected LpPagP to incorporate

a 15-carbon long *iso*-methyl branched C16 acyl chain (i.e. C15 straight chain with a methyl branch on the second to last carbon), because of the available phospholipids in *L. pneumophila*, and the inference that the hydrocarbon ruler of LpPagP is lined at its base by an Ala, instead of a Gly residue in *E. coli* PagP (Figure 2.5). Mutation of Gly88Ala in EcPagP causes the enzyme to select unbranched C15 saturated acyl chains (Khan et al. 2007). It is possible that PagP is in fact a dedicated palmitoyltransferase in *L. pneumophila*, regardless of the peculiarities in its lipids and in its hydrocarbon ruler. The enzyme may be tolerant of the Ala that lines the base of the hydrocarbon ruler instead of a Gly, and in any case selects a palmitate in the bacterial OM (Ahn et al. 2004; Khan et al. 2007). On the other hand, LpPagP may very well prefer to incorporate an *iso*- or *anteiso*-methyl branched acyl chain into lipid A in *L. pneumophila* OMs, but because of the limitations in our assays this cannot be concluded at this time. We were unable to recapitulate *L. pneumophila* PagP regiospecificity in *E. coli* OMs, likely because the enzyme was not able to use the lipids available in an *E. coli* background, or it is also possible that the enzyme did not express. We could have confirmed the latter by expressing the enzyme with a tag and its signal peptide which targets the protein to the bacterial OM, isolate the OM, and analyze by Western blotting. However, previous experiments have taught us that PagP is unable to be detected using traditional western blot procedure possibly due to the very hydrophobic nature of the protein and the presence of detergent used to isolate the proteins from the membrane (Kaur & Bachhawat 2009). The enzyme was able to use less than optimal substrates *in vitro* because its

properties were likely enhanced by the defined detergent assay conditions (Hite et al. 2008).

The discovery of two PagP homologs in the same bacteria was intriguing. It did not cross our minds that the KoPagP homologs and EcPagP could have different lipid A regiospecificity since *K. oxytoca* exhibits a hexa-acylated Kdo_2 lipid A like that of *E. coli* (Süsskind et al. 1998). We expected that Ko1PagP and Ko2PagP would palmitoylate lipid A at the 2-position as observed for EcPagP (Bishop et al., 2000). However, both Ko1PagP and Ko2PagP palmitoylated lipid A at the 2-position as expected, but also at the 3' position, both *in vitro* and in bacterial OMs. This result may not be valid under normal conditions where the wild type *K. oxytoca* would display a lipid A with the 3'-position blocked by a myristate and, therefore, would not accommodate palmitate incorporation at this site (Süsskind et al. 1998).

Alternatively, the observed relaxed lipid A regioselectivity in these enzymes for the 2 and 3' positions, suggests that the lipid A structure may not be the only determinant of lipid A regiospecificity. Süsskind and colleagues did not mention the origin of *K. oxytoca* isolates that were used in obtaining the structure of *K. oxytoca* LPS, but it probably was a clinical isolate (Süsskind et al. 1998). *K. oxytoca* is a clinically significant pathogen, known for nosocomial infections, but it is also a plant growth promoting bacterium (Darby et al. 2014; Cakmakci et al. 1981; Raju et al. 1972). It is possible that *K. oxytoca* could have variability in their lipid A structures due to the different hosts it

colonizes, as seen in *Bordetella* species (El Hamidi et al. 2009a; Zarrouk et al. 1997). Considering this possibility, PagP from *K. oxytoca* could be necessary to palmitoylate lipid A at the 2 and/or 3' position in a lipid A species that has the available positions. The lipid A 3'-position could become available by deacylation at this position possibly in a plant environment. Silipo et al., reported that different species of *Xanthomonas* (plant pathogenic and non-pathogenic bacteria) showed varied acylation patterns in lipid A that influence activation of the immune response in plants (Silipo etal. 2008). Probably double palmitoylation is a strategy used by *K. oxytoca* to modify its lipid A structure to evade the onslaught of the immune response system in plants during colonization (Tam et al. 2015; Molinaro et al. 2009; Silipo et al. 2008).

We attempted to understand how PagP interacted with lipid A during acyltransferase reactions as it concerns the enzyme's lipid A positional regiospecificity. A Thr residue that aligns with Pro28 in *E. coli* PagP on the surface of the *B. bronchiseptica* PagP appears to be necessary for optimal lipid A palmitoylation. It is not unusual for an integral membrane enzyme to bind to its lipid A substrate by electrostatic interactions or hydrogen bonding. Lipid A 1 and 4' phosphate groups were observed binding to surface exposed positively charged residues in the crystal structure of LpxK that was solved with bound substrate. LpxK is a membrane-bound tetraacyldissacharide-1-phosphate 4'-kinase that catalyzes the sixth step of the lipid A biosynthesis pathway by phosphorylating the 4'-position of the tetraacyldiasaccharide-1-phosphate intermediate to form lipid IV_A (Chapter 1 - Figure 1.3) (Emptage et al. 2014; Raetz et al. 2007). Although not a

positively charged residue, it is possible that the γ-OH of Thr28 forms a hydrogen bond with one of the phosphate groups to stabilize the lipid A enzyme transition state (Lee & Imae 1990; Graf et al. 1988). However, it is necessary to consider if lipid A could be stabilized for the acyltransferase reaction by binding to a single residue on the enzyme surface. Likely, more residues need to be investigated before a final conclusion can be reached. Additionally, activity of the enzyme with mutations in surface exposed residues *in vitro* can be quite different as opposed to their activity in bacterial OMs (Bishop Unpublished; Hite et al. 2008). Hence, investigations are required within bacterial OMs. A reduction in lipid A palmitoylation alone is insufficient to decide if Thr28 residue is a binding residue. Further studies may include spectroscopic studies of the mutant and wild type with and without substrate to analyze conformational changes. If Thr28 is a lipid A regiospecific binding residue, is it possible to mutate Thr28 to a corresponding residue in a lipid A 2-position regiospecific enzyme and reverse its regiospecificity? We have already elucidated the mechanism for how the enzyme selects a specific length of acyl chain (Khan et al. 2007; Khan et al. 2010a; Khan et al. 2010). Answers to such questions would enable us to engineer an enzyme that can also select a specific position to acylate in the lipid A backbone, which could have therapeutic value.

The question of the significance of the L3 loop CSI from Ko1PagP and Ko2PagP was also addressed. The L3 loop CSI was shown to correlate with Ko1PagP and Ko2PagP ability to palmitoylate PG *in vitro*. The CSI in the L3 loop of PagP is represented by a deletion in Ko1PagP and an insertion in Ko2PagP. This CSI in the L3 loop is in close

proximity to R114 of the extracellular catalytic triad, which stabilizes the phospholipid headgroup during the acyltransferase reaction (Bishop Unpublished). Ko1PagP and Ko2PagP had no preference for a particular phospholipid headgroup, consistent with previous reports for EcPagP (Bishop et al. 2000; Brozek et al. 1987). The realization that the L3 loop CSI affects PG palmitoylation was unexpected because to our knowledge of acceptor substrates lipid A and, by extension, PG access the hydrocarbon ruler through the embrasure (Khan & Bishop 2009; Bishop Unpublished). Therefore, both PG and lipid A palmitoylation should be affected. We concluded that PG binds non-specifically on the surface of the enzyme when used as an acceptor substrate. The enzyme could use two possible routes, including the embrasure, for acyl chain extraction to palmitoylate PG, but only the embrasure is known for lipid A access (Cuesta-Seijo et al. 2010; Khan & Bishop 2009). This is reiterated in the significant changes in CD molar ellipticity at 218 nm for Ko2PagP CSI mutants. The changes observed suggest that a conformational change occurred, which affected PG palmitoylation, but not lipid A palmitoylation because PG possibly binds non-specifically at a site other than the embrasure during the acyltransferase reaction. This distinction in alternative routes may not be possible in bacterial OM due to lamellar bilayer restrictions (Cuesta-Seijo et al. 2010; Hite et al. 2008).

Similarly, a four-amino acid CSI was identified in the T2 turn of the minor clade PagP proteins (Figure 2.1). Current results suggests that this CSI is required for function (Dixon Unpublished). A two-amino acid CSI was also identified in the T2 turn of major

clade homologs, but the significance was not determined. It would be interesting to know if the two-amino acid CSI in the T2 turn of the major clade has a similar effect as the four-amino acid CSI in the T2 turn of minor clade PagP proteins.

Overall, it is clear that the determinant for PagP lipid A positional specificity is multifactorial, but the biochemical principle that can be concluded here is that all the PagP proteins investigated, from both the minor and major clades, function to modify lipid A by the addition of a palmitate. Further, the specific incorporation of the palmitate at the 3'-position of lipid A that is observed by the major clade BbPagP and minor clade PaPagP and HePagP is yet another similarity between the two clades of PagP proteins. This lipid A 3'-position regiospecificity may have been the original design of the enzyme, which has evolved to acquire lipid A 2-position regiospecificity as is exhibited in EcPagP (Bishop et al. 2000; Thaipisuttikul et al. 2014).

Chapter 3.0

Characterization of chromosomal and plasmid-based subclades of PagP

3.1 Preface

This chapter is focused on the characterization of chromosomal and plasmid-based subclades of PagP. Dr. Bishop and I designed the experiments and wrote the manuscript together. The *E. coli* DIXCO3 strain and EcPagP mutants were constructed by Charneal Dixon. Lipids for mass spectrometry were prepared by Charneal Dixon and analyzed by Dr. Theresa Garett of Vassar College.

3.2 Summary

The *pagP* gene is usually found as a single copy, but some bacteria have two copies located either on the chromosome, or one on the chromosome and one on a plasmid. These PagP homologs branch into two subclades: namely, “chromosomal”, and “plasmid”-based PagP homologs. Our objective was to elucidate PagP structure-function relationships in order to distinguish the lipid interactions associated with these two PagP subclades. We characterized chromosomal Ko1PagP and plasmid-based Ko2PagP homologs from *Klebsiella oxytoca* and compared them with PagP from *E. coli* (EcPagP) using both *in vitro* detergent micellar assays and *in vivo* expression in bacterial outer membranes (OMs). Both Ko1PagP and EcPagP exhibit a putative charge relay system reminiscent of the chymotrypsin active site on the periplasmic side of the enzyme where the residues D61 and H67 interact with Y87. The putative charge relay residues are naturally mutated to N61 (or S61) and S67 in Ko2PagP and other plasmid-based PagPs. EcPagP and Ko1PagP palmitoylate both lipid A and PG *in vitro*, whereas Ko2PagP only palmitoylates lipid A. Furthermore, EcPagP and Ko1PagP effectively use PG as an

acceptor substrate to form palmitoyl-PG (PPG), *bis*(monoacylglycero)phosphate (BMP), and lysophosphatidylglycerol (LPG) *in vitro*. Switching the charge relay residues between Ko1PagP and Ko2PagP resulted in a conformational change that is associated with phospholipid::lysophospholipid transacylation and palmitoylation of PG. However, in bacterial OMs, unlike EcPagP, Ko1PagP and Ko2PagP only palmitoylate lipid A. The periplasmic Y87 residue is critical for production of BMP and LPG, but H67 is not required. The putative charge relay system residues probably function instead to influence the PagP β-barrel shear number, which can be translated across the bilayer to influence the expansion of PG into other glycerophosphoglycerol phospholipids PPG, BMP, and LPG.

3.3 Introduction

Protein function is often intimately related to conformational dynamics. The change in protein conformation may be subtle, involving the interplay of a few amino acid side chains, or large, involving drastic changes within the entire structure (Teilum et al. 2011; Horovitz & Fersht 1990). Proteins are highly cooperative structures, a perturbation that changes conformation can potentially interfere with ligand interaction (Seo et al. 2014; Hammes 2002). For membrane proteins, this correlation between subtle conformational changes and ligand interaction is not easily assessed because of their naturally hydrophobic microenvironment. To gain a comprehensive understanding of a protein it is beneficial to know the three-dimensional structure, preferably with bound substrates, but this takes the protein out of its natural environment and is often difficult to

achieve (Hite et al. 2008). In this study, duplicate copies of the outer membrane (OM) enzyme PagP from *Klebsiella oxytoca* afford a unique opportunity to investigate structure-function relationships that illustrate how control of conformational flexibility relates to enzymatic catalysis. Understanding how to manipulate the interplay between intrinsic conformational changes and function is not only of basic scientific interest, but it can be applied to protein engineering (Teilum et al. 2011).

PagP enzymatically transfers a palmitate chain from a phospholipid to lipid A in many Gram-negative bacteria. Palmitoyl-lipid A confers resistance to host immune defenses and influences the activation of the mammalian host immune response during bacterial infection (Bishop et al. 2000; Bishop 2005). In some bacteria PagP also palmitoylates the headgroup of phosphatidylglycerol (PG) forming palmitoyl-PG (PPG). PPG is believed to increase the hydrophobicity of the OM and, therefore, could contribute to the local barrier function at specific sites on the bacterial cell surface (Dalebroux et al. 2014).

PagP is a small eight-stranded β-barrel protein with an *N*-terminal amphiphatic α-helix (Ahn et al. 2004; Cuesta-Seijo et al. 2010; Hwang et al. 2004; Hwang et al. 2002) (Figure 3.1A). The PagP x-ray crystal structure spans the OM with a 25^{o} tilt to the membrane normal (Ahn et al. 2004) and exhibits an extracellular active site with residues H33, S77 and R114 on flexible loops (Hwang et al., 2002; Bishop Unpublished). The interior of the enzyme has an unusual hydrophobic ligand-binding pocket called the

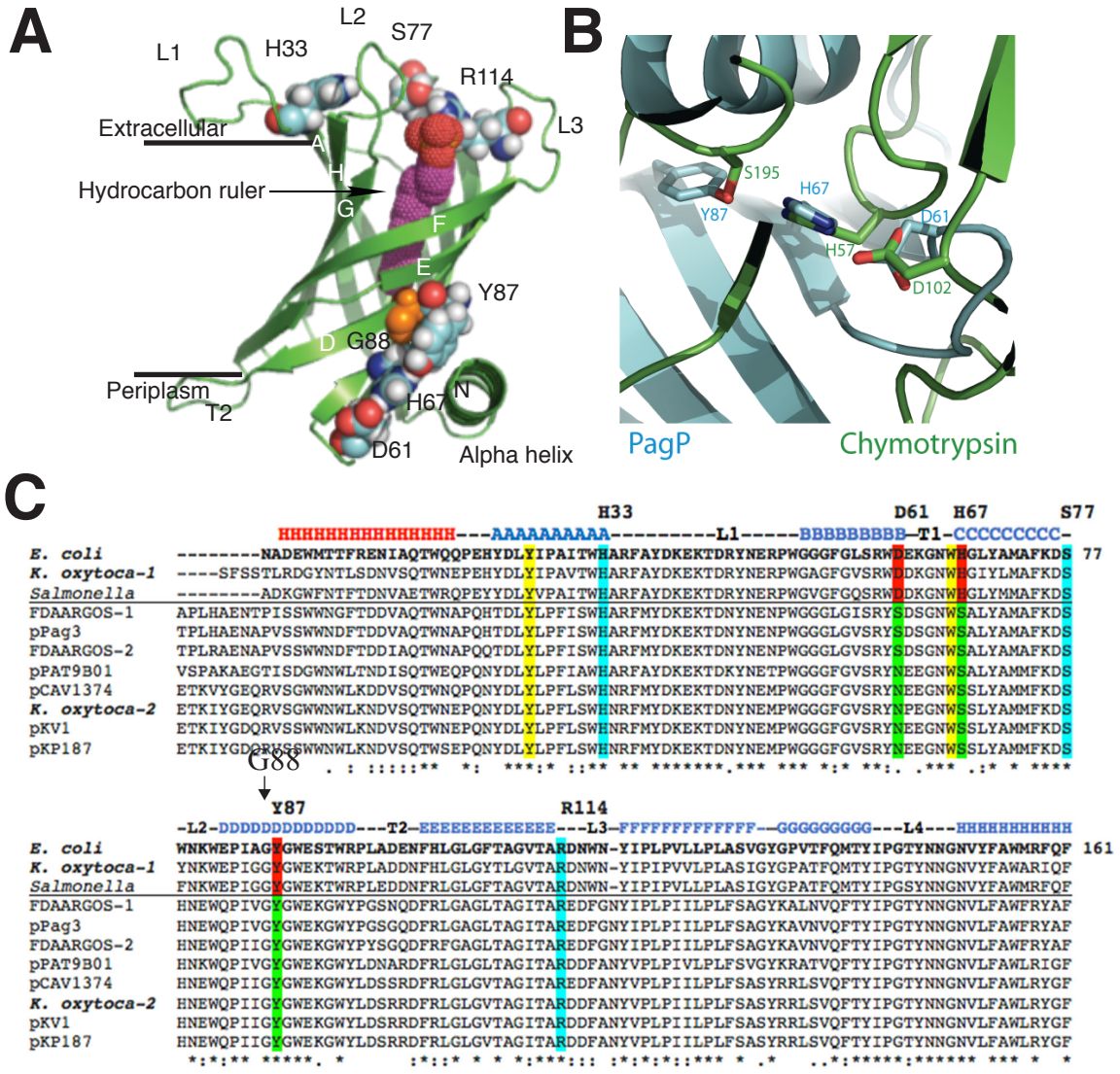

Figure 3.1. Putative charge relay system or catalytic triad on the periplasmic side of PagP. A. PagP crystal structure in SDS/MPD (PDB 3GP6). PagP is an eight stranded antiparallel β-barrel protein. It has extracellular catalytic residues H33, S77 and R114, and proposed catalytic triad D61, H67 and Y87 on the periplasmic side. The hydorcarbon ruler is delineated with a SDS molecule. G88 is at the base of the hydrocarbon ruler (orange spheres). B. PagP superimposed onto chymotrypsin showing the proposed novel catalytic triad residues D61, H67 and Y87. C. Multiple sequence alignment of the plasmid PagPs compared to known chromosomal PagPs. PagP homologs from the chromosome are italized and those found on plasmids have regular fonts. The extracellular catalytic residues are highlighted in blue, the periplasmic catalytic triad for the chromosomal PagPs is in red and the plasmid-based triad is in green. The conserved residues T26 and W66 responsible for the exciton are highlighted in yellow.

hydrocarbon ruler (Ahn et al. 2004). Structural dynamics revealed by NMR spectroscopy illustrate that PagP alternates between a relaxed R state, possibly to facilitate substrate access, and a tense T state, when substrates bind through an induced-fit mechanism (Hwang et al. 2004; Hwang et al. 2002).

PagP remains dormant in the OM and is triggered by OM lipid asymmetry perturbations, which allow phospholipids and lipid A to access the active site from the external leaflet (Jia et al. 2004). PagP selects a C16 palmitate chain with exquisite specificity by using an elaborate mechanism involving the hydrocarbon ruler and a gate in the β-barrel wall known as the crenel. Phospholipid acyl chains enter the hydrocarbon ruler through the crenel, which effectively blockades C18 acyl chains esterified at the phospholipid *sn*-2 position (Cuesta-Seijo et al. 2010; Khan et al. Unpublished). The hydrocarbon ruler tightly binds to the distal six methylene units, enabling a C16 palmitate when fully extended to be in perfect registration with the active site residues, therefore excluding C14 acyl chains esterified at the *sn*-1 position (Khan et al. Unpublished). An unrestrained molecular dynamics simulation of PagP in a membrane environment revealed that R114 stabilizes the phospholipid head-group as the *sn*-1 palmitoyl group docks into the hydrocarbon ruler (Bishop Unpublished). H33 and S77 are the key catalytic residues that facilitate the acyltransferase reaction in accordance with a sequential or ternary complex reaction mechanism (Unpublished observations). Lipid A accesses the *sn*-1 palmitoyl group bound in the hydrocarbon ruler PagP through another opening in the β-barrel wall known as the embrasure, located opposite the crenel and

flanked by residues Pro28 and Pro50. The embrasure is the main site from which acyl chain extraction from the hydrocarbon ruler is possible, but a minor site between β-strands B and C is also implicated (Figure 3.1A) (Cuesta-Seijo et al. 2010). Reversibly blocking the embrasure with a disulfide bridge in a Pro28Cys/Pro50Cys double mutant prevented lipid A palmitoylation without affecting the slow phospholipase reaction, but lipid A palmitoylation activity was again restored when the disulfide bridge was reduced (Khan & Bishop 2009).

An interesting feature observed on the periplasmic side of PagP is a motif resembling the catalytic triad of the proteolytic enzyme chymotrypsin (Figure 3.1B). The main difference is that S195 in chymotrypsin is replaced by Y87 in PagP, and the charge relay residues D102 and H57 in chymotrypsin are replaced by D61 and H67 in PagP (Figure 3.1B). The analogous mechanism we initially imagined for this putative catalytic triad involved D61 polarizing H61 so it could function as a general base to deprotonate the phenolic hydroxyl group of Y87, thus rendering it nucleophilic for catalysis. Y87 is conserved among all PagP homologs from this clade (Figure 3.1C), but D61 and H67 are substituted by asparagine and/or serine, respectively, in PagP homologs that are plasmid-based. This suggests that mutational pressure may have selected an "inactive" charge relay system in PagP homologs originating from plasmids.

PagP homologs from plasmids belong to a group of bacteria from the γ-Proteobacteria that encode two copies of *pagP* on the chromosome, or one on the

chromosome and another on a plasmid. Chromosomal PagP homologs are syntenic or conserved in the same genetic locus, whereas plasmid-based PagP homologs are randomly placed on the chromosome if they are not present in plasmids (Figure 3.1C). All bacteria with two PagP homologs are associated with plants and have a role in nitrogen fixation or denitrification (Cakmakci et al. 1981; Raju et al. 1972; Lin et al. 2012; Sandhiya et al. 2001; Thijs et al. 2014).

In this work, the two PagP homologs from *Klebsiella oxytoca* were investigated. *K. oxytoca* is a member of the *Enterobacterales* order and the *Klebsiella* clade, and it is closely related to the highly pathogenic *K. pneumoniae* (Alnajar and Gupta 2017). It is now considered a clinically significant pathogen associated with nosocomial infections (Darby et al. 2014; Singh et al. 2016). *K. oxytoca* has two *pagP* genes in its genome that we identify as Ko1PagP and Ko2PagP. The two *pagP* genes are found on separate strands of the chromosomes. Ko1*pagP* is the first of the two that shows up at 3074Kb on the positive strand, while the second Ko2*pagP* shows up at 5235Kb on the negative strand, using strain KCTC 1686 (ATCC 8724) as reference. At the amino acid level, Ko1PagP is 61% identical to Ko2PagP. EcPagP shares 83% and 59% amino acid identity with Ko1PagP and Ko2PagP, respectively.

Here we report the biochemical characterization of chromosomal and plasmid-based subclades of PagP. The chromosomal PagP exhibits a putative D61/H67 charge relay system at the periplasmic side of the enzyme in addition to an extracellular active

site that palmitoylates lipid A and PG. Plasmid-based PagP palmitoylates lipid A, but not PG, and lacks the putative charge relay residues. Mutational switching of the charge relay residues caused a conformational change that affected the function of the enzymes in PG transacylation and palmitoylation. Our results show that we can control these reactions in a detergent micellar assay system. Although our results show the duplicated homologs from *K. oxytoca* can only palmitoylate lipid A in bacterial OMs, we established that Y87 from EcPagP was critical to control the expansion of glycerophosphoglycerol phospholipids PG and PPG to form *bis*(monoacylglycero)phosphate (BMP), and lysophosphatidylglycerol (LPG). Therefore, we have established that EcPagP is a multifunctional enzyme with active sites disposed on either side of the OM. Furthermore, we establish that PagP has been adapted during evolution in plasmids to be monofunctional as a lipid A palmitoyltransferase. Based on our results, and known PagP structure-function relationships, we propose a model for how PagP structural perturbations allow it to switch between multifunctional and monofunctional conformational states.

3.4 Materials and methods

3.4.1 Bacterial strains, plasmids and growth conditions

The bacterial strains and plasmids used are described in Table 3.1. Cells were generally grown at 37 ºC on semi-solid or liquid LB media consisting of 10 g Tryptone, 5 g yeast extract, 10 g NaCl and 15 g agar (for semi-solid media). Antibiotics were added as necessary at final concentrations of 100 μg/mL for ampicillin, 15 μg/mL for gentamicin,

25 μg/mL for kanamycin and 30 μg/mL for chloramphenicol. The term "overnight culture" refers to a liquid culture in LB broth inoculated with a single bacterial colony from semi-solid media and allowed to incubate for 16 to 18 hours.

Table 3.1. Bacterial strains and plasmids used

Strains /Plasmids	Description	Source
***E. coli* K-12 strains**		
W3110	Wild type	Smith et al. 2008
MC1061	F^-, λ^-, *araD139,* Δ*(ara-leu)7697,* Δ *(lac)X74, galU, galK, hsdR2* (r_K-m_K+), *mcrB1, rpsL*	Casadaban & Cohen 1980
WJ0124	MC1061 *pagP::amp*^{r}	Jia et al. 2004
SK1061	MC1061 *msbB::*Tn5 (kan^r), *pagp::amp*^{r}	Smith et al. 2008
C41(DE3)	F^- *ompT hsdS*B (rB- mB-) *gal dcm* (DE3)	Lucigen
BKT09	BW25113Δ*pagP*, Δ*lpxP*, Δ*lpxL*, Δ*lpxM::*Kan	Tan et al. 2012
BKT12	W3110 Δ*clsA,* Δ*clsB,* Δ*clsC*:: Kan^R	Tan et al. 2012
DIXC03	BKT12 Δ*pagP::*Apr^R	Charneal Dixon
Plasmids		
pBADGr	*ori araC-*P_{BAD} *dhfr*::Gm^r mob^+	Asikyan et al. 2008
pKo1PagP	pBADGr with *Klebsiella Ko1pagP*	This study
pKo2PagP	pBADGr with *Klebsiella Ko2pagP*	This study
pEcPagPS77A	pBADGr with *E. coli EcPagPS77A*	Charneal Dixon
pEcPagPY87F	pBADGr with *E. coli EcPagPY87F*	Charneal Dixon
pUCP20	*Escherichia-Pseudomonas* shuttle vector, *bla*, P*lac*	West et al. 1994
p'Ko1PagP	pUCP20 with *Ko1pagP*	This study
p'Ko2PagP	pUCP20 with *Ko2pagP*	This study
p'EcPagPS77A	pUCP20 with *EcpagPS77A*	This study
p'EcPagPY87	pUCP20 with *EcpagPY87F*	This study
pET21a(+)	*T7 lac promoter and terminator MCS, C-terminal His-tag* Amp^R	Novagen
Ko1PagP	pET21a(+) with *Ko1pagP*	This study
Ko1PagPD61N	Derivative of pET21a/*Ko1PagP*	This study
Ko1PagPH67S	Derivative of pET21a/*Ko1PagP*	This study
Ko1PagPD61N/H67S	Derivative of pET21a/*Ko1PagP*	This study
Ko1PagP117::118N	Derivative of pET21a/*Ko1PagP*	This study
Ko2PagP	pET21a(+) with *Ko2PagP*	This study
Ko2PagPN61D	Derivative of pET21a/*Ko2PagP*	This study
Ko2PagPS67H	Derivative of pET21a/*Ko2PagP*	This study
Ko2PagPN61D/S67H	Derivative of pET21a/*Ko2PagP*	This study
Ko2PagPΔN118	Derivative of pET21a/*Ko2PagP*	This study
Ko2PagPN118A	Derivative of pET21a/*Ko2PagP*	This study
Ko2PagPN118R	Derivative of pET21a/*Ko2PagP*	This study

3.4.2 DNA manipulations

Plasmid were isolated using a QIAprep Spin Miniprep Kit from Qiagen or Invitrogen. Isolations were done according to manufacturer's instructions for high copy number plasmids (e.g. pET21a+). For low copy plasmids (e.g. pBADGr) 5 or 10 mL of the sample was harvested initially and the remainder of the protocol followed according to manufacturer's instruction. Site directed mutagenesis on various protein sequences were done using the QuikChange site directed mutagenesis kit by Agilent according to the manufacturer's specification, primers are listed in Table 3.2. Briefly, the reaction included 20 ng DNA template, 125 ng each of the forward and reverse primers, 5 µL 10X reaction buffer, 1 µL dNTPs, 3 µL QuikSolution, sterile distilled water was added for a total volume of 50 µL and 1 µL pfu DNA polymerase. The PCR conditions for site directed mutagenesis includes an initial 1 min denaturation at 95 ^{o}C, 18 cycles of 50 secs at 95 ^{o}C, 50 secs at 60 ^{o}C, 1 min/kb of plasmid length at 68 ^{o}C, final extension for 7 mins at 68 ^{o}C and the reaction was held at 4 ^{o}C. 1 µL of Dpn1 enzyme was added to the reaction mixture and then it was incubated at 37 ^{o}C for 1 hr. The mutated DNA was transformed into XL1 Gold competent cells and the cells of interested selected on LB agar supplemented with ampicillin. Mutations were confirmed by DNA sequencing (MOBIX, McMaster University).

Table 3.2. Primers used for site directed mutagenesis

KoPagP mutants	Primers (5'-3')
Ko1PagP	
D61N	**F**: ATGCCAATTACCTTTATCATTCCAACGGCTAACACCAAAAC **R**: GTTTTGGTGTTAGCCGTTGGAATGATAAAGGTAATTGGCAT
D61N/H67S	**F**: ATGCCAATTACCTTTATCATTCCAACGGCTAACACCAAAAC **R**: GTTTTGGTGTTAGCCGTTGGAATGATAAAGGTAATTGGCAT **F**: GAAGGCCATCAGATAAATACCACTCCAATTACCTTTATCATCCCAACG **R**: CGTTGGGATGATAAAGGTAATTGGAGTGGTATTTATCTGATGGCCTTC
Ko2PagP	
N67D	**F**: TTACCTTCCGGATCATAACGGCTAACACCAAAACCACC **R**: GGTGGTTTTGGTGTTAGCCGTTATGATCCGGAAGGTAA
N61D/S67H	**F**: TAAACATCATTGCATACAGGCTGTGCCAATTACCTTCCGGATTATAAC **R**: GTTATAATCCGGAAGGTAATTGGCACAGCCTGTATGCAATGATGTTTA **F**: TTACCTTCCGGATCATAACGGCTAACACCAAAACCACC **R**: GGTGGTTTTGGTGTTAGCCGTTATGATCCGGAAGGTAA

3.4.2.1 Chemical transformation

To prepare chemically competent cells for protein analysis in the outer membrane, the calcium chloride method was applied. 50 mL of LB was inoculated with 1% overnight culture of the appropriate bacteria and was allowed to grow at 37 ºC at 200 rpm to OD 0.4-0.6. The cells were placed on ice for 10 mins. All remaining steps were carried out at 4 ºC. The cells were harvested at 6000 rpm for 3 mins. The supernatant was discarded, and the pellet was gently resuspended in 10 mL cold 0.1 M $CaCl_2$. The resuspended cells were incubated on ice for 20 mins then centrifuged as above. The supernatant was discarded and gently resuspended in 5 mL solution of cold 0.1 M $CaCl_2$ and 15% glycerol. The competent cells were dispensed into microtubes and used immediately (kept on ice) or stored at 80 ºC.

To transform these cells, 1 µL of the plasmid DNA was added to 100 µL of freshly made or thawed competent cells in a microtube. The microtube was then placed on ice for 30 mins. The cells were then heat shocked at 42 ºC for 45 secs and then chilled on ice for 2 mins. 500 µL of SOC media was added to the cells and they were outgrown at 37 ºC for 1 hr. The cells were centrifuged at 8000 rpm for a min, 400 µL of the supernatant was discarded. The remaining 100 µL of supernatant was used to resuspend the cells and plate on LB with appropriate antibiotic.

3.4.2.2 Electroporation

To transform *E. coli* cells by electroporation, 10 mL of LB was inoculated with 1% overnight culture, grew at 37 ºC and 200 rpm until the cells reached an OD_{600} of 0.4. Cultures were transferred into centrifuge tubes and placed on ice for 15 mins. Cultures were then centrifuged at 4000 rpm for 15 mins, and the supernatant was discarded. Cells were washed with 10% cold glycerol and centrifuged at 3800 rpm for 20 mins and the supernatant discarded (this step was repeated). The pellet was re-suspended in 50 µL of 10% cold glycerol. 100 ng of DNA was added to the re-suspended culture and then transferred to a cold electroporation cuvette, a voltage of 1800 was used. Cells were then outgrown at 37 ºC and 200 rpm for 90 mins and then selected for by the appropriate antibiotic on LB plates.

3.4.3 Protein expression and purification

The DNA sequences for all proteins without the signal peptide used in this study were synthesized and purchased from Invitrogen GeneArt™. The sequences were cloned into the pET21a+ plasmid using restriction enzymes NdeI, which adds a Met residue to the mature N-terminal end of the protein and XhoI, which add two residues Leu and Glu to the carboxylic end of the protein preceding the X6 His-tag from the plasmid. The procedure depends on isopropyl β-D-thiogalactoside (IPTG) induction in *E. coli* C41(DE3) (Khan et al. 2007).

3.4.3.1 Small scale protein analysis

10 mL cultures were grown at 37 ºC and 200 rpm, after a 1% overnight inoculum, until the culture reached an OD_{600} of 0.5 (~2.5 hrs). pET21a+ (empty negative control) was also grown and analyzed. The cells were then inoculated with and without IPTG for a final concentration of 1 mM and grown for 4 hrs. 1 mL of the cells was collected and harvested in 1.5 mL microtubes for 3 mins at 8000 rpm. The supernatant was discarded, and the pellet was used for analysis or stored at -20 ºC for later use.

The cells are re-suspended in 100 µL lysis buffer (50 µM Tris HCl pH 8, 150 mM NaCl, 1% SDS). Samples were boiled at 100 ºC for 10 mins. 5 µL of the lysed cells was used for protein concentration determination using bicinchoninic acid assay (BCA) (Smith et al. 1985). 80 µg of crude protein extracts were mixed in an equal volume of 2X SDS buffer (100 mM Tris-HCl pH 6.8, 4% (w/v) SDS, 0.2% (w/v) bromophenol blue,

200 mM dithiothreitol (DTT)) and boiled at 100 °C for 10 min. The SDS-PAGE on 1.5 mm thick 13% acrylamide gels was performed with Bio-Rad Protean II XI apparatus and operated at 150 V. Gels were stained with Coomassie Blue dye and destained (methanol, acetic acid and water 40/10/50 v/v) overnight.

3.4.3.2 Large scale protein expression and purification

1L cultures were grown at 37 °C and 200 rpm, after a 1% overnight inoculum, until the culture reached an OD_{600} of 0.5 (2.5 hrs). Cells were then inoculated with IPTG for a final concentration of 1 mM, and left to grow for 4 hrs. Cells are harvested by centrifugation, the supernatant was discarded, and the pellet stored at -80 °C or isolation was continued. Harvested cells were re-suspended in isolation buffer (50 mM Tris-HCl at pH 8.0, 5mM EDTA) and lysed mechanically with a French Press 40K cell at 800 psi. The lysate is pelleted at 27000 rpm using an optima ultracentrifuge MLA-80 rotor at 4 °C for 20 mins. This pellet is re-suspended in 50 mM Tris-HCl pH 8.0, 2% Triton X-100 and centrifuged as above. This pellet is re-suspended in 50 mM Tris-HCl at pH 8.0 and centrifuged using a Sorval RC-58 at 8000 rpm in a sorval SS-34 rotor for 20 mins. This pellet is re-suspended in 50 mM Tris-HCl at pH 8.0, 6 M guanidine-HCl, centrifuge as previous and the resulting supernatant is the crude denatured protein. All supernatants were collected for further analysis if necessary.

Crude protein samples were purified using Ni^{2+} charged ion-exchange chromatography. The column was charged with 5 column volumes of 50 mM $NiSO_4$ and

equilibrated with 3 column volumes of 100 mM Tris-HCl (pH 8.0), 250 mM NaCl, 6 M guanidine and 5 mM imidazole. Crude protein sample is added to the column slowly and washed with 10 column volumes of the previous buffer and then with 20 column volumes with the same buffer containing 20 mM imidazole. The protein was then eluted step-wise with 5 mL of the same buffers, but with increasing concentration of imidazole 35, 50, 75, 100 and 125 mM. The 100 and 125 mM fractions were pooled and dialyzed against water. The precipitated protein is collected by centrifugation using the Sorval SS-34 rotor at 8000 rpm for 20 mins.

3.4.4 Protein Electrospray Mass Spectrometry

Approximately 1μg of the wet pellet from the water dialyzed protein was sent to the McMaster Regional Centre of Mass Spectrometry (MRCMS). The protein was diluted 50 folds into a solution of 1:1 (v/v) 1% formic acid and acetonitrile just prior to injection into Agilent 6210 TOF mass spectrometer using methanol as the mobile phase. The multiple charged ion region was selected and the mass to charge of the protein was deconvoluted using max entropy.

3.4.5 Protein refolding and analysis on SDS PAGE

Precipitated protein samples were dissolved in 10 mM Tris-HCl (pH 8.0) and 6 M Gdn-HCl. These samples were diluted dropwise into a 10-fold excess of 100 mM Tris-HCl and 0.5% lauroyldimethylamine-*N*-oxide (LDAO) at room temperature with vigorous stirring and left to stir overnight at 4 ^{o}C. The samples were then loaded on a 4

mL bed of His-bind resin charged with 50 mM $NiSO_4$ and equilibrated with 10 mM Tris-HCl (pH 9.0), 0.1% LDAO, and 5 mM imidazole. The protein samples were washed with 10 column volumes wof the equilibrium buffer and then with 10 column volumes of 10 mM Tris-HCl (pH 9.0), 0.1% LDAO, and 20 mM imidazole. The refolded proteins were eluted with 10 mM Tris-HCl (pH 9.0), 0.1% LDAO, and 250 mM imidazole. The protein is then dialyzed against 100 mM Tris-HCl (pH 9.0), 0.1% LDAO overnight.

Refolded protein concentrations were determined using the BCA (Smith et al., 1985). 80 μg of protein extracts were solubilized in an equal volume of 2X SDS buffer (100 mM Tris-HCl pH 6.8, 4% (w/v) SDS, 0.2% (w/v) bromophenol blue, 200 mM DTT) with or without boiling for 10 min where indicated. SDS-PAGE on 1.5 mm thick 15% acrylamide gels was performed with Bio-Rad Protean II XI apparatus and operated at 150 V. Gels were stained with Coomassie Blue dye and destained (methanol, acetic acid and water 40/10/50 v/v) overnight.

3.4.6 Far-UV circular dichroism spectroscopy

The samples were analyzed by CD according to Khan et al (2007). Briefly, samples were maintained at 0.3 mg/mL in 0.1% LDAO and 100 mM Tris-HCl (pH 8.0) in a 1 mm path length cuvette specific for CD analysis. The samples were analyzed with an Aviv 250 CD spectrometer which was linked to a Peltier device Merlin Series M25 for temperature control. The temperature was maintained at 25 ^{o}C for wavelength scans and data sets were obtained between 200 to 260 nm for most samples. The samples were

maintained at the same concentration for thermal unfolding profiles. The samples were heated from 25 to 100 ºC at a rate of 2 ºC/min, with a response time of 16 secs.

3.4.7 Phospholipase activity assay

Phospholipase reactions were set up with a final concentration of 20 μM of ^{14}C-*sn-1,2*-dipalmitoyl phosphatidylcholine (^{14}C-DPPC) at 4000 cpm/uL to monitor the phospholipase reaction on a thin layer chromatography (TLC) plate. To the ^{14}C-DPPC were added final concentrations of 1 mM cold DPPC and 10 ng/μL of the enzyme in a 25 μL reaction that was buffered by100 mM Tris HCl (pH 8.0), 0.25% *n*-dodecyl-β-D-maltoside (DDM) and 10 mM EDTA. Phospholipids dissolved in chloroform were first dried down (one and then the other) under a stream of nitrogen prior to the addition of 22.5 μL of reaction buffer, and the reaction was initiated with the addition of 2.5 μL of a 10 ng/μL of the enzyme. The enzyme was serially diluted from the inhibitory LDAO detergent into a DDM dilution buffer that supports activity (100 mM Tris HCl pH 8 and 0.25% DDM). A no enzyme negative control (DDM dilution buffer), and a phospholipase A_2 (PLA_2) positive control were also used in these reactions. PLA_2 uses its own aqueous reaction buffer (100 mM Tris HCl pH 8.0, 0.25% DDM and 10 mM $CaCl_2$). Reactions were carried out at 30 ºC overnight (16-18 hrs) and were terminated by adding 2.5 μL (10000 cpm ^{14}C-DPPC) of the reaction directly to the origin of G25 silica TLC plates. The plates were resolved in sealed glass tanks that were previously equilibrated for ~ 3 hrs with solvent system chloroform/methanol/water (65:25:4 v/v), dried and exposed to a

Molecular Dynamics Phosphorimager screen overnight. The products were visualized using a Molecular Dynamic Typhoon 9200 Phosphorimager.

3.4.8 Lipid A acyltransferase assay

Acyltransferase assays were done either with ^{14}C-DPPC or with ^{32}P orthophosphate-lipid IV_A to monitor the reactions. Final concentrations of 20 μM ^{14}C-DPPC, 1 mM of cold DPPC, 100 μM of synthetic lipid IV_A (re-suspended in the reaction buffer 100 mM Tris HCl pH 8.0, 0.25% DDM and 10 mM EDTA) with 10 ng/μL of the enzyme were used in a 25 μL reaction volume. Whereas for ^{32}P orthophosphate monitored assays, reactions were set up with final concentrations of 1 mM of cold DPPC, 100 μM ^{32}P orthophosphate-lipid IV_A (extracted from *E. coli* cells see below) along with 10 ng/μL of the enzyme were used. The phospholipids dissolved in chloroform were dried separately under a stream of N_2 prior to the addition of 22.5 μL of lipid IV_A dissolved in the aqueous reaction buffer. The lipids were re-suspended by alternately sonicating and vortexing. A no enzyme control and a PLA_2 positive control (PLA_2 control only for ^{14}C monitored reactions) were also used for these reactions. The reactions are initiated with the addition of 2.5 μL of a 10 ng/μL of the enzyme. The reactions progressed for various time periods from 10 mins to 16 hrs and are terminated by adding 2.5 μL (~10000 cpm for ^{14}C or 200 cpm for ^{32}P orthophosphate) of the reaction directly to the origin of a G25 (^{14}C-radiolabeled reactions) or Silica 60 (^{32}P orthophosphate-radiolabeled) TLC plate. For ^{14}C monitored reactions the plates were resolved in sealed glass tanks that were equilibrated with solvent system chloroform/methanol/water 65:25:4 (v/v). For ^{32}P

orthophosphate-monitored reactions, the plates were resolved in sealed glass tanks that were previously equilibrated for ~ 3 hrs with solvent system chloroform/pyridine/88% formic acid/water 50:50:16:4 (v/v). The plates were dried and exposed to a Molecular Dynamics Phosphorimager screen overnight. The products were visualized using a Molecular Dynamic Typhoon 9200 Phosphorimager and quantified by ImageQuant software.

3.4.8.1 Hydrocarbon ruler assay

These reactions were conducted as acyltransferase assays with a suite of phospholipid donors and a radiolabeled acceptor for monitoring on a TLC plate. Reactions were set up with final concentrations of 1 mM of cold *sn-1,2*- diacyl-phosphatidylcholines ranging from C12 to C18, 100 μM ^{32}P orthophosphate-labeled lipid IV_A (extracted from *E. coli* cells see below) along with 10 ng/μL of the enzyme. The phospholipids in chloroform were dried separately under a stream of N_2 prior to the addition of 22.5 μL of ^{32}P orthophosphate-labeled lipid IV_A dissolved in the aqueous reaction buffer. The lipids are re-suspended by alternately sonicating and vortexing. The remainder of the procedure is as described for acyltransferase assays above.

3.4.9 PG acyltransferase assay

PG acyltransferase reactions were conducted with ^{14}C-DPPC to monitor the reaction. Cold *sn*-1,2-dipalmitoyl phosphatidylglycerol (DPPG) or 1-palmitoyl-2-oleoyl-*sn*-glycero-3-phosphatidylglycerol (POPG) were used as the acceptor substrates. For

these reactions, final concentrations of 20 μM of ^{14}C-DPPC, 1 mM of cold DPPC were added to the tube and dried separately under a stream of N_2, 100 μM of DPPG or POPG dissolved in the reaction buffer (100 mM Tris HCl pH 8.0, 0.25% DDM and 10 mM EDTA) was added and re-suspended by alternately sonicating and vortexing. 10 ng/μL of the enzyme was used in a total reaction volume of 25 μL. A no enzyme negative control (DDM dilution buffer), and a phospholipase A_2 (PLA_2) positive control were also used in these reactions. PLA_2 uses its own aqueous buffer (100 mM Tris HCl pH 8.0, 0.25% DDM and 10 mM $CaCl_2$). 2.5 μL of the reaction was spotted on the TLC plate to stop the reaction at appropriate time. Reactions times are usually 30, 60, 120, 240, 360 mins intervals. The plates were resolved in sealed tanks that were previously equilibrated for ~ 3 hrs with solvent system consisting of chloroform/methanol/acetic acid in a ratio of 65:25:5 (v/v). The plates were dried and exposed to a Phosphorimager screen overnight. The products were visualized using a Molecular Dynamic Typhoon 9200 Phosphorimager and quantified by ImageQuant software.

3.4.10 ^{32}P orthophosphate-lipid IV_A extraction

^{32}P orthophosphate-lipid IV_A extractions were performed using a mild acid hydrolysis reaction that disrupts the labile ketosidic bond and cleaves the Kdo sugar residues from lipid A without affecting the distribution of acyl chains (Smith et al. 2008; Zhou et al. 1999). *E. coli* BKT09 strain (Table 3.1) was used for these extractions. A 1% inoculum of overnight culture was subcultured into 20 mL fresh LB media with 12.5 μg/μL kanamycin and 50 μL of ^{32}P orthophosphate for labeling. The cells were grown for

2 hrs 55 mins after which 25 mM of EDTA was added and the cells allowed to grow for an additional 5 mins prior to harvesting in a clinical centrifuge at high speed for 10 mins. The cells were then washed with 10 mL 1 X PBS before re-suspended in 0.8 mL PBS and subsequent addition of 1 mL chloroform and 2 mL methanol, then left at room temperature for 1 hr. The cells were pelleted and washed with 5 mL of single phase Bligh/Dyer (chloroform/methanol/PBS - 1:2:0.8) and pelleted at high speed in a clinical centrifuge for 5 mins. The pellet was then dispersed in 1.8 mL of 12.5 mM sodium acetate pH 4.5 and 1% SDS by sonic irradiation. This suspension was incubated at 100 ^{o}C for 30 mins and then cooled. The mixture was then converted to two-phase Bligh/Dyer by adding 2 mL chloroform and 2 mL methanol, vortexed and centrifuged at high speed for 10 mins. The lower phase was collected and washed with 4 mL upper phase of the two-phase Bligh/Dyer (chloroform/methanol/PBS – 2:2:1.8) centrifuged for 8 mins, collected lower phase and dried under a stream of N_2. The dried lipid was re-suspended in 100 µL of chloroform/methanol (4:1 v/v) by sonication with periodic icing. The re-suspended lipid was loaded on a TLC plate and was resolved in a sealed tank that was previously equilibrated for ~3 hrs with solvent system chloroform/ pyridine/ 88% formic acid/ water (50:50:16:5 v/v).

The resolved plate was air-dried or blow dried on cool setting. The TLC plate was exposed to a Phosphorimager screen for 1 hr. The relevant spot for lipid IV_A was located and scratched from the plate. The lipid was extracted from the scrapings with 5 mL single phase Bligh/Dyer after incubation for 1 hour. The mixture was centrifuged at high speed

for 5 mins and passed through a glass Pasteur pipette fitted with about a 2 cm glass wool. The filtered liquid was converted to two-phase by adding 1.3 mL chloroform and 1.3 mL 1x PBS vortexed and centrifuged for 5 mins. The lower phase was collected and dried under a stream of N_2. The dried pure lipid IV_A is re-suspended in 100 μL of chloroform/methanol (4:1 v/v). 2 μL was used for scintillation counts and the remaining lipid dried again. The lipid was then re-suspended in a sufficient volume of reaction buffer (100 mM Tris HCl pH 8.0, 0.25% DDM and 10 mM EDTA) to give each reaction spot a count of 200 cpm on the TLC plate. The pure ^{32}P orthophosphate-labeled lipid IV_A is then fed into enzymatic assays as described above.

3.4.11 PagP expression in bacterial OM: ^{32}P orthophosphate-labeled lipid analysis

PagP sequences with signal peptide from *K. oxytoca* were purchase from Invitrogen GeneArt™ in carrier plasmids. The sequences were designed for cloning into *Eco*RI and *Hin*dIII restriction sites of plasmid pBADGr (Table 3.1). Double digestion of the carrier plasmid (with the *pagP* gene) and pBADGr plasmid were conducted by standard cloning methods according to manufactures' protocol for Invitrogen restriction enzymes. The cut plasmid and *pagP* insert were gel purified and then extracted using Qiagen gel extraction kit. These were ligated with T4 ligase from the Invitrogen DNA ligase kit according to manufacturers' protocol. The ligated plasmid-PagP construct is transformed into XL1-Blue competent cells according to manufacturers' protocol. The plasmid-construct is isolated and transformed using chemically competent cells or

electroporation into *E. coli* strain or *K. oxytoca* strain for outer membrane protein expression.

Lipid A species and phospholipids from *E. coli* strain or *K. oxytoca* strains were analyzed by the mild acid hydrolysis method. The respective strains of bacteria from *E. coli* (and *K. oxytoca*) with and without *pagP* genes and complementation of *pagP* on low copy number plasmids (pBADGr or pUCP20) were analyzed for their lipid content (Table 3.1). A 1% inoculum of overnight culture was subcultured into 5 mL fresh LB media with 100 mg/mL ampicillin for cultures with pUCP20 and 15 mg/mL gentamicin for cultures with pBADGr, and 5 μL of ^{32}P orthophosphate for labeling. The cells were grown for 2 hrs 55 mins after which 25 mM of EDTA was added and the cells allowed to grow for an additional 5 mins prior to harvesting in a clinical centrifuge at high speed for 10 mins. The cells were then washed with 4 mL 1 X PBS before re-suspended in 0.8 mL PBS, and subsequent addition of 1 mL chloroform and 2 mL methanol, then left at room temperature for 1 hr. The cells were pelleted and the supernatant* was collected for phospholipid analysis. The remainder of this protocol is only for lipid A isolation. The pellet was washed with 5 mL of single phase Bligh/Dyer (chloroform/methanol/PBS - 1:2:0.8) and centrifuged at high speed. The pellet was then dispersed in 1.8 mL of 12.5 mM sodium acetate pH 4.5 and 1% SDS by sonic irradiation. This suspension was incubated at 100 ºC for 30 mins and then cooled. The mixture was then converted to two-phase Bligh/Dyer by adding 2 mL chloroform and 2 mL methanol vortexed and centrifuged at high speed for 10 mins. The lower phase was collected and washed with 4

mL upper phase of the two-phase Bligh/Dyer (chloroform/methanol/PBS – 2:2:1.8) centrifuged for 8 mins, collected lower phase and dried under a stream of nitrogen. 2 µL was added to 2 mL scintillation fluid for radiolabeled counts. 1000 cpm of the lipid A samples were spotted on the silica 60 TLC plate. The plate was resolved in a sealed tank that was previously equilibrated for ~ 3 hrs with solvent system chloroform/ pyridine/ 88% formic acid/ water (50:50:16:5 v/v).

3.4.12 Phospholipids analysis

To the supernatant* 2 mL of chloroform and 2 mL 1 X PBS were added, the suspension was vortexed and centrifuged at high speed. The lower phase was collected and dried under a low stream of N_2. The dried lipid was re-suspended in 200 µL of chloroform/methanol (4:1 v/v) by sonication with periodic icing. 2 µL was added to 2 mL scintillation fluid for radiolabeled counts. 10,000 cpm of the phospholipid samples were spotted on the silica 60 TLC plate. The plate was resolved in a sealed tank that was previously equilibrated for ~ 3 hrs with solvent system chloroform/methanol/acetic acid (65:25:5 v/v). The resolved plate was air-dried or blow dried on cool setting. The TLC plate was exposed to a Phosphorimager screen overnight. The products were visualized using a Molecular Dynamic Typhoon 9200 Phosphorimager.

3.4.13 Mass Spectrometry analysis of total phospholipids from *E. coli*

50 mL cultures were grown with appropriate antibiotic and induced with 0.2% arabinose to OD_{600} 1. Cells were harvested, and lipids were extracted as described in

phospholipid analysis, but without radiolabeling. The dried lipid was resuspended in 100 μL of chloroform/methanol (2:1, v/v) was analyzed using LC-ESI-Q-TOF mass as previously described (Bulat & Garrett 2011). The HPLC effluent (0.4 ml/min) from normal-phase chromatography on a Zorbax Rx-SIL column was analyzed using an Agilent 6520 quadrupole time-of-flight mass spectrometer in the negative-ion mode. Mass spectra were obtained for 100 to 2000 at 1 spectra per second with the following instrument parameters: fragmentor voltage -175 V, drying gas temperature -325 °C, drying gas flow -11 l/min, nebulizer pressure -45 psig, capillary voltage -4000V. Data were collected in profile mode with the instrument set to 3200 mass range under high resolution conditions at 2 GHz data acquisition rate. The instrument was calibrated using Agilent ESI- L low concentration tuning mix and under normal operating conditions the resolution of the instrument was ~15,000. The mass accuracy of the instrument was between 1 and 5 ppm, and, therefore measured masses are given to three decimal places. Data acquisition and analysis was performed using Agilent MassHunter Workstation Acquisition Software and Agilent MassHunter Work- station Qualitative Analysis Software (Agilent Technologies, Santa Clara, CA), respectively.

3.5 Results

3.5.1 Characterization of KoPagP homologs *in vitro*

The two PagP homologs from *K. oxytoca* and mutants obtained from site directed mutagenesis (Table 3.2 for primers) were expressed, purified and refolded. To achieve high concentrations, sequences were designed without their signal peptides so that the

proteins were overexpressed in the cytoplasm in the unfolded state and then refolded in detergent. Additionally, the *pagP* gene was placed behind the T7-RNA polymerase promoter and ribosome-binding site in plasmid pET21a+ (Bishop et al. 2000). The plasmid added a *C*-terminal His-tag to allow for affinity chromatography. DNA sequencing and ESI-MS verified the target proteins (Table 3.3).

Table 3.3 Electrospray mass spectrometry for Ko1PagP, Ko2PagP, and mutants

Protein	Theoretical Mass (Da)	ESI mass (Da)	Sequences
Ko1PagP	20367	20366	**M**SFSSTLRDGYNTLSDNVSQTWNEPEHYDLYIPAVT WHARFAYDKEKTDRYNERPWGAGFGVSRWDDKGN WHGIYLMAFKDSYNKWEPIGGYGWEKTWRPLADDN FHLGLGYTLGVTARDNWN-YIPIPVVLPLASIGYGPAT FQMTYIPGTYNNGNVYFAWARIQF**LEHHHHHH***
Ko1PagPD61N	20366	20365	**M**SFSSTLRDGYNTLSDNVSQTWNEPEHYDLYIPAVT WHARFAYDKEKTDRYNERPWGAGFGVSRW<u>N</u>DKGN WHGIYLMAFKDSYNKWEPIGGYGWEKTWRPLADDN FHLGLGYTLGVTARDNWN-YIPIPVVLPLASIGYGPAT FQMTYIPGTYNNGNVYFAWARIQF**LEHHHHHH***
Ko1PagPD61N/H67S	20316	20315	**M**SFSSTLRDGYNTLSDNVSQTWNEPEHYDLYIPAVT WHARFAYDKEKTDRYNERPWGAGFGVSRW<u>N</u>DKGN W<u>S</u>GIYLMAFKDSYNKWEPIGGYGWEKTWRPLADDN FHLGLGYTLGVTARDNWN-YIPIPVVLPLASIGYGPAT FQMTYIPGTYNNGNVYFAWARIQF**LEHHHHHH***
Ko2PagP	21404	21403	**M**ETKIYGEQRVSGWWNWLKNDVSQTWNEPQNYDL YLPFLSWHNRFMYDKEKTDNYNEMPWGGGFGVSRY NPEGNWSSLYAMMFKDSHNEWQPIIGYGWEKGWYL DSRRDFRLGLGVTAGITARDDFANYVPLPIILPLFSAS YRRLSVQFTYIPGTYNNGNVLFAWLRYGF**LEHHHH HH***
Ko2PagPN61D	21405	21406	**M**ETKIYGEQRVSGWWNWLKNDVSQTWNEPQNYDL YLPFLSWHNRFMYDKEKTDNYNEMPWGGGFGVSRY <u>D</u>PEGNWSSLYAMMFKDSHNEWQPIIGYGWEKGWYL DSRRDFRLGLGVTAGITARDDFANYVPLPIILPLFSAS YRRLSVQFTYIPGTYNNGNVLFAWLRYGF**LEHHHH HH***
Ko2PagPN61D/S67H	21455	21455	**M**ETKIYGEQRVSGWWNWLKNDVSQTWNEPQNYDL YLPFLSWHNRFMYDKEKTDNYNEMPWGGGFGVSRY <u>D</u>PEGNW<u>H</u>SLYAMMFKDSHNEWQPIIGYGWEKGWYL DSRRDFRLGLGVTAGITARDDFANYVPLPIILPLFSAS YRRLSVQFTYIPGTYNNGNVLFAWLRYGF**LEHHHH HH***

Wild type Ko1PagP and Ko2PagP were used as templates for subsequent point mutations. All protein sequences used in this study lacks the *N*-terminal signal peptide, which is replaced by a Met (in bold), and includes a C-terminal 6X His tag*. The amino acids that are substituted are underlined.

3.5.1.1 Evaluation of KoPagP refolding

EcPagP readily refolds in LDAO and exhibits temperature dependent shifts in electrophoretic mobility by SDS-PAGE (Ahn et al. 2004; Bishop et al. 2000). β-barrel OM proteins have a unique feature when analyzed using SDS-PAGE heat modifiability assays. The boiled samples run at a different rate than the unboiled samples due to the strong hydrogen bonding that holds the β-barrel together enabling these proteins to withstand denaturation by SDS in the absence of heating (Noinaj et al. 2015; Khan et al. 2007). We expected the KoPagP homologs to refold and show similar temperature related shifts on SDS-PAGE. Ko1PagP and Ko2PagP had single bands in each lane illustrating pure monomeric proteins. Both proteins were heat modifiable in that they showed band-shifts on the SDS-PAGE (Figure 3.2). In this SDS-PAGE (prepared inhouse) analysis the heated samples ran faster, while the unheated folded samples ran at the expected molecular weight of ~20 kDa. In previous studies, heated and unheated bands of EcPagP were observed in the reversed order in commercial precast SDS-PAGE system (Khan et al. 2007). Some studies have concluded that factors such as the gel matrix, differences in solvation of the protein by SDS and detergent interactions may be involved (Rath et al. 2008).

Protein secondary structural conformation can be obtained from CD signals in the far-UV wavelength region (240-190 nm) due to amide chromophores of the peptide bonds. Although detergents are suitable for isolating and purifying membrane proteins

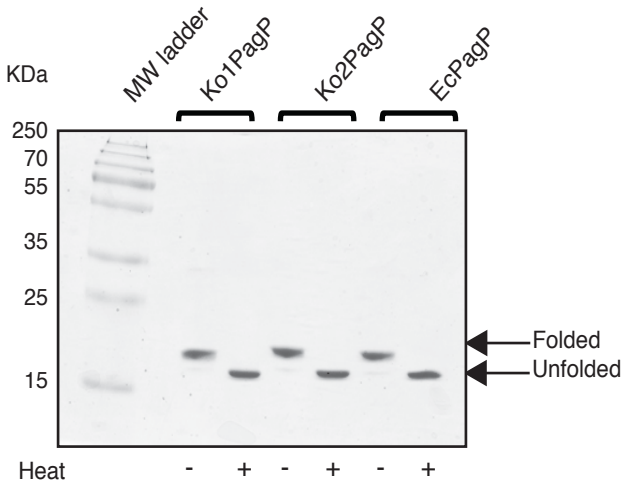

Figure 3.2. Chromosome and plasmid-based PagPs refolded in LDAO detergent shows heat modifiability on 15% SDS-PAGE. 40 µg of Ko1PagP, Ko2PagP and EcPagP samples heated (100 °C for 10 mins) and unheated (room temperature) for analysis by SDS-PAGE. The gel was stained by Coomassie blue dye and destained in a methanol, acetic acid and water solution. The state of the protein is indicated on the right of gel, and the molecular weight standards are indicated on the left.

like PagP, they are not always appropriate for spectroscopic studies (Miles & Wallace 2016). LDAO is a zwitterionic detergent, its micelles are transparent down to 200 nm and is therefore suitable for CD analysis of our proteins. Far-UV wavelength scans and thermal unfolding profiles provided spectroscopic evaluation of KoPagP homologs refolded in LDAO (Figures 3.3). EcPagP, Ko1PagP, and Ko2PagP had a negative ellipticity maximum at 218 nm characteristic of an n $\rightarrow\pi^*$ transition due to peptide bonds in a mostly β-sheet conformation (Saxena & Wetlaufer 1971; Khan et al. 2007). Ko1PagP and EcPagP showed a positive ellipticity at 232 nm known as an exciton due to an interaction between buried aromatic side chains of Y26 and W66 (Khan et al. 2007). Ko2PagP did not have this exciton effect (Figure 3.3A) despite conservation of the same two buried aromatic side chains (Figure 3.1C). The exciton effect arises from the delocalization of the excited electronic states between Y26 and W66 when they adopt a particular geometric arrangement (Khan et al. 2007). As such, the absence of the exciton in Ko2PagP indicates that this protein exhibits a distinctly different geometric arrangement of the buried Y26 and W66 residues.

Monitoring the loss of the negative ellipticity maximum 218 nm allows for the determination of the thermal stability within the protein structure (Greenfield 2007). Ko1PagP and Ko2PagP were monitored at increasing temperatures from 25-100 ^{o}C at 218 nm (the characteristic wavelength for β-barrel proteins) (Figure 3.3B). Ko1PagP and Ko2PagP were highly stable with unfolding temperatures of 88 ^{o}C for Ko1PagP, the same

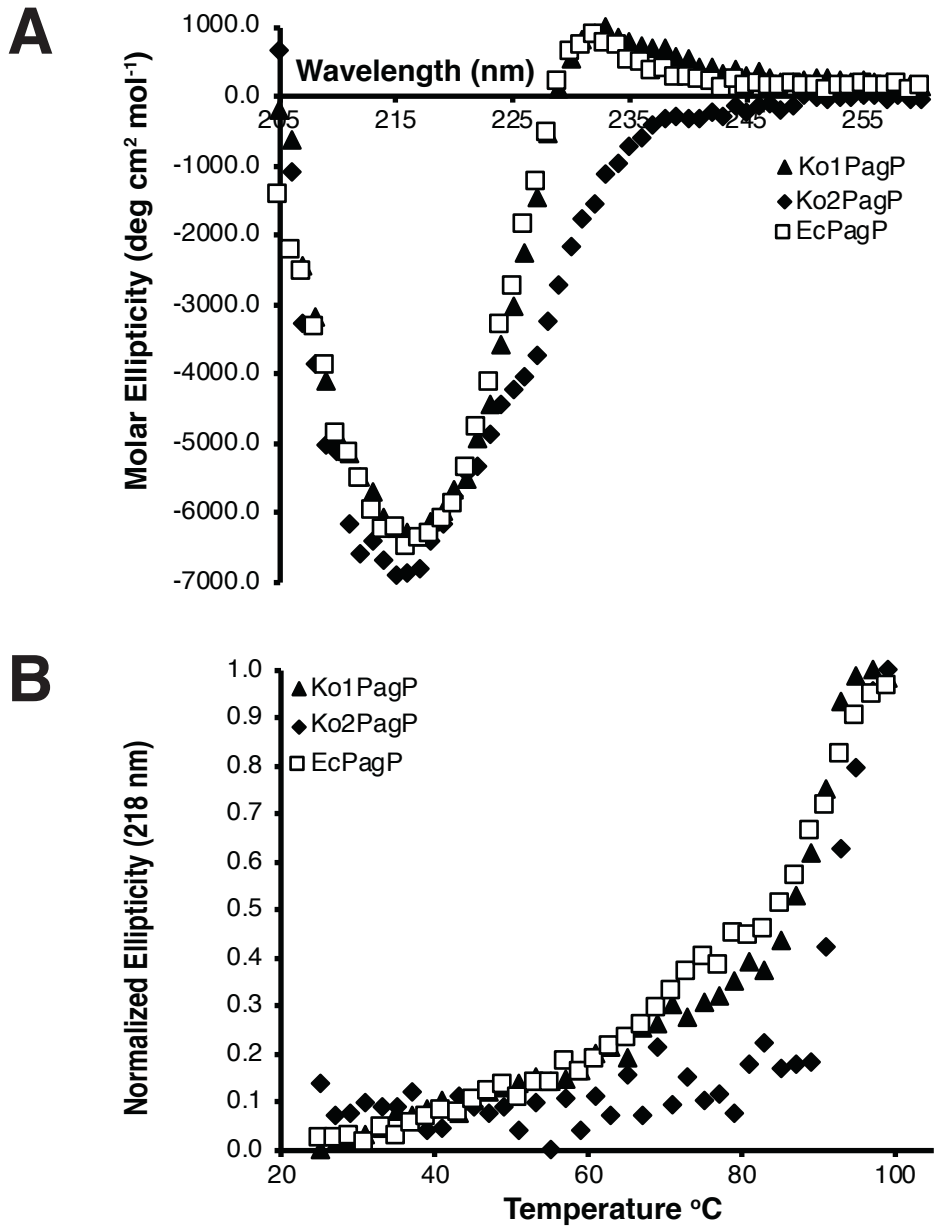

Figure 3.3. Far-UV spectroscopic evaluation of refolded chromosomal and plasmid-based PagPs. A. Wavelength scans for Ko1PagP, Ko2PagP and EcPagP. Samples were maintained at 0.3 mg/mL in 0.1% LDAO and 10 mM Tris-HCl (pH 8.0). Scans were done between 200-260 nm while the temperature remained at 25 °C. B. Thermal unfolding profiles for Ko1PagP, Ko2PagP and EcPagP. The same protein samples for wavelength scans were used and monitored from 25-100 °C by following the loss of negative ellipticity at 218 nm.

as for EcPagP, and 92 °C for Ko2PagP. The graphs plateaued at ~100 °C signifying complete unfolding of the proteins.

3.5.1.2 The exciton effect correlates with the charge relay system residues

The presence or absence of the exciton was the first major difference observed between Ko1PagP and Ko2PagP (Figure 3.3A). We wondered why there was a difference in CD between the two homologs from *K. oxytoca*, especially since both proteins had Y26 and W66 residues that were responsible for the exciton effect (Khan et al. 2007). In the amino acid sequence alignment, the putative active charge relay residues D61 and H67 found in chromosomal PagP homologs were naturally substituted by N or S and S in the chromosomal and plasmid-based PagP, respectively (Figure 3.1C). Due to the location of the charge relay residues in the folded protein, we reasoned that the presence of the exciton in the chromosomal PagP is a result of having the putative active charge relay residues, which provided the optimal geometrical and distance constraints for the chromophores in Y26 and W66 to interact forming the exciton couplet (Figure 3.1C). We hypothesized that mutating the putative charge relay residues to N and S, respectively, may cause a conformational change in Ko1PagP protein structure resulting in the loss of the exciton, and the reverse should be true for Ko2PagP (mutating to D and H). Consistent with this hypothesis, a mutation of H67N in EcPagP caused a conformational change that resulted in the loss of the exciton and produced an unstable protein with a thermal unfolding temperature of 60 °C, which is 28 °C less than that of the wild type protein (Smith 2008). Therefore, we mutated the charge relay residues of Ko1PagP to

those of Ko2PagP and vice-versa (Table 3.1). The single and double point mutations were confirmed using DNA sequencing and ESI MS (Table 3.3). Small scale protein expression revealed that all the mutant proteins expressed except the Ko1PagPH67S mutant (Figure 3.4). Although Ko2PagPS67H was expressed, we were unable to refold this protein in LDAO detergent as we did for the other proteins. We reasoned that the electrostatic association between H67 and D61 might create an instability in single mutants at position "67" that could be compensated for in a corresponding double mutant.

To analyze the effect of the point mutations on the conformation of the protein, far-UV CD spectroscopy was used (Figure 3.5 and 3.6). The single point mutations of Ko1PagPD61N and Ko2PagPN61D had no observable effect of the presence or absence of the exciton suggesting that the single mutation was not sufficient to perturb the geometric arrangement of the chromophores in Y26 and W66. However, the double point mutations in the charge relay residues, Ko2PagPN61D/S67H saw an emergence of the exciton, while Ko1PagPD61N/H67S saw what appears to be an extinguishing exciton (Figure 3.5A and 3.6A). These results suggest that the double point mutation in Ko2PagPN61D/S67H provided the optimal conditions of distance and geometric constraints for coupling of the chromophores in Y26 and W66 to generate the exciton effect. The exciton was still partially intact in Ko1PagPD61N/H67S due to possibly greater conformational plasticity in structure for Ko1PagP (Figure 3.6A). We also observed a decrease in the negative ellipticity maximum for Ko1PagPD61N/H67S and Ko2PagPN61D/S67H compared to wild type Ko1PagP and Ko2PagP, respectively

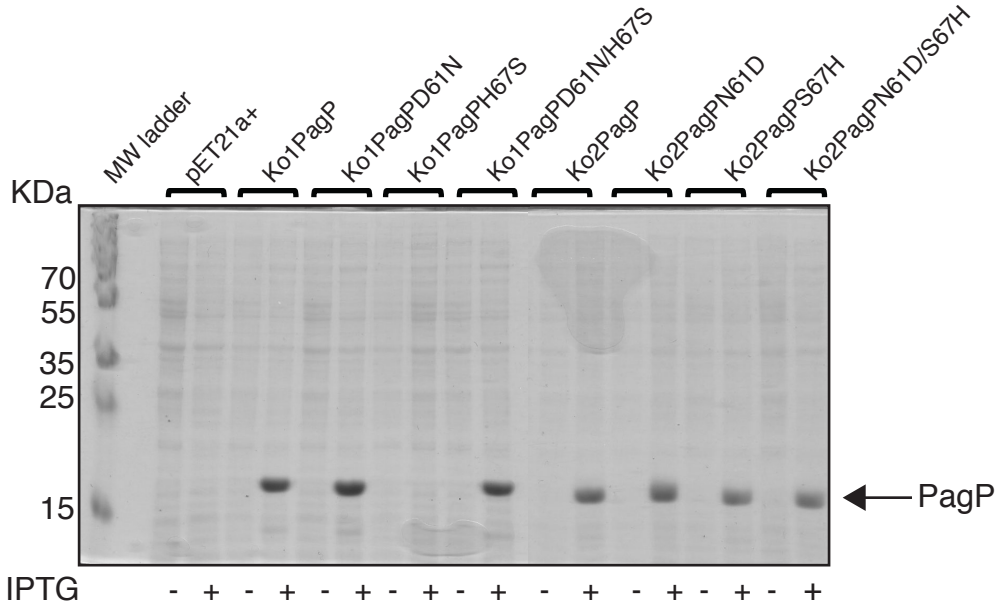

Figure 3.4. 13.5% SDS PAGE of putative charge relay mutants. Ko1PagP, Ko2PagP and their charge relay mutants are overexpressed from the pET21a+ plasmid. IPTG induced and uninduced samples are shown.

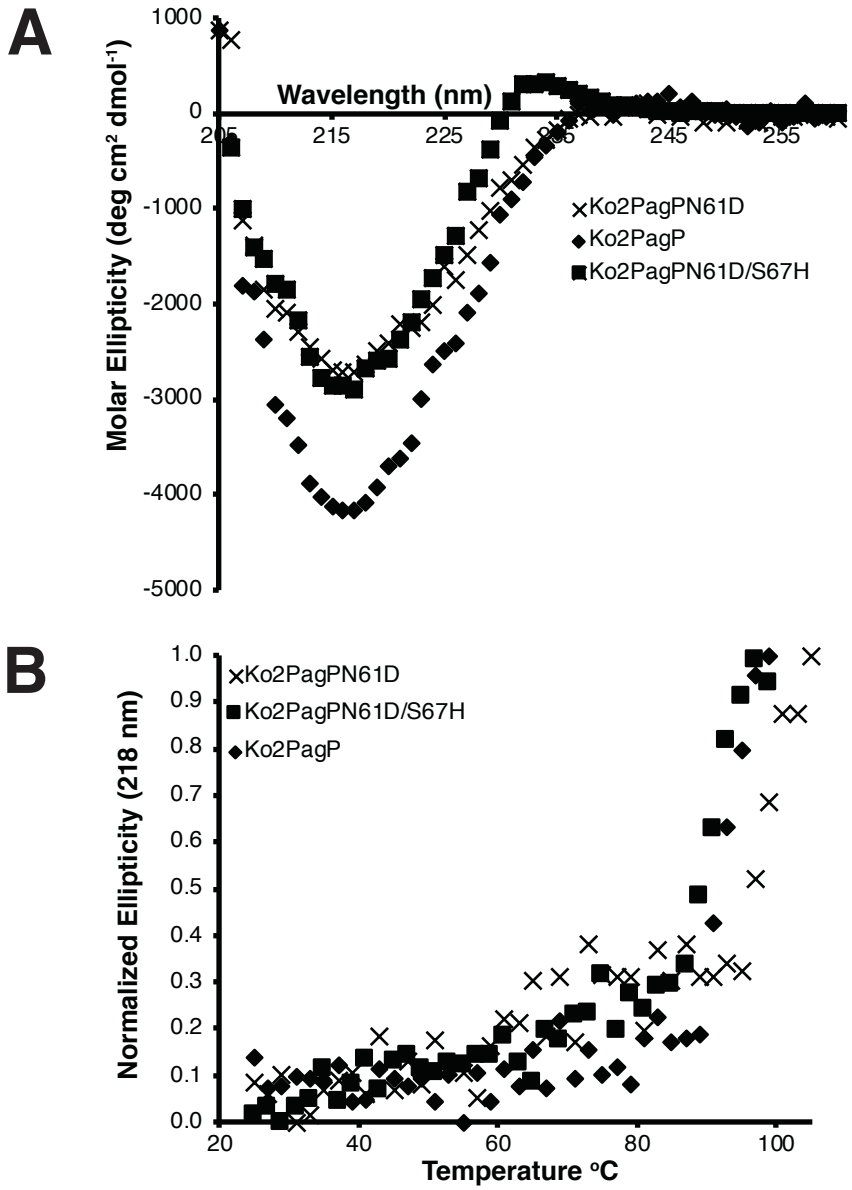

Figure 3.5. Far-UV spectroscopic analysis of Ko2PagP and charge relay mutants. A. Wavelength scans for Ko2PagP, Ko2PagPD61N and Ko2Pag-PD61N/H67S. Samples were maintained at 0.3 mg/mL in 0.1% LDAO and 10 mM Tris-HCl (pH 8.0). Scans were done between 200-260 nm while the temperature remained at 25 °C. B. Thermal unfolding profiles for Ko2PagP, Ko2PagPD61N and Ko2PagPD61N/H67S. The same protein samples for wavelength scans were used and monitored from 25-100 °C by following the loss of negative ellipticity at 218 nm.

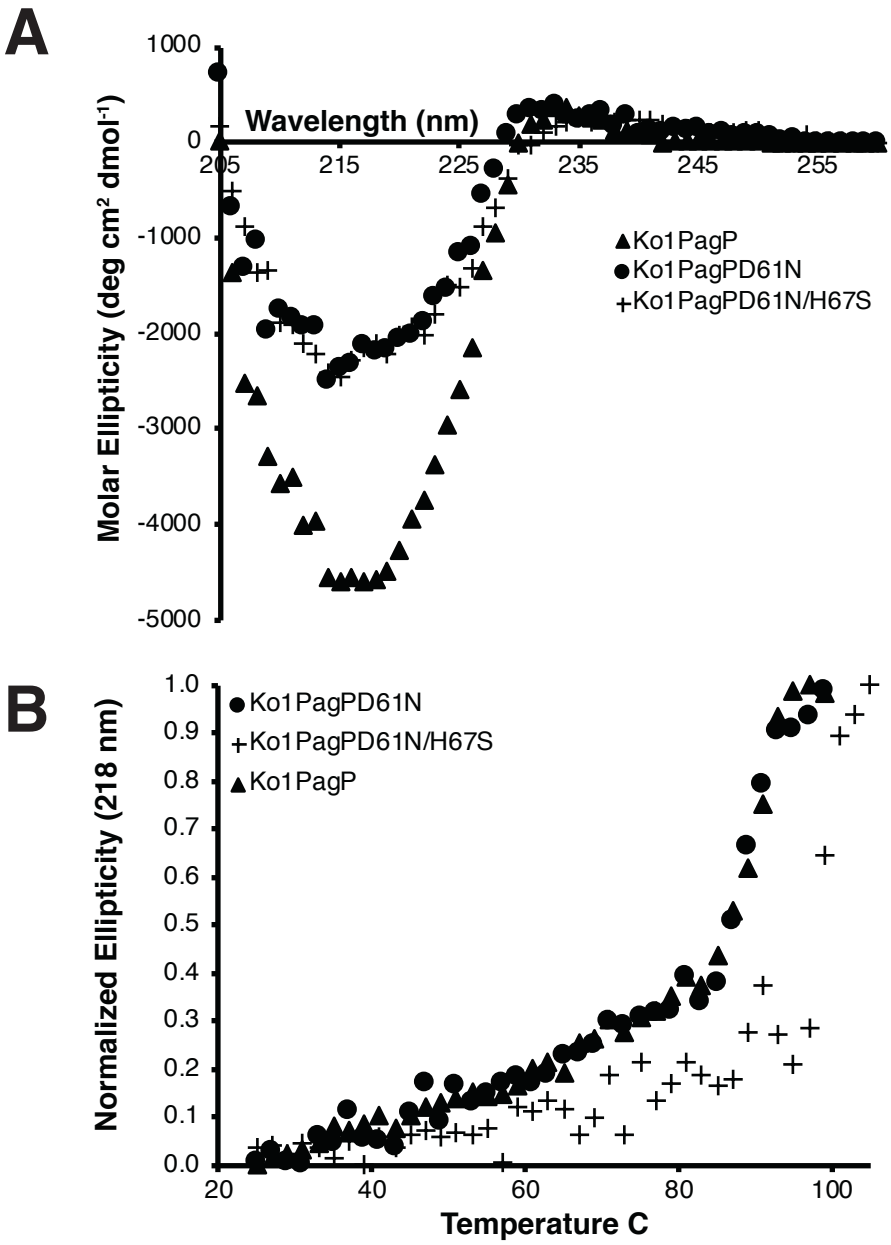

Figure 3.6. Far-UV spectroscopic analysis of Ko1PagP and charge relay mutants. A. Wavelength scans for Ko1PagP, Ko1PagPD61N and Ko1Pag-PD61N/H67S. Samples were maintained at 0.3 mg/mL in 0.1% LDAO and 10 mM Tris-HCl (pH 8.0). Scans were done between 200-260 nm while the temperature remained at 25 °C. B. Thermal unfolding profiles for Ko1PagP, Ko1PagPD61N and Ko1PagPD61N/H67S. The same protein samples for wavelength scans were used and monitored from 25-100 °C by following the loss of negative ellipticity at 218 nm.

(Figure 3.5A and 3.6A). This suggests less β-sheet formation in the double charge relay mutants. The loss/appearance of the exciton and the change in negative ellipticity maximum suggests a conformation change in Ko1PagP and Ko2PagP structure due to the switch in the proposed charge relay system.

We followed loss of the negative ellipticity at 218 nm in thermal unfolding profiles for Ko1PagP and Ko2PagP. The double point mutant Ko1PagPD61N/H67S was more stable than the single point mutant Ko1PagPD61N, and the latter had the same unfolding temperature as wild type Ko1PagP (Figure 3.6B), whereas Ko2PagPN61D single mutant was more stable than its double mutant Ko2PagPN61D/S67H and wild type Ko2PagP (Figure 3.5B). In both cases, proteins without an exciton or with an "inactive charge relay system" were more stable.

3.5.1.3 Ko1PagP and Ko2PagP are dedicated palmitoyltransferases

EcPagP is very specific in selecting a palmitate due to its hydrocarbon ruler, which is lined at the base by a glycine residue (G88) that distinguishes acyl chains by a single methylene unit *in vitro* (Figure 3.1A and 3.1C) (Khan et al. 2007; Ahn et al. 2004). Ko1PagP and Ko2PagP also has a Gly residue at position 88 possibly at the base of their hydrocarbon ruler (Figure 3.1A). We asked if Ko1PagP and Ko2PagP were also dedicated palmitoyltransferases. To determine the acyl chain selection of KoPagP homologs, an acyl chain length specificity or hydrocarbon ruler assay was conducted (Ahn et al. 2004; Thaipisuttikul et al. 2014). To assay our enzymes in our defined detergent micelle system,

the enzymes that were refolded in the inhibitory LDAO had to be serially diluted into an activity buffer that included *n*-dodecyl-β-D-maltoside (DDM) that supports PagP activity (Khan et al. 2007; Bishop et al. 2000). The acyltransferase assays were set up using ^{32}P orthophosphate lipid IV_A (prepared by a mild acid hydrolysis from *E. coli* BKTO9 cells, Table 3.1) as an acceptor with nonradioactive phosphatidylcholines (PC) of defined acyl chain composition as donor substrates for each enzyme. The products from the reactions were separated by TLC and quantified (Figure 3.7). *E. coli* and related bacteria do not make PC, but the availability of synthetic PC with defined acyl-chain composition and the relaxed specificity of PagP for the polar head group, suits them for our enzymatic studies of acyl chain selection. The results demonstrated that Ko1PagP and Ko2PagP were selective for C16 acyl chain by discriminating acyl chains that differ in length by just one methylene unit (Ahn et al. 2004; Khan et al. 2007). Ko2PagP seems to be more specific for the palmitate than Ko1PagP, which seems less specific in that C15 and C17 acyl chains were also incorporated at similar rates compared to C16 acyl chains (Figure 3.7). Despite this, only even numbered acyl chains are present in the OM of *K. oxytoca* and related bacteria from the *Enterobacterales* order (Alnajar & Gupta 2017); therefore, a C15 or C17 acyl chain would not be selected by this protein in bacterial OMs (Parsons & Rock 2013). In addition, Ko1PagP had a significantly higher specific activity than that of Ko2PagP for the C16 palmitate chain when the symmetrical dipalmitoyl-PC (DPPC) is being used, suggesting that Ko1PagP palmitoylates lipid IV_A more rapidly (Figure 3.7).

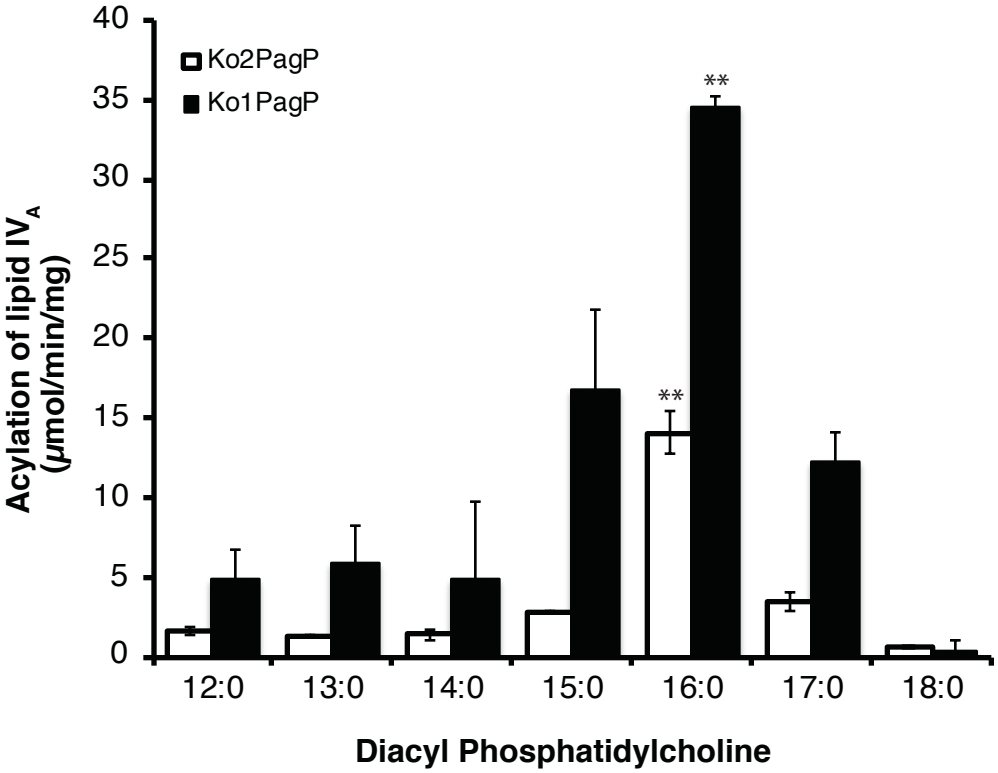

Figure 3.7. Ko1PagP and Ko2PagP are selective for a C16 palmitate chain. Hydrocarbon ruler measurements demonstrate acyl chain selectivity for Ko1PagP and Ko2PagP. 10 ng/μl enzymes were incubated with 1 mM of phospholipids (a suite of diacyl phosphatidylcholines from C12-C18) and 50 μM of ^{32}P orthophosphate labeled lipid IV$_A$. 2.5 μl of samples were spotted on a TLC plate every 20 mins up to 120 mins. The TLC plates were exposed to Phosphorimager screen and quantification was done by ImageQuant software. The average specific activity for three replicates for each enzyme and each phospholipid donor was calculated and plotted. The preference for a C16 chain for each enzyme was significant by unpaired Student t test, *P<0.005.

3.5.1.4 Ko1PagP, but not Ko2PagP uses PG as an acceptor substrate to make PPG, BMP and LPG.

PagP palmitoylates PG and lipid A to the same order in *Salmonella* OM. The *E. coli* PagP is also reported to catalyze the reaction to form palmitoyl-PG (PPG) *in vitro.* This suggests a biological function for PagP activity in the formation of PPG (Dalebroux et al. 2014). So far, the only difference observed enzymatically between Ko1PagP and Ko2PagP is the rate of reaction for lipid A palmitoylation. Therefore, we asked if Ko1PagP and Ko2PagP were also able to catalyze the palmitoylation of PG to form PPG. Enzymatic assays were set up with ^{14}C-DPPC as a donor to monitor the reaction on a TLC plate (Figure 3.8). We observed that Ko1PagP and EcPagP both palmitoylated PG to similar extents; however, Ko2PagP did not. Closer examination of the products of this reaction on TLC plates reveal the formation of two other products from EcPagP and Ko1PagP catalyzed reactions: *bis*(monoacylglycero)phosphate (BMP) and lyso-phosphatidylglycerol (LPG) (Figure 3.8). PG, PPG, BMP, and LPG belong to a group of related glycerophosphoglycerol (GPG) phospholipids (Figure 3.8) (Hullin-Matsuda et al. 2007). Previous description of this reaction for EcPagP did not mention the production of these compounds for three possible reasons: 1. the *in vitro* reaction has to go for several hours for all the products to be visible by autoradiography. 2. BMP is a structural isomer of PG, they have identical molecular masses in mass spectrometry studies. 3. BMP has physical properties like that of CL with which it co-migrates in TLC in most solvent systems. BMP is usually found in animal tissues in 1-2% of the total phospholipid content. Yet, it is enriched (~18%) in the multi lamellar vesicles found in endosomes.

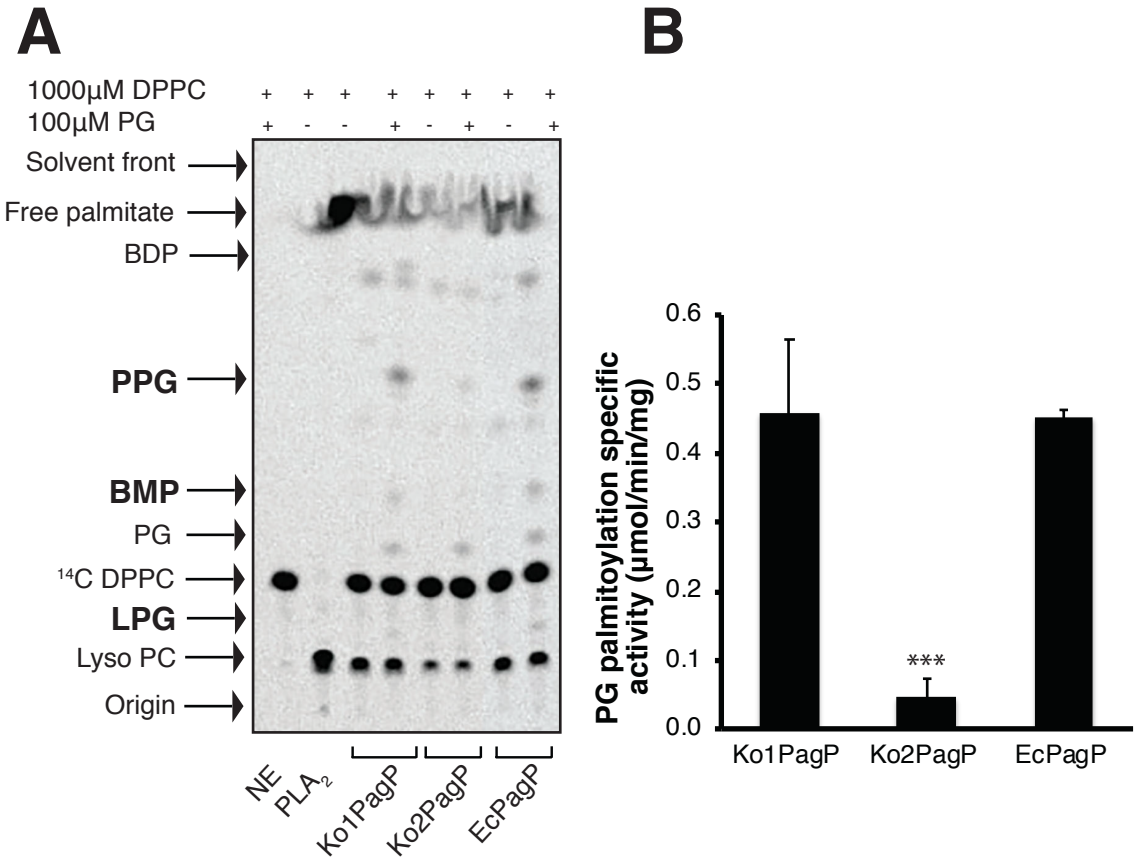

Figure 3.8. Purified Ko2PagP does not palmitoylate PG. A. Purified Ko1PagP, Ko2PagP and EcPagP were incubated with ^{14}C-DPPC and non-radiolabeled PG overnight. Samples were separated by TLC and the plate was exposed and visualized by phosphorimaging. The solvent system used to resolve the TLC plate was chloroform/methanol/water 65:25:4 (v/v). B. The same reaction as (A) over a time course (30, 60, 120, 240, 360 min) with specific activity determined by quantifying the intensity of the PPG spot on the TLC plate using ImageQuant software. These assays were done 3-4 times. Value for Ko2PagP significantly less than EcPagP and Ko1PagP by unpaired Student t test, ***P<0.001. Abbreviations: BDP, bis(diacylglycero)phosphate; BMP, bis(monoacylglycero)phosphate; DPPC, *sn*-1,2-dipalmitoyl-phosphatidylcholine; LPG, lyso-PG; PPG, palmitoyl-PG.

Interestingly, eukaryotic BMP is derived from PG, but it is found only as the *sn*-1-glycerolphosphate isomer as the result of a putative enzymatic inversion in the PG backbone stereochemistry (Hullin-Matsuda et al. 2007; Thornburg et al. 1991). There is one report of BMP being isolated from alkalophilic Bacillus bacteria. Nishihara et al concluded that the occurrence of BMP was due to the alkalophilicity of the bacteria (1982). No reference of this lipid is found in Gram-negative bacteria (Akgoc et al. 2015; Nishihara et al. 1982).

3.5.1.5 The ability of KoPagPs to transacylate and palmitoylate PG correlate with the charge relay residues.

The realization that Ko1PagP and EcPagP were able to produce the full range of glycerophosphoglycerols while Ko1PagP could not, prompted us to investigate the reasons for this difference. A switch in the proposed charge relay residues correlated with a conformational change in the structure of the enzyme observed by CD (Figure 3.5A and 3.6A). We reasoned that such a change in conformation is often related to function, and that the putative charge relay residues could be associated with the differences that are observed when PG is used as an acceptor substrate in the acyltransferase reaction (Hammes 2002). Studies have shown that lipid A and PG are being palmitoylated at the extracellular surface active site because an EcPagP extracellular catalytic residue mutant EcPagPS77A does not palmitoylate lipid A or PG (Hwang et al. 2002; Bishop Unpublished). We hypothesized that the putative catalytic site on the periplasmic surface

might act as a lipase to hydrolyze PPG to BMP and then further hydrolyze BMP to LPG (Figure 3.9).

We tested this idea by first establishing that the formation of PPG or palmitoylated lipid A was not affected by mutation in the proposed charge relay residues. We assayed wild type Ko1PagP, Ko2PagP, and charge relay mutants in two separate acyltransferase reactions, first with PG as the acceptor and then with lipid A as the acceptor, using ^{14}C-DPPC as the donor in both cases (Figure 3.10, 3.11 and 3.12). Qualitative analysis of the acyltransferase reaction with PG as an acceptor substrate suggests that the Ko2PagP charge relay mutants have gained function, but more obvious in the transacylation of PG (Figure 3.10A). Quantitative analysis confirms a gain in function in Ko2PagP mutants for both PG transacylation and palmitoylation (Figure 3.10B). Transacylation is the enzymatic exchange of acyl chains between phospholipids and lyso-phospholipids (LP), and we take advantage of this feature in our assays to incorporate radiolabeling into substrates and products (Figure 3.11) (Homma et al. 1987). This reaction is believed to occur through the binding of PG at the embrasure because it is abolished when the P28C/P50C double mutant is oxidized (Unpublished observations). Ko1PagP charge relay mutants seem to have lost some function in transacylation reactions, but the difference is not significant (Figure 3.10B). BMP was undetectable in these reactions for Ko2PagP and charge relay mutants, and no difference in BMP formation was observed for Ko1PagP and its charge relay mutants (Figure 3.10A and B). This suggests that neither BMP nor LPG are affected by a switch in the charge relay

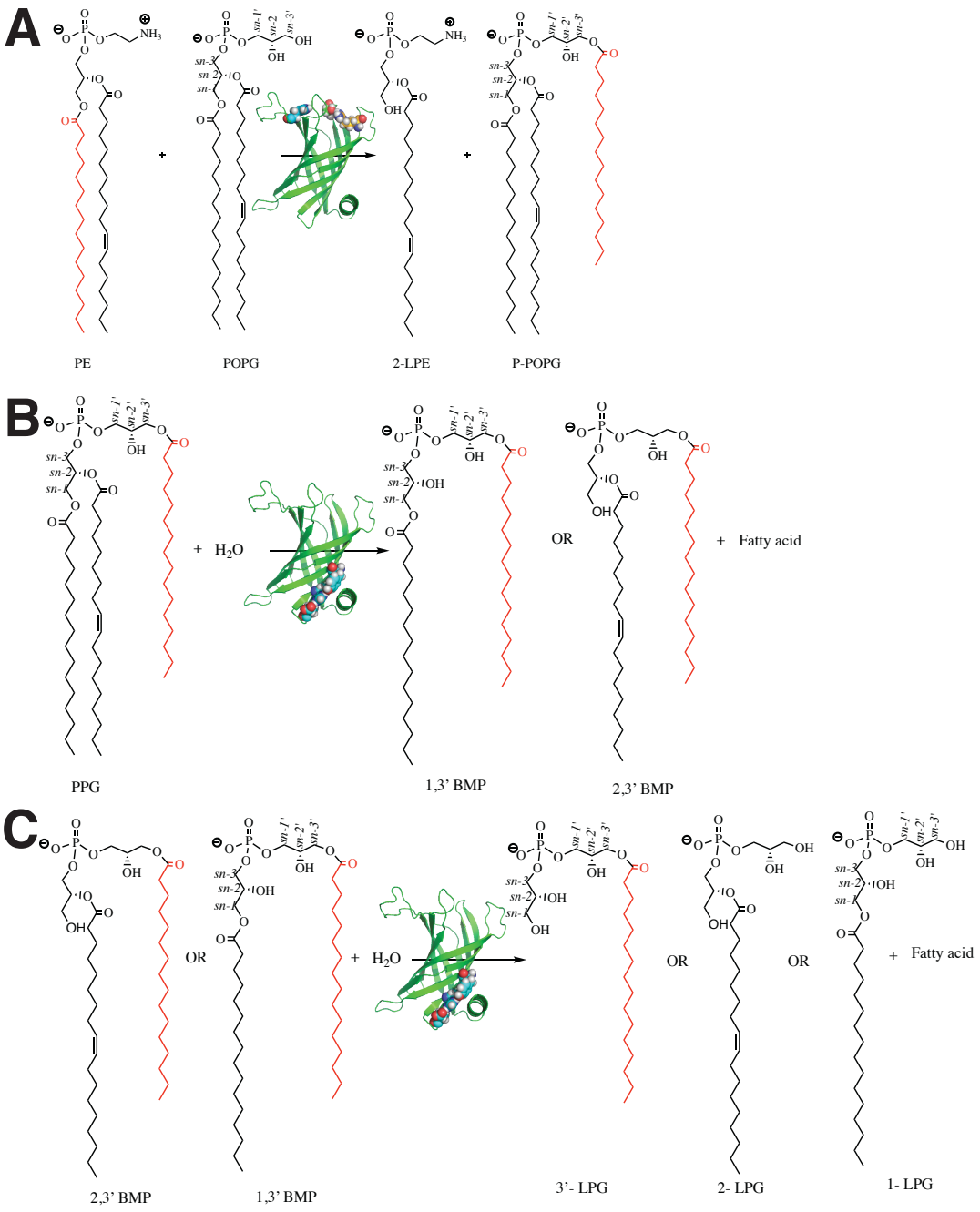

Figure 3.9. Proposed biochemical reactions for glycerophosphoglycerol production. A. PagP enzymatically transfers a palmitate to POPG forming palmitoyl-POPG (P-POPG); this reaction occurs at the extracellular active site of the outer leaflet of the outer membrane. B. P-POPG is flipped to the inner leaflet of the outer membrane where it is hydrolyzed to one of the two forms of BMP by PagP's periplasmic active site. C. PagP's periplasmic active site further hydrolyzes BMP to one of the three forms of LPG.

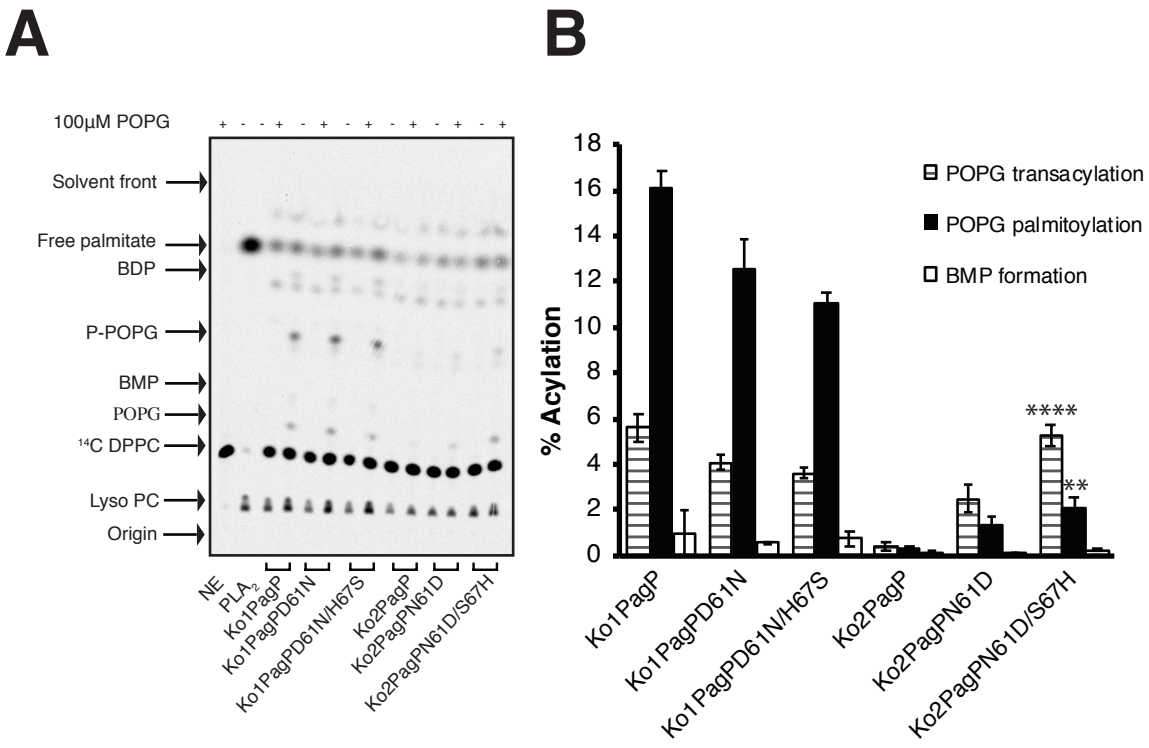

Figure 3.10. POPG palmitoylation by Ko1PagP, Ko2PagP, and charge relay mutants. A. Autoradiograph showing acyltransferase reaction using 10 ng/µL of each enzyme, 1000 µM of DPPC, 100 µM of POPG and 20 µM ^{14}C-DPPC. The TLC plate was developed in a solvent system of chloroform/methanol/water 65:25:4 (v/v), scanned, and visualized by Phosphorimaging. B. Quantification of spots representing POPG, P-POPG and BMP. The average percentage acylation was calculated for three replicates. Values for Ko2PagP double point mutant significantly greater than for wild type for both transacylation and palmitoylation of POPG by unpaired Student t test, ****P<0.0001, **P=0.003.

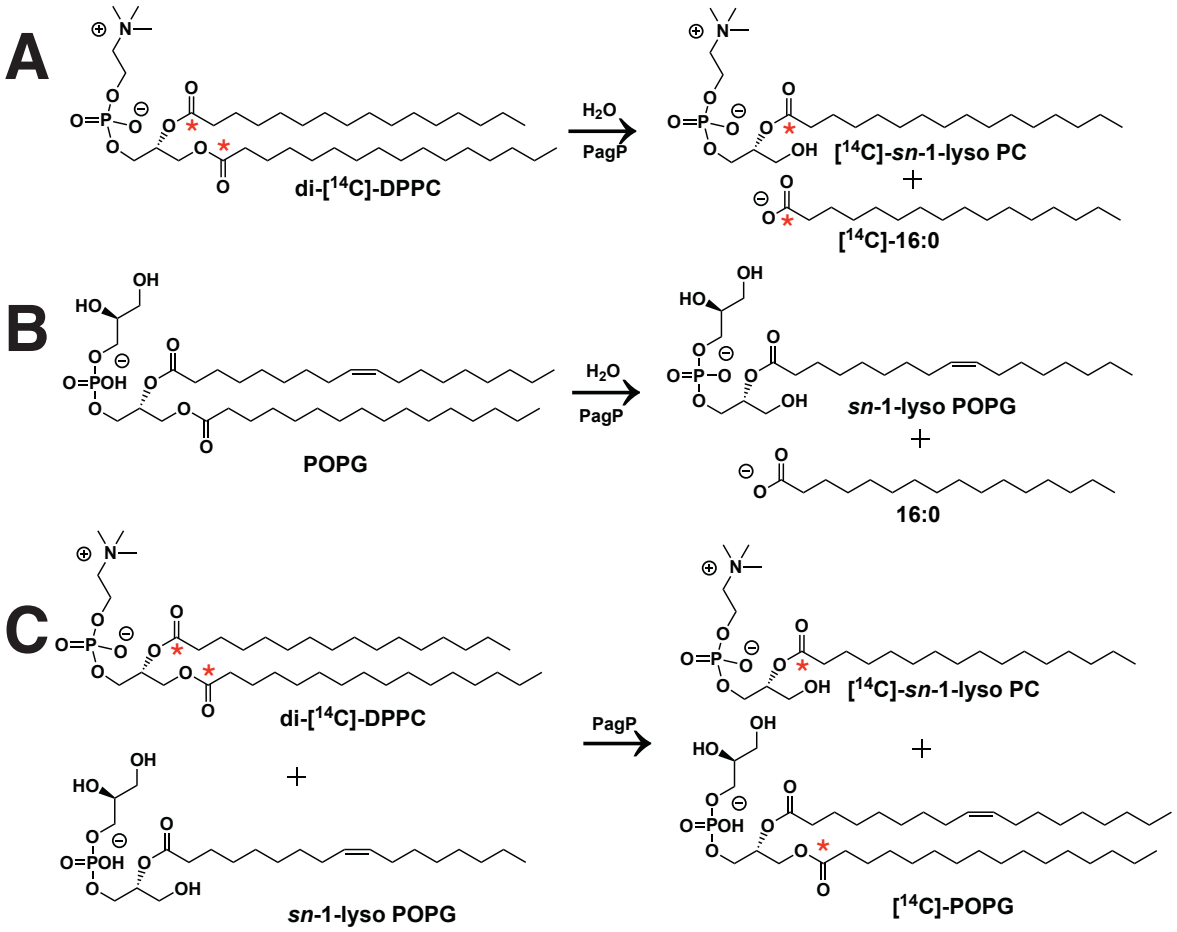

Figure 3.11. PagP transacylation reaction using POPG as an acceptor substrate. A. PagP hydrolyzes ^{14}C-DPPC to form ^{14}C-lyso-PC and ^{14}C-palmitate. B. Non-radiolabeled POPG is hydrolyzed by PagP to form non-radiolabeled lyso-POPG and free palmitate. C. PagP uses ^{14}C-DPPC to enzymatically re-acylates non-radiolabeled lyso-POPG to form ^{14}C-POPG, and ^{14}C-lyso-PC. Red asterisk denotes radiolabeling.

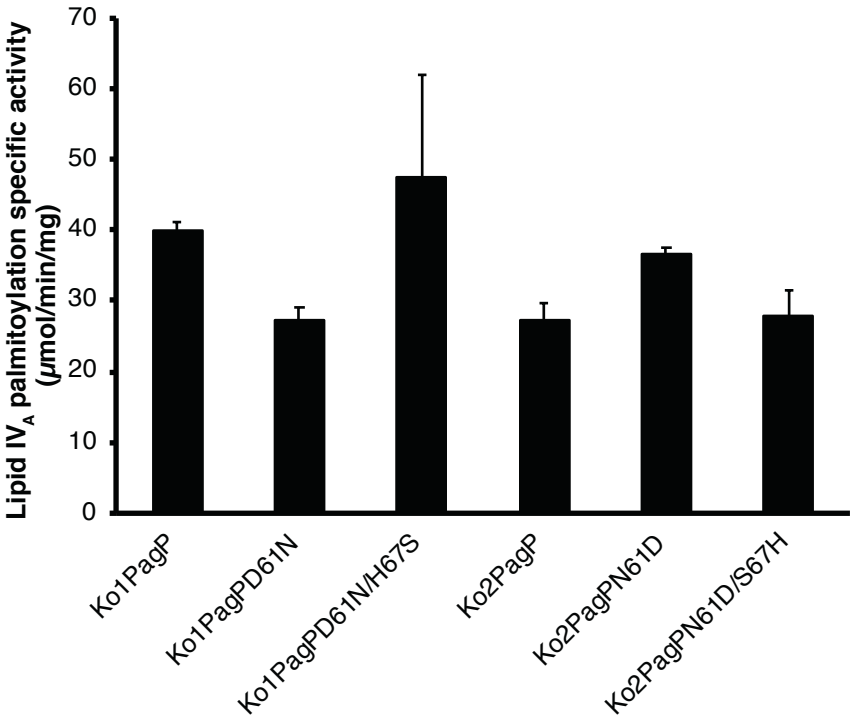

Figure 3.12. Lipid IV_A palmitoylation by Ko1PagP, Ko2PagP, and charge relay mutants. 10 ng/μL of each enzyme was incubated with 1 mM DPPC as donor 100 μM lipid IV_A as acceptor, and 20 μM ^{14}C-DPPC for monitoring on a TLC plate. The reaction was monitored over a time course of every 20 mins up to 120 mins. TLC plates were exposed to Phosphorimager screens and quantification was done by ImageQuant software. The average specific activity of three replicates for each enzyme was calculated and plotted. No significant differences between mutant proteins and wild type Ko1PagP or Ko2PagP by unpaired Student t test.

residues. Palmitoylated lipid A was unaffected by the mutations in the charge relay residues (Figure 3.12). Altogether, these results suggest that the charge relay residues correlate with the enzyme's extracellular active site ability to convert cold PG to ^{14}C-PG and in further palmitoylating PG to PPG.

3.5.2 Characterization of KoPagP homologs in OMs *in vivo*

3.5.2.1 Neither Ko1PagP nor Ko2PagP form glycerophosphoglycerols

Protein dynamics is enhanced in detergents compared to lipids and it is possible that enzymes may have different physical properties in a detergent micellar environment than in a restricted lamellar OM bilayer (Hite et al. 2008; Womack et al. 1983). We asked if the *in vitro* results observed when PG is used as an acceptor substrate for EcPagP, Ko1PagP, and Ko2PagP could be recapitulated in bacterial OMs. Usually, we express the proteins on a plasmid in an *E. coli* PagP knockout strain and isolate the lipids, but we learned from previous experiments that BMP co-migrates with cardiolipin on a TLC plate. Accordingly, we decided to express the proteins in a PagP and cardiolipin synthases (*clsA, clsB,* and *clsC*) knockout strain (DIXCO3, Table 3.1). We used ^{32}P orthophosphate for labeling and grew the cells expressing PagP on a plasmid with relevant controls, with and without the addition of EDTA to activate PagP. We extracted phospholipids and lipid A species and analyzed them by TLC (Figures 3.13). For EcPagP expressed in the *E. coli* DIXCO3 strain PPG, BMP and LP (lyso-phospholipids) were observed in cells as they were observed in *in vitro* acyltransferase reactions (Figure 3.13A and 3.8A). Surprisingly,

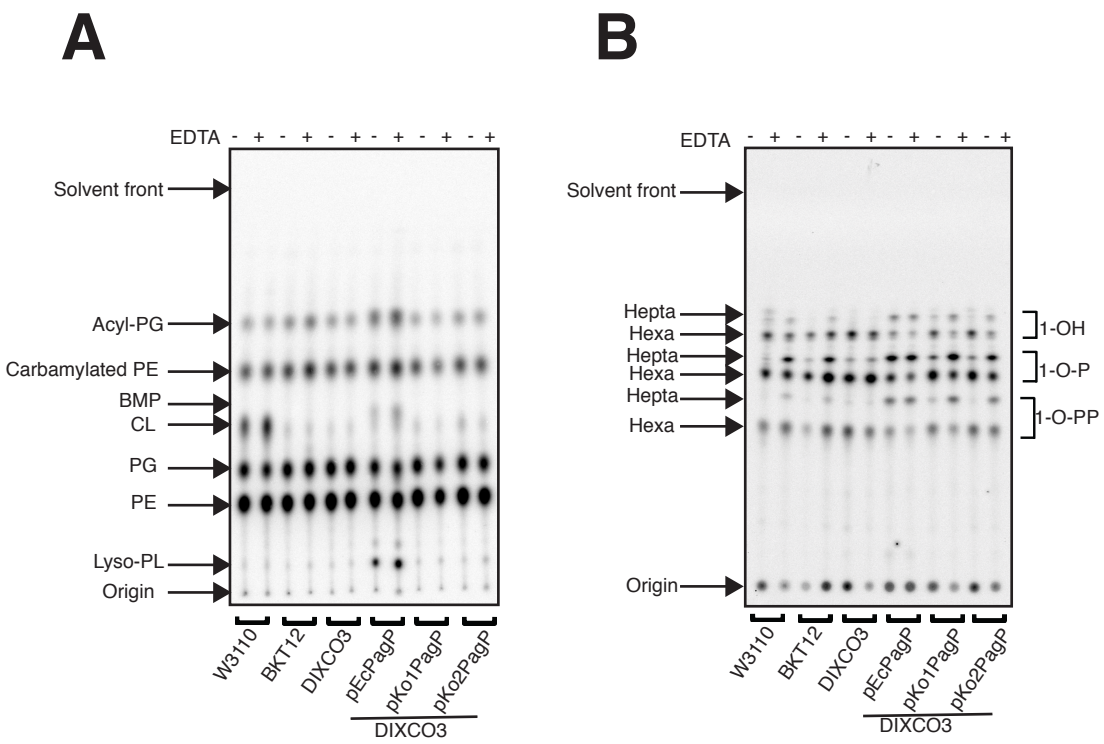

Figure 3.13. EcPagP makes PPG, BMP and LPLs in bacterial OMs, but KoPagPs do not. A. Autoradiograph showing phospholipid profile for *E. coli* strains W3110 (wild type), BKT12 (W3110 Δ*clsA*, Δ*clsB*, Δ*clsC*) and DIXCO3 (BKT12 Δ*pagP*) harbouring pEcPagP, pKo1PagP and pKo2PagP expressed from an arabinose-inducible promoter. Cells were grown and treated with and without EDTA to activate PagP. ^{32}P orthophosphate radiolabeled phospholipids were isolated using Bligh and Dyer solvents (1959), resolved by TLC (solvent system chloroform/methanol/ acetic acid, 65:25:5 (v/v)), and visualized using Phosphorimaging. B. Autoradiograph showing lipid A profile from the same cultures as in (A). ^{32}P orthophosphate radiolabeled lipid A species were isolated using the mild acid hydrolysis method, separated by TLC (solvent system chloroform/pyridine/88% formic acid/ water, 50:50:16:5 (v/v)), and visualized using Phosphorimaging.

neither Ko1PagP nor Ko2PagP generated BMP or LPs when expressed in this *E. coli* background. PPG made by PagP in the OM co-migrates with other types of acyl-PG from the inner membrane; therefore, it is difficult to rectify PPG production from KoPagPs because perhaps PPG is not being produced at high levels in bacterial OMs. Additionally, to be certain the enzymes were being expressed, the lipid A profiles were also analyzed from the same cultures. All the proteins were being expressed as evidenced by lipid A palmitoylation (Figure 3.13B). We reasoned that the KoPagP homologs were unable to perform as expected because they were expressed heterologously with their native signal peptides in an *E. coli* background. Perhaps if these enzymes were expressed in a *K. oxytoca* OM background we would be able to observe formation of the full range of glycerophosphoglycerols.

Consequently, we created *K. oxytoca pagP* single and double knockouts for homologous expression of the KoPagP homologs. Although a complete PagP knockout was never obtained, we were still able to analyze lipid A and PG palmitoylation (Figure 3.14A and B) (See Chapter 4 for discussion). The autoradiograph of the separated lipids showed lipid A palmitoylation occurred but there was no PG palmitoylation or BMP and LPG formation for the KoPagP homologs in a *K. oxytoca* OM bilayer environment when PagP was activated with EDTA. This confirms that the KoPagP homologs palmitoylate lipid A, but do not make the glycerophosphoglycerols in bacterial OMs.

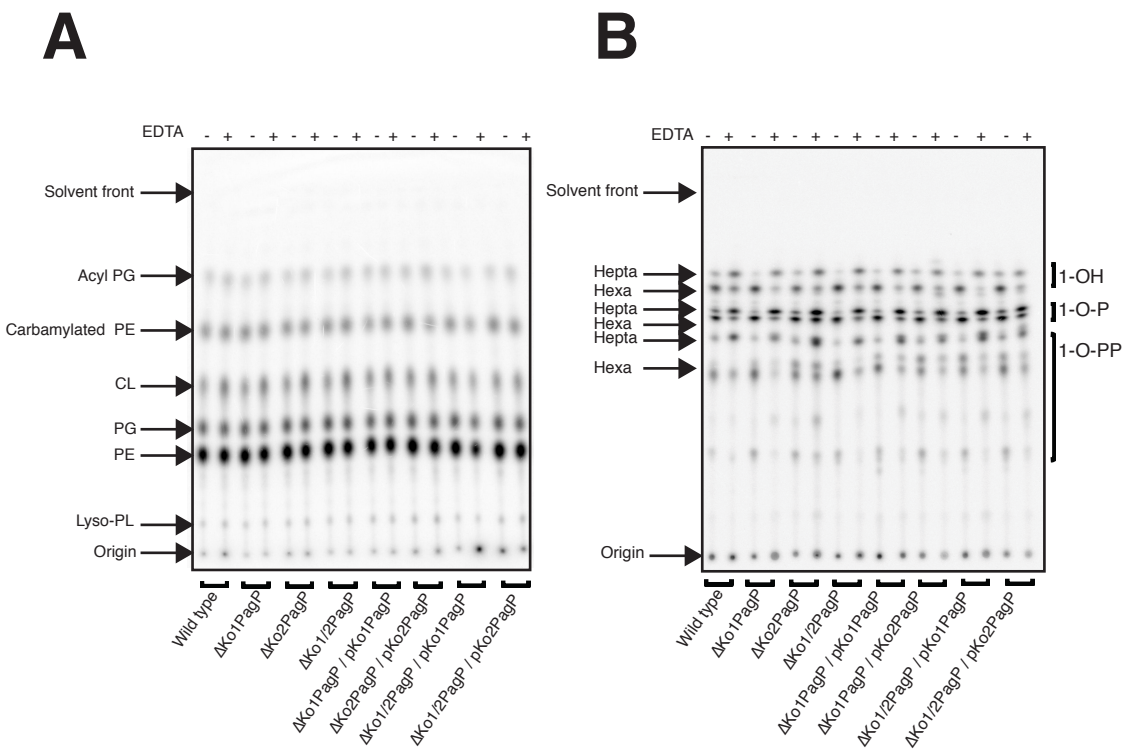

Figure 3.14. KoPagPs acylate lipid A, but not PG in *K. oxytoca* OMs. A. ^{32}P orthophosphate labeled phospholipids were isolated from *K. oxytoca* wild type, ΔKo1PagP, ΔKo2PagP, ΔKo1/2PagP with pKo1PagP and pKo2PagP expressed from an arabinose-inducible promoter. The phospholipids were isolated by Bligh and Dyer solvents (1959), separated by TLC and visualized by Phosphorimaging. The TLC plate was resolved in solvent system chlorform/ methanol/ acetic acid, 65:25:5 v/v. B. ^{32}P orthophosphate labeled lipid A species were isolated from the same cultures as in (A) except they were isolated by mild acid hydrolysis and the lipid A species were separated by TLC. The plate was resolved in solvent system chlorform/ pyridine/ 88%formic acid/ water, 50:50:16:5 v/v. and visualized by Phosphorimaging.

3.5.2.2 EcPagP requires Y87 from the proposed periplasmic active site to make the glycerophosphoglycerols

Considering that we were not be able to resolve if the putative charge relay residues or periplasmic catalytic triad from Ko1PagP was affecting the full range of glycerophosphoglycerol production in bacterial OMs, we decided to execute further studies with EcPagP. We used EcPagP mutants EcPagPS77A in the cell surface active site, EcPagPH67A(S) in the proposed charge relay residue mutant, and EcPagPY87F in the proposed periplasmic active site nucleophile mutant (Smith 2008). These proteins were expressed on arabinose-inducible promoter in *E. coli* strain DIXCO3 as before, and the lipids were isolated and separated by TLC (Figure 3.15). The H67 mutants produced the full range of glycerophosphoglycerols comparable to the wild type, but the Y87 mutant failed to accumulate acyl-PG, BMP and LPG (Figure 3.15A). Both EcPagPH67 and EcPagPY87F mutants palmitoylated lipid A as expected (Figure 3.15B) (Smith 2008), whereas the EcPagPS77A mutant did not form any PPG or palmitoylated lipid A as expected (Figures 3.15A and B) (Bishop Unpublished; Hwang et al. 2002).

We decided to confirm the results observed in bacterial OMs by mass spectrometry. We expressed EcPagP wild type, EcPagPS77A, EcPagPY87F, EcPagPH67A and H67S, Ko1PagP and Ko2PagP in *E. coli* WJ0124 (*pagP* knockout, Table 3.1). We wanted to be sure cardiolipin was not affected by the presence or absence of *pagP*, but we were unable to observe this difference using TLC to separate the lipids

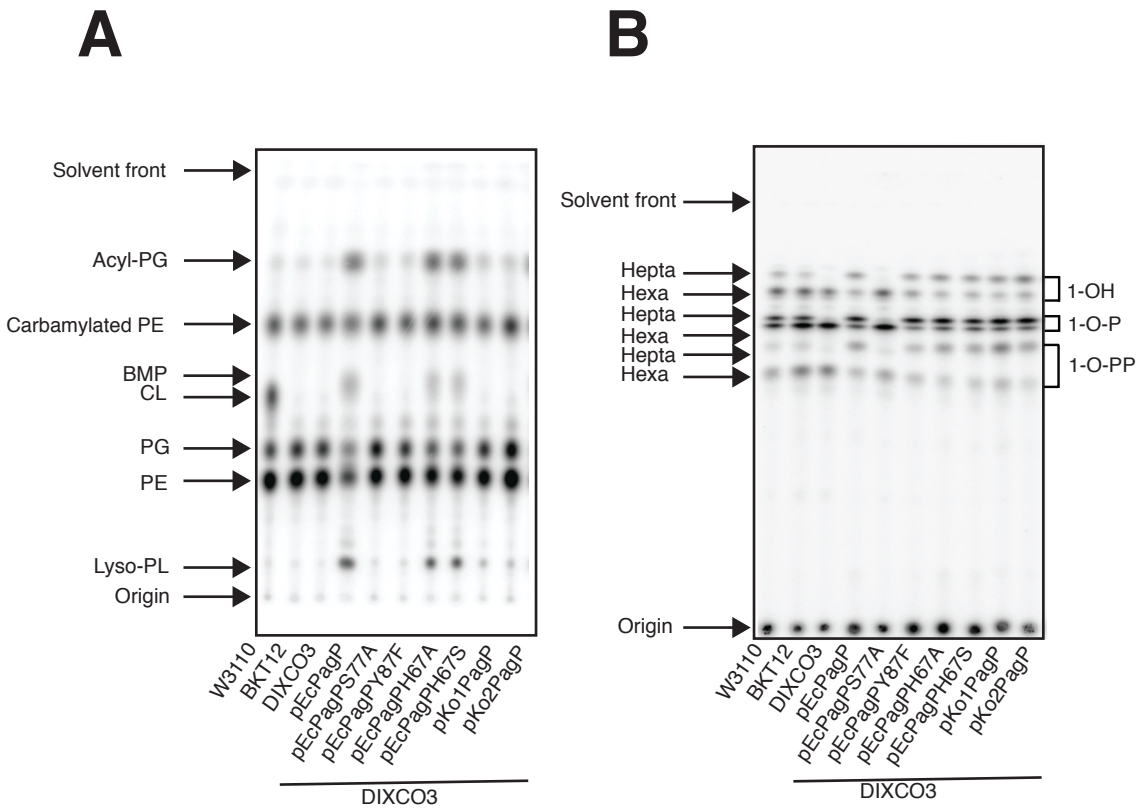

Figure 3.15. EcPagP requires Y87 to make glycerophosphoglycerols in the *E. coli* OMs. A. Autoradiograph showing phospholipid profile for *E. coli* strains W3110 (wild type), BKT12 (W3110 Δ*clsA*, Δ*clsB*, Δ*clsC*) and DIXCO3 (BKT12 Δ*pagP*) harbouring EcPagP, EcPagPS77A, EcPagPY87F, EcPagPH67A (S), Ko1PagP and Ko2PagP expressed from an arabinose-inducible promoter. Cells were grown and treated with and without EDTA to activate PagP. ^{32}P orthophosphate radiolabeled phospholipids were isolated using Bligh and Dyer solvents (1959) and resolved by TLC (solvent system chloroform/methanol/ acetic acid, 65:25:5 (v/v)). B. Autoradiograph showing lipid A profile from the same cultures as in (A). ^{32}P orthophosphate radiolabeled lipid A species were isolated using mild acid hydrolysis and were separated by TLC (solvent system chloroform/pyridine/88% formic acid/ water, 50:50:16:5 (v/v)). Plates were exposed to and visualized using Phosphorimaging.

using a strain that produced cardiolipin (Dalebroux et al. 2014). The lipids were isolated, dried down and analyzed by electrospray ionization mass spectrometry (ESI-MS or MS/MS) for acyl-PG, BMP, lyso-PLs and cardiolipin (Figure 3.16, 3.17 and Table 3.4) (Bulat & Garrett 2011; Garrett & Moncada 2014; Hsu et al. 2004). All samples had acyl-PG, because acyl-PG content includes those from IM and OM but shows variation in relative abundances (Hsu et al. 2004). IM acyl-PG is enriched with different acyl chain compositions than those of the OM. IM acyl-PG includes those with *m/z* of 955.9 for *sn*-3' acyl chains C14:0 or C14:1, and *m/z* of 983.9 for *sn*-3' acyl chains C16:0 or C16:1, whereas the predominant OM acyl-PG had *m/z* values of 957.9, 985.6 and 1011.7 each predicted to have a palmitate at the *sn*-3' position (Figure 3.16) (Dalebroux et al. 2014; Hsu et al. 2004). Bacteria overexpressing the EcPagPY87F mutant had some acyl-PG from the OM with the palmitate at the *sn*-3' position, *m/z* value 1011.7, whereas bacteria overexpressing EcPagP and the H67 mutant were enriched with all the known acyl-PG species from the OM that had a palmitate at the *sn*-3' position (Figure 3.16) (Hsu et al. 2004). These results confirm that EcPagP transfers a palmitate to the *sn*-3' position of PG, and that Y87 is required to degrade all the palmitoyl-PG produced in the OM, but that H67 mutants had no effect on palmitoyl-PG formation (Dalebroux et al. 2014; Hsu et al. 2004).

MS/MS in the negative mode yields similar spectra for PG and BMP, but previous analysis of MS/MS in the positive mode have distinguished BMP with a palmitate attached to the 3'-position with *m/z* value of 747.5 (Figure 3.9) (Garrett 2016). Therefore,

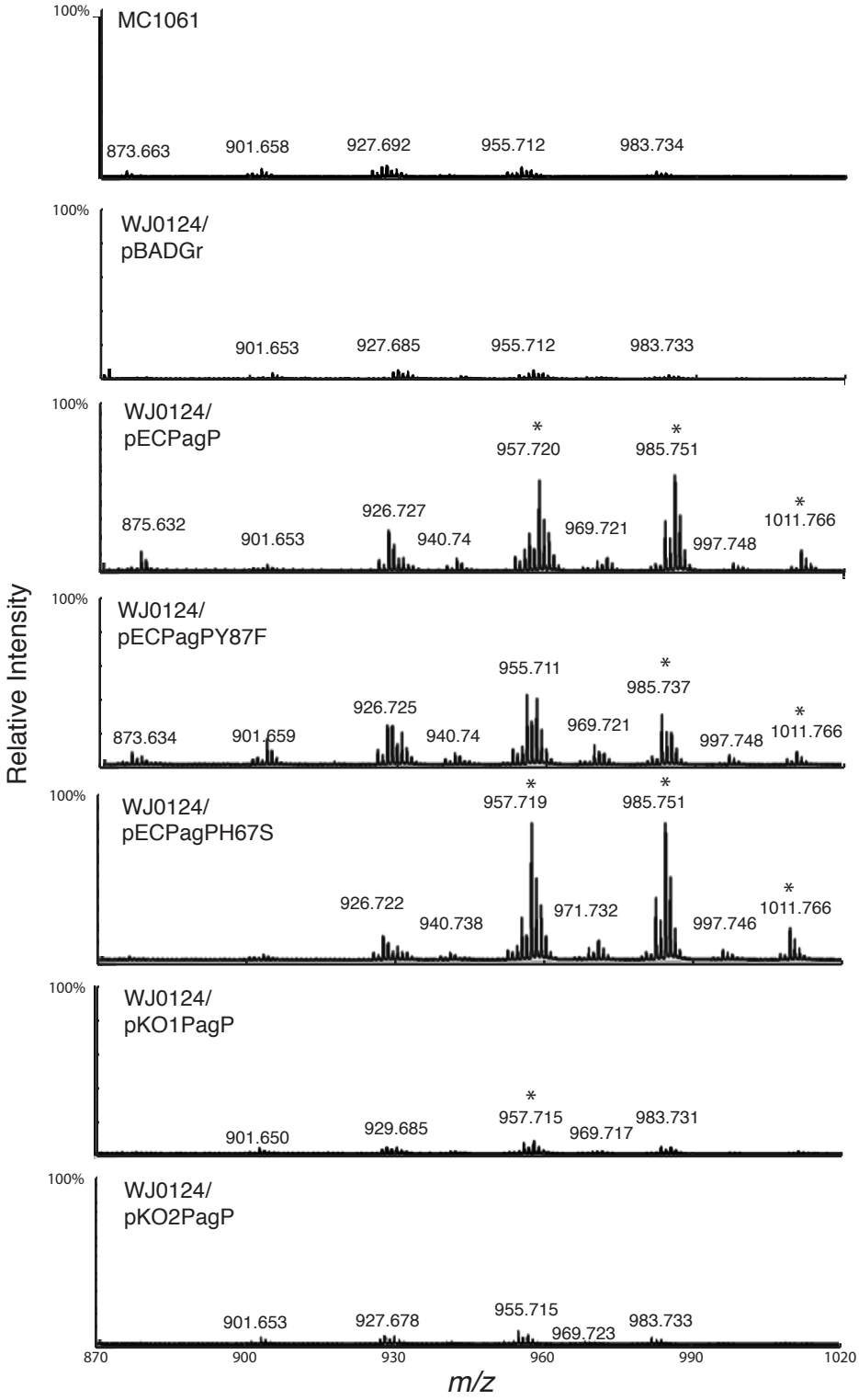

Figure 3.16. Continues on following page

Figure 3.16. The negative-ion MS/MS of acyl-PG from *E. coli*. MC1061 (wild type), *E. coli* WJ0124 (MC1061 Δ*pagP*) and *E. coli* WJ0124 transformed with pBADGr constructs that express PagP from an arabinose-inducible promoter were grown and phospholipids extracted using Bligh and Dyer solvents (1959).The lipids were subjected to ESI-MS and data for *m/z* values 870-1020 are shown (Bulat and Garrett. 2011). ESI-MS $[M-H]^-$ ions of lipid extracts were prepared from: MC1061, WJ0124 /pBADGr, WJ0124/ pEcPagP, WJ0124/ pEcPagPY87F, WJ0124/ pEcPagPH67S, WJ0124/ pKo1PagP and WJ0124/ Ko2PagP. * Signifies a palmitoyl-PG from the OM with C16 at the *sn-3* position (Hsu et al. 2004).

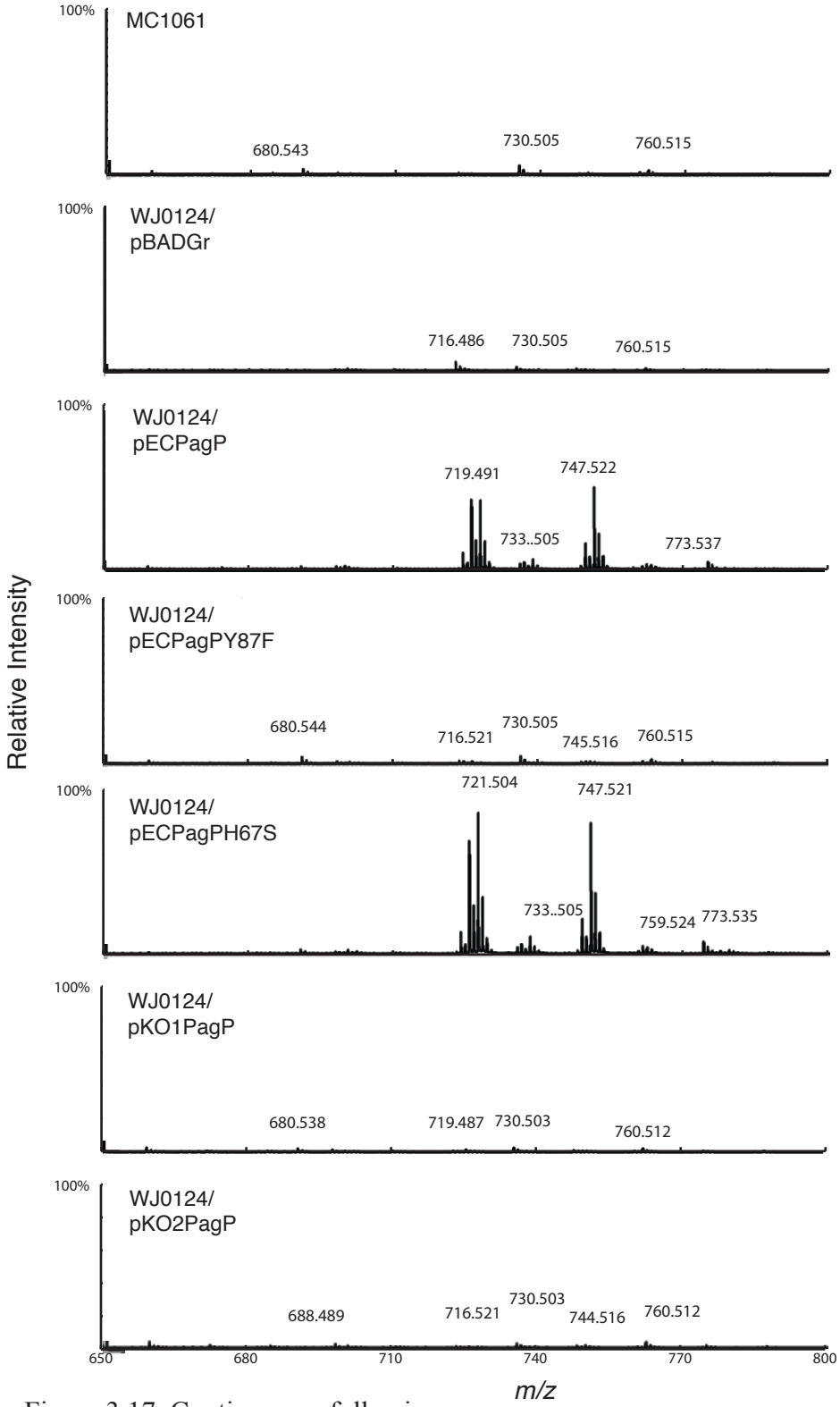

Figure 3.17. Continues on following page

Figure 3.17. Negative-ion MS/MS of BMP from *E. coli. E. coli*. MC1061 (wild type), *E. coli* WJ0124 (MC1061 Δ*pagP*) and *E. coli* WJ0124 transformed with pBADGr constructs that express PagP from an arabinose-inducible promoter were grown and phospholipids extracted using Bligh and Dyer solvents (1959).The lipids were subjected to liquid chromotography which elutes BMP at ~18 mins (Data not shown). This ion was further analysed in the negative ion mode, *m/z* values 650-800 are shown (Bulat and Garrett. 20011; Garrett 2016). MS/MS $[M-H]^-$ ions of lipid extracts were prepared from: MC1061, WJ0124 /pBADGr, WJ0124/ pEcPagP, WJ0124/ pEcPagPY87F, WJ0124/ pEcPagPH67S, WJ0124/ pKo1PagP and WJ0124/ Ko2PagP.

for these investigations MS/MS in the negative mode was performed generating major products with *m/z* values 747.5 and 721.5 (with possibly a C14:0 or C14:1 at the 3'-position) that were only observed from cells overexpressing EcPagP and the H67 mutant (Figure 3.17) (Garrett 2016). Lyso-PG rather than lyso-PE species were also consistent with the production of lyso-PL in bacterial OMs lipids separated by TLC (Table 3.4). Cardiolipin was unaffected by the presence or absence of PagP (Table 3.4).

Table 3.4. Phospholipid relative abundances in *E. coli* with PagP overexpressed determined by ESI-MS

	Relative Intensity (%)						
[M-H]$^-$	MC1061	WJ0124	WJ0124 pEcPagP	WJ0124 pEcPagPY87F	WJ0124 pEcPagPH67S	WJ0124 pKo1PagP	WJ0124 pKo2PagP
				Lyso-PG			
481	0	0	50	0	31	18	0
483	0	0	62	18	18	0	0
495	0	0	18	0	0	0	0
509	0	0	100	18	43	0	0
				Lyso-PE			
450	0	0	50	25	50	12	12
456	0	0	18	18	25	0	0
464	0	0	18	6	25	6	6
478	0	0	62	37	100	6	6
				CL			
673	41	41	50	41	41	41	50
680	8	8	10	8	8	8	8
687	66	66	66	66	50	50	66
693	33	33	41	33	33	33	41
701	25	25	30	25	25	25	30
				PG			
718	40	86	27	67	27	60	70
733	7	13	0	7	0	13	13
747	47	43	27	43	20	40	43
773	13	0	7	10	7	10	10
				PE			
688	27	90	23	64	45	50	69
702	9	32	9	18	14	18	27
716	45	43	32	36	27	27	32
742	14	9	9	9	5	9	9

Relative abundances of zero were close to background signals.

Additionally, we reasoned that if we could co-express EcPagP mutant proteins (S77A and Y87F) in *E. coli* OMs we could determine if the proposed periplasmic active site is responsible for the expansion of the glycerophospholipids. Theoretically, EcPagPY87F will palmitoylate PG (and lipid A) forming PPG (and palmitoylated lipid A), while the S77A mutant should hydrolyze PPG to BMP and BMP to LPG. Likewise, we thought that a similar scenario would play out in the OM for Ko1PagP and Ko2PagP, since both are naturally being expressed in bacterial OMs. The *E. coli* DIXCO3 strain co-expressing the EcPagP mutants did not produce the full range of glycerophospholipids (Figure 3.18). The KoPagPs also did not expand the lipid pool when both were expressed in a *E. coli* background (Figure 3.18). Further, it has been described that the OM is not a continuous bilayer but is made up of lipid domains and islands (Kleanthous et al. 2015). In the OM the two enzymes with the different point mutations would need to be in very close proximity for the product of EcPagPY87F (PPG) to be available as a substrate to EcPagPS77A for hydrolysis of BMP and LPG; this scenario might not present itself in the bacterial OM.

3.6 Discussion

Conformational flexibility within a protein is an important feature and is usually associated with ligand binding, and some enzymes manage catalytic function through such changes (Plapp 2010; Döring et al. 1999). NMR studies reveals that PagP is dynamic and alternates between two distinct relaxed (R) and a tensed (T) states, two conformations possibly associated with ligand binding in the outer membrane (Hwang et al. 2004). PagP

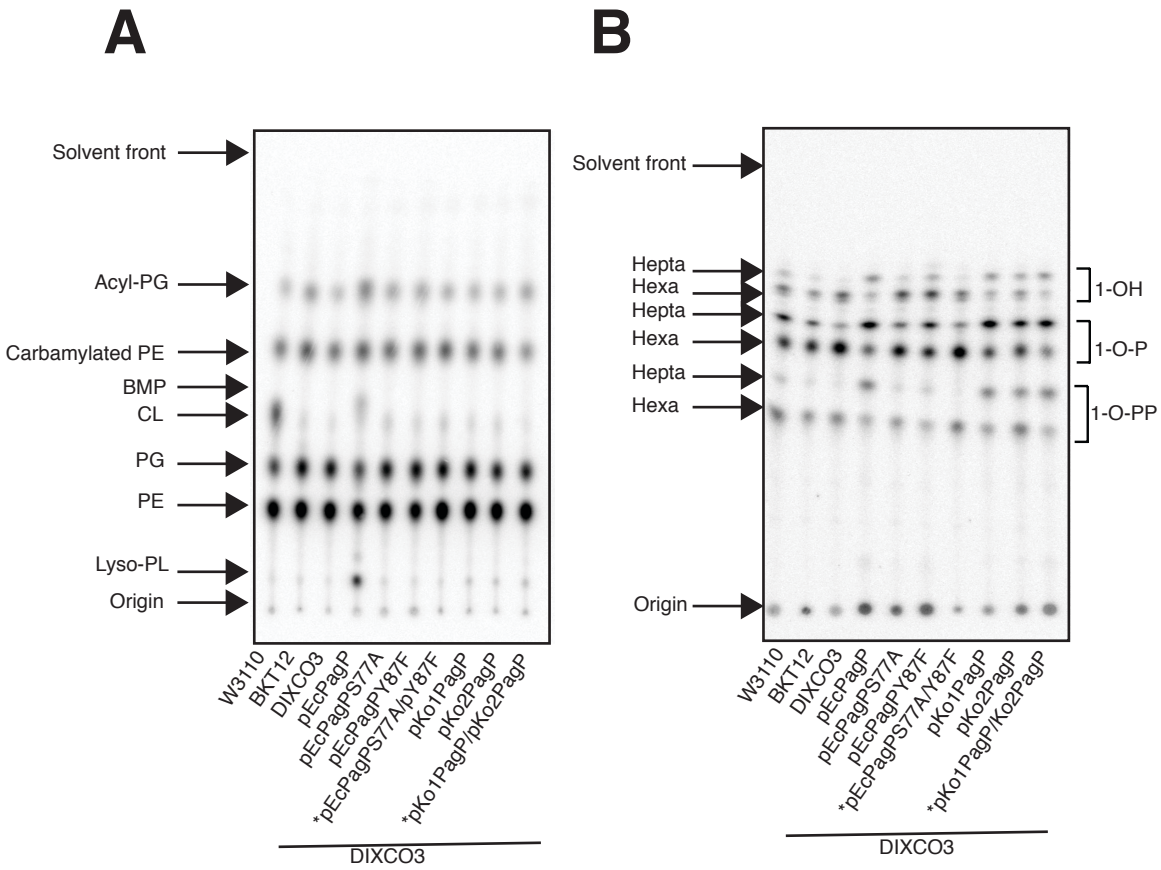

Figure 3.18. Co-expression of EcPagP mutants or KoPagPs does not form glycerophosphoglycerols. A. Autoradiograph showing phospholipid profile for *E. coli* strains W3110 (wild type), BKT12 (W3110 Δ*clsA*, Δ*clsB*, Δ*clsC*) and DIXCO3 (BKT12 Δ *pagP*) harbouring pEcPagP, pEcPagPS77A, pEcPagPY87F, pKo1PagP and pKo2PagP expressed from an arabinose-inducible promoter.*pEcPagPS77A/Y87F and *pKo1PagP/pKo2PagP means that pEcPagPS77A and p'EcPagPY87F, and pKo1PagP and p'Ko2PagP were co-expressed from compatible pBADGr and pUCP20 plasmids (Table 3.1), respectively. Cells were grown and treated with and without EDTA to activate PagP. ^{32}P orthophosphate radiolabeled phospholipids were isolated using Bligh and Dyer solvents (1959), resolved by TLC (solvent system chloroform/methanol/ acetic, 65:25:5 (v/v)), and visualized using Phosphorimaging. B. Autoradiograph showing lipid A profile from the same cultures as in (A). ^{32}P orthophosphate radiolabeled lipid A species were isolated using the mild acid hydrolysis method, resolved by TLC (solvent system chloroform/pyridine/88% formic acid/ water, 50:50:16:5 (v/v)), and visualized using Phosphorimaging.

lies dormant with a 25^{o} tilt in the OM bilayer, but we suspect binding to its phospholipid and lipid A or PG substrates will change the hydrophobic surface potential of PagP causing it to tilt in a upright position on the β-barrel axis during catalytic reactions (Ahn et al. 2004). During these major changes, small internal changes between amino acid side chains may have a coupling effect (indirect) with the enzyme's lipid interaction (Teilum et al. 2011; Horovitz & Fersht 1990).

Evidence is mounting that there is a putative charge relay system or catalytic triad buried between the β-barrel wall and the *N*-terminal α-helix on the periplasmic side of the enzyme that might be necessary for structure-function relationships in PagP (Smith et al. 2008; Bishop Unpublished). The natural substitution in the putative charge relay residues between chromosomal and plasmid-based PagP homologs gives us a unique opportunity to investigate these residues, even though these homologs in *K. oxytoca* are not otherwise completely identical. Our data suggests that the putative charge relay residues have a structural and functional relationship that can be controlled *in vitro* in these *K. oxytoca* PagP homologs. The natural mutation in both residues of the putative charge relay systems seems to have created a stable equivalent with a conformational change that can be detected by circular dichroism. We showed that the switch in the putative charge relay system results in a conformational change that correlates with the presence and absence of the exciton. The residue at position 67 seems to be a highly unstable position but only depending on the substitution within the purified protein, because PagP with substitutions at this position was functional in the bacterial OMs (Smith 2008). This suggests that

folding and insertion of proteins into the membrane bilayer through initiation by chaperones in the periplasm (Sikdar et al. 2017) and/or by mediation by the BAM complex are able to facilitate proper folding despite a single mutation in the protein (Noinaj et al. 2013; Kleinschmidt 2015; Schiffrin et al. 2017). The detergent micelle is unable to replicate similar assistance in the folding of the mutant proteins (Kleinschmidt 2015).

Additionally, we showed that these putative charge relay residues, when switched between the two homologs affects the enzyme ability to transacylate and palmitoylate PG, although lipid A palmitoylation was not affected. We believe this transacylation function is only an *in vitro* feature because in the lamellar OM bilayer under normal conditions PagP is topologically separated from its phospholipid substrate as a donor or acceptor and would not be able to exchange acyl chains between phospholipids (Bishop 2005; Homma et al. 1987). Furthermore, PagP is not believed to be functioning as a phospholipase at its extracellular active site in bacterial OMs where it is more likely to be continuously exposed to lipid A (Bishop 2005; Leive 1968). The results suggest a connection between PG transacylation reaction and palmitoylation reaction (Figure 3.10). For PPG to be detected by autoradiography, first cold PG needs to be transacylated to radiolabeled PG, which is then palmitoylated to PPG. Both reactions take place at the extracellular active site of PagP, indicating a connection between the putative charge relay system and the extracellular active site. Yet, this connection only affected PG as an acceptor substrate and not lipid A. We believed that PagP's phospholipid transacylation reaction occurs

through binding at the embrasure because the reaction is abolished when the P28C/P50C (EcPagP) double mutant is oxidized (unpublished observations). Similarly, we assumed that PG binds non-specifically at the embrasure to form PPG. However, it has been described that lipid A gains access through the embrasure (Khan & Bishop 2009), so there must be some flexibility in the ability of the embrasure to be specific for lipid A or merely selective for a combination of lipid A and PG acceptors. Two other probable routes for acyl chain extraction were identified by steered molecular dynamics simulations, through the crenel and between strands B and C (Figure 3.19) (Cuesta-Seijo et al. 2010). The crenel is the access site for phospholipid acyl chain entry, and considering that PagP acyltransferase reactions proceeds through a sequential mechanism that involves a ternary complex, we do not expect that acyl chain entry and exit would occur at the crenel. This leaves a plausible route through B/C for acyl chain extraction during the transacylation or palmitoylation reaction (Figure 3.19) (Cuesta-Seijo et al. 2010).

Realizing the importance of an "active charge relay system" in Ko1PagP and Ko2PagP in our detergent micelle system, we imagined a similar situation in bacterial OMs. Instead, it seems that palmitoylating PG is not important to *K. oxytoca*, even though at least one of the enzymes have the ability to do so *in vitro*. Physical properties such as hydrophobic and electrostatic interactions in addition to the OM bilayer topology presents a restrictive environment for the protein compared to the detergent micelle environment (Hite et al. 2008). Therefore, the protein may have distinctly different properties in the

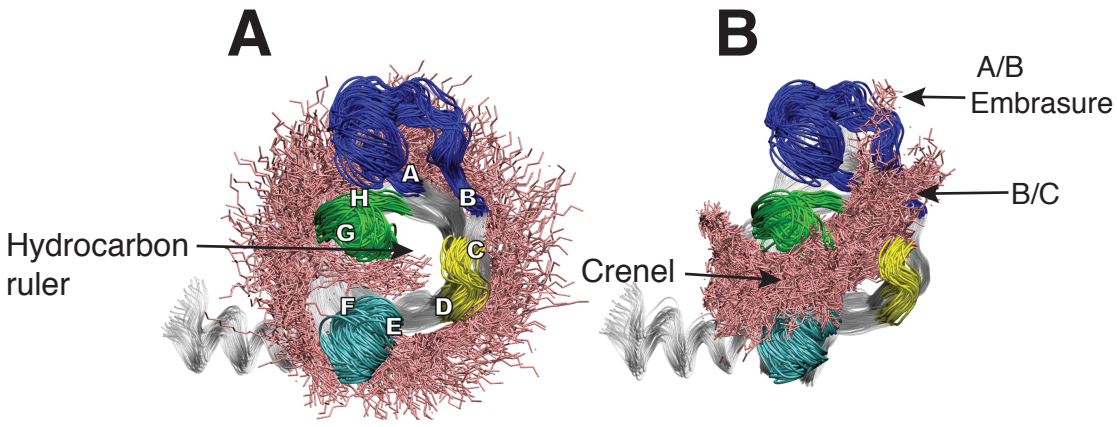

Figure 3.19. Plausible routes for phospholipid acyl chain entry and exit from steered molecular dynamics simulations. The β-barrel strands are labeled A-H and extracellular loops L1, L2, L3 and L4 are dark blue, yellow, light blue and green, respectively. The acyl chains are shown in pink. A. The crenel or opening between F/G is the only route available for acyl chain entry. B. Both F/G and B/C routes can be used for the removal of the acyl chain from the binding site (Cuesta-Seijo et al., 2010).

two environments. Yet, the reactions performed by the enzymes in both environments are quite specific. It would be interesting to know the evolution of the two PagP homologs from *K. oxytoca*. It is possible that the ancestral enzyme had the ability to palmitoylate lipid A and PG, but selective pressure in the OM (for Ko1PagP) and in the primary sequence (Ko2PagP) has deemed both enzymes unable to perform this reaction.

Perhaps the simplest model for switching PagP between being monofunctional in lipid A palmitoylation and bifunctional in palmitoylation of both lipid A and PG comes from a subtle change in β-barrel Shear number associated with the D61/H67 pair. The Shear number of a β-barrel is measure of the extent to which the β-strands are staggered with respect to each other and the barrel axis (Murzin et al. 1994). The loss of the exciton in Ko2PagP, despite the presence of the Y26/W66 exciton partners, indicates that these residues are geometrically organized in a manner that is distinctly different from EcPagP and Ko1PagP. Since Ko2PagP displays a thermal unfolding temperature that is 4˚C higher than EcPagP/Ko1PagP, we can argue that Ko2PagP represents a ground state structure. Introduction of the D61/H67 pair on the β-barrel exterior on the periplasmic side of the membrane can raise the β-barrel structure into an excited state conformation with a corresponding reduction of 4˚C in thermal unfolding temperature. If this excited state structure is altered in the β-barrel Shear number, then a reorganization of the geometric arrangement of the Y26/W66 exciton partners is expected to occur with the consequent elicitation of the previously invisible exciton effect. By demonstrating that the exciton effect can be restored in Ko2PagP upon introduction of the D61/H67 pair we have

confirmed that the excited state structure is modified in its Shear number. Since Shear translates globally in the structure of a β-barrel, we can presume that there is an associated repositioning of the β-strands with respect to each other on the cell surface. Such a global repositioning of β-strands emanating for the periplasmic side of the membrane could easily be translated to the embrasure on the cell surface and influence its ability to recognize lipid A or both lipid A and PG.

We had hypothesized that the D61, H67 and Y87 might be a novel catalytic triad on the periplasmic side of the enzyme that acts as a lipase to hydrolyze PPG to BMP and BMP to LPG. Otherwise, the D61 and H67 could just be a "charge relay system" that is involved in maintaining conformational stability and function (Antonov & Vorotyntseva 1972). We have proven the latter in our detergent micelle system, but this may not translate to the bacterial OM, at least not in the case for *K. oxytoca.* Due to the limitations of the KoPagP homologs to perform both reactions (palmitoylating lipid A and PG) in the bacterial OMs, we continued our investigation with EcPagP and available mutants in the proposed periplasmic catalytic active site. EcPagP requires Y87 to hydrolyze PPG to BMP and BMP to LPG in the bacterial OM. However, H67 is not required for these reactions, suggesting that this putative charge relay system residue is not involved in the periplasmic lipase activity of PagP, but that Y87 plays an important role. Interestingly, our results imply that the enzyme requires Y87 for the accumulation of PPG. It would also appear that the Y87 residue has a correlation with the extracellular active site but only when PG is palmitoylated in bacterial OM. The question of how Y87 functions as a

catalyst remains, but our initial suspicion based on the similarity of the D61/H67/Y87 cluster with the catalytic triad of chymotrypsin fortuitously led us to the discovery of a novel active site despite the structural and non-catalytic role we uncovered for the putative charge relay system residues.

Finally, we had theorized that all PagP homologs that were from the same genetic locus would have the same functions in terms of palmitoylating lipid A and producing the glycerophosphoglycerols, whereas PagPs with a plasmid origin would not be able to form the latter products. This might be true in an *in vitro* setting for the *K. oxytoca* PagPs, but we are unable to make a general statement for duplicated PagP homologs from other bacteria. It would seem that although we can predict the behavior of the enzyme *in vitro* based on the primary sequence or even the structural architecture, in bacterial OMs these enzymes are specific for the lifestyle of different bacteria. The one consistent feature is that PagP is a dedicated palmitoyltransferase both in detergent micelles and bacterial OMs, which suggests that this is the main function of PagP (Bishop 2005; Bishop et al. 2000). We can also argue that selective pressure acting on Ko2PagP has adapted it to function as a monofunctional lipid A palmitoyltransferase because it displays this activity both *in vitro* and *in vivo*. EcPagP is clearly a bifunctional enzyme because it palmitoylates lipid A and expands the pool of glycerophosphoglycerol phospholipids both *in vitro* and *in vivo*. Ko1PagP is somewhat of an anomaly because it behaves as a bifunctional enzyme *in vitro* and as a monofunctional enzyme *in vivo*. The fact that there appears to be a third

pagP gene in *K. oxytoca* (see Chapter 4) might help to clarify why multiple PagP structure-function relationships exist in this organism.

Chapter 4.0

Elucidation of a role for duplicated PagP homologs in *Klebsiella oxytoca*

4.1 Preface

The work presented here describe our attempts to understand the function of the two PagP homologs found in *Klebsiella oxytoca*. Dr. Bishop and I designed the experiments and wrote the manuscript together. Tony Lee assisted with experiments in creating *pagP* knockout strains in *K. oxytoca* and lipid analysis for bacteria grown under various conditions. Saad Syed assisted with data analysis of sequenced plasmid. I performed all other experiments.

4.2 Summary

PagP is an outer membrane (OM) enzyme that transfers a palmitate chain from the *sn*-1 position of a phospholipid to either lipid A or the polar headgroup of phosphatidylglycerol (PG). PagP is encoded by a single gene located on the chromosomes of β- and γ-Proteobacteria, but a subset of bacteria from the γ-Proteobacteria class live as endophytes within plant hosts and encode two *pagP* genes with either both located on the chromosome or one located on the chromosome and the other borne on a plasmid. We wanted to understand the function of the two *pagP* genes in the *Klebsiella oxytoca* genome. The first *pagP* gene encodes Ko1PagP and is located in the same chromosomal locus that corresponds with the location of the *pagP* gene from *Escherichia coli* (EcPagP), but the second *pagP* gene encodes Ko2PagP and is never observed in the same locus between organisms. Ko1PagP and Ko2PagP differ from EcPagP because they are monofunctional lipid A palmitoyltransferases that do not palmitoylate PG in the OM. We created single and double knockouts of the genes that encode Ko1PagP and Ko2PagP in

K. oxytoca and were surprised to discover that these cells still express lipid A palmitoyltransferase activity that can be triggered by EDTA-treatment of cells. These findings imply that a third PagP enzyme is either encoded in the *K. oxytoca* genome at an unannotated plasmid locus or that it lacks sufficient sequence identity to be detected. We demonstrate that Ko1PagP, but not Ko2PagP, increases lipid A acylation under PhoPQ inducing conditions. Both PagP homologs confer some resistance to C18G, the synthetic α-helical cationic antimicrobial peptide. These results indicate that Ko2PagP complements Ko1PagP, but the two homologs might be expressed in response to different environmental signals.

4.3 Introduction

Klebsiella oxytoca is an emerging pathogen (Singh et al. 2016). *K. oxytoca* along with its close relative pathogenic *Klebsiella pneumoniae* are among the top ten most commonly isolated Gram-negative bacteria from intensive care units in the US, Canada and Europe (Neuhauser et al. 2003; Zhanel et al. 2008; Hanberger 1999). *K. oxytoca*, like *K. pneumoniae,* possess several mechanisms that lead to multidrug resistance, such as extended-spectrum β-lactamases (ESBLs), AmpC β-lactamases and aminoglycoside-modifying enzymes (Sato et al. 2015; Jayol et al. 2015; Singh et al. 2016). Their prevalence, combined with the spread of antibiotic resistant strains, testifies to the need for effective alternative or improved traditional anti-infective agents.

Interestingly, *K. oxytoca* and some strains of *K. pneumoniae* are also plant endophytes that promote plant growth. These bacterial strains are mutualistic diazotrophs that provide fixed atmospheric N_2 in the form of ammonia by colonizing the plant host while receiving nutrients and protection without causing disease symptoms (Fouts et al. 2008). *K. oxytoca* has been isolated from a number of plants including wheat, corn, and orchids, where its plant growth promoting features have been described (Pavlova et al. 2017; Cakmakci et al. 1981; Raju et al. 1972). Bacteria with such varied lifestyles are expected to have ingenious adaptation strategies. Changes in environmental cues can cause remodeling of the bacterial outer membrane for the maintenance of optimal membrane architecture (Li et al. 2012).

Lipopolysaccharide (LPS) is the major component of the outer leaflet of the outer membrane of Gram-negative bacteria. LPS is a tripartite molecule with an O-antigen, core oligosaccharide, and lipid A anchor. Lipid A is the biologically active component of LPS that is recognized by host innate immune system (Nikaido 2003; Rietschel et al. 1994). Gram-negative bacteria that colonize and adapt in multiple hosts usually synthesize multiple lipid A structures (Zarrouk et al. 1997; Basheer et al. 2011). Lipid A modification is a strategy used by bacteria to fortify the OM, alter its susceptibility to host antimicrobial peptides, modulate immunity, and control pathogenesis (Needham & Trent 2013; Raetz et al. 2007; Li et al. 2012). Although the LPS from *K. oxytoca* is not well studied, the lipid A from a rough mutant (without O antigen) was characterized to reveal a predominant hexa-acylated structure (like that of the *Escherichia coli* lipid A) with β-1’-6

linked disaccharide of glucosamine as its backbone, phosphorylated at the 1 and 4' position, and acylated with four *R*-3-hydroxymyristate chains with secondary acylation of one laurate and one myristate. Two 3-deoxy-D-*manno*-oct-2-ulosonic acid (Kdo) residues from the inner core are attached to the lipid A backbone (Figure 4.1). A less abundant hepta-acylated form was also identified with a C16 palmitate incorporated at the 2-position of lipid A (Figure 4.1) (Süsskind et al. 1998). The palmitate is incorporated by PagP, a lipid A modification enzyme located in the OM (Bishop 2005; Bishop et al. 2000).

PagP palmitoylates lipid A and phosphatidylglycerol in a number of Gram-negative bacteria (Bishop et al. 2000; Bishop 2005; Dalebroux et al. 2014). Palmitoyl-lipid A increases the bacterial ability to resist host cationic antimicrobial peptides (CAMPs) and modulates the activation of mammalian host immune responses (Bishop 2005), whereas palmitoyl-PG might be involved in fortifying the local barrier function of the OM (Dalebroux et al. 2014). PagP is transcriptionally regulated by the PhoPQ two component system that senses low magnesium concentrations and CAMPs (Guo et al. 1998; Eguchi et al. 2004). PagP is also activated post-transcriptionally by treatment of cells with EDTA, which disrupts OM lipid asymmetry and promotes the ectopic exposure of phospholipids in the external leaflet of the OM (Jia et al. 2004).

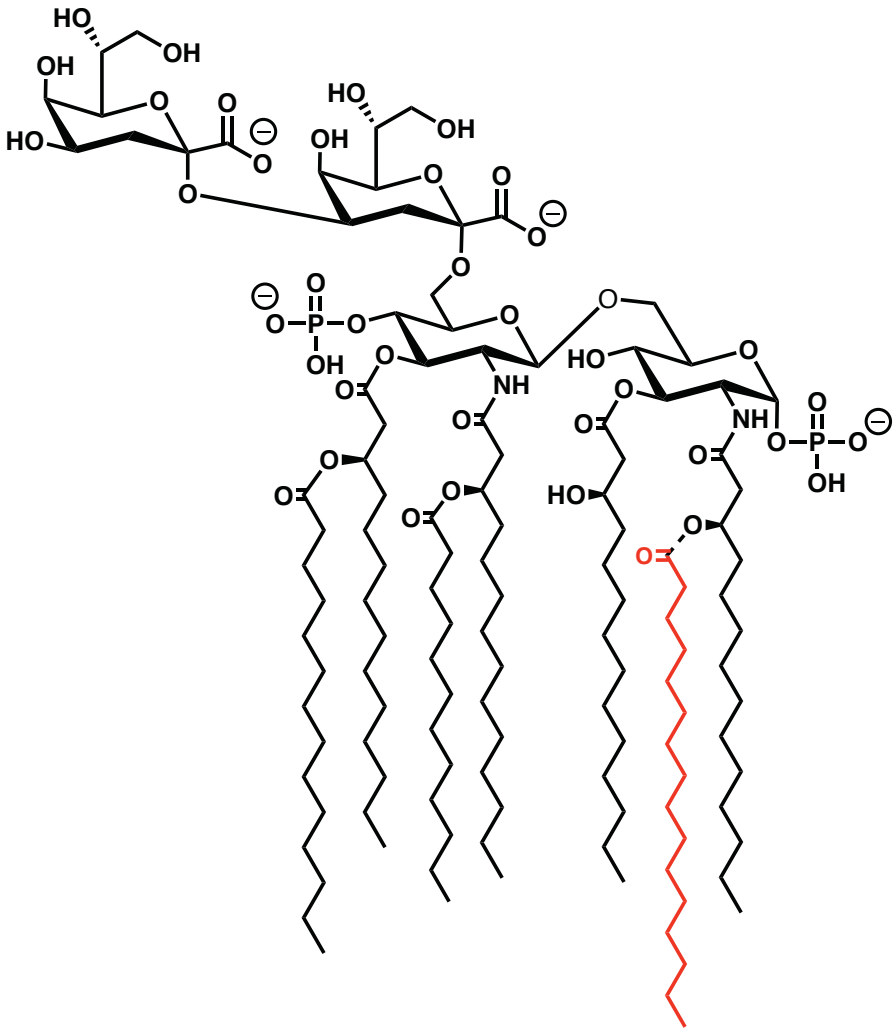

Figure 4.1. Structure of lipid A exhibited by *K. oxytoca*. *K. oxytoca* displays a predominantly hexa-acylated lipid A with a β-1'-6 linked disaccharide, acylated with four *R*-3-hydroymyristates which are further acylated with a laurate (C12) and a myristate (C14). The glucosamine backbone is attached to two Kdo sugars and phosphorylated at the 1 and 4' positions. A C16 palmitate (in red) is found attached to the hydromyristate at the 2-position in a less predominant species of lipid A (Süsskind et al. 1998).

PagP has been described previously to be encoded by a single copy gene (Bishop 2005). *K. oxytoca* is one of a small group of γ-Proteobacteria that encode two *pagP* genes on its chromosome. The other bacteria with two *pagP* genes on the chromosome are *Raoultella ornithinolytica, Enterobacter cloacae, Erwinia billingiae* and *Serratia fonticola* (Raju et al. 1972; Sandhiya et al. 2001; Thijs et al. 2014). Additionally, some bacteria encode *pagP* on a plasmid that accompanies the original *pagP* on the chromosome. Although multiple copies of a lipid A biosynthetic acyltransferase have been described for LpxB in *Legionella pneumophila* and LpxL in *K. pneumoniae*, to our knowledge this is the first report on multiple copies of a lipid A modification enzyme that is embedded in the OM (Mills et al. 2017; Albers et al. 2007). The aim of this study was to elucidate the role(s) of the two PagP homologs in *K. oxytoca.*

4.4 Methods

4.4.1 Bacterial strains, plasmids and growth conditions

The bacterial strains and plasmids used are described in Table 4.1. Cells were generally grown at 37 ºC on semi-solid or liquid LB media consisting of 10 g Tryptone, 5 g yeast extract, 10 g NaCl and 15 g agar (for semi-solid media). To create *pagP* knockouts cells that required hygromycin, cells had to be grown in low salt LB with 5 g NaCl, all other components remain as in regular LB. Antibiotics were added as necessary at final concentrations of 50 and 100 μg/mL for apramycin, 100 μg/mL for hygromycin, 15 μg/mL for gentamicin and 25 μg/mL for kanamycin. The term “overnight culture”

refers to a liquid culture in LB broth inoculated with a single bacterial colony from semi-solid media and allowed to incubate for 16 to 18 hours.

For anaerobic growth glycerol-fumarate medium was used (Spencer & Guest 1973). The medium contained per liter: KH_2PO_4, 5.44 g; K_2HPO_4, 10.49 g; $(NH_4)_2SO_4$, 2 g; $MgSO_4.7H_2O$, 0.05 g; $MnSO_4.4H_2O$, 5 mg; $FeSO_4.7H_2O$, 0.125 mg; $CaCl_2$, 0.5 mg; Fumaric acid, 4.6 g, casamino acid, 0.5 g and 15 mL of 50% filter sterilized glycerol was added after sterilization. Cultures were grown in flasks or tubes with screw caps and media was added to fill tubes or flasks. Anaerobic incubation on solid media (in regular petri dishes) was carried out in a gas generating system incubation container for cultivating anaerobic microorganisms (BD GasPak™ EZ container systems and anaerobic indicators).

Table 4.1 Bacterial strains and plasmids

Strains /Plasmids	Description	Source
***E. coli* strains**		
MC1061	F^-, λ^-, *araD139,* Δ*(ara-leu)7697,* Δ *(lac)X74, galU, galK, hsdR2* (r_K-m_K+), *mcrB1, rpsL*	(Casadaban & Cohen 1980)
WJ0124	MC1061 *pagP::amp*^{r}	(Jia et al. 2004)
***K. oxytoca* strains**		
ATCC 8724	Wild type	ATCC
ΔKo1PagP	ΔKo1*pagP*	This study
ΔKo2PagP	ΔKo2*pagP*	This study
ΔKo1/2PagP	ΔKo1/2*pagP*	This study
Plasmids		
pBADGr	*ori araC-*P_{BAD} *dhfr*::Gm^r *mob*$^+$	(Asikyan et al. 2008)
pKo1PagP	pBADGr with *Klebsiella Ko1pagP*	This study
pKo2PagP	pBADGr with *Klebsiella Ko2pagP*	This study
pIJ773	Apramycin resistance cassette, Amp^R	(Gust et al. 2004)
pACBSR-Hyg	p15A replicon plasmid, arabinose P_{BAD} promoter, red recombinase, Hyg^R	(Huang et al. 2014)
pFLP-Hyg	p15A replicon, heat shock inducible FLP recombinase, Hyg^R	(Huang et al. 2014)

4.4.2 DNA isolation and manipulations

Plasmids were isolated using a QIAprep Spin Miniprep Kit from Qiagen or Invitrogen. Isolations were done according to manufacturer's instructions. For low copy plasmids (e.g. pBADGr) 5 or 10 mL of the sample was harvested initially and the remainder of the protocol followed according to manufacturer's instruction.

4.4.2.1 Large plasmid isolation

The alkaline lysis method was used with some modification (Sambrook & Russell 2001). Cultures were grown overnight, and 1 mL aliquots were harvested for 2 mins at 5000 rpm. The supernatant was discarded, and the pellet was washed twice with 150 µL of tris-EDTA (10 mM Tris, 1 mM EDTA pH 8). The pellet was then re-suspended (by vortexing vigorously) in 100 µL ice cold freshly made 25 mM Tris HCl with 10 mM EDTA. 200 µL of 1M NaOH with 1% SDS was added to the suspension and mixed thoroughly without vortexing, before placing on ice for 5 mins. 150 µL of ice cold acidic potassium acetate (1.5 mL glacial acetic acid, 28.5 ml distilled water and 60 ml of 5M potassium acetate) was added and the mixture was gently mixed by inversion. The mixture was centrifuged at 12000 rpm for 5 mins at 4 ^{o}C. The supernatant with the plasmid was transferred to a fresh microtube and 20 µL of DNase free RNase (10 mg/mL) was added to ensure removal of any traces of RNA. This was placed on ice for 10 min. Equal volumes of phenol/chloroform/isoamyl alcohol (DNA grade) was added to the supernatant and the suspension was mixed gently. This was centrifuged at 12000 rpm, 5 min at 4 ^{o}C. The upper layer without precipitate was transferred to a fresh microtube.

Centrifugation was repeated if the upper layer was not clear. Two volumes of ice cold ethanol were added to the supernatant and the suspension mixed and left to incubate at room temperature for 60 min. The plasmid DNA was precipitated by centrifugation at maximum speed at room temperature for 10 mins. Plasmid DNA was air dried by inverting the tubes to drain on paper towel. Plasmid DNA was washed twice with 1µL 70% ethanol at 4 ^{o}C to remove ethanol. Plasmid DNA was re-dissolved in 50 µL of TE buffer or water, pH 8 and stored at 4 ^{o}C.

4.4.2.2 Plasmid sequencing and analysis

The isolated plasmid from the *pagP* double knockout was separated and excised from 1% agaraose gel. The excised band was purified using Invitrogen PCR and gel extraction kit. Plasmid DNA was shut-gun sequenced using Illumina next generation sequencing platform (Illumina, San Diego, CA). The sequenced data was processed and *de novo* assembled using SPAdes and annotated with Prokka (Seemann 2014; Bankevich et al. 2012). Analysis of assembled contigs was done using Geneious 8.1.2, an integrated and extendable desktop software platform for the organization and analysis of sequence data (Kearse et al. 2012). Contigs with chromosomal contamination were discarded. Nucleotide BLAST was used to compare our data to sequences in the NCBI database.

4.4.3 Construction of Ko1PagP and Ko2PagP single and double knockouts

We attempted to generate *pagP* single and double knockouts in *K. oxytoca* by using the Red recombinase method adopted from Huang et al. (2014). Three plasmids

were used to assist in creating these knockouts; pIJ773, pACBSR-Hyg and pFLP-Hyg. pIJ773 contains an apramycin cassette with flanking FRT sites that replaced the gene of interest. The apramycin cassette was cut from pIJ773 with restriction enzymes *Eco*RI and *Hin*dIII. The products were separated on a 1% agarose gel; the smaller 1.3 kb band was excised from the gel and extracted using a commercial (Qiagen) gel extraction kit. This DNA was used as the template for priming the homologous region of the chromosome using the specially designed 80 bp primers which include 60 bp of the homologous region flanking gene of interest (Table 4.2). pACBSR-Hyg (hygromycin resistance gene) contains the λ-Red system, it is used to facilitate homologous recombination between the apramycin cassette and the target locus in the chromosome. This plasmid contains the three genes necessary for the process to occur; *beta*, *gam* and *exo* under the control of an arabinose-inducible promoter. pACBSR-Hyg was electroporated into *K. oxytoca* ATCC 8724, cells were grown out and plated on low salt LB agar supplemented with hygromycin and incubated at 37 ºC. Next, the PCR product (linear DNA with the apramycin cassette with flanking FRT sites and homologous region) was electroporated into the cells containing lambda red function. The enzymes of the λ-Red system assist the linear DNA to be recombined into the chromosome swapping out the gene of interest for the apramycin cassette. Overnight cultures of *K. oxytoca* harboring the pACBSR-Hyg plasmid was subcultured into 90 mL low salt LB, 10 mL of sterile 1 M L-arabinose solution, and 100 μg/mL hygromycin, and grown at 30 ºC at 200 rpm. 200-500 ng of the knockout cassette was introduced into the cell by electroporation. Cells were grown out and plated on LB agar with 50 μg/mL apramycin. Conformation primers (Table 4.2) were

used to detect colonies with the appropriate knockout cassette. Confirmation primer pairs spanned ~250 bp upstream and 250 bp within the gene of interest. Colonies with the correct PCR product were then passed through LB with apramycin for several days until cells were sensitive to hygromycin. Next, pFLP-Hyg (containing FLP recombinase) was introduced into the cells with the knockout cassette that are sensitive to hygromycin by electroporation. pFLP-Hyg facilitates the excision of the apramycin cassette from the chromosome. The cells were grown overnight at 30 ºC, plated on LB and heat-shocked at 43 ºC overnight. The colonies were then streaked onto matching LB and LB apramycin plates to screen for loss of the apramycin gene from the knockout cassette. Colonies that were sensitive to apramycin were passed several times in LB media at 37 ºC until they had regained hygromycin sensitivity. PCR was used to confirm apramycin gene deletion.

Table 4.2 Primers used in construction and confirmation of *pagP* knockouts and plasmid *pagP* identification

Primer	Sequence 5'-3'
Ko1PagP_ko_Fwd	cctaataccgttaaggtagtattaagattatctttgttatcttactccgctttaaaaatg attccggggatccgtcgacc
Ko1PagP_ko_Rev	tctttgtttttcaacaagacagtccgcttatctcttttattgctataaaaaatcgcatca tgtaggctggagctgcttc
Ko2PagP_ko_Fwd	ctgtttttttgttcccaaactgaatgaacaccgggcgactttctttaaggaa taaaacgatgattccggggatccgtcgacc
Ko2PagP_ko_Rev	tcaaaaaagtgattacgatttgacgatcgccggttcagctcatggccg cctgcgcatttatgtaggctggagctgcttc
Ko1PagP_Conf_Fwd	gggaatgtgcctaaaaaacggg
Ko1PagP_Conf_Rev	taaaccacttaacgttaccttt
Ko2PagP_Conf_Fwd	catctatttctcaatcactgcg
Ko2PagP_Conf_Rev	ctcgccaccattagcaaaacga
pPagP_ Fwd	gcgacgttgtctgcggatag
pPagP_Rev	agcacgttgccgttattgtag

4.4.3.1 Chemical transformation

To prepare chemically competent cells for protein analysis in bacterial outer membranes, the calcium chloride method was applied. 50 mL of LB was inoculated with 1% overnight culture of the appropriate bacteria and was allowed to grow at 37 ºC at 200 rpm to OD_{600} 0.4-0.6. The cells were placed on ice for 10 mins. All remaining steps were carried out at 4 ºC. The cells were harvested at 6000 rpm for 3 mins. The supernatant was discarded and the pellet re-suspended in 10 mL cold 0.1M $CaCl_2$, very gently. The re-suspended cells were incubated on ice for 20 mins then centrifuged as above. The supernatant was discarded and gently re-suspended in 5 mL cold 0.1M $CaCl_2$. This was then dispensed into microtubes and placed at 80 ºC.

To transform these cells, 1 µL of the plasmid DNA, then 100 µL of competent cells were added to a microtube. The microtube was then placed on ice for 30 mins. The cells were then heat shocked at 42 ºC for 45 secs and then chilled on ice for 2 mins. 500 µL of SOC media was added to the cells and they were outgrown at 37 ºC for 1 hr. The cells were centrifuged at 8000 rpm for a min, 400 µL of the supernatant was discarded. The remaining 100 µL of supernatant was used to resuspend the cells and plate on LB with appropriate antibiotic.

4.4.3.2 Electroporation

To transform *K. oxytoca* cells by electroporation, 100 mL of LB was inoculated with 1% overnight culture, grew at 37 ºC and 200 rpm until the cells reached an OD_{600} of 0.4, ~2.5 hours. Cultures were transferred into centrifuge tubes and placed on ice for 15

mins. Everything was kept cold for the remainder of the procedure. Cultures were then centrifuged at 6500 rpm for 5 mins, and the supernatant was discarded. Cells were washed with 50 mL of 10% cold glycerol and centrifuged at 6500 rpm for 5 mins and the supernatant discarded (this step was repeated twice). As much as the glycerol as possible was removed from the pellet and then the pellet was re-suspended in residual (~50 μL) 10% cold glycerol with a 1000 μL pipette tip. 200-400 ng of DNA was added to the re-suspended culture and then transferred to a cold electroporation cuvette, a voltage of 2500 was used. Cells were then outgrown at 37 ºC and 200 rpm for 90 mins and then selected for by the appropriate antibiotic on LB plates.

4.4.4 *In silico* analysis of *pagP* gene

PagP sequences from bacteria of interest were analyzed using tBLASTn (Gertz et al. 2006). The sequences were found in genomes of bacterial species of interest. The gene arrangement from each bacterium was examined for size, orientation, and location within the genome. The *pagP* gene arrangements from bacteria of interest were aligned.

4.4.5 ^{32}P orthophosphate labeled lipid analysis from bacterial OM

PagP sequences with signal peptide from *K. oxytoca* were purchase from Invitrogen GeneArt™ in carrier plasmids. The sequences were designed for cloning into *Eco*RI and *Hin*dIII restriction sites of plasmid pBADGr (Table 4.1). Double digestion of the carrier plasmid (with the *pagP* gene) and pBADGr plasmid were conducted by standard cloning methods according to manufacturers' protocol for Invitrogen restriction

enzymes. The digested plasmid and *pagP* insert were gel purified and then extracted using a Qiagen gel extraction kit. These were ligated with T4 ligase from the Invitrogen DNA ligase kit according to the manufacturers' protocol. The ligated plasmid-*pagP* construct was transformed into XL1-Blue competent cells according to manufacturers' protocol. The plasmid is isolated and transformed using chemically competent cells or electroporation into *E. coli* strain or *K. oxytoca* strain for outer membrane protein expression.

Lipid A species and phospholipids from *E. coli* strain or *K. oxytoca* strains were analyzed by the mild acid hydrolysis method. The respective strains of bacteria from *K. oxytoca* with and without *pagP* genes and complementation of *pagP* on low copy number plasmids (pBADGr) were analyzed for their lipid content (Table 3.1). A 1% inoculum of an overnight culture was subcultured into 5 mL fresh LB media with 15 mg/mL gentamicin for cultures with pBADGr, and 5 μC_i/mL of ^{32}P orthophosphate for labeling. The cells were grown for 2 hrs 55 mins after which 25 mM of EDTA was added and the cells allowed to grow for an additional 5 mins prior to harvesting in a clinical centrifuge at high speed for 10 mins. The cells were then washed with 4 mL 1 X PBS before re-suspended in 0.8 mL PBS, and subsequent addition of 1 mL chloroform and 2 mL methanol, then left at room temperature for 1 hr (Bligh & Dyer 1959). The cells were pelleted and the supernatant* was collected for phospholipid analysis. The remainder of this protocol is only for lipid A isolation. The pellet was washed with 5 mL of single phase Bligh/Dyer solvents (chloroform/methanol/PBS - 1:2:0.8) and centrifuged at high

speed. The pellet was then dispersed in 1.8 mL of 12.5 mM sodium acetate pH 4.5 and 1% SDS by sonic irradiation. This suspension was incubated at 100 ^{o}C for 30 mins and then cooled. The mixture was then converted to two-phase Bligh/Dyer solvents by adding 2 mL chloroform and 2 mL methanol vortexed and centrifuged at high speed for 10 mins. The lower phase was collected and washed with 4 mL upper phase of the two-phase Bligh/Dyer solvents (chloroform/methanol/PBS – 2:2:1.8) centrifuged for 8 mins, collected lower phase and dried under a stream of nitrogen. 2 µL was added to 2 mL scintillation fluid for radiolabeled counts. 1000 cpm of the lipid A samples were spotted on the silica 60 TLC plate. The plate was resolved in a sealed tank that was previously equilibrated for ~ 3 hrs with solvent system chloroform/ pyridine/ 88% formic acid/ water (50:50:16:5 v/v).

4.4.5.1 Phospholipids analysis

To the supernatant* 2 mL of chloroform and 2 mL of 1 X PBS were added, the suspension was vortexed and centrifuged at high speed (Bligh & Dyer 1959). The lower phase was collected and dried under a low stream of N_2. The dried lipid was re-suspended in 200 µL of chloroform/methanol (4:1 v/v) by sonication with periodic icing. 2 µL was added to 2 mL of scintillation fluid for radiolabeled counts. 10,000 cpm of the phospholipid samples were spotted on the silica 60 TLC plate. The plate was resolved in a sealed tank that was previously equilibrated for ~ 3 hrs with solvent system chloroform/methanol/acetic acid (65:25:5 v/v). The resolved plate was air-dried or blow-dried on cool setting. The TLC plate was exposed to a Phosphorimager screen overnight.

The products were visualized using a Molecular Dynamic Typhoon 9200 Phosphorimager

4.4.6 Antimicrobial peptide susceptibility assays

MICs were determined by the microdilution method according to Clinical and Laboratory Standards Institute (CLSI) guidelines. Cells were plated on Mueller Hinton II (MHII) media and grown overnight (MHII media was used because it is cation-adjusted and is suitable for this antimicrobial peptide MIC study). Overnight bacterial cultures grown in MHII broth were subcultured by 1:50 in fresh MHII broth and grown to an OD_{600} of 0.6-0.8 at 37 ºC, with shaking at 200 rpm. Bacterial cultures were standardized to OD_{600} 0.5 and then further diluted 1:200 in MHII broth. A total of 100 μL of standardized samples were plated in 96 well microtiter plates including serial dilutions of C18G. Plates were sealed and incubated for 18 hours at 37 ºC. MICs were determined as the concentration which no visible growth was observed after incubation. Experiments were done three times with two technical replicates each time.

4.5 Results

4.5.1 KoPagP homologs acylate lipid A in *K. oxytoca* OMs

In vitro, both Ko1PagP and Ko2PagP palmitoylate lipid A, but only Ko1PagP palmitoylates PG to form PPG, which then expands the PG glycerophosphoglycerols (Chapter 3, Figure 3.7 and 3.8). To investigate the function of PagP homologs in the *K. oxytoca* OM we decided to create *pagP* single and double knockout strains. We obtained a non-cytotoxic *K. oxytoca* strain ATCC 8724 from the American Type Culture

Collection and we adapted the red recombinase system protocol for creating knockouts in *K. pneumoniae* (Table 4.1; Table 4.2) (Huang et al. 2014; Shin et al. 2012). This method uses two selection markers, an apramycin resistance cassette to replace the target gene and hygromycin resistance to select for two plasmids at different times, that mediated homologous recombination and excision of the apramycin cassette (Huang et al. 2014). To verify *pagP* knockout strains, we designed confirmation primers to span the middle of the *pagP* gene to ~200 bp upstream of the gene resulting in a product of about 500 bp for each knockout. PCR and DNA sequencing were used to verify knockouts (Figure 4.2A). Ko1*pagP* and Ko2*pagP* genes were completely deleted from the single and double mutants, respectively (Figure 4.2A). An 81 bp scar region of the FRT sites replaced the Ko1*pagP* and Ko2*pagP* genes in the *pagP* deleted strains.

To confirm the absence of enzyme activity we extracted and examined the lipid A profiles in *K. oxytoca* OMs in wild type and *pagP* knockout strains. Cells were grown to early log phase, briefly treated with EDTA to activate the enzyme, and lipid A species were extracted using mild acid hydrolysis and separated by TLC (Figure 4.2B). Although PCR analysis confirmed that the genes were absent, lipid A profiles suggested lipid A acylation occurred in response to EDTA treatment (Figure 4.2B) (Jia et al. 2004). For Ko1*pagP* and Ko2*pagP* single knockouts we observed slightly less lipid A acylation than the wild type, which is expected because these knockout strains still had a *pagP* gene present in their genomes. Unexpectedly, the double *pagP* gene knockout strain also showed lipid A acylation, even though both genes were deleted (Figure 4.2B). We

decided to overexpress Ko1PagP and Ko2PagP on plasmids in the knockout strains in order to extract lipid species to investigate the function of *pagP* in the *K. oxytoca* OMs (Figure 4.3 and 4.4). We observed the same level of lipid A acylation in all the strains investigated, suggesting that Ko1PagP complements the Ko2*pagP* knockout and vice versa (Figure 4.3B). The same level of lipid A acylation was also seen in the double knockout strain, suggesting that there might be a third lipid A palmitoyltransferase enzyme in *K. oxytoca* ATCC 8724 OMs. When we examined the phospholipid profile of the mutants and the overexpression of PagP in these mutants we realized that neither the deletion nor overexpression of either Ko1PagP or Ko2PagP affected the phospholipid profiles of the *pagP* knockout strains (Figure 4.4). These findings confirm that Ko1PagP and Ko2PagP acylate lipid A in response to EDTA treatment, but have no effect on PPG production in the OM of *K. oxytoca.* We conclude that there is possibly a third PagP encoded in the genome of *K. oxytoca* ATCC 8724.

4.5.2 Possibly a third lipid A palmitoyltransferase enzyme in *K. oxytoca* ATCC 8724 OMs

Prior to understanding the distribution of PagP in Gram-negative bacteria, *pagP* was known to be a single copy gene in bacterial genomes (Chapter 2). We are now aware that some bacteria have two copies, and not only is *pagP* found in the main chromosome but also in plasmids (Chapter 2 Figure 2.6; Table 4.3). The results observed for the lipid A profiles of wild type and *pagP* deleted strains in *K. oxytoca* indicate that there might be

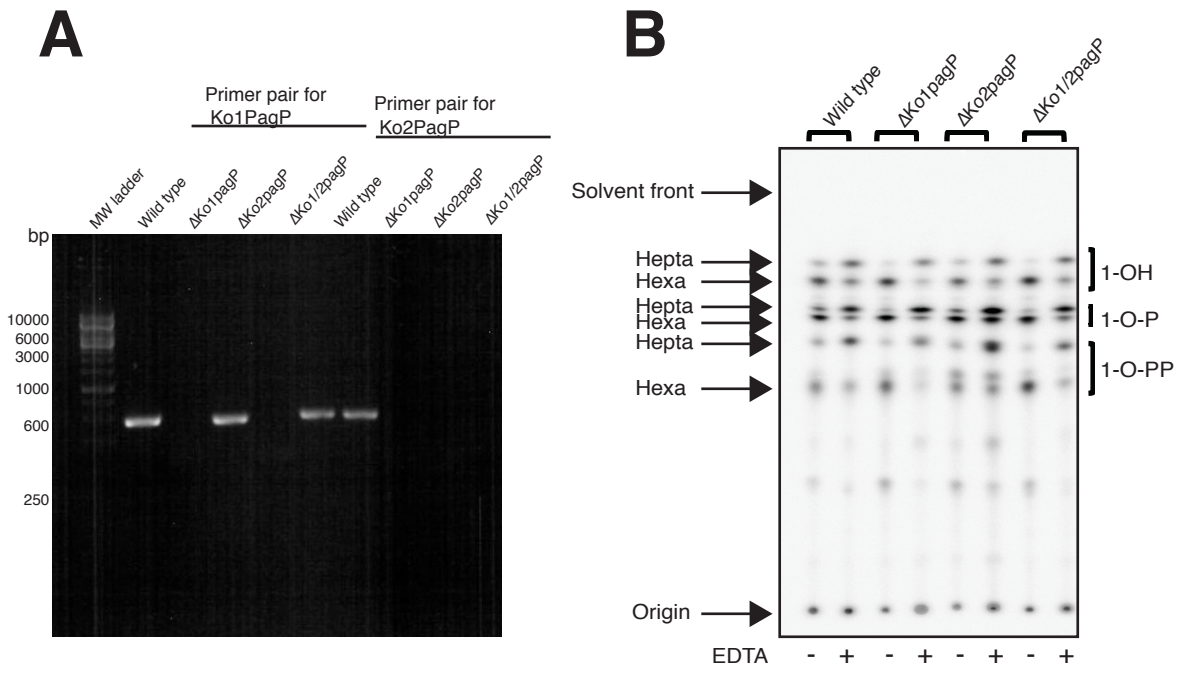

Figure 4.2. Confirmation of single and double *pagP* knockout ΔKo1*pagP*, ΔKo2*pagP* and ΔKo1/Ko2*pagP* . A. 1% agarose gel showing PCR products with knockout confirmation primer pairs for Ko1*pagP* (left four lanes not including ladder) and the four lanes on the right are PCR procducts for primer pairs for Ko2*pagP* knock-out confirmation. B. Lipid A profile for *K. oxytoca* single and double *pagP* knockouts. Cells were grown to early log phase, treated with and without EDTA to activate PagP and lipids isolated by mild acid hydrolysis. The lipids were separated by TLC and visualized by Phosphorimaging. TLC plates were resolved in solvent system chloro-form/ pyridine/ 88%formic acid/ water, 50:50:16:5 (v/v). The main lipid A species are indicated on the left and include the hepta, hexa and penta-acylated lipid A with the 4'-monophosphate (1-OH), 1,4' *bis*-phosphate (1-O-P) or 1-diphosphate (1-O-P-P) derivatives of each species.

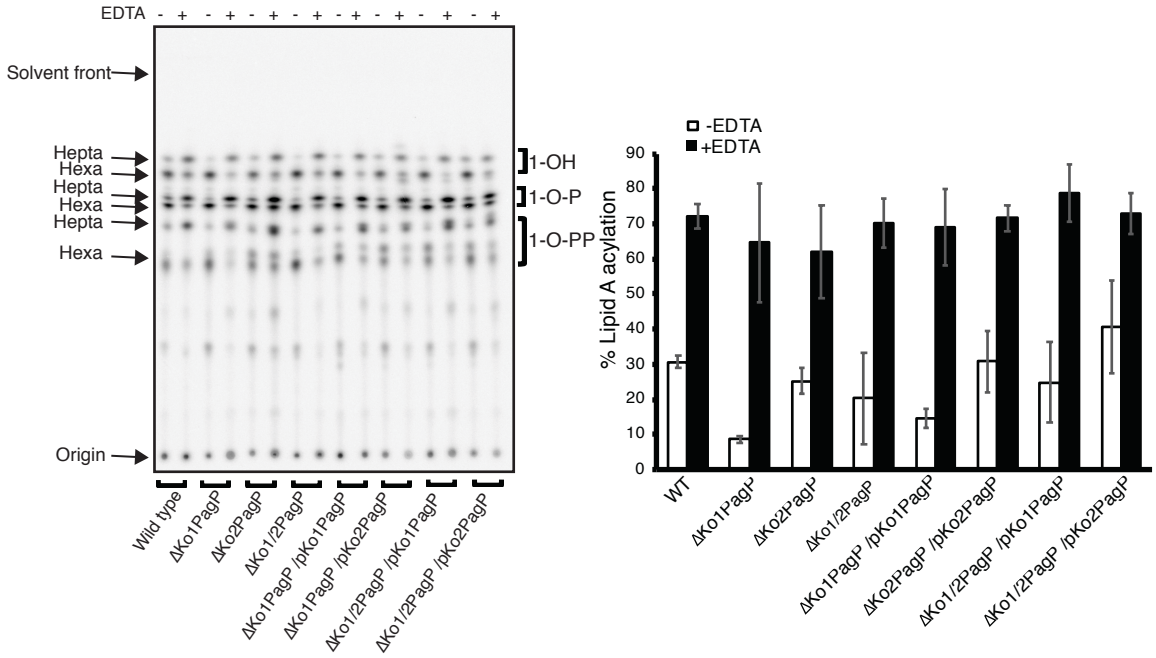

Figure 4.3. Lipid A profiles for *K. oxytoca* wild type, *pagP* knockouts and *pagP* complemented strains. Cells were grown with ^{32}P orthophosphate to early log phase and treated with or without EDTA. ^{32}P orthophosphate labeled lipid A species were isolated using mild acid hydrolysis from *K. oxytoca* wild type, ΔKo1PagP, ΔKo2PagP, Δ Ko1/2PagP with pKo1PagP, pKo2PagP expressed from an arabinose-inducible promoter. A. The lipids were separated by TLC and visualized by Phosphorimaging. TLC plates were resolved in solvent system chlorform/ pyridine/ 88%formic acid/ water, 50:50:16:5 (v/v). The main lipid A species are indicated on the left and include the hepta, hexa and penta-acylated lipid A with the 4'-monophosphate (1-OH), 1,4' *bis*-phosphate (1-O-P) or 1-diphosphate (1-O-P-P) derivatives of each species. B. The hexa and hepta-acylated lipid A species for the 1, 4' bis-phosphoryl lipid A form (1-O-P) were quantified using ImageQuant software. Error bars represents the mean +/- standard deviation of three biological replicates.

a third *pagP* gene in the genome of this bacterium, possibly on a plasmid. *K. oxytoca* strain CAV1374 has three *pagP* genes in its genome; two on the chromosome and one on plasmid pCAV1374-150 (Table 4.3) (Sheppard et al. 2015). Therefore, it would not be unusual to find *pagP* on a plasmid in *K. oxytoca* strain ATCC 8724. However, the complete genome of *K. oxytoca* ATCC 8724 strain was published with no mention of an associated plasmid (Shin et al. 2012). Despite these findings, it is known that megaplasmids with sizes of 100 Kbp or larger are often found in *Klebsiella spp*. and sometimes go undetected because they do not separate readily from chromosomal DNA, and often get trapped in the sample wells in conventional gel electrophoresis (Barton et al. 1995). Plasmids with a *pagP* gene have an average size of 300 Kbp (Table 4.3). As such, we carried out plasmid extraction using the commercial Qiagen kit and alkaline lysis large plasmid isolation protocols from wild type and *pagP* deleted strains and ran the results on a 1% agarose gel (Figure 4.5A) (Sambrook & Russell 2001). Surprisingly, we observed bands at ~20 Kbp and just below the well in the wild type and *pagP* deleted strains, which could represent supercoiled and relaxed plasmid DNA, respectively (Higgins et al. 2016). The band just below the sample well could also be plasmid DNA contaminated with chromosomal DNA (Barton et al. 1995). Plasmid isolation and electrophoretic mobility of a laboratory strain *E. coli* MC1061, which is known to have no associated plasmid (Table 4.1) yielded no bands on a 1% agarose gel (Casadaban & Cohen 1980). This suggests that the bands observed from the *K. oxytoca* strains could be plasmids.

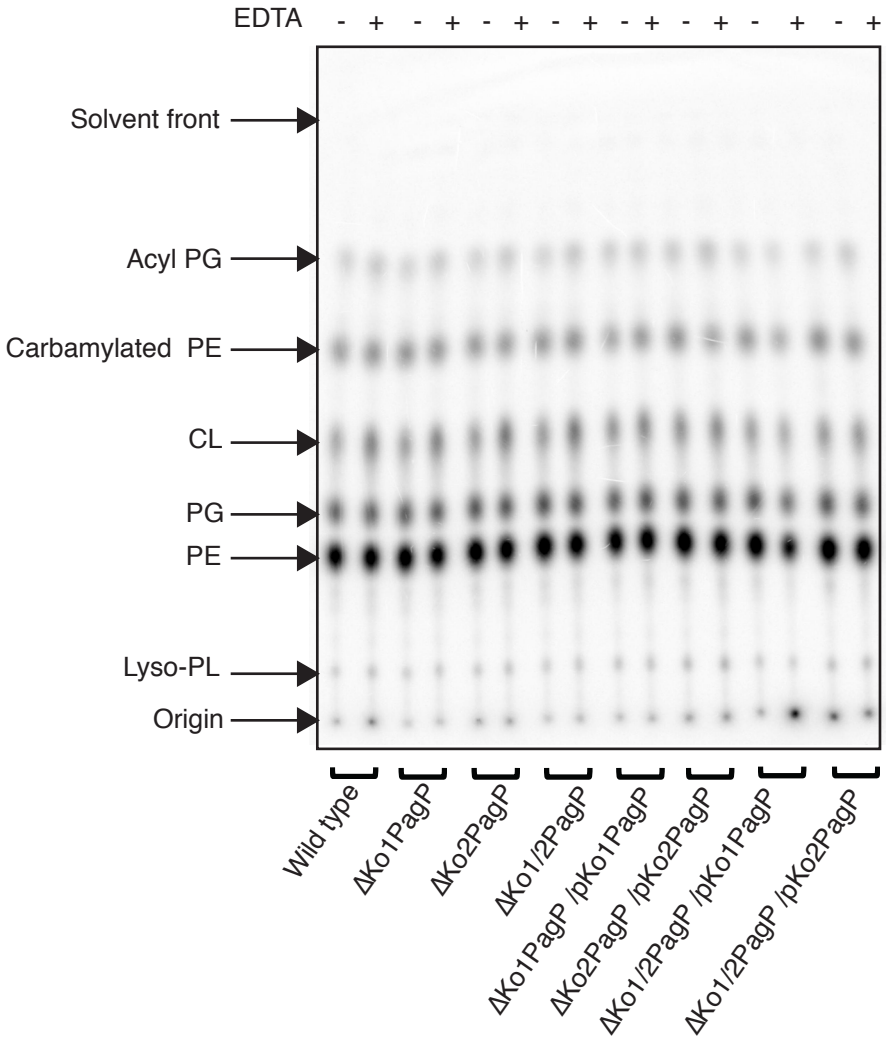

Figure 4.4. Phospholipid profiles for *K. oxytoca* wild type, *pagP* knock-outs and *pagP* complemented strains. Cells were grown with ^{32}P ortho-phosphate to early log phase and treated with or without EDTA. ^{32}P ortho-phosphate labeled phospholipids were isolated using Bligh and Dyer solvents (1959) from *K. oxytoca* wild type, ΔKo1PagP, ΔKo2PagP, ΔKo1/2PagP with pKo1PagP or pKo2PagP expressed from an arabinose-inducible promotor. The lipids were separated by TLC and visualized by Phosphorimaging. The TLC plate was resolved in solvent system chlor-form/ methanol/ acetic acid, 65:25:5 v/v.

We asked if there could be a *pagP* gene on this plasmid. We designed internal primers based on the *pagP* gene found on plasmid pCAV1374-150 from *K. oxytoca* strain CAV1374 and performed PCR (Table 4.2 and Figure 4.5B). The bands detected on the agarose gel would suggest that there is a *pagP* gene. Although the primers could have been non-specific, the size of the bands observed was ~550 bp as expected and confirmed by DNA sequencing. Interestingly, only DNA templates from the wild type and ΔKo1*pagP* samples gave PCR products, even though all four strains of *K. oxytoca* appeared to have plasmids. A pairwise alignment of the plasmid *pagP* (pPagP) from pCAV1374-150 and the second *pagP* from *K. oxytoca* ATCC 8724 revealed a 96% amino acid sequence identity (Figure 4.5C). Therefore, the PCR results confirmed that the plasmid extract was contaminated with genomic DNA, and that the second *pagP* was indeed deleted (Figure 4.1A and 4.5B). The results also suggested that if there is a third PagP in *K. oxytoca* ATCC 8724 the amino acid sequence is not identical to that of the *pagP* found on pCAV1374-150.

We decided to sequence what we had determined to be a plasmid. We isolated the plasmid from the *pagP* double knockout strain (to ensure there was no chance of a known *pagP* gene showing up from contaminated chromosomal DNA), separated the extract on an agarose gel and excised the band that ran at ~20 Kbp. The excised band was purified, and the DNA was sequenced using Illumina next-generation sequencing platform (Illumina, San Diego. CA). The sequenced DNA was processed and *de novo* assembled using SPAdes and annotated with Prokka (Seemann 2014; Bankevich et al. 2012). Ten

contigs were assembled. Assembled contigs were analyzed using Geneious 8.1.2 (Kearse et al. 2012). Nucleotide BLAST was used to compare our data to sequences in the NCBI database. BLAST analysis of contigs suggested that there might be a plasmid, and evidence of chromosomal DNA contamination was also observed. The two top hits were plasmids from *K. pneumoniae* kp15 plasmid pENVA size 253,984 bp and *K. pneumoniae* strain SKGHO1 plasmid unnamed 1 size 281,190 bp (Schlüter et al. 2014; Alfaresi 2017). No *pagP* gene was found on these plasmids. We also found no *pagP* gene in any contigs when we searched against the known *pagP* genes. It is possible that a different enzyme is acylating lipid A in response to EDTA treatment in *K. oxytoca* OM, or a PagP with little or no homology in amino acid sequence to Ko1PagP, Ko2PagP or the EcPagP (all three sequences were used in the search).

Table 4.3 Bacterial strains bearing plasmids with *pagP* gene

Bacteria strain	Plasmid	Size (Kbp)	Reference
Klebsiella oxytoca CAV1374	pCAV1374-150	150	(Sheppard et al. 2015)
Klebsiella oxytoca KONIH2	pKOR-e3cb	51	(Weingarten et al. 2018)
Klebsiella pneumoniae 342	pKP187	187	(Fouts et al. 2008)
Klebsiella varicola DX120E	pKV1	162	(Lin et al. 2015)
Pantoea agglomerans FDAARGOS	Unnamed plasmid 2	90	(Goldberg et al. 2018)
Pantoea agglomerans C410P1	Unnamed plasmid 1	470	(Li 2016)
Panteoa vagans C9-1	pPag3	535	(Smits et al. 2010)
Panteoa sp. At-9b	pPAT9B01	790	(Lucas et al. 2010)

4.5.3 *In silico* analysis of *pagP* gene arrangement in bacteria with duplicate copies on chromosomes

To gain some understanding or possible reasons for why two copies of the *pagP*

gene are found in this group of bacteria from the Enterbacterales order of the γ-Proteobacteria class, we decided to comparatively analyze the arrangement of *pagP* genes on the chromosomes. The PagP sequences from *K. oxytoca*, *Raoultella ornithinolytica, Enterobacter cloacae, Erwinia billingiae* and *Serratia fonticola* were analyzed using tBLASTn (protein to translated nucleotide) (Gertz et al. 2006). PagP from *Salmonella* and *E. coli* (conserved *pagP* gene), *Yersinia, Legionella* and *Bordetella* were also analyzed. The gene arrangement from each bacterium was examined for size and orientation in relation to neighboring genes (Figure 4.6). For the first *pagP* gene, some level of synteny was observed, that is, the gene was conserved in the same genetic locus in different bacterial species, as seen in *E. coli* and *Salmonella* (Guo et al. 1998). Generally, the first *pagP* gene is located between C_4-dicarboxylate uptake C (*dcuC*) and cold shock protein (*cspE*) (Figure 4.6). Some bacteria analyzed also had *crcB*, that encodes for a fluoride ion transporter, located downstream of *cspE*, in the exact arrangement of genes observed in this chromosomal region of *E. coli* and *Salmonella* (Guo et al. 1998; Hu et al. 1996). Expression of *crcA* (*pagP*), *cspE* and *crcB* on a high copy plasmid led to camphor resistance and chromosome condensation in *E. coli* (Hu et al. 1996). PagP in this locus of the chromosome found in other bacteria from the β- and γ-Proteobacteria does not have this gene organization. This arrangement was also not apparent for the second *pagP* gene on the chromosome or the *pagP* gene found on plasmids (Figure 4.6; Chapter 2, Figure 2.6). This observation might indicate *pagP* is a part of an operon along with *dcuC* and *cspE*. However, analysis of the *pagP* gene in *E. coli* K12, *Salmonella* and *Legionella*

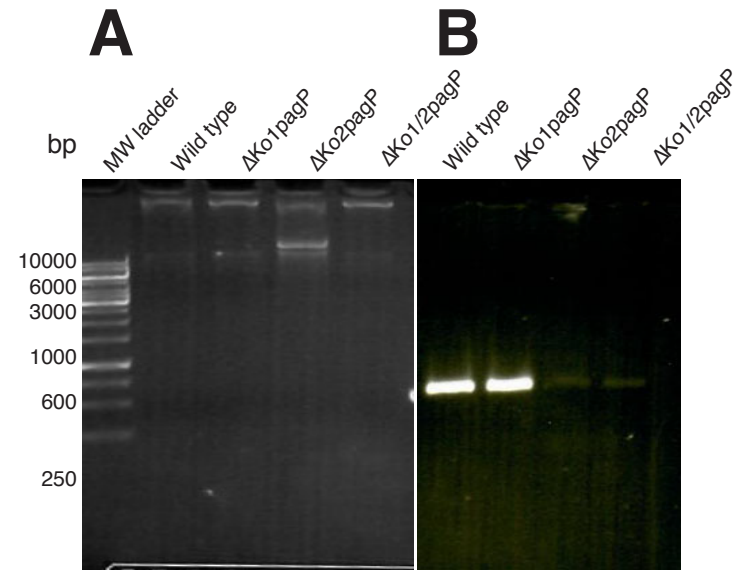

C

```
KO2     1 ETKIYGEQRVSGWWNWLKNDVSQTWNEPQNYDLYLPFLSWHNRFMYDKEKTDNYNEMPWGGGFGVSRYNPEGNWSSLYAMMFKDS 85
pPagP   1 ETKVYGEQRVSGWWNWLKDDVSQTWNQPQNYDLYLPFLSWHNRFMYDKEKTDNYNEMPWGGGFGVSRYNEEGNWSSLYAMMFKDS 85
          ***:**********************:*******************************************.***************

KO2       HNEWQPIIGYGWEKGWYLDSRRDFRLGLGVTAGITARDDFANYVPLPIILPLFSASYRRLSVQFTYIPGTYNNGNVLFAWLRYGF 170
pPagP     HNEWQPIIGYGWEKGWYLDSSRDFRLGLGVTAGITAREDFANYVPLPIILPLFSASYRRLSVQFTYIPGTYNNGNVLFAWLRYGF 170
          ************************************.************************************************


KO1     1 SFSSTLRDGYNTLSDNVSQTWNEPEHYDLYIPAVTWHARFAYDKEKTDRYNERPWGAGFGVSRWDDKGNWHGIYLMAFKDSYN  83
pPagP   4 YGEQRVSGWWNWLKDDVSQTWNQPQNYDLYLPFLSWHNRFMYDKEKTDNYNEMPWGGGFGVSRYNEEGNWSSLYAMMFKDSHN  87
          .....:...:*.*.*:******:*::****:*.::**.**.*******.***.***.******::::***..:*.*.**.***

KO1       KWEPIGGYGWEKTWRPLADDNFHLGLGYTLGVTARDNW-NYIPIPVVLPLASIGYGPATFQMTYIPGTYNNGNVYFAWARIQF  166
pPagP     EWQPIIGYGWEKGWYLDSSRDFRLGLGVTAGITAREDFANYVPLPIILPLFSASYRRLSVQFTYIPGTYNNGNVLFAWLRYGF  170
          .*:**.******.*...:..:*.****.*.*:***::: **:*:*::***.*..*...:.*.************.***.*..*
```

Figure 4.5. 1% agarose gel analysis of plasmid isolated from *K. oxytoca* wild type and *pagP* knockout strains. A. Plasmid isolation was done using the alkaline lysis method (Sambrook & Russell 2001). The two bands observed could be super-coiled (smaller Mw band) and linear plasmid DNA or plasmid DNA with genomic DNA (larger Mw band) (Higgins et al. 2016; Barton et al.1995). B. PCR analysis of plasmid DNA from *K. oxytoca* wild type and *pagP* knockouts, using internal primers for *pagP* from pCAV1374-150 (Table 4.3). C. Pairwise sequence analysis for Ko2PagP (KO2) and Ko1PagP (KO1) with PagP from plasmid *K. oxytoca* CAV1374-150 (pPagP) (Table 4.3).

confirms that it is monocistronic, and is not a part of an operon (Sand et al. 2003; Robey et al. 2001; Guo et al. 1998). Additionally, in most instances *dcuC* is oriented in the opposite direction and always has its own promoter, therefore it is not being co-transcribed with *pagP* (Figure 4.6) (Zientz et al. 1996). The second *pagP* gene product shares about 50% amino acid sequence identity with the first PagP, but it is randomly placed on the chromosome, suggesting that the second *pagP* genes were products of horizontal gene transfer (HGT), rather than an internal gene duplication (Figure 4.6) (Treangen & Rocha 2011).

4.5.4 KoPagP homologs do not occur under anaerobic conditions

K. oxytoca is a facultative anaerobe that has a pathogenic lifestyle in humans, but an endophytic lifestyle in plants, where it fixes atmospheric nitrogen in plant roots (Podschun & Ullmann 1998; Cakmakci et al. 1981). Nitrogen fixation is an anaerobic process and is identified as a common trait among Gram-negative bacteria with more than one *pagP* gene in their genomes (Sandhiya et al. 2001; Lin et al. 2012; MacLean et al. 2007; Fouts et al. 2008). Lipid A modification is a strategy employed by Gram-negative bacteria to adapt to environmental changes and to evade immune responses (Needham & Trent 2013; Raetz et al. 2007). We hypothesized that a possible function for at least one of the PagP homologs in *K. oxytoca* was to palmitoylate lipid A during the anaerobic process of N_2 fixation in plant roots, to increase the hydrophobicity of the bacterial OM during this process. If this is so, *pagP* could possibly be regulated by the fumarate nitrate reduction regulator (FNR). Furthermore, *pagP* is located downstream of *dcuC*, which is

regulated by FNR, so it is also possible that FNR could play a role in the regulation of the divergently oriented *pagP* promoter (Figure 4.6) (Zientz et al. 1996; Unden and Bongaerts 1997). FNR is a transcriptional regulator that is essential for the expression of over a hundred genes during anaerobic respiratory processes (Volbeda et al. 2017). Accordingly, we decided to analyze the lipids from *K. oxytoca* OM grown under anaerobic conditions. In previous studies, wild type *E. coli* K12 cells were able to grow anaerobically on glycerol-fumarate media, where glycerol was the carbon source and fumarate was the electron acceptor (Spencer & Guest 1973). We adopted this glycerol-fumarate media to grow *K. oxytoca* strains anaerobically, isolated the lipids and separated them by TLC (Figure 4.7). These cultures were also treated with and without EDTA to activate PagP, but no lipid A acylation was observed for either treatment (Figure 4.7A). No differences were observed for the phospholipids that were isolated from the same cultures grown under anaerobic conditions (Figure 4.7B). When grown under aerobic conditions, both KoPagP homologs respond to EDTA treatment to form acylated lipid A but not acylated phospholipids (Figure 4.2B, 4.3 and 4.4). This confirms that lipid acylation by PagP homologs from *K. oxytoca* does not occur during anaerobic respiration. This further suggests that *K. oxytoca* PagP homologs are not activated by FNR. The expression of the enzymes could be repressed under FNR inducing conditions, but this was not investigated.

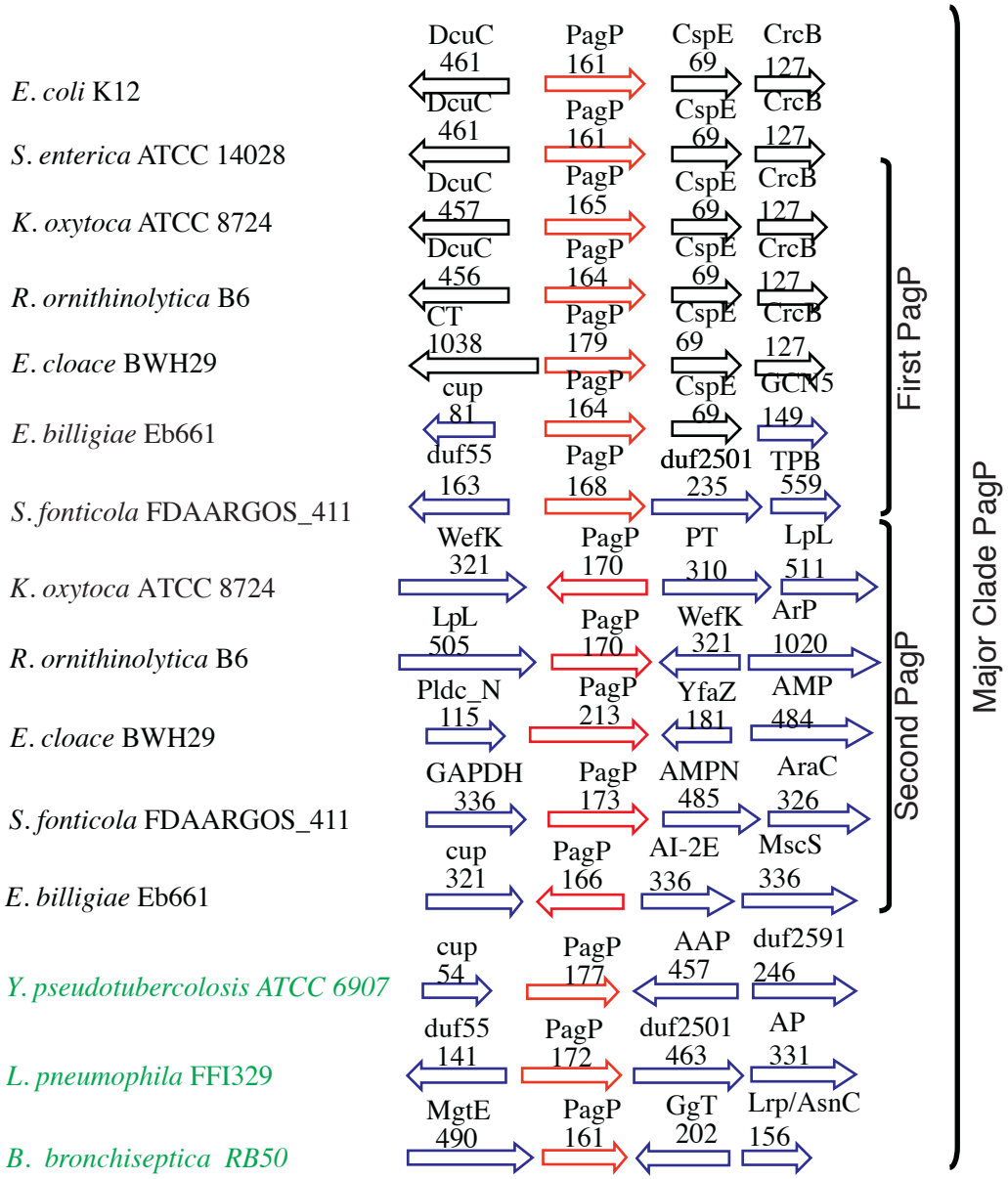

Figure 4.6. Gene arrangement for first and second PagP. The first PagP is located in a conserved region of the chromosome in four of five of the bacteria with two *pagP* genes. This region is also conserved in *E. coli* and *S. typhimurium.* The second PagP is randomly place on the chromosome. Single copy PagP in other bacteria are not found in a conserved region of the chromosome (highlighted in green). Arrows represent genes in the orientations observed on chromosomes; red arrows reprensents PagP; black arrows represents conserved regions; blue arrows represents non-conserved regions. Continues unto next page...

Figure 4.6 (continued). Gene arrangement for first and second PagP. Names of proteins: DcuC - C4-dicarboxylate transporter, CspE-cold shock protein, CrcB-camphor resistant/flouride ion transporter, CT- cation transporter, cup-conserved uncharacterized protein, GCN5-related N-acetyltransferase, duf proteins-domain of unknown function, TPB-thiamine pyrophosphate binding protein, WefK-acyltransferase, PT-phosphotransferase, LpL-lysophospholipase, ArP-acriflavin resistance protein, Pldc_N-acyltransferase membrane protein, YfaZ-porin, AMP-adenine monophosphate nucleosidase, GAPDH-glyceraldehyde-3-phosphate dehydrogenase, AI-2E-autoinducer-2 exporter, MscS-small conductance mechanosensitive channel, AAP-amino acid permease, AP- anion permease, MgtE- magnesium transporter, GgT - gamma glutamylcyclotransferase, Lrp/AsnC-transcriptional regulator.

4.5.5 Ko1PagP, but not Ko2PagP, is activated by PhoPQ inducing conditions

In *S. typhimurium* and *E. coli,* PagP is a PhoPQ-activated gene, which is regulated by PhoPQ that sense Mg^{2+}-limited growth conditions or CAMPs (Guo et al. 1998; Eguchi et al. 2004). Bacterial growth in Mg^{2+}-limited conditions promotes expression of PhoPQ-activated genes whereas high magnesium concentration represses the expression to levels similar to *phoPQ* null mutants (Groisman, 2001). A comparison of Ko1*pagP* and Ko2*pagP* promoter regions with the promoter regions of *E. coli* and *S. typhimurium* depicts a putative PhoPQ direct repeat consensus sequences for Ko1*pagP* and Ko2*pagP* even though variable spacing was observed (Figure 4.8) (Eguchi et al. 2004; e Silva & Echeverrigaray 2012; Solovyev & Salamov 2011). Consequently, we decided to investigate the effect of PhoPQ inducing and repressing conditions on the lipid A profile from *K. oxytoca* wild type and *pagP* deletion strains. We grew the cells in N-minimal media containing 8 μM Mg^{2+} for PhoPQ inducing and 1 mM Mg^{2+} for PhoPQ repressing conditions, extracted the lipids and separated them by TLC (Figure 4.9) (Gibbons et al. 2005). The lipid A profile suggests the occurrence of several lipid A modifications, including lipid A acylation by PagP, for the PhoPQ induced condition based on the variety and migration of spots on the TLC plate (Gibbons et al. 2005). This is expected as many lipid A modification enzymes are regulated by PhoPQ (Needham & Trent 2013; Gibbons et al. 2005). Quantitative analysis of three replicates demonstrates that the percentage lipid A acylation for the Ko1*pagP* single and Ko1*pagP*/Ko2*pagP* double knockouts was significantly less when cells were grown in N-minimal media with 1 mM Mg^{2+} compared to cells grown with 8 μM Mg^{2+} (Figure 4.10). No significant differences

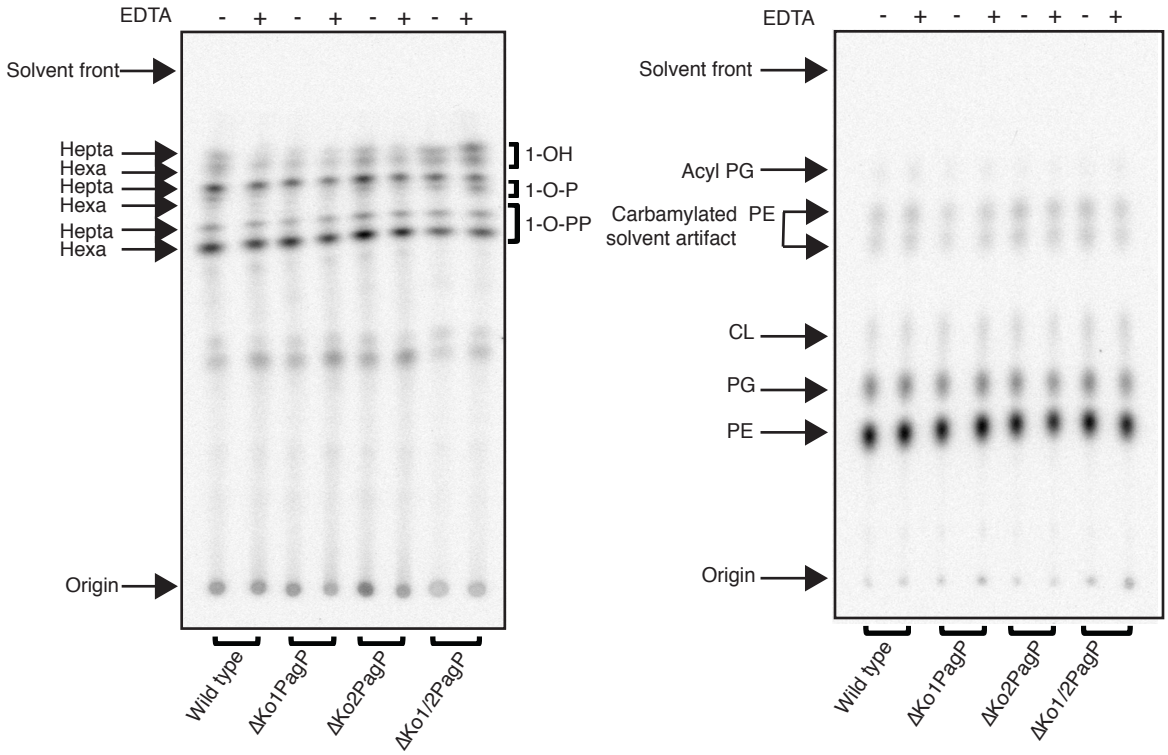

Figure 4.7. Lipid profile from *K. oxytoca* wild type and *pagP* knockout strains grown anaerobically. Cells were grown in glycerol-fumarate media (Spencer & Guest 1973) with ^{32}P orthophosphate for labeling. Cells were treated with and without EDTA prior to harvesting. A. Lipid A isolation was done using a mild acid hydrolysis procedure. Lipids were separated by TLC and visualized using Phosphorimaging. The TLC plate was resolved in solvent system chlorform/ pyridine/ 88%formic acid/ water, 50:50:16:5 (v/v). The main lipid A species are indicated on the left and include the hepta, hexa and penta-acylated lipid A with the 4'-monophosphate (1-OH), 1,4' *bis*-phosphate (1-O-P) or 1-diphosphate (1-O-P-P) derivatives of each species. B. Phospholipids were isolated using Bligh and Dyer solvents (1959). Lipids were separated by TLC and visualized using Phosphorimaging. The TLC plates were resolved in solvent system chloroform/methanol/acetic acid, 65/25/5 (v/v).

Figure 4.8. *In silico* promoter analysis for *E. coli, S. typhimurium*, and *K. oxytoca* PagPs. *In silico* promoter analysis was conducted using BPROM, prediction of bacterial promoter software (Solovyev and Salamov, 2011) and manual inspection. The promoter region for each *pagP* gene has the proposed -10 region boxed, and the transcription start site, thick arrows. Putative PhoP promoter region with approximate -10 and -35 hexamers and consensus PhoP box **(T/G)GTTTA**nnnnn**(T/G)GTTTA,** are highlighted with bold capitalized letters, as described for the *E. coli pagP* promoter region (Eguchi et al. 2004). The gene ATG start site is also shown in bold letter **M** for methionine.

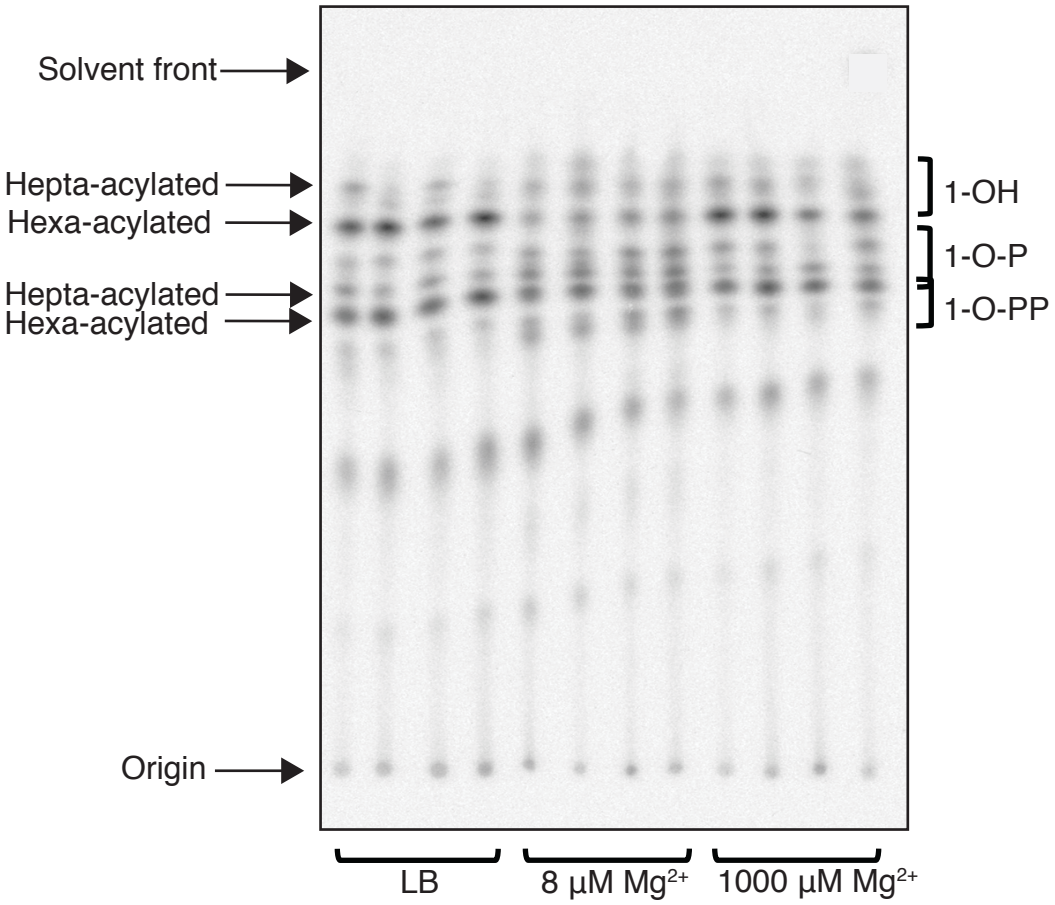

Figure 4.9. Lipid A profile for *K. oxytoca* cells grown in PhoP/Q inducing and repressing conditions. Cells were grown in N-minimal media supplemented with 8 μM Mg^{2+} (PhoPQ inducing condition), 1000 μM Mg^{2+} (PhoPQ repressing condition), and LB (rich media) as a control repressing condition. ^{32}P orthophosphate labeled lipids were isolated using mild acid hydrolysis, separated by TLC and visualized by Phosphorimaging. The TLC plate was resolved in solvent system chlorform/ pyridine/ 88%formic acid/ water, 50:50:16:5 (v/v). Lipid A species assignments are based on *E. coli* and *S. typhimurium* lipid A profiles from cells grown in N-minimal media supplemented with low and high Mg^{2+} concentrations (Gibbons et al. 2005).

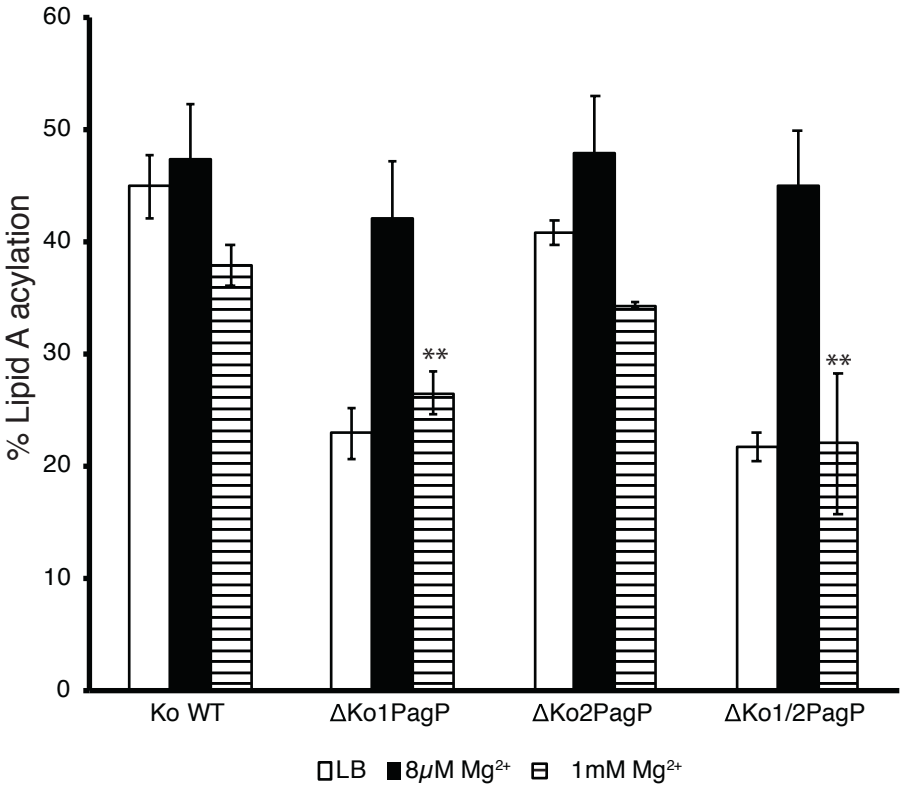

Figure 4.10. Lipid A acylation by PagP is affected by PhoPQ inducing conditions. Percentage acylation of lipid As isolated from *K. oxytoca* wild type, Ko1PagP and Ko2PagP single and double knockouts grown in N-minimal media supplemented with 8μM (PhoPQ inducing condition) and 1mM $MgCl_2$ (PhoPQ repressing condition) and LB as a negative control. ^{32}P orthophosphate labeled lipids were isolated using mild acid hydrolysis, separated by TLC and visualized by Phosphorimager. Quantification of lipid A species was done using ImageQuant software and the percentage lipid A acylation was calculated for three replicates. Lipid A palmitoylation was significantly reduced when Ko1PagP was knocked out and the strain was grown in 1mM Mg^{2+} as opposed to 8μM Mg^{2+} concentrations. Statistical analysis was done by unpaired Student t test, **$P<0.05$.

in lipid A acylation were observed between the *K. oxytoca* wild type and *pagP* single and double knockout strains grown in N-minimal media supplemented with 8 μM Mg^{2+} (Figure 4.10). These results suggest that knocking out the *pagP* genes did not affect lipid A acylation under these conditions or there is another enzyme producing acylated lipid A, as was described in section 4.4.1. Percentage lipid A acylation was also the same for all three growth conditions for wild type and Ko2*pagP* knockout strain, and for Ko2*pagP* and Ko1*pagP*/Ko2*pagP* double knockout strains (Figure 4.10). These results are unclear because they imply that Ko1*pagP*, but not Ko2*pagP*, may be repressed under high Mg^{2+} conditions, although not necessarily activated under low Mg^{2+} conditions. No differences were observed for phospholipids isolated from the same cultures under the same conditions (Figure 4.11). Interestingly, although the *S. typhimurium* and *E. coli* PagP have similarities in their promoter region, the *S. typhimurium* PagP is activated when the bacterium is grown with 8 μM Mg^{2+} forming palmitate, phosphoethanolamine, and 4-amino-4-deoxy-L-arabinose modified species, but *E. coli* PagP does not (Figure 4.8) (Gibbons et al. 2005; Kim et al. 2004; Zhou et al. 1999). The *E. coli* PagP can be activated in a PhoPQ independent manner by treating with ammonium metavanadate, a non-specific phosphatase inhibitor, to form these various lipid A modifications (Zhou et al. 1999). Perhaps Ko2PagP behaves like the *E. coli* PagP. It will be necessary to investigate the regulation of these genes using reporter fusions and/or RT-PCR in *phoPQ* null mutants to gain a better understanding.

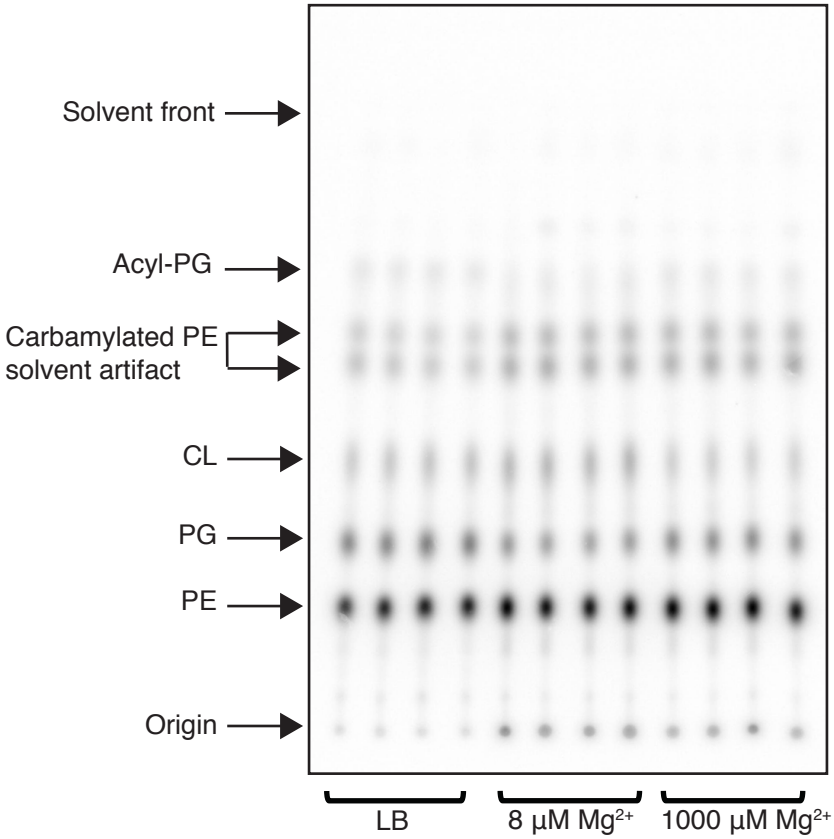

Figure 4.11. Phospholipid profile for *K. oxytoca* cells grown in PhoPQ inducing and repressing conditions. Cells were grown in N-minimal media supplemented with 8 μM Mg^{2+} (PhoPQ inducing condition), 1000 μM Mg^{2+} (PhoPQ repressing conditions) and LB (rich media) as a control for repressing condition. ^{32}P orthophosphate labeled phospholipids were isolated using Bligh and Dyer solvents (1959), separated by TLC and visualized by Phosphorimaging. The TLC plate was resolved in solvent system chlorform/ methanol/ acetic acid, 65:25:5 (v/v).

4.5.6 Ko1PagP and Ko2PagP play a role in bacterial resistance to C18G

Lipid A palmitoylation by PagP was reported to confer resistance to CAMPs possibly because of an increase in the hydrophobicity of the OM (Thaipisuttikul et al. 2014; Ernst et al. 2001; Guo et al. 1998). Ko1PagP and Ko2PagP are dedicated lipid A palmitoyltransferases (Chapter 3, Figure 3.7). We asked if these PagP homologs had any effects against CAMPs. We investigated the effect of C18G (a synthetic α-helical peptide derived from human platelet factor IV) on wild type and *pagP* knockout *K. oxytoca* strains (Table 4.1) (Darveau et al. 1992). We determined the minimal inhibitory concentration (MIC) using the microdilution method for the different strains (Table 4.4). The MIC is the lowest concentration of the assayed antimicrobial peptide that inhibits the visible growth of the microorganism tested. Experiments were done three times with two technical replicates each time (Table 4.4). Differences were observed in MICs for wild type compared to *pagP* knockout strains, but these were not significant.

Recall that although we had deleted the two PagP homologs from *K. oxytoca*, lipid A acylation was being observed in response to EDTA treatment (Figure 4.2 and 4.3). This could potentially affect the MIC values (Thaipisuttikul et al. 2014; Ernst et al. 2001; Guo et al. 1998). Therefore, we also conducted MICs in *E. coli* strains with and without *pagP,* and heterologously expressed Ko1PagP and Ko2PagP on low copy number plasmids (Table 4.5). Similar values were obtained for *E. coli* MC1061 (wild type), WJ0124 (*pagP* knockout) and WJ0124 strains overexpressing Ko1PagP and Ko2PagP. Differences of

two-fold or greater between the wild type and mutants are necessary to proceed to another form of susceptibility studies (Clinical Laboratory Standards Institutes).

Table 4.4 Minimal inhibitory concentrations for *K. oxytoca*

Bacterial strain	MIC of C18G (μg/ml)
K. oxytoca ATCC 8724	1.0
ΔKo1PagP	0.5
ΔKo2PagP	0.5
ΔKo1-Ko2PagP	0.5
ΔKo1PagP /pKo1PagP	1.0
ΔKo2PagP /pKo2PagP	1.0
ΔKo1-Ko2PagP /pKo1PagP	1.25
ΔKo1-Ko2PagP /pKo2PagP	1.25

MIC for the wild type not significantly different from mutants (P>0.05, by unpaired student t test)

Table 4.5 Minimal inhibitory concentrations for *E. coli*

Bacterial strain	MIC of C18G (μg/mL)
E. coli MC1061(Wild type)	1.0
E. coli WJ0124 *(*MC1061 Δ*pagP*)	1.0
WJ0124 /pKo1PagP	2.0
WJ0124 /pKo2PagP	2.0

MIC for the wild type not significantly different from mutants (P>0.05, by unpaired student t test)

4.6 Discussion

The work in this study demonstrates that *K. oxytoca* ATCC 8724 encodes two PagP acyltransferases that are homologous to the *E. coli* PagP, and each adds a seventh chain to the hexa-acylated lipid A in its OM (Süsskind et al. 1998). Neither Ko1PagP nor Ko2PagP acylates PG in the *K. oxytoca* OM. Our data also suggest that a third lipid A palmitoyltransferase enzyme may be present in this bacterium. Comparison of the location of *pagP* genes in *K. oxytoca* and other bacteria with two *pagP* genes reveals that

the first *pagP* gene is usually located in a conserved locus, whereas the second *pagP* gene is randomly placed on the chromosome. KoPagP homologs do not acylate lipid A or PG under anaerobic conditions. Analysis of lipid A species from *K. oxytoca* wild type and *pagP* mutant strains that were grown in magnesium limited condition suggests that Ko1PagP, but not Ko2PagP may be activated by the PhoPQ two component system. Ko1PagP and Ko2PagP confer moderate resistance to the alpha helical CAMP C18G.

PagP is encoded by a single copy gene in a number of bacteria mainly from the β- and γ-Proteobacteria (Chapter 2). PagP is an OM enzyme that palmitoylates lipid A and /or PG. A subset of bacteria from the Enterobacterales order of the γ-Proteobacteria class have two or more copies of PagP in their genomes. *K. oxytoca* is one such bacterium, and it is a nosocomial pathogen and a plant endophyte (Singh et al. 2016; Cakmakci et al. 1981; Darby et al. 2014). In an effort to understand the function of PagP homologs in *K. oxytoca* we created single and double gene knockouts and then assessed the activities based on the presence or absence of the enzymes. The KoPagP homologs complement each other, by showing lipid A acylation in the absence of the other enzyme in the single *pagP* knockout strains, but no sign of phospholipid modification, indicating that *K. oxytoca* PagP homologs are strictly lipid A palmitoyltransferases.

Surprisingly, the double *pagP* knockout also had lipid A acylation with levels compared to wild type when cells were treated with EDTA. This implies that there is another palmitoyltransferase enzyme that modifies lipid A. Although rare, this has been

observed in the *K. oxytoca* CAV1374 strain, which has two *pagP* genes on its chromosomes and one on a plasmid (Sheppard et al. 2015). Even though a plasmid may have been found that was never reported, the search for another *pagP* homolog to the two known *pagP* homologs on a plasmid was futile. It is possible that the other palmitoyltransferase enzyme is not homologous to the known PagPs at the amino acid level. This would not be an unusual case because the *Pseudomonas* PagP has no amino acid sequence identity to the *E. coli* PagP. For several years palmitoylated lipid A was observed in *Pseudomonas aeruginosa* that was isolated from the airways of cystic fibrosis patients, but a *pagP* gene was never identified. A combined genetic and biochemical approach was used to identify the PA1343 gene, that encodes for PagP. *Pseudomonas* PagP palmitoylates lipid A *in vitro* (purified protein) and in bacterial OMs (Thaipisuttikul et al. 2014; Ernst et al. 2007).

In *E. coli* and *Salmonella,* PagP is regulated by the PhoPQ two-component system that senses low magnesium concentrations (Eguchi et al. 2004; Guo et al. 1998). Ko1*pagP* is found in the same genetic locus as the *E. coli pagP* and *S. typhimurium pagP*, which are activated by a magnesium limited environment (Gibbons et al., 2005). Conversely, the *K. oxytoca* Ko2*pagP* gene seems to be unaffected compared to the wild type when grown under similar conditions. This implies that Ko1PagP, but not Ko2PagP, is activated by PhoPQ system, which displays known interspecies variation in activation signals used and genes that are regulated (Needham & Trent 2013). For lipid A modifications in *Salmonella*, PhoPQ system activation induces the PmrAB system, which

is also regulated by the post-transcriptional activator PmrD that responds to Fe^{3+}, Al^{3+}, and low pH, but these systems are uncoupled in *E. coli* for the incorporation of a palmitate by PagP (Needham & Trent 2013; Raetz et al. 2007; Winfield & Groisman 2004). Even though Ko1PagP and Ko2PagP are from the same bacterium, it is possible that Ko2PagP could be regulated by PhoPQ but by a different stimulus, possibly at a low pH or with the addition of a metal. The other possibility is that Ko2PagP could be negatively regulated when grown in a Mg^{2+}-limited medium, since both Ko1PagP and Ko2PagP are active and similarly palmitoylate lipid A post-transcriptionally when either gene was deleted and treated with EDTA (Jia et al. 2004). In a similar study, *K. pneumoniae* encodes two LpxL late-acyltransferases, LpxL1 transfers a laurate (C12) acyl chain and LpxL2 transfers a myristate (C14) acyl chain. Only LpxL2 is expressed *in vivo* in *K. pneumoniae*. LpxL1 had a putative PhoPQ consensus sequence upstream of the gene, but was negatively regulated by this two component system (Mills et al. 2017). Had our investigations included a *phoP* knockout, a *phoP/*Ko1*pagP* and a Ko2*pagP* double knockouts, as well as transcriptional studies of each gene, a stronger conclusion could be reached, but very little is known about the genetics of these systems in *K. oxytoca* as this bacterium is not well studied; therefore, these knockouts were not created.

Lipid A acylation is a major factor governing the immunological activity of LPS (Park et al. 2009). Additionally, lipid A acylation affects the hydrophobicity of the outer leaflet of the OM because of the van der Waals interactions between the acyl chains (Nikaido 2003). Many Gram-negative bacteria modify the acyl chains of lipid A in

response to stressful stimuli to increase resistance to antimicrobial peptides (Needham & Trent 2013). Lipid A acylation modification by Ko1PagP and Ko2PagP likely contribute to the bacteria moderate resistance to the α-helical CAMP C18G, but this was possibly complicated by the presence of another lipid A palmitoyltransferase that responded to EDTA treatment in the absence of Ko1PagP and Ko2PagP. Interestingly, deletion of either homolog in *K. oxytoca* had the same effect to C18G as well as when both homologs were deleted. Similarly, either enzyme can fully complement the double *pagP* knockout strain. This suggests that both homologs are functionally equivalent as it relates to conferring resistance to C18G. It would be interesting to know how the wild type compares with the different mutants when treated with other structural classes of antimicrobial peptides including some from plants, because a *pagP* mutant in *Legionella pneumophila* is susceptible to both C18G and polymyxin B, whereas a *Salmonella pagP* mutant is susceptible to C18G and protegrin, but the *P. aeruginosa* PagP only conferred resistance to C18G (Robey et al. 2001; Guo et al. 1998; Thaipisuttikul et al. 2014). These previous reports would suggest that PagP confers various levels of resistance to different classes of CAMPs probably based on the bacterial niche (Guo et al. 1998; Li et al. 2012; Needham & Trent 2013).

Finally, it seems that genomes encoding two copies of lipid A acyltransferases are not an unusual feature in Gram-negative bacteria. Similar to the example mentioned in *K. pneumoniae*, two LpxM were also found in *Shigella flexneri* and in *E. coli* O157:H7, but the second gene was found on plasmids. This gene is found as a part of the *shf* locus

found on plasmid pO157 of *E. coli* O157:H7 and the virulence plasmid pWR100 of *S. flexneri* (Kim et al. 2004; d'Hauteville et al. 2002). In *S. flexneri*, LpxM is required for maximum acylation of lipid A and invasion of the gut (d'Hauteville et al. 2002). In *E. coli*, the additional LpxM complements the chromosomal copy in generating fully hexa-acylated lipid A and suppressing the micro-heterogeneity of lipid A species (Kim et al. 2004). Both enzymes catalyze the transfer of C14 myristate chains and were positively regulated by PhoPQ (Kim et al. 2004; d'Hauteville et al. 2002). Multiple copies of a gene usually indicate importance towards environmental adaptation, virulence or other survival strategies. A new gene function could have been created or, both could have the same function (complementing each other) or, they are activated under different conditions (Bratlie et al. 2010; Zhang 2003). Although more studies need to be conducted it would appear that Ko1PagP and Ko2PagP complement each other under normal conditions, but probably the colonization of various hosts may trigger different stimuli that affect regulation.

Chapter 5.0

5.1 Conclusions

The focus of this thesis was to understand how PagP has been adapted in nature to interact with multiple lipid substrates and products. A great deal of work was already accomplished when I began my graduate career with regards to PagP structural and functional relationships. Two crystal structures and NMR structures for the *Escherichia coli* PagP (EcPagP) were already resolved (Ahn et al. 2004; Cuesta-Seijo et al. 2010; Hwang et al. 2004; Hwang et al. 2002). A robust defined detergent micelle system, which employs close to physiological substrates was developed (Bishop et al. 2000). A relatively simple but effective method was established to analyze lipid A acylation by PagP in the lamellar outer membrane bilayer (Jia et al., 2004). Additionally, the elaborate mechanism by which PagP selects a palmitate chain was elucidated (Cuesta-Seijo et al. 2010; Khan et al. Unpublished. 2007). These discoveries were fundamental and played a great role in exploring and characterizing the molecular diversity of lipid palmitoylation in various PagP homologs.

PagP shows diversity in its lipid A palmitoylation ability (Bishop 2005), but there was no established system that described how this protein is distributed or if there was a correlation between PagP lipid A regioselectivity with its distribution. Furthermore, PagP is separated into a minor and major clade with no clear phylogenetic relatedness. This led to our initial phylogenetic investigations with the aim of understanding the distribution

and relations of PagP homologs among Gram-negative bacteria in order to choose appropriate homologs for our study. Although the evolutionary relationships were not resolved using a sequence-based method, we now have the understanding that PagP is distributed between a major clade - proteins that are found in β- and γ-Proteobacteria, and a minor clade - proteins that are found in β-, γ- and δ-Proteobacteria, and Firmicute. Our investigations of structure-function relationships of key homologs within the major clade confirmed all possible cases of lipid A 2-position regiospecificity (*Legionella pneumophila* PagP - LpPagP), 3'-position regiospecificity (*Bordetella bronchiseptica* PagP - BbPagP) and, 2 and 3'- positions regioselectivities (*Klebsiella oxytoca* PagP homologs – Ko1PagP and Ko2PagP). The T29 surface residue in the embrasure region of PagP from *B. bronchiseptica* was found to be important for lipid A palmitoylation at the 3'-position. The PagP from *Legionella* seemed to have adapted to select a C16 palmitate to the 2-position of lipid A, even though majority of the phospholipids in this bacterium are of the *iso* and *anteiso*-methyl branched forms (Geiger 2010). Interestingly, although the minor and the major clades have no clear relation based on the sequence-based analysis, structure-function relationships suggest that they are structurally related and share the very specific characteristic of displaying lipid A 3'-position regiospecificity, suggesting that the two clades derived from a common ancestor (Chapter 2).

Within the major clade homologs from the γ-Proteobacteria we identified a number of endophytic bacteria including *K. oxytoca* that encodes two *pagP* genes in their genomes, either both on the chromosome or one on a chromosome and one on a plasmid.

The homolog that shows up first in the chromosome is conserved (chromosomal) whereas, the second homolog is randomly placed on the chromosome or found on plasmids (plasmid-based). Our studies revealed that a one amino acid conserved signature indel (CSI) in the L3 loop alters the protein structural conformation which correlates to the enzymes' ability to palmitoylate PG, but not lipid A. We conclude that PG as an acceptor substrate binds non-specifically on the surface of the enzyme during the acyltransferase reaction, but the enzyme could potentially use two routes for acyl chain extraction, whereas acyl chain extraction for lipid A palmitoylation is known to occur only at embrasure (Cuesta-seijo et al. 2010; Khan & Bishop 2009) (Chapter 2). Further biochemical characterization of these two PagP homologs from *K. oxytoca* highlighted a mechanism by which the interplay between amino acid side chains caused a conformational change within the structure that affected PagP::PG interactions.

We demonstrated how PagP intrinsic structural perturbations allow the enzyme to switch between multifunctional and monofunctional states. Sequence analysis of the two subclades of proteins revealed a network of residues resembling a classic chymotrypsin charge relay network (D61, H67) or a novel catalytic triad with a Y87 residue in place of the nucleophilic S195, on the periplasmic surface of the first PagP found on the chromosome (as well as in EcPagP). The "charge relay" residues were naturally mutated in the second (plasmid-based) PagP homolog. Switching the D/H pair to the naturally mutated N/S residues between the two homologs from *K. oxytoca* resulted in an internal structural perturbation that was coupled to the enzymes' extracellular active site for PG

palmitoylation reaction. Significantly, EcPagP and Ko1PagP did not only generate palmitoyl-PG, when PG was the acceptor substrate *in vitro* (Dalebroux et al. 2014), but also *bis*(monoacylglycerol)phosphate (BMP) and lyso-phosphatidylglycerol (LPG), which are called the glycerophosphoglycerols. Surprisingly, Ko1PagP did not perform this reaction in bacterial outer membranes, but EcPagP did. Using EcPagP and mutants for *in vivo* expression investigations, we found that the Y87 residue of the proposed novel catalytic triad is indeed required to form the full range of glycerophosphoglycerols, but the H67 residue is not important. As such, we conclude that D61/H67 pair are not functioning as a charge relay network, but instead affects the conformation of the protein. This change in conformation translates to the extracellular active site and across the bilayer to affect the expansion of PG into the other glycerophosphoglycerol phospholipids PPG, BMP, and LPG. It is not yet clear how Y87 functions as a catalytic residue on its own, but our initial suspicion based on the similarity of the D61/H67/Y87 cluster with the catalytic triad of chymotrypsin pointed us in the right direction to discover a novel active site despite the structural and non-catalytic role we uncovered for the putative charge relay network residues. From this study we also conclude that EcPagP is multifunctional to palmitoylate lipid A and form the glycerophosphoglycerols *in vitro* and *in vivo*, whereas Ko1PagP is only multifunctional *in vitro*, and that Ko2PagP is a monofunctional lipid A palmitoyltransferase both *in vitro* and *in vivo* (Chapter 3).

Multiple copies of PagP appears to be important to bacteria that live endophytic lifestyles. Based on our findings that neither Ko1PagP nor Ko2PagP used PG as an

acceptor substrate in the OM, we attempted to establish the purpose of these homologs in nature. Creating single and double PagP knockouts in *K. oxytoca* revealed that there might be a third PagP with little or no sequence homology to the known PagP homologs. This was a major challenge as this acyltransferase affected all the known functions of PagP in the bacteria OMs. Although not entirely clear, we believe that Ko1PagP and Ko2PagP complement each other in acylating lipid A and conferring some resistance to the α-helical structures of CAMPs. Questions regarding the regulation of these proteins surfaced, but we were unable to address these because of our limited knowledge of the genetics in *K. oxytoca,* and the time allotted for the completion of this work. Based on our initial results that Ko1PagP, but not Ko2PagP is activated under PhoPQ inducing conditions we suspect that colonization of various hosts may trigger different stimuli that affect regulation (Chapter 4).

The work presented in this thesis will broaden our knowledge of PagP::lipid interactions among other Gram-negative bacteria, which has been dominated by studies of the *E. coli* PagP. Our understanding of how conformational flexibility within PagP can manipulate function can be applied to protein engineering. Additionally, our initial understanding of how PagP can palmitate lipid A in a regiospecific manner can be further developed to engineer an enzyme that could have therapeutic value (Raetz et al. 2007; Bishop 2005)

5.1.1 Current considerations

The ability to work with PagP in a defined detergent system and *in vivo* conditions affords an opportunity to analyze outer membrane protein folding. We saw in these and previous studies where PagP H67 single mutant did not express or refold in our detergent micelle system, but the protein refolded and was fully functional in bacterial OMs (Smith, 2008). This suggests that factors in the *in vivo* environment such as periplasmic chaperones and/or BAM complex facilitate folding of the mutant protein that did not fold in the detergent micelle system (Kleinschmidt, 2015; Schiffrin et al., 2017). Assessing an OM protein such as PagP with and without site mutations, in a detergent micelle and bacterial OMs with knockouts in periplasmic chaperones and/or BAM components, could potentially answer a number of questions in this poorly understood area of OM protein folding.

Another area for consideration is the inability of the detergent system to fully recapitulate physiological environment to for studies of PagP. In bacterial OMs, PagP extracellular active site is at the membrane aqueous environment interface, a situation that is not achieved in detergent micelles. A promising alternative to detergents are styrene-maleic acid copolymers (SMALPs), which solubilizes and reconstitutes membrane proteins into nanodiscs (Fiori et al. 2017). Using these copolymers to solubilize or reconstitute PagP for structural and functional studies could be instrumental in understanding how lipid A and PG binds to the enzyme.

5.1.2 Future studies

From the studies described in this thesis, we have recognized a new role for PagP in making minor lipids that involves the periplasmic surface of the enzyme and gained a better understanding of how PagP interacts with its lipid substrates, but some details are still outstanding, such as: understanding how the Y87 residue is involved in the hydrolysis of PPG to BMP and BMP to LPG; determining the of functions for the glycerophosphoglycerols and completing studies of a how lipid A and PG binds to PagP. Additionally, we need to determine how Ko1PagP and Ko2PagP are being regulated, but first we need to identify and knockout the third PagP from *K. oxytoca*.

Elucidation of the mechanism by which the Y87 residue is involved in the hydrolysis of PPG to BMP and BMP to LPG.

We have discovered that the Y87 residue is involved in PagP periplasmic hydrolysis reactions, but that it may not be a constituent of the proposed D61, H67 and Y87 catalytic triad (Chapter 3). We have already developed a method to prepare millimolar amounts of radiolabeled PPG to be used as substrate for the lipase activity of the periplasmic surface of PagP *in vitro* (Unpublished data). Structure-functional relationships involving various point mutations on the periplasmic surface of the enzyme and using PPG as a substrate could aid in our understanding of the mechanism by which PagP hydrolyses PPG to BMP.

Determination of functions for the glycerophosphoglycerols

We now have the ability to control the production of the glycerophosphoglycerols (PPG, BMP and LPG) in *E. coli* (Chapter 3). Recently, the outer membrane phospholipase PldA that hydrolyses phospholipids to form lyso-phospholipids and free fatty acid was found to have a secondary role in signal transduction (May & Silhavy 2017). Additionally, we have the capacity to separate the inner and outer membranes using sucrose density gradient centrifugation because the inner membrane PldB also generates acyl-PG (Bishop et al. 2000; Hsu et al. 1989). To separate the roles of PldA and PldB from that of PagP, we can then express wild type PagP and relevant mutants in a *E. coli* PldA mutant background and analyze the outer membrane lipidome. This will determine phospholipids specifically generated by PagP, which will initiate investigations for possible functions.

Determination of the mechanism by which lipid A and PG binds to PagP

In two separate occasions in this thesis we saw where a mutation in PagP D/H pair and CSI in the L3 loop affected PG palmitoylation but not lipid A, suggesting that PG and lipid A access the enzyme at different locations or that PG unspecifically binds at various locations on the surface of the enzyme and due to the conformational change, that affects the β-barrel shear structure (Chapter 2 and 3). We already have in our possession the EcPagPPro28Cys/Pro50Cys double point mutant with a disulfide bond blocking the embrasure carried on a plasmid (Khan & Bishop 2009). The same mutation could be carried out on the *K. oxytoca* PagP homologs, since they too have Pro28 and Pro50 residues. Additionally, a similar mutation should be installed between β-strands B and C (Cuesta-Seijo et al. 2010). Acyltransferase reactions should then be carried out with these

proteins and compare to the *E. coli* PagP embrasure and B/C mutant using PG and lipid A as the acceptor. This experiment will determine if lipid A and PG access the enzyme at the same location. After which point mutations on the surface of the enzyme within the access site can determine residues involved in binding.

References

Abellón-Ruiz, J., Kaptan, S. S., Baslé, A., Claudi, B., Bumann, D., Kleinekathöfer, U., & Van Den Berg, B. (2017). Structural basis for maintenance of bacterial outer membrane lipid asymmetry. *Nature Microbiology*, *2*(12), 1616–1623.

Ahn, V. E., Lo, E. I., Engel, C. K., Chen, L., Hwang, P. M., Kay, L. E., Bishop, R. E, Privé, G. G. (2004). A hydrocarbon ruler measures palmitate in the enzymatic acylation of endotoxin. *The EMBO Journal*, *23*(15), 2931–41.

Akgoc, Z., Sena-Esteves, M., Martin, D. R., Han, X., d'Azzo, A., & Seyfried, T. N. (2015). Bis(monoacylglycero)phosphate: a secondary storage lipid in the gangliosidoses. *Journal of Lipid Research, 56,* 1006-1013.

Albers, U., Tiaden, A., Spirig, T., Alam, D. Al, Goyert, S. M., Gangloff, S. C., & Hilbi, H. (2007). Expression of *Legionella pneumophila* paralogous lipid A biosynthesis genes under different growth conditions. *Microbiology*, *153*(11), 3817–3829.

Alfaresi, M. (2017). Complete genome of a pandrug-resistant *Klebsiella pneumoniae* isolate, representing a Carbapenem resistant Enterobacteriaceae (CRE) resistant to all commercially available antibiotics in the UAE, Pathology and Laboratory Medicine, Sheikh Khalifa General Hospital (SKGH), UAE. Retrieved from: *NCBI website* accession number: NZ_CP015500

Alnajar, S., & Gupta, R. S. (2017). Phylogenomics and comparative genomic studies delineate six main clades within the family Enterobacteriaceae and support the reclassification of several polyphyletic members of the family. *Infection, Genetics and Evolution*, *54*, 108–127.

Altschul, S. (1997). Gapped BLAST and PSI-BLAST: a new generation of protein database search programs. *Nucleic Acids Research*, *25*(17), 3389–3402.

Anandan, A., Evans, G. L., Condic-Jurkic, K., O'Mara, M. L., John, C. M., Phillips, N. J., Jarvis, G. A., Wills, S. S., Stubbs I. M., Kahler, C. M., & Vrielink, A. (2017). Structure of a lipid A phosphoethanolamine transferase suggests how conformational changes govern substrate binding. *Proceedings of the National Academy of Sciences*, *114*(9), 2218–2223.

Anisha, C., Mathew, J., & Radhakrishnan, E. (2013). Plant Growth Promoting Properties of endophytic *Klebsiella sp.* isolated from Curcuma longa. *Ijbpas.Com*, *2*(3), 593–601.

Antonov, V. K., & Vorotyntseva, T. I. (1972). Effect of methylation of the histidine residue in the active site of α-chymotrypsin on the conformational stability of the

enzyme. *FEBS Letters*, *23*(3), 361–363.

Aravind, L., Mazumder, R., Vasudevan, S., & Koonin, E. V. (2002). Trends in protein evolution inferred from sequence and structure analysis. *Current Opinion in Structural Biology*, *12*(3), 392–399.

Asikyan, M. L., Kus, J. V., & Burrows, L. L. (2008). Novel proteins that modulate type IV pilus retraction dynamics in *Pseudomonas aeruginosa*. *Journal of Bacteriology*, *190*(21), 7022-7034

Asmar, A. T., Ferreira, J. L., Cohen, E. J., Cho, S. H., Beeby, M., Hughes, K. T., & Collet, J. F. (2017). Communication across the bacterial cell envelope depends on the size of the periplasm. *PLoS Biology*, *15*(12), e2004303

Baars, L., Wagner, S., Wickstrom, D., Klepsch, M., Ytterberg, A. J., van Wijk, K. J., & de Gier, J.-W. (2008). Effects of SecE Depletion on the Inner and Outer Membrane Proteomes of *Escherichia coli*. *Journal of Bacteriology*, *190*(10), 3505–3525.

Bader, M. W., Sanowar, S., Daley, M. E., Schneider, A. R., Cho, U., Xu, W., Klevit, R. E., Moual H, L., & Miller, S. I. (2005). Recognition of antimicrobial peptides by a bacterial sensor kinase. *Cell*, *122*(3), 461–72.

Bankevich, A., Nurk, S., Antipov, D., Gurevich, A. A., Dvorkin, M., Kulikov, A. S., Lesin, V, M., Nikolenko, S. I., Pham, S., Prjibelski, A, D., Pyshkin A V., Sirotkin, A V., Vyahhi, N., Tesler, G., Alekseyev M, A., & Pevzner, P. A. (2012). SPAdes: A New Genome Assembly Algorithm and Its Applications to Single-Cell Sequencing. *Journal of Computational Biology*, *19*(5), 455–477.

Bannwarth, M., & Schulz, G. E. (2003). The expression of outer membrane proteins for crystallization. *Biochimica et Biophysica Acta (BBA) - Biomembranes*, *1610*(1), 37–45.

Barton, B. M., Harding, G. P., & Zuccarelli, A. J. (1995). A general method for detecting and sizing large plasmid. *Analytical Biochemistry*, *226*, 235–240.

Basheer, S. M., Guiso, N., Tirsoaga, A., Caroff, M., & Novikov, A. (2011). Structural modifications occurring in lipid A of *Bordetella bronchiseptica* clinical isolates as demonstrated by matrix-assisted laser desorption/ionization time-of-flight mass spectrometry. *Rapid Communications in Mass Spectrometry*, *25*(8), 1075–1081.

Batra, J., Szabó, A., Caulfield, T. R., Soares, A. S., Sahin-Tóth, M., & Radisky, E. S. (2013). Long-range Electrostatic Complementarity Governs Substrate Recognition by Human Chymotrypsin C, a Key Regulator of Digestive Enzyme Activation. *Journal of Biological Chemistry*, *288*(14), 9848–9859.

Begley, M., Gahan, C. G. M., & Hill, C. (2005). The interaction between bacteria and bile. *FEMS Microbiology Reviews*, *29*(4), 625–651.

Beveridge, T. J. (1999). Minireview Structures of Gram-Negative Cell Walls and Their Derived Membrane Vesicles. *Journal of Bacteriology*, *181*(16), 4725–4733.

Bishop, R. (Unpublished). Enzymatic Modification of Endotoxins.

Bishop, R. E . (2005). Fundamentals of Endotoxin Structure and Function. *Contributions to Microbiology*, *12*, 1–27.

Bishop, R. E. (2005). The lipid A palmitoyltransferase PagP: molecular mechanisms and role in bacterial pathogenesis. *Molecular Microbiology*, *57*(4), 900–12.

Bishop, R. E. (2008). Structural biology of membrane-intrinsic β-barrel enzymes: Sentinels of the bacterial outer membrane. *Biochimica et Biophysica Acta - Biomembranes*, *1778*, 1881–1896.

Bishop, R. E. (2014). Emerging roles for anionic non-bilayer phospholipids in fortifying the outer membrane permeability barrier. *Journal of Bacteriology*, *196*(18), 3209–3213.

Bishop, R. E. (2016). Polymorphic Regulation of Outer Membrane Lipid A Composition. *MBio*, *7*(6), e01903-16.

Bishop, R. E., Gibbons, H. S., Guina, T., Trent, M. S., Miller, S. I., & Raetz, C. R. (2000). Transfer of palmitate from phospholipids to lipid A in outer membranes of gram-negative bacteria. *The EMBO Journal*, *19*(19), 5071–80.

Bonifacino, J. S., & Glick, B. S. (2004). The Mechanisms of Vesicle Budding and Fusion. *Cell*, *116*(2), 153–166.

Bonnington, K. E., & Kuehn, M. J. (2016). Outer Membrane Vesicle Production Facilitates LPS Remodeling and Transitions. *MBio*, *7*(5), 1–15.

Bowie, J. U. (2005). Solving the membrane protein folding problem. *Nature*, *438*(7068), 581–589.

Bratlie, M. S., Johansen, J., Sherman, B. T., Huang, D. W., Lempicki, R. A., & Drabløs, F. (2010). Gene duplications in prokaryotes can be associated with environmental adaptation. *BMC Genomics*, *11*(1), 588.

Brigulla, M., & Wackernagel, W. (2010). Molecular aspects of gene transfer and foreign

DNA acquisition in prokaryotes with regard to safety issues. *Applied Microbiology and Biotechnology*, *86(4)*, 1027-1041.

Brozek, K. A., Bulawa, C. E., & Raetz, C. R. (1987). Biosynthesis of lipid A precursors in *Escherichia coli*. A membrane-bound enzyme that transfers a palmitoyl residue from a glycerophospholipid to lipid X. *Journal of Biological Chemistry*, *262*(11), 5170–5179.

Brozek, K. A., & Raetz, C. R. (1990). Biosynthesis of lipid A in *Escherichia coli*. Acyl carrier protein-dependent incorporation of laurate and myristate. *The Journal of Biological Chemistry*, *265*(26), 15410–7.

Bulat, E., & Garrett, T. A. (2011). Putative N-acylphosphatidylethanolamine synthase from *Arabidopsis thaliana* is a lysoglycerophospholipid acyltransferase. *Journal of Biological Chemistry*, *286*(39), 33819–33831.

Cakmakci, M. L., Evans, H. J., & Seidler, R. J. (1981a). Characteristics of nitrogen-fixing *Klebsiella oxytoca* isolated from wheat roots. *Plant and Soil*, *61*(1–2), 53–63.

Caroff, M. (1988). Detergent-accelerated hydrolysis of bacterial endotoxins and determination of the anomeric configuration of the glycosyl phosphate present in the "Isolated lipid A" fragment of the *Bordetella pertussis* endotoxin**.** *Carbohydrate Research*, *175*, 273–282.

Caroff, M., & Karibian, D. (2003). Structure of bacterial lipopolysaccharides. *Carbohydrate Research*, *338*(23), 2431–2447.

Casadaban, M. J., & Cohen, S. N. (1980b). Analysis of gene control signals by DNA fusion and cloning in *Escherichia coli*. *Journal of Molecular Biology*, *138*(2), 179–207.

Casella, C. R., & Mitchell, T. C. (2013). Inefficient TLR4/MD-2 Heterotetramerization by Monophosphoryl Lipid A. *PLoS ONE*, *8*(4), 19–21.

Chalabaev, S., Chauhan, A., Novikov, A., Iyer, P., Szczesny, M., Beloin, C., Caroff, M & Ghigo, J.-M. (2014). Biofilms Formed by Gram-Negative Bacteria Undergo Increased Lipid A Palmitoylation, Enhancing *In Vivo* Survival. *MBio*, *5*(4), e01116-14-e01116-14.

Chisholm, S. T., Coaker, G., Day, B., & Staskawicz, B. J. (2006). Host-microbe interactions: Shaping the evolution of the plant immune response. *Cell*, 124(4), 803-814.

Chong, Z. S., Woo, W. F., & Chng, S. S. (2015). Osmoporin OmpC forms a complex

with MlaA to maintain outer membrane lipid asymmetry in *Escherichia coli*. *Molecular Microbiology*, *98*(6), 1133–1146.

Clifton, L. A., Skoda, M. W. A., Le Brun, A. P., Ciesielski, F., Kuzmenko, I., Holt, S. A., & Lakey, J. H. (2014). Effect of Divalent Cation Removal on the Structure of Gram-Negative Bacterial Outer Membrane Models. *Langmuir*, *31*(1), 404–412.

Costerton, J. W., Ingram, J. M., & Cheng, K.-J. (1974). Structure and Function of the Cell Envelope of Gram-Negative Bacteria. *Bacteriological Reviews*, *38*(1), 87–110.

Cronan, J. E. (2003). Bacterial Membrane Lipids: Where Do We Stand? *Annual Review of Microbiology*, *57*(1), 203–224.

Cuesta-Seijo, J. A., Neale, C., Khan, M. A., Moktar, J., Tran, C. D., Bishop, R. E., Pomes, R., Privé, G. G. (2010). PagP crystallized from SDS/cosolvent reveals the route for phospholipid access to the hydrocarbon ruler. *Structure (London, England : 1993)*, *18*(9), 1210–9.

d'Hauteville, H., Khan, S., Maskell, D. J., Kussak, A., Weintraub, A., Mathison, J., Ulevitch, R. J., Wuscher, N., Parsot, C., & Sansonetti, P. J. (2002). Two msbB Genes Encoding Maximal Acylation of Lipid A Are Required for Invasive *Shigella flexneri* to Mediate Inflammatory Rupture and Destruction of the Intestinal Epithelium. *The Journal of Immunology*, *168*(10), 5240–5251.

Dalebroux, Z. D., Edrozo, M. B., Pfuetzner, R. A., Ressl, S., Kulasekara, B. R., Blanc, M.-P., & Miller, S. I. (2015). Delivery of Cardiolipins to the *Salmonella* Outer Membrane Is Necessary for Survival within Host Tissues and Virulence. *Cell Host & Microbe*, *17*(4), 441–451.

Dalebroux, Z. D., Matamouros, S., Whittington, D., Bishop, R. E., & Miller, S. I. (2014). PhoPQ regulates acidic glycerophospholipid content of the *Salmonella Typhimurium* outer membrane. *Proceedings of the National Academy of Sciences of the United States of America*, *111*(5), 1963–8.

Darby, A., Lertpiriyapong, K., Sarkar, U., Seneviratne, U., Park, D. S., Gamazon, E. R., & Fox, J. G. (2014). Cytotoxic and pathogenic properties of *Klebsiella oxytoca* isolated from laboratory animals. *PloS One*, *9*(7), e100542.

Darveau, R. P., Blake, J., Seachord, C. L., Cosand, W. L., Cunningham, M. D., Cassiano-Clough, L., & Maloney, G. (1992). Peptides related to the carboxyl terminus of human platelet factor IV with antibacterial activity. *Journal of Clinical Investigation*, *90*(2), 447–455.

de Kruijff, B. (1987). Polymorphic regulation of membrane lipid composition. *Nature*,

329(6140), 587–588.

DeChavigny, A., Heacock, P. N., & Dowhan, W. (1991). Sequence and inactivation of the pss gene of *Escherichia coli*. Phosphatidylethanolamine may not be essential for cell viability. *The Journal of Biological Chemistry*, *266*(8), 5323–32.

den Dunnen, J., & Antonarakis, S. (2001). Nomenclature for the description of human sequence variations. *Human Genetics*, *109*(1), 121–124.

Didierlaurent, A. M., Laupèze, B., Di Pasquale, A., Hergli, N., Collignon, C., & Garçon, N. (2017). Adjuvant system AS01: helping to overcome the challenges of modern vaccines. *Expert Review of Vaccines*, *16*(1), 55–63.

Dixon, C. (Unpublished). *New Roles for PagP in the Bacterial Outer Membrane Stress Response*. Thesis. McMaster University, Hamilton, Ontario, Canada.

Doerrler, W. T. (2006). Lipid trafficking to the outer membrane of Gram-negative bacteria. *Molecular Microbiology*, *60*(3), 542–552.

Dong, H., Xiang, Q., Gu, Y., Wang, Z., Paterson, N. G., Stansfeld, P. J., & Dong, C. (2014). Structural basis for outer membrane lipopolysaccharide insertion. *Nature*, *511*(7507), 52–6.

Dong, H., Zhang, Z., Tang, X., Huang, S., Li, H., Peng, B., & Dong, C. (2016). Structural insights into cardiolipin transfer from the Inner membrane to the outer membrane by PbgA in Gram-negative bacteria. *Scientific Reports*, *6*(1), 30815.

Dong, H., Zhang, Z., Tang, X., Paterson, N. G., & Dong, C. (2017). Structural and functional insights into the lipopolysaccharide ABC transporter LptB2FG. *Nature Communications*, *8*(1), 222.

Döring, K., Surrey, T., Nollert, P., & Jähnig, F. (1999). Effects of ligand binding on the internal dynamics of maltose-binding protein. *European Journal of Biochemistry*, *266*(2), 477–483.

Durfee, T., Nelson, R., Baldwin, S., Plunkett, G., Burland, V., Mau, B., Petrosino, J. F., Qin, X., Muzny, D. M., Ayele, M., Gibbs, R. A., Weinstock, G. M., & Blattner, F. R. (2008). The complete genome sequence of *Escherichia coli* DH10B: Insights into the biology of a laboratory workhorse. *Journal of Bacteriology*, *190*(7), 2597–2606.

e Silva, S. de A., & Echeverrigaray, S. (2012). Bacterial Promoter Features Description and Their Application on *E. coli* in silico Prediction and Recognition Approaches. In *Bioinformatics* (pp. 61–78). InTech. Retrieved from: http://doi.org/10.5772/48149

Eguchi, Y., Okada, T., Minagawa, S., Oshima, T., Mori, H., Yamamoto, K., & Utsumi, R. (2004). Signal Transduction Cascade between EvgA/EvgS and PhoP/PhoQ Two-Component Systems of *Escherichia coli*. *Journal of Bacteriology*, *186*(10), 3006–3014.

Ekiert, D. C., Bhabha, G., Isom, G. L., Greenan, G., Ovchinnikov, S., Henderson, I. R., & Vale, R. D. (2017). Architectures of Lipid Transport Systems for the Bacterial Outer Membrane. *Cell*. 169(2), 273-285.e17.

El Hamidi, A., Novikov, A., Karibian, D., Perry, M. B., & Caroff, M. (2009). Structural characterization of *Bordetella parapertussis* lipid A. *Journal of Lipid Research*.

Emptage, R. P., Tonthat, N. K., York, J. D., Schumacher, M. A., & Zhou, P. (2014). Structural basis of lipid binding for the membrane-embedded tetraacyldisaccharide-1-phosphate 4'-kinase LpxK. *Journal of Biological Chemistry*, *289*(35), 24059–24068.

Epand, R. M., & Epand, R. F. (2011). Bacterial membrane lipids in the action of antimicrobial agents. *Journal of Peptide Science : An Official Publication of the European Peptide Society*, *17*(5), 298–305.

Ernst, R. K., Guina, T., & Miller, S. I. (2001). *Salmonella typhimurium* outer membrane remodeling: role in resistance to host innate immunity. *Microbes and Infection*, *3*(14–15), 1327–1334.

Ernst, R. K., Hajjar, A. M., Tsai, J. H., Moskowitz, S. M., Wilson, C. B., & Miller, S. I. (2003). *Pseudomonas aeruginosa* lipid A diversity and its recognition by Toll-like receptor 4. *Journal of Endotoxin Research*. 9(6), 395-400.

Ernst, R. K., Moskowitz, S. M., Emerson, J. C., Kraig, G. M., Adams, K. N., Harvey, M. D., & Miller, S. I. (2007). Unique lipid a modifications in *Pseudomonas aeruginosa* isolated from the airways of patients with cystic fibrosis. *The Journal of Infectious Diseases*, *196*(7), 1088–92.

Erridge, C., Bennett-Guerrero, E., & Poxton, I. R. (2002). Structure and function of lipopolysaccharides. *Microbes and Infection*, *4*(8), 837–851.

Evans, J. T., Cluff, C., Johnson, D., Lacy, M., Persing, D., & Baldridge, J. (2003). Enhancement of antigen specific immunity via the TLR4 ligands MPL adjuvant and Ribi.529. *Expert Review of Vaccines*, *2*(2), 219–229.

Feist, W., Ulmer, A. J., Musehold, J., Brade, H., Kusumoto, S., & Flad, H. D. (1989). Induction of Tumor Necrosis Factor-Alpha Release by Lipopolysaccharide and Defined Lipopolysaccharide Partial Structures. *Immunobiology*, *179*(4–5), 293–307.

Fiori, M. C., Jiang, Y., Altenberg, G. A., & Liang, H. (2017). Polymer-encased nanodiscs with improved buffer compatibility. *Scientific Reports*, *7*(1), 7432.

Fouts, D. E., Tyler, H. L., DeBoy, R. T., Daugherty, S., Ren, Q., Badger, J. H., & Methé, B. A. (2008). Complete genome sequence of the N_2-fixing broad host range endophyte *Klebsiella pneumoniae* 342 and virulence predictions verified in mice. *PLoS Genetics*, *4*(7), e1000141

Furse, S., & Scott, D. J. (2016). Three-Dimensional Distribution of Phospholipids in Gram Negative Bacteria. *Biochemistry*, *55*(34), 4742–4747.

Galdiero, S., Galdiero, M., & Pedone, C. (2007). -Barrel Membrane Bacterial Proteins: Structure, Function, Assembly and Interaction with Lipids. *Current Protein and Peptide Science*, *8*, 63–82.

Garçon, N., Chomez, P., & Van Mechelen, M. (2007). GlaxoSmithKline Adjuvant Systems in vaccines: Concepts, achievements and perspectives. *Expert Review of Vaccines*, *6*(5), 723–739.

Garrett, T. A. (2016). Major roles for minor bacterial lipids identified by mass spectrometry. *BBA - Molecular and Cell Biology of Lipids*, *1862*, 1319–1324.

Garrett, T. A. (2017). Major roles for minor bacterial lipids identified by mass spectrometry. *Biochimica et Biophysica Acta (BBA) - Molecular and Cell Biology of Lipids*, *1862*(11), 1319–1324.

Garrett, T. A., & Moncada, R. M. (2014). The *Arabidopsis thaliana* lysophospholipid acyltransferase At1g78690p acylates a variety of lysophospholipids including bis(monoacylglycero)phosphate. *Biochemical and Biophysical Research Communications*, *452*(4), 1022–1027.

Garrett, T. J., Merves, M., & Yost, R. A. (2011). Characterization of protonated phospholipids as fragile ions in quadrupole ion trap mass spectrometry. *Int J Mass Spectrom*, *308*(352), 299–306.

Geiger, O. (2010). Lipids and Legionella virulence. In K. N. Timmis (Ed.), *Handbook of Hydrocarbon and Lipid Microbiology* (pp. 3196–3201). Berlin, Heidelberg: Springer Berlin Heidelberg.

Gertz, E. M., Yu, Y.-K., Agarwala, R., Schäffer, A. A., & Altschul, S. F. (2006). Composition-based statistics and translated nucleotide searches: improving the TBLASTN module of BLAST. *BMC Biology*, *4*, 41.

Gibbons, H. S., Kalb, S. R., Cotter, R. J., & Raetz, C. R. H. (2005). Role of Mg2+ and pH in the modification of *Salmonella* lipid A after endocytosis by macrophage tumour cells. *Molecular Microbiology*, *55*(2), 425–440.

Gibbons, H. S., Reynolds, C. M., Guan, Z., & Raetz, C. R. H. (2008). An Inner Membrane Dioxygenase that Generates the 2-Hydroxymyristate Moiety of *Salmonella* Lipid A †. *Biochemistry*, *47*(9), 2814–2825.

Glauert, A. M., & Thornley, M. J. (1969). The topography of the bacterial cell wall. *Annual Review of Microbiology*, *23*, 159–198.

Goldberg, B., Campos, J., Tallon, L., Sadzewicz, L., Sengamalay, N., & Ott, S. (2018). FDA database for Regulatory Grade microbial Sequences (FDA-ARGOS): Supporting development and validation of Infectious Disease Dx tests. Baltimore, MA. USA. Retrieved from: *NCBI website*, asscession number: CP014127

Graf, L., Jancso, A., Szilagyi, L., Hegyi, G., Pinter, K., Naray-Szabo, G., & Rutter, W. J. (1988). Electrostatic complementarity within the substrate-binding pocket of trypsin. *Proceedings of the National Academy of Sciences*, *85*(14), 4961–4965.

Greenfield, N. J. (2007). Using circular dichroism collected as a function of temperature to determine the thermodynamics of protein unfolding and binding interactions. *Nature Protocols*, *1*(6), 2527–2535.

Gregg, K. A., Harberts, E., Gardner, F. M., Pelletier, M. R., Cayatte, C., Yu, L., & Ernst, R. K. (2017). Rationally designed TLR4 ligands for vaccine adjuvant discovery. *MBio*. 8(3). Retrieved from: http://doi.org/10.1128/mBio.00492-17

Groisman, E. A. (2001). The Pleiotropic Two-Component Regulatory System PhoP-PhoQ Minireview The Pleiotropic Two-Component Regulatory System PhoP-PhoQ. *Journal of Bacteriology*, *183*(6), 1835–1842.

Gunn, J. S. (2008). The *Salmonella* PmrAB regulon: lipopolysaccharide modifications, antimicrobial peptide resistance and more. *Trends in Microbiology*, *16*(6), 284–290.

Guo, D., & Tropp, B. E. (2000). A second *Escherichia coli* protein with CL synthase activity. *Biochimica et Biophysica Acta - Molecular and Cell Biology of Lipids*, *1483*(2), 263–274.

Guo, L., Lim, K., Poduje, C., & Daniel, M. (1998). Lipid A acylation and bacterial resistance against vertebrate antimicrobial peptides. *Cell*, *95*, 189–198.

Gupta, R. S. (1998). Protein Phylogenies and Signature Sequences: A Reappraisal of Evolutionary Relationships among Archaebacteria, Eubacteria, and Eukaryotes,

62(4), 1435–1491.

Gupta, R. S. (2014). Identification of Conserved Indels that are Useful for Classification and Evolutionary Studies. In *Methods in Microbiology* (Vol. 41, pp. 153–182). Elsevier. Retrieved from: http://doi.org/10.1016/bs.mim.2014.05.003

Gupta, R. S., & Epand, R. M. (2017). Phylogenetic analysis of the diacylglycerol kinase family of proteins and identification of multiple highly-specific conserved inserts and deletions within the catalytic domain that are distinctive characteristics of different classes of DGK homologs. *PLOS ONE*, *12*(8), e0182758.

Gupta, R. S., Nanda, A., & Khadka, B. (2017). Novel molecular, structural and evolutionary characteristics of the phosphoketolases from bifidobacteria and Coriobacteriales. *PLOS ONE*, *12*(2), e0172176. http://doi.org/10.1371/journal.pone.0172176

Gust, B., Chandra, G., Jakimowicz, D., Yuqing, T., Bruton, C. J., & Chater, K. F. (2004). λ Red-Mediated Genetic Manipulation of Antibiotic-Producing Streptomyces. In *Advances in Applied Microbiology* (pp. 107–128).

Guzman, L. L. M., Belin, D., Carson, M. J., Beckwith, J., Luz-Maria Guzman Michael J. Carson, and Jon Beckwith, D. B., & Luz-Maria Guzman Michael J. Carson, and Jon Beckwith, D. B. (1995). Tight Regulation, Modulation, and High-Level Expression by Vectors Containing the Arabinose PBAD Promoter. *Journal of Bacteriology*, *177*(14), 4121–4130.

Hammes, G. G. (2002). Multiple conformational changes in enzyme catalysis. *Biochemistry, 41*(26), 8221-8228.

Hanberger, H. (1999). Antibiotic Susceptibility Among Aerobic Gram-negative *Bacilli* in Intensive Care Units in 5 European Countries. *JAMA*, *281*(1), 67.

Hancock, R. E. W., & Bell, A. (1988). Antibiotic uptake into gram-negative bacteria. *European Journal of Clinical Microbiology & Infectious Diseases*, *7*(6), 713–720.

Hegde, R. S., & Bernstein, H. D. (2006). The surprising complexity of signal sequences. *Trends in Biochemical Sciences, 31*(10), 563-571.

Hester, S. E., Goodfield, L. L., Park, J., Feaga, H. A., Ivanov, Y. V., Bendor, L., & Harvill, E. T. (2015). Host Specificity of Ovine *Bordetella parapertussis* and the Role of Complement. *PLOS ONE*, *10*(7), e0130964. Retrieved from: http://doi.org/10.1371/journal.pone.0130964

Higgins, N. P., Vologodskii, A. V, & Genetics, M. (2016). Topological Behaviour of

Plasmid DNA. *Microbiologiy Spectrum*, *3*(2), 1–49.

Hite, R., Gonen, T., Harrison, S., & Walz, T. (2008). Interactions of lipids with aquaporin-0 and other membrane proteins. *Pflügers Archiv-European Journal*, *456*(4), 651–661.

Hittle, L. E., Jones, J. W., Hajjar, A. M., Ernst, R. K., & Preston, A. (2015a). *Bordetella parapertussis* PagP mediates the addition of two palmitates to the lipopolysaccharide lipid A. *Journal of Bacteriology*, *197*(3), 572–580.

Ho, H., Miu, A., Alexander, M. K., Garcia, N. K., Oh, A., Zilberleyb, I., & Koth, C. M. (2018). Structural basis for dual-mode inhibition of the ABC transporter MsbA. *Nature*, *557*(7704), 196–201.

Holliday, G. L., Mitchell, J. B. O., & Thornton, J. M. (2009). Understanding the functional roles of amino acid residues in enzyme catalysis. *Journal of Molecular Biology*, *390*(3), 560–77.

Homma, H., Kudo, I., Inoue, K., & Nojima, S. (1987). Characteristics of phospholipid transacylase of *Escherichia coli*. *Journal of Biochemistry*, *101*(4), 1033–9.

Horovitz, A., & Fersht, A. R. (1990). Strategy for analysing the co-operativity of intramolecular interactions in peptides and proteins. *Journal of Molecular Biology*, *214*(3), 613–617.

Hsu, F. F., Turk, J., Shi, Y., & Groisman, E. A. (2004). Characterization of acylphosphatidylglycerols from *Salmonella typhimurium* by tandem mass spectrometry with electrospray ionization. *Journal of the American Society for Mass Spectrometry*, *15*(1), 1–11.

Hsu, L., Jackowski, S., & Rock, C. O. (1989). Uptake and acylation of 2-acyl-lysophospholipids by *Escherichia coli*. *Journal of Bacteriology*, *171*(2), 1203–1205.

Hu, K. H., Liu, E., Dean, K., Gingras, M., DeGraff, W., & Trun, N. J. (1996). Overproduction of three genes leads to camphor resistance and chromosome condensation in *Escherichia coli*. *Genetics*, *143*(4), 1521–1532.

Huang, T.-W., Lam, I., Chang, H.-Y., Tsai, S.-F., & Palsson B, Ø, C, P., (2014). Capsule deletion via a λ-Red knockout system perturbs biofilm formation and fimbriae expression in *Klebsiella pneumoniae* MGH 78578. *BMC Research Notes*, *7*, 13.

Hullin-Matsuda, F., Kawasaki, K., Delton-Vandenbroucke, I., Xu, Y., Nishijima, M., Lagarde, M., & Kobayashi, T. (2007). De novo biosynthesis of the late endosome lipid, *bis*(monoacylglycero)phosphate. *Journal of Lipid Research*, *48*(9), 1997–2008.

Huysmans, G. H. M., Radford, S. E., Brockwell, D. J., & Baldwin, S. A. (2007). The *N*-terminal Helix Is a Post-assembly Clamp in the Bacterial Outer Membrane Protein PagP. *Journal of Molecular Biology*, *373*(3), 529–540.

Hwang, P., Bishop, R., & Kay, L. (2004). The integral membrane enzyme PagP alternates between two dynamically distinct states. *Proceedings of the National Academy of Sciences of the United States of America*, *101*(6234).

Hwang, P. M., Choy, W.-Y., Lo, E. I., Chen, L., Forman-Kay, J. D., Raetz, C. R. H., Prive, G. G., Bishop, R. E., and Kay, L. E. (2002). Solution structure and dynamics of the outer membrane enzyme PagP by NMR. *PNAS*, *99*(21), 13560–5.

Isom, G. L., Davies, N. J., Chong, Z.-S., Bryant, J. A., Jamshad, M., Sharif, M., & Henderson, I. R. (2017). MCE domain proteins: conserved inner membrane lipid-binding proteins required for outer membrane homeostasis. *Scientific Reports*, *7*(1), 8608.

Iyer, B., & Mahalakshmi, R. (2016). Distinct Structural Elements Govern the Folding, Stability, and Catalysis in the Outer Membrane Enzyme PagP. *Biochemistry*, *35*(55), 4960–70.

Jayol, A., Poirel, L., Villegas, M. V., & Nordmann, P. (2015). Modulation of mgrB gene expression as a source of colistin resistance in *Klebsiella oxytoca*. *International Journal of Antimicrobial Agents*, *46*(1), 108–110.

Jia, W., El Zoeiby, A., Petruzziello, T. N., Jayabalasingham, B., Seyedirashti, S., & Bishop, R. E. (2004). Lipid trafficking controls endotoxin acylation in outer membranes of *Escherichia coli*. *The Journal of Biological Chemistry*, *279*(43), 44966–75.

Jogl, G., Hsiao, Y.-S., & Tong, L. (2004). Structure and Function of Carnitine Acyltransferases. *Annals of the New York Academy of Sciences*, *1033*(1), 17–29.

Jogl, G., & Tong, L. (2003). Crystal structure of carnitine acetyltransferase and implications for the catalytic mechanism and fatty acid transport. *Cell*, *112*, 113–122.

Jones, J. D. G., & Dangl, J. L. (2006). The plant immune system. *Nature*, *444*(7117), 323–329.

Jones, N. C., & Osborn, M. J. (1977). Translocation of phospholipids between the outer and inner membranes of *Salmonella typhimurium*. *Journal of Biological Chemistry*, *252*(20), 7405–7412.

Kaur, J., & Bachhawat, A. K. (2009). A modified Western blot protocol for enhanced sensitivity in the detection of a membrane protein. *Analytical Biochemistry*, *384*(2), 348–349.

Kawasaki, K., Ernst, R. K., & Miller, S. I. (2004). 3-O-Deacylation of Lipid A by PagL, a PhoP/PhoQ-regulated Deacylase of *Salmonella typhimurium*, Modulates Signaling through Toll-like Receptor 4. *Journal of Biological Chemistry*, *279*(19), 20044–20048.

Kearse, M., Moir, R., Wilson, A., Stones-Havas, S., Cheung, M., Sturrock, S., & Drummond, A. (2012). Geneious Basic: An integrated and extendable desktop software platform for the organization and analysis of sequence data. *Bioinformatics*, *28*(12), 1647–1649.

Khadka, B., & Gupta, R. S. (2017). Identification of a conserved 8 aa insert in the PIP5K protein in the Saccharomycetaceae family of fungi and the molecular dynamics simulations and structural analysis to investigate its potential functional role. *Proteins: Structure, Function and Bioinformatics*, *85*(8), 1454–1467.

Khan, M. A., & Bishop, R. E. (2009). Molecular mechanism for lateral lipid diffusion between the outer membrane external leaflet and a beta-barrel hydrocarbon ruler. *Biochemistry*, *48*(41), 9745–56.

Khan, M. A., Moktar, J., Mott, P. J., & Bishop, R. E. (2010a). A thiolate anion buried within the hydrocarbon ruler perturbs pagP lipid acyl chain selection. *Biochemistry*, *49*, 2368–2379.

Khan, M. A., Moktar, J., Mott, P. J., Vu, M., McKie, A. H., Pinter, T., Hof, F., & Bishop, R. E. (2010). Inscribing the perimeter of the PagP hydrocarbon ruler by site-specific chemical alkylation. *Biochemistry*, *49*(42), 9046–57.

Khan, M. A., Neale, C., Michaux, C., Pomès, R., Privé, G. G., Woody, R. W., & Bishop, R. E. (2007). Gauging a hydrocarbon ruler by an intrinsic exciton probe. *Biochemistry*, *46*, 4565–4579.

Khan, M. A., Sapiano, M. J., Vu, M., Mott, P. J., Lewis, R. N. A. H., Mcelhaney, R. N., & Bishop, R. E. (Unpublished). PagP Crenel Gating Impedes Lipid A Stearoylation by Enforcing Phospholipid Regioselectivity and Blockading sn-1-Stearate Chain Access to the Hydrocarbon Ruler.

Kim, H. M., Park, B. S., Kim, J. I., Kim, S. E., Lee, J., Oh, S. C., & Lee, J. O. (2007). Crystal Structure of the TLR4-MD-2 Complex with Bound Endotoxin Antagonist Eritoran. *Cell*. 130(5), 906-917.

Kim, S. H., Jia, W., Bishop, R. E., & Gyles, C. (2004). An msbB Homologue Carried in Plasmid pO157 Encodes an Acyltransferase Involved in Lipid A Biosynthesis in *Escherichia coli* O157:H7. *Infection and Immunity*, *72*(2), 1174–1180.

Kleanthous, C., Rassam, P., & Baumann, C. G. (2015). Protein-protein interactions and the spatiotemporal dynamics of bacterial outer membrane proteins. *Current Opinion in Structural Biology*, *35*, 109-115.

Kleinschmidt, J. H. (2015). Folding of β -barrel membrane proteins in lipid bilayers — Unassisted and assisted folding and insertion. *Biochimica et Biophysica Acta (BBA) - Biomembranes*, *1848*(9), 1927–1943.

Koebnik, R., Kaspar, Locher, P., & Gelder, P. Van. (2000). Structure and function of bacterial outer membrane proteins: barrels in a nutshell. *Molecular Microbiology*, *37*(2), 239–253.

Koonin, E. V., Makarova, K. S., & Aravind, L. (2001). Horizontal Gene Transfer in Prokaryotes: Quantification and Classification. *Annual Review of Microbiology*, *55*(1), 709–742.

Lambert, M. a., & Moss, C. W. (1989). Cellular fatty acid compositions and isoprenoid quinone contents of 23 *Legionella* species. *Journal of Clinical Microbiology*, *27*(3), 465–473.

Langley, K. E., Hawrot, E., & Kennedy, E. P. (1982). Membrane assembly: Movement of phosphatidylserine between the cytoplasmic and outer membranes of *Escherichia coli*. *Journal of Bacteriology*, *152*(3), 1033–1041.

Lee, L., & Imae, Y. (1990). Role of threonine residue 154 in ligant recognition of the Tar chemoreceptor in *Escherichia coli*. *Journal of Bacteriology*, *172*(1), 377–382.

Leive, L. (1968). Studies on the permeability change produced in coliform bacteria by ethylenediaminetetraacetate. *Journal of Biological Chemistry*, *243*, 2373–2380.

Lerouge, I., & Vanderleyden, J. (2001). O-antigen structural variation: mechanisms and possible roles in animal/plant-microbe interactions. FEMS Microbiology Reviews, *26*(2001), 17-47.

Li, C. (2016). *Complete genome sequence of a biocontrol organism Pantoea agglomerans C410P1*. Institute of Health Sciences, Anhui University, China. Retrieved from: *NCBI website,* accession number: CP016890.

Li, C., Guan, Z., Liu, D., & Raetz, C. R. H. (2011). Pathway for lipid A biosynthesis in

Arabidopsis thaliana resembling that of *Escherichia coli*. *PNAS*, *108*(28), 11387–11392.

Li, Y., Powell, D. A., Shaffer, S. A., Rasko, D. A., Pelletier, M. R., Leszyk, J. D., & Ernst, R. K. (2012). LPS remodeling is an evolved survival strategy for bacteria. *Proceedings of the National Academy of Sciences*, *109*(22), 8716–8721.

Lin, L., Li, Z., Hu, C., Zhang, X., Chang, S., Yang, L., & An, Q. (2012). Plant Growth-Promoting Nitrogen-Fixing Enterobacteria Are in Association with Sugarcane Plants Growing in Guangxi, China. *Microbes Environ*, *27*(4), 391–398.

Lin, L., Wei, C., Chen, M., Wang, H., Li, Y., Li, Y., & An, Q. (2015). Complete genome sequence of endophytic nitrogen-fixing *Klebsiella variicola s*train DX120E. *Standards in Genomic Sciences*, *10*(1), 22.

Lin, T. Y., & Weibel, D. B. (2016). Organization and function of anionic phospholipids in bacteria. *Applied Microbiology and Biotechnology*, *100*(10), 4255–4267.

Lin, Z., Cai, X., Chen, M., Ye, L., Wu, Y., Wang, X., Lv, Z., Shang, Y., & Qu, D. (2018). Virulence and stress responses of *Shigella flexneri* regulated by PhoP/PhoQ. *Frontiers in Microbiology*, *8*(JAN).

López-Lara, I. M., & Geiger, O. (2017). Bacterial lipid diversity. *Biochimica et Biophysica Acta (BBA) - Molecular and Cell Biology of Lipids*, *1862*(11), 1287–1299.

Lu, Y.-H., Guan, Z., Zhao, J., & Raetz, C. R. H. (2010). Three Phosphatidylglycerol-phosphate Phosphatases in the Inner Membrane of *Escherichia coli.* Journal of Biological Chemical, *286*(7), 5506-5518.

Lucas, S., Copeland, A., Lapidus, A., & Cheng, J. (2010). Complete sequence plasmid1 of *Pantoea sp.* At-9b. *EMBL/GenBank/DDBJ Databases*. Retrieved from: https://www.uniprot.org/proteomes/UP000001624

Luo, Q., Yang, X., Yu, S., Shi, H., Wang, K., Xiao, L., Tingting, L., Dianfan, L., Zhang, Min, Z., & Huang, Y. (2017). Structural basis for lipopolysaccharide extraction by ABC transporter LptB2FG. *Nature Structural & Molecular Biology*. 24(5), 469-474.

MacLean, A. M., Finan, T. M., & Sadowsky, M. J. (2007). Genomes of the symbiotic nitrogen-fixing bacteria of legumes. *Plant Physiology*, *144*(2), 615–22.

Malinverni, J. C., & Silhavy, T. J. (2009). An ABC transport system that maintains lipid asymmetry in the Gram-negative outer membrane. *Proceedings of the National Academy of Sciences*, *106*(19), 8009–8014.

May, K. L., & Silhavy, T. J. (2017). Making a membrane on the other side of the wall. *Biochimica et Biophysica Acta - Molecular and Cell Biology of Lipids*, *1862*(11), 1386–1393.

Mi, W., Li, Y., Yoon, S. H., Ernst, R. K., Walz, T., & Liao, M. (2017). Structural basis of MsbA-mediated lipopolysaccharide transport. *Nature*. *549*(7671), 233-237.

Miles, A. J., & Wallace, B. A. (2016). Circular dichroism spectroscopy of membrane proteins. *Chemical Society Reviews*, *45*(18), 4859–4872.

Miller, S. I., & Salama, N. R. (2018). The gram-negative bacterial periplasm: Size matters. *PLoS Biology*. Retrieved from: http://doi.org/10.1371/journal.pbio.2004935

Mills, G., Dumigan, A., Kidd, T., Hobley, L., & Bengoechea, J. A. (2017). Identification and Characterization of Two *Klebsiella pneumoniae* lpxL Lipid A Late Acyltransferases and Their Role in Virulence. *Infection and Immunity*, *85*(9).

Molinaro, A., Newman, M. A., Lanzetta, R., & Parrilli, M. (2009). The structures of lipopolysaccharides from plant-Associated Gram-negative bacteria. *European Journal of Organic Chemistry*, (34), 5887–5896.

Murzin, A. G., Lesk, A. M., & Chothia, C. (1994). Principles determining the structure of beta-sheet barrels in proteins. I. A theoretical analysis. *Journal of Molecular Biology*, *236*(5), 1369–1381.

Nakamura, Y., Itoh, T., Matsuda, H., & Gojobori, T. (2004). Biased biological functions of horizontally transferred genes in prokaryotic genomes. *Nature Genetics*, *36*(7), 760–766.

Naushad, H. S., Lee, B., & Gupta, R. S. (2014). Conserved signature indels and signature proteins as novel tools for understanding microbial phylogeny and systematics: Identification of molecular signatures that are specific for the phytopathogenic genera *Dickeya*, *Pectobacterium* and *Brenneria*. *International Journal of Systematic and Evolutionary Microbiology, 64, 366-383*.

Needham, B. D., & Trent, M. S. (2013). Fortifying the barrier: the impact of lipid A remodelling on bacterial pathogenesis. *Nature Reviews. Microbiology*, *11*(7), 467–81.

Neuhauser, M. M., Weinstein, R. A, Rydman, R., Danziger, L. H., Karam, G., & Quinn, J. P. (2003). Antibiotic Resistance Among Gram-Negative *Bacilli* in US Intensive Care Units. *JAMA*, *289*(7), 885.

Nicolson, G. L. (2014). The Fluid—Mosaic Model of Membrane Structure: Still relevant to understanding the structure, function and dynamics of biological membranes after more than 40 years ☆. *BBA - Biomembranes*, *1838*, 1451–1466.

Nikaido, Hiroshi Vaara, M. (1985). Molecular Basis of Bacterial Outer Membrane Permeability, *49*(1), 1–32.

Nikaido, H. (2003). Molecular Basis of Bacterial Outer Membrane Permeability Revisited. *Microbiology and Molecular Biology Reviews*, *67*(4), 593–656.

Nishihara, M., Morii, H., & Koga, Y. (1982). Bis(monoacylglycero)phosphate in Alkalophilic Bacteria. *J. Biochem*, *92*, 1469–1479.

Noinaj, N., Kuszak, A. J., Gumbart, J. C., Lukacik, P., Chang, H., Easley, N. C., & Buchanan, S. K. (2013). Structural insight into the biogenesis of β-barrel membrane proteins. *Nature*, *501*(7467), 385–390.

Okuda, S., Sherman, D. J., Silhavy, T. J., Ruiz, N., & Kahne, D. (2016). Lipopolysaccharide transport and assembly at the outer membrane: The PEZ model. *Nature Reviews Microbiology*, *14*(6), 337–345.

Oursel, D., Loutelier-Bourhis, C., Orange, N., Chevalier, S., Norris, V., & Lange, C. M. (2007). Lipid composition of membranes of *Escherichia coli* by liquid chromatography/tandem mass spectrometry using negative electrospray ionization. *Rapid Communications in Mass Spectrometry : RCM*, *21*(11), 1721–1728.

Palade, G. (1975). Intracellular Aspects of the Process of Protein Synthesis. *Science*, *189*(4206), 867–867.

Park, B. S., Song, D. H., Kim, H. M., Choi, B.-S., Lee, H., & Lee, J.-O. (2009). The structural basis of lipopolysaccharide recognition by the TLR4-MD-2 complex. *Nature*, *458*(7242), 1191–5.

Parkhill, J., Sebaihia, M., Preston, A., Murphy, L., Thomson, N., Harris, D., & Maskell, D. (2003). Comparative analysis of the genome sequences of *Bordetella pertussis*, *Bordetella parapertussis* and *Bordetella bronchiseptica*. *Nat Genet*, *35*(1), 32–40.

Parsons, J. B., & Rock, C. O. (2013). Bacterial lipids: Metabolism and membrane homeostasis. *Progress in Lipid Research*, *52*(3), 249–276.

Pattengale, N. D., Alipour, M., Bininda-Emonds, O. R. P., Moret, B. M. E., & Stamatakis, A. (2009). How Many Bootstrap Replicates Are Necessary? In *Lecture Notes in Computer Science (including subseries Lecture Notes in Artificial Intelligence and Lecture Notes in Bioinformatics)* (pp. 184–200). DOI: 10.1007/978-3-642-02008-

7_13

Pavlova, A. S., Leontieva, M. R., Smirnova, T. A., Kolomeitseva, G. L., Netrusov, A. I., & Tsavkelova, E. A. (2017). Colonization strategy of the endophytic plant growth-promoting strains of *Pseudomonas fluorescens* and *Klebsiella oxytoca* on the seeds, seedlings and roots of the epiphytic orchid, Dendrobium nobile Lindl. *Journal of Applied Microbiology*, *123*(1), 217–232.

Petrou, V. I., Herrera, C. M., Schultz, K. M., Clarke, O. B., Vendome, J., Tomasek, D., & Mancia, F. (2016). Structures of aminoarabinose transferase ArnT suggest a molecular basis for lipid A glycosylation. *Science*, *351*(6273), 608–612.

Pilione, M. R., Pishko, E. J., Preston, A., Maskell, D. J., & Harvill, E. T. (2004). pagP Is Required for Resistance to Antibody-Mediated Complement Lysis during Bordetella bronchiseptica Respiratory Infection pagP Is Required for Resistance to Antibody-Mediated Complement Lysis during *Bordetella bronchiseptica* Respiratory Infection. *Infection and Immunity*, *72*(5), 2837–2842.

Plapp, B. V. (2010). Conformational changes and catalysis by alcohol dehydrogenase. *Archives of Biochemistry and Biophysics*, *493*(1), 3-12.

Podschun, R., & Ullmann, U. (1998). *Klebsiella spp*. as nosocomial pathogens: epidemiology, taxonomy, typing methods, and pathogenicity factors. *Clinical Microbiology Reviews*, *11*(4), 589–603.

Preston, A., Maxim, E., Toland, E., Pishko, E. J., Harvill, E. T., Caroff, M., & Maskell, D. J. (2003). *Bordetella bronchiseptica* PagP is a Bvg-regulated lipid A palmitoyl transferase that is required for persistent colonization of the mouse respiratory tract. *Molecular Microbiology*, *48*(3), 725–736.

Preston, A., Petersen, B. O., Duus, J., Kubler-Kielb, J., Ben-Menachem, G., Li, J., & Vinogradov, E. (2006). Complete structures of *Bordetella bronchiseptica* and *Bordetella parapertussis* lipopolysaccharides. *Journal of Biological Chemistry*, *281*(26), 18135–18144.

Qiao, S., Luo, Q., Zhao, Y., Zhang, X. C., & Huang, Y. (2014). Structural basis for lipopolysaccharide insertion in the bacterial outer membrane. *Nature*, *511*(7507), 108–11.

Raetz, C. R., & Dowhan, W. (1990). Biosynthesis and function of phospholipids in *Escherichia coli*. *The Journal of Biological Chemistry*, *265*(3), 1235–1238.

Raetz, C. R. H., Guan, Z., Ingram, B. O., Six, D. A., Song, F., Wang, X., & Zhao, J. (2009). Discovery of new biosynthetic pathways: the lipid A story. *Journal of Lipid*

Research, *50*(Supplement), S103–S108.

Raetz, C. R. H., Reynolds, C. M., Trent, M. S., & Bishop, R. E. (2007). Modification, Lipid A In, Systems. *Annu Rev Biochem.*, *76*(3), 295–329.

Raju, P. N., Evans, H. J., & Seidler, R. J. (1972a). An asymbiotic nitrogen-fixing bacterium from the root environment of corn. *Proceedings of the National Academy of Sciences of the United States of America*, *69*(11), 3474–8.

Raju, P. N., Evans, H. J., & Seidler, R. J. (1972b). An Asymbiotic Nitrogen-Fixing Bacterium from the Root Environment of Corn (Enterobacter cloacae/acetylene reduction/nonleguminous plants), *69*(11), 3474–3478.

Ranf, S. (2016). Immune Sensing of Lipopolysaccharide in Plants and Animals: Same but Different. *PLoS Pathogens*, *12*(6).

Ranf, S., Gisch, N., Schäffer, M., Illig, T., Westphal, L., Knirel, Y. A., Sanchez-Carballo, P. M., Zähringer, U., Huckelhoven, R., Lee, J., & Scheel, D. (2015). A lectin S-domain receptor kinase mediates lipopolysaccharide sensing in *Arabidopsis thaliana*. *Nature Immunology*, *16*(4), 426–433.

Reynolds, C. M., Kalb, S. R., Cotter, R. J., & Raetz, C. R. H. (2005). A Phosphoethanolamine Transferase Specific for the Outer 3-Deoxy-D- manno - octulosonic Acid Residue of *Escherichia coli* Lipopolysaccharide. *Journal of Biological Chemistry*, *280*(22), 21202–21211.

Rietschel, E. T., Kirikae, T., Schade, F. U., Mamat, U., Schmidt, G., Loppnow, H., Ulmer, A. J., Zähringer, U., Seydel, U., & Di Padova, F. (1994). Bacterial endotoxin: molecular relationships of structure to activity and function. *FASEB Journal : Official Publication of the Federation of American Societies for Experimental Biology*, *8*(2), 217–25.

Rietveld, a G., Killian, J. a, Dowhan, W., & de Kruijff, B. (1993). Polymorphic regulation of membrane phospholipid composition in *Escherichia coli*. *The Journal of Biological Chemistry*, *268*(17), 12427–33.

Rietveld, T. G., Chupin, V. V., Koorengevel, M. C., Wienk, H. L. J., Dowhan, W., & De Kruijff, B. (1994). Regulation of lipid polymorphism is essential for the viability of phosphatidylethanolamine-deficient *Escherichia coli* cells. *Journal of Biological Chemistry*. 269(46), 28670-28675.

Rilfors L, Lindblom G, Wieslander Å, C. A. (1984). Lipid bilayer stability in biological membranes. In M. LA Kates M (Ed.), *Membrane fluidity* (pp. 205–245). Plenum Press.

Robey, M., Connell, W. O., & Cianciotto, N. P. (2001). Identification of *Legionella pneumophila* rcp , a pagP -Like Gene That Confers Resistance to Cationic Antimicrobial Peptides and Promotes Intracellular Infection. *Infection and Immunity*, *69*(7), 4276–4286.

Rollauer, S. E., Sooreshjani, M. A., Noinaj, N., & Buchanan, S. K. (2015). Outer membrane protein biogenesis in Gram-negative bacteria. *Philosophical Transactions of the Royal Society B: Biological Sciences*, *370*(1679), 20150023.

Rosenfeld, Y., & Shai, Y. (2006). Lipopolysaccharide (Endotoxin)-host defense antibacterial peptides interactions: Role in bacterial resistance and prevention of sepsis. *Biochimica et Biophysica Acta - Biomembranes*, *1758*(9), 1513–1522.

Rosner, M. R., Verret, R. C., & Khorana, H. G. (1979). The structure of lipopolysaccharide from an *Escherichia coli* heptose-less mutant. III. Two fatty acyl amidases from *Dictyostelium discoideum* and their action on lipopolysaccharide derivatives. *Journal of Biological Chemistry*, *254*(13), 5926–5933.

Rowlett, V. W., Mallampalli, V. K. P. S., Karlstaedt, A., Dowhan, W., Taegtmeyer, H., Margolin, W., & Vitrac, H. (2017). Impact of membrane phospholipid alterations in *Escherichia coli* on cellular function and bacterial stress adaptation. *Journal of Bacteriology*. 199(13), e00849-16. Retrieved from: http://doi.org/10.1128/JB.00849-16

Roy, A., Kucukural, A., & Zhang, Y. (2010). I-TASSER: a unified platform for automated protein structure and function prediction. *Nature Protocols*, *5*(4), 725–738.

Rutten, L., Geurtsen, J., Lambert, W., Smolenaers, J. J. M., Bonvin, A. M., de Haan, A., & Tommassen, J. (2006). Crystal structure and catalytic mechanism of the LPS 3-O-deacylase PagL from *Pseudomonas aeruginosa*. *Proceedings of the National Academy of Sciences of the United States of America*, *103*(18), 7071–6.

Sambrook, J., & Russell, D. (2001). *Molecular cloning: A laboratory manual* (3rd ed.). Cold Spring Harbor, NY: Cold Spring Harbor Laboratory Press.

Sand, O., Gingras, M., Beck, N., Hall, C., & Trun, N. (2003). Phenotypic characterization of overexpression or deletion of the *Escherichia coli* crcA, cspE and crcB genes. *Microbiology*, *149*(8), 2107-2117

Sandhiya, G. S., Sugitha, T. C., Balachandar, D., & Kumar, K. (2001). Endophytic Colonization and In Planta Nitrogen Fixation by a diazotrophic *Serratia sp*. in rice. *Indian Journal of Environmental Biology* , *43*, 802–807.

Sapiano, M. (2014). *Lipid A Regioselectivity Of The Escherichia coli Palmitoyl Transferase PagP*. Thesis. McMaster University, Hamilton, Ontario, Canada.

Sato, T., Hara, T., Horiyama, T., Kanazawa, S., Yamaguchi, T., & Maki, H. (2015). Mechanism of resistance and antibacterial susceptibility in extended-spectrum β-lactamase phenotype *Klebsiella pneumoniae* and *Klebsiella oxytoca* isolated between 2000 and 2010 in Japan. *Journal of Medical Microbiology*, *64*, 538–543.

Saxena, V., & Wetlaufer, D. (1971). A new basis for interpreting the circular dichroic spectra of proteins. *Proceedings of the National Academy of Sciences of the United States of America* , *68*(5), 969–972.

Schiffrin, B., Calabrese, A. N., Higgins, A. J., Humes, J. R., Ashcroft, A. E., Kalli, A. C., & Radford, S. E. (2017). Effects of Periplasmic Chaperones and Membrane Thickness on BamA-Catalyzed Outer-Membrane Protein Folding. *Journal of Molecular Biology*, *429*(23), 3776–3792.

Schlüter, A., Nordmann, P., Bonnin, R. A., Millemann, Y., Eikmeyer, F. G., Wibberg, D., & Poirel, L. (2014). IncH-Type Plasmid Harboring bla CTX-M-15 , bla DHA-1 , and qnrB4 Genes Recovered from Animal Isolates. *Antimicrobial Agents and Chemotherapy*, *58*(7), 3768–3773.

Schulz, G. E. (2002). The structure of bacterial outer membrane proteins. *Biochimica et Biophysica Acta*, *1565*(2), 308–317.

Seemann, T. (2014). Prokka: Rapid prokaryotic genome annotation. *Bioinformatics*. Retrieved from: http://doi.org/10.1093/bioinformatics/btu153

Sheppard, A., Stoesser, N., Wilson, D., & Sebra, R. (2015). Rapid spread of a carbapenem resistance gene driven by multiple levels of genetic mobility. Oxford, United Kingdom. Retrieved from: *NCBI website*, accession number: CP011633

Sherman, D. J., Xie, R., Taylor, R. J., George, A. H., Okuda, S., Foster, P. J., & Kahne, D. (2018). Lipopolysaccharide is transported to the cell surface by a membrane-to-membrane protein bridge. *Science*, *359*(6377), 798–801.

Shevchuk, O., Jäger, J., & Steinert, M. (2011). Virulence properties of the *Legionella pneumophila* cell envelope. *Frontiers in Microbiology*, *2*(APR).

Shin, S. H., Kim, S., Kim, J. Y., Lee, S., Um, Y., Oh, M. K., & Heum, S. (2012). Complete Genome Sequence of *Klebsiella oxytoca* KCTC 1686, Used in Production of 2,3-Butanediol. *Journal of Bacteriology*, *194*(9), 2371–2.

Shrivastava, R., Jiang, X., & Chng, S.-S. (2017). Outer membrane lipid homeostasis via

retrograde phospholipid transport in *Escherichia coli*. *Molecular Microbiology*, *106*(3), 395–408.

Sievers, F., Wilm, A., Dineen, D., Gibson, T. J., Karplus, K., Li, W., Lopez, R., Thompson, J, D., & Higgins, D. G. (2011). Fast, scalable generation of high-quality protein multiple sequence alignments using Clustal Omega. *Molecular Systems Biology*, *7*(1), 539–539.

Sikdar, R., Peterson, J. H., Anderson, D. E., & Bernstein, H. D. (2017). Folding of a bacterial integral outer membrane protein is initiated in the periplasm. *Nature Communications*, *8*(1), 1309.

Silhavy, T. J., Kahne, D., & Walker, S. (2010). The Bacterial Cell Envelope. *Cold Spring Harbour Perspectives in Biology*, *2*, 1–17.

Silipo, A., Sturiale, L., Garozzo, D., Erbs, G., Jensen, T. T., Lanzetta, R., & Molinaro, A. (2008). The Acylation and Phosphorylation Pattern of Lipid A from *Xanthomonas Campestris* Strongly Influence its Ability to Trigger the Innate Immune Response in Arabidopsis. *ChemBioChem*, *9*(6), 896–904.

Singer, S. J., & Nicolson, G. L. (1972). The Fluid Mosaic Model of the Structure of Cell Membranes. *Source: Science, New Series*, *175113111*(18), 720–731.

Singh, L., Cariappa, M. P., & Kaur, M. (2016). *Klebsiella oxytoca*: An emerging pathogen? *Medical Journal Armed Forces India*, *72*, S59–S61.

Sjostrom, M., Wold, S., Wieslander1, A., & Rilfors2, L. (1987). Signal peptide amino acid sequences in *Escherichia coli* contain information related to fmal protein localization. A multivariate data analysis. *The EMBO Journal*, *6*(3), 823–831.

Smith, A. (2008). *How Outer Membrane Lipid Asymmetry Control PagP*. Thesis. McMaster University, Hamilton, Ontario, Canada.

Smith, A. E., Kim, S.-H., Liu, F., Jia, W., Vinogradov, E., Gyles, C. L., & Bishop, R. E. (2008). PagP activation in the outer membrane triggers R3 core oligosaccharide truncation in the cytoplasm of *Escherichia coli* O157:H7. *The Journal of Biological Chemistry*, *283*(7), 4332–43.

Smith, E. W., Zhang, X., Behzadi, C., Andrews, L. D., Cohen, F., & Chen, Y. (2015). Structures of *Pseudomonas aeruginosa* LpxA Reveal the Basis for Its Substrate Selectivity. *Biochemistry*, *54*(38), 5937–5948.

Smith, P. K., Krohn, R. I., Hermanson, G. T., Mallia, A. K., Gartner, F. H., Provenzano, M. D., & Klenk, D. C. (1985). Measurement of protein using bicinchoninic acid.

Analytical Biochemistry, *150*, 76–85.

Smits, T. H. M., Rezzonico, F., Kamber, T., Goesmann, A., Ishimaru, C. A., Stockwell, V. O., & Duffy, B. (2010). Genome sequence of the biocontrol agent *Pantoea vagans* strain C9-1. *Journal of Bacteriology*, *192*(24), 6486–6487.

Solovyev, V., & Salamov, A. (2011). Automatic Annotation of Microbial Genomes and Metagenomic Sequences. In *Metagenomics and its Applications in Agriculture, Biomedicine and Environmental Studies* (pp. 61–78). Nova Science Publishers.

Spencer, M. E., & Guest, J. R. (1973). Isolation and Properties of Fumarate Reductase Mutants of *Escherichia coli*. *Journal of Bactriology*, *114*(2), 563–570.

Strahl, H., & Errington, J. (2017). Bacterial Membranes: Structure, Domains, and Function Changes may still occur before final publication. *Annual review of microbiology, 71,* 519-538.

Süsskind, M., Lindner, B., Weimar, T., Brade, H., & Holst, O. (1998). The structure of the lipopolysaccharide from *Klebsiella oxytoca* rough mutant R29 (O1-/K29-). *Carbohydrate Research*, *312*(1–2), 91–95.

Sweet, C. R., Williams, A. H., Karbarz, M. J., Werts, C., Kalb, S. R., Cotter, R. J., & Raetz, C. R. H. (2004). Enzymatic synthesis of lipid A molecules with four amide-linked acyl chains: LpxA acyltransferases selective for an analog of UDP-N-acetylglucosamine in which an amine replaces the 3″-hydroxyl group. *Journal of Biological Chemistry*, *279*(24), 25411–25419.

Tam, J. P., Wang, S., Wong, K. H., & Tan, W. L. (2015). Antimicrobial peptides from plants. *Pharmaceuticals*. *8(4),* 711-757.

Tamura, K., Stecher, G., Peterson, D., Filipski, A., & Kumar, S. (2013). MEGA6: Molecular Evolutionary Genetics Analysis Version 6.0. *Molecular Biology and Evolution*, *30*(12), 2725–2729.

Tan, B. K., Bogdanov, M., Zhao, J., Dowhan, W., Raetz, C. R. H., & Guan, Z. (2012). Discovery of a cardiolipin synthase utilizing phosphatidylethanolamine and phosphatidylglycerol as substrates. *Proceedings of the National Academy of Sciences*, *109*(41), 16504–16509.

Teilum, K., Olsen, J. G., & Kragelund, B. B. (2011). Protein stability, flexibility and function. *Biochimica et Biophysica Acta - Proteins and Proteomics*. *1814*(8), 969-976

Thaipisuttikul, I., Hittle, L. E., Chandra, R., Zangari, D., Dixon, C. L., Garrett, T. A.,

Goodlett, D. R., Miller, S. I., Bishop, R. E., & Ernst, R. K. (2014). A divergent *Pseudomonas aeruginosa* palmitoyltransferase essential for cystic fibrosis-specific lipid A. *Molecular Microbiology*, *91*(1), 158–174.

Thijs, S., Hamme, J. Van, Gkorezis, P., Rineau, F., Weyens, N., Vangronsveld, J., & Vangronsveld, J. (2014). Draft Genome Sequence of Raoultella ornithinolytica TNT, a Trinitrotoluene-Denitrating and Plant Growth-Promoting Strain Isolated from Explosive-Contaminated Soil. *Genome Announcements*, *2*(3), 13–14.

Thong, S., Ercan, B., Torta, F., Fong, Z. Y., Alvina Wong, H. Y., Wenk, M. R., & Chng, S. S. (2016). Defining key roles for auxiliary proteins in an ABC transporter that maintains bacterial outer membrane lipid asymmetry. *ELife*, *5*(AUGUST). Retrieved from: http://doi.org/10.7554/eLife.19042

Thornburg, T., Miller, C., Thuren, T., King, L., & Waite, M. (1991). Glycerol reorientation during the conversion of phosphatidylglycerol to Bis(monoacylglycerol)phosphate in macrophage-like RAW 264.7 cells. *Journal of Biological Chemistry*, *266*(11), 6834-6840

Treangen, T. J., & Rocha, E. P. C. (2011). Horizontal transfer, not duplication, drives the expansion of protein families in prokaryotes. *PLoS Genetics*, *7*(1), e1001284.

Trent, M. S. (2004). Biosynthesis, transport, and modification of lipid A. *Biochemistry and Cell Biology = Biochimie et Biologie Cellulaire*, *82*, 71–86.

Trent, M. S., Stead, C. M., Tran, A. X., & Hankins, J. V. (2006). Diversity of endotoxin and its impact on pathogenesis. *Journal of Endotoxin Research*, *12*(4), 205–223.

Unden, G., Philipp, A. S. & Degreif-Dunnwald, P., (2014). The Aerobic and Anaerobic Respiratory Chain of *Escherichia coli* and *Salmonella enterica*: Enzymes and Energetics. EcoSal Plus 2014; doi:10.1128/ ecosalplus.ESP-0005-2013.

Unden, G., & Bongaerts, J. (1997). Alternative respiratory pathways of *Escherichia coli*: Energetics and transcriptional regulation in response to electron acceptors. *Biochimica et Biophysica Acta - Bioenergetics*, *1320*(3), 217–234.

Ursell, T. S., Trepagnier, E. H., Huang, K. C., & Theriot, J. A. (2012). Analysis of Surface Protein Expression Reveals the Growth Pattern of the Gram-Negative Outer Membrane. *PLoS Comput. Biol.*, *8*(9), e1002680.

Volbeda, A., Nicolet, Y., & Fontecilla-Camps, J. C. (2017). Fumarate and Nitrate Reduction Regulator (FNR). *Encyclopedia of Inorganic and Bioinorganic Chemistry*, 1–11.

Vollmer, W., Blanot, D., & De Pedro, M. A. (2008). Peptidoglycan structure and architecture. *FEMS Microbiology Reviews*, *32*(2), 149–167.

Ward, A., Reyes, C. L., Yu, J., Roth, C. B., & Chang, G. (2007). Flexibility in the ABC transporter MsbA: Alternating access with a twist. *Proceedings of the National Academy of Sciences*, *104*(48), 19005–19010.

Weingarten, R. ., Johnson, R. ., Conlan, S., Ramsburg, A. ., & Dekker, J. (2018). Genomic Analysis of Hospital Plumbing Reveals Diverse Reservoir of Bacterial Plasmids Conferring Carbapenem Resistance. *mBio, 9(1)*, e02011-17

West, S. E. H., Schweizer, H. P., Dall, C., Sample, A. K., & Runyen-Janecky, L. J. (1994). Construction of improved *Escherichia-Pseudomonas* shuttle vectors derived from pUC18/19 and sequence of the region required for their replication in *Pseudomonas aeruginosa*. *Gene*, *148*(1), 81-86.

Wiedenbeck, J., & Cohan, F. M. (2011). Origins of bacterial diversity through horizontal genetic transfer and adaptation to new ecological niches. *FEMS Microbiology Reviews*, *35*(5), 957–976.

Winfield, M. D., & Groisman, E. A. (2004). Phenotypic differences between *Salmonella* and *Escherichia coli* resulting from the disparate regulation of homologous genes. *Proceedings of the National Academy of Sciences*, *101*(49), 17162–17167.

Winn, W. C. (1988). Legionnaires disease: historical perspective. *Clinical Microbiology Reviews*, *1*(1), 60–81.

Womack, M. D., Kendall, D. A., & Macdonald, R. C. (1983). Detergent effects on enzyme activity and solubilization of lipid bilayer membranes. *Biochimica et Biophysica Acta*, *733*(210), 215–71793.

Wu, T., Malinverni, J., Ruiz, N., Kim, S., Silhavy, T. J., & Kahne, D. (2005). Identification of a multicomponent complex required for outer membrane biogenesis in *Escherichia coli*. *Cell*, *121*(2), 235–245.

Wu, T., McCandlish, A. C., Gronenberg, L. S., Chng, S.-S., Silhavy, T. J., & Kahne, D. (2006). Identification of a protein complex that assembles lipopolysaccharide in the outer membrane of *Escherichia coli*. *Proceedings of the National Academy of Sciences*, *103*(31), 11754–11759.

Yan, A., Guan, Z., & Raetz, C. R. H. (2007). An Undecaprenyl Phosphate-Aminoarabinose Flippase Required for Polymyxin Resistance in *Escherichia coli*. *Journal of Biological Chemistry*, *282*(49), 36077–36089.

Zähringer, U., Knirel, Y. A., Lindner, B., Helbig, J. H., Sonesson, A., Marre, R., & Rietschel, E. T. (1995). The lipopolysaccharide of *Legionella pneumophila* serogroup 1 (strain Philadelphia 1): chemical structure and biological significance. *Progress in Clinical and Biological Research*, *392*, 113–39.

Zarrouk, H., Karibian, D., Bodie, S., Perry, M. B., Richards, J. C., & Caroff, A. M. (1997). Structural Characterization of the Lipids A of Three *Bordetella bronchiseptica* Strains: Variability of Fatty Acid Substitution. *Journal of Bacteriology*, *179*(11), 3756–3760.

Zasloff, M. (2002). Antimicrobial peptides of multicellular organisms. *Nature*, *415*(January), 389–395.

Zhanel, G. G., DeCorby, M., Laing, N., Weshnoweski, B., Vashisht, R., Tailor, F., & Hoban, D. J. (2008). Antimicrobial-resistant pathogens in intensive care units in Canada: Results of the Canadian National Intensive Care Unit (CAN-ICU) study, 2005-2006. *Antimicrobial Agents and Chemotherapy*, *52*(4), 1430–1437.

Zhang, B., Jaroszewski, L., Rychlewski, L., & Godzik, A. (1997). Similarities and differences between nonhomologous proteins with similar folds: Evaluation of threading strategies. *Folding and Design*, 2(5), 307-317.

Zhang, J. (2003). Evolution by gene duplication: An update. *Trends in Ecology and Evolution*, *18*(6), 292–298.

Zhou, Z., Lin, S., Cotter, R. J., & Raetz, C. R. H. (1999). Lipid A Modifications Characteristic of *Salmonella typhimurium* Are Induced by NH4 VO3 in Escherichia coli K12. *Journal of Biological Chemistry*, *274*(26), 18503–18514.

Zientz, E., Six, S., & Unden, G. (1996). Identification of a third secondary carrier (DcuC) for anaerobic C4-dicarboxylate transport in *Eschenchia coli*: Roles of the three Dcu carriers in uptake and exchange. *Journal of Bacteriology*, *178*(24), 7241–7247.